Modeling of Asphalt Pavement Performance Indices in Different Climate Regions Using Soft Computing Techniques

By

Abdualmtalab Abdualaziz Yeklef Ali

A thesis
presented to Memorial University
in fulfillment of the
thesis requirement for the degree
of Doctor of Philosophy
in
Civil Engineering

October (2022)

St. John's Newfoundland and Labrador Canada

AUTHOR'S DECLARATION

I hereby declare that I am the sole author of this thesis. This is a true copy of the thesis, including any required final revisions, as accepted by my examiners.

I understand that my thesis may be made electronically available to the public.

ABSTRACT

Pavement Management Systems (PMS) enhance pavement performance over the pavements' predicted lifespan by maximizing pavement life. PMS have become an essential aspect of construction and maintenance in the road domain, providing significant cost and energy emission reductions. In addition, using pavement performance prediction models have become an important part of PMS as a technically method for road engineers and various transportation agencies during the past several decades. The Pavement Condition Index (PCI) and International Roughness Index (IRI) are generally accepted methods for gauging ride quality and pavement conditions. Asphalt pavements are highly sensitive to various parameters, including pavement distress, environment, and traffic volume. Hence, studying these variables while developing prediction models is a vital step that can help develop asphalt pavement performance indices.

This research aimed to introduce an effective method for developing asphalt pavement performance indices in different climate regions. This research provided a methodology to develop performance models using three soft computing techniques, namely the fuzzy inference system (FIS), multiple linear regression (MLR), and artificial neural networks (ANNs). Two sources were used for the extracted dataset: the long-term pavement performance (LTPP) data set for four climate regions in the U.S. and Canada and filed survey data of section roads of St. John's, Newfoundland, Canada.

First, for the classification section, the research presented in this study provided a FIS that uses appropriate membership functions for computing PCI and IRI values. A fuzzy input was calculated by considering the degree of distress from nine density types of pavement distress coefficients (rutting, fatigue cracking, block cracking, longitudinal cracking, transverse cracking, patching, potholes, bleeding, and ravelling), which were considered as fuzzy input variables. Results

presented that the rutting and transverse cracking had the most significant influence on the PCI model, while rutting and patching had the most significant impact on the IRI model.

Second, the MLR and ANNs techniques were used for predicting and developing models for the PCI and IRI of flexible pavements. The LTPP database was used to obtain three fundamental variables (pavement distress, environmental, and traffic volume) as input variables for four climate regions.

Finally, for the case study, the research developed a second set of pavement distress models based on a field survey of St. John's city's input variables for predicting PCI and IRI models. A high determination coefficient (R^2), low root mean square error (RMSE) and mean absolute error (MAE)indicated good accuracy for the prediction models. The results showed that the ANNs have more precision than the MLR techniques. However, the results showed that both methods perform well.

ACKNOWLEDGEMENTS

I would like to first and foremost thank Allah for granting me good health, a good state of mind, and a way to finish this thesis. All praise and thanks to Allah, without his help, it won't be easy to complete this degree.

The author would like to express deep gratitude to my supervisor, Professor Amgad Hussein, for his guidance, encouragement, for this research, as well as my co-supervisor, Professor Usama Heneash, for his help and support throughout the study. I would also like to thank my committee members, Professor Samer Nakhla for his support.

I would dedicate my thesis to my mother's and father's soul; may Allah bless them.

I owe a debt of gratitude to my wife and my kids for their patience and help. Big thanks go to my brothers for their encouragement and kindness.

I greatly appreciate the support of the Azzaytuna University-Tarhuna and the Ministry of Higher Education in Libya, which sponsored the research and funded my study period.

List of Contents

List of Figures

List of Tables

List of Abbreviations

FHWA	Federal Highway Administration
AASHTO	American Association of State Highway Officials
PMS	Pavement Management System
SHRP	Strategic Highway Research Program
M&R	Maintenance and Rehabilitation
LTPP	Long-Term Pavement Performance
AC	Asphalt Concrete
GPS	General Pavement Studies
GPS-1	GPS for Asphalt Concrete Pavement on Granular Base
SPS	Specific Pavement Studies
PCI	Pavement Condition Index
IRI	International Roughness Index
FIS	Fuzzy Inference Systems
ANNs	Artificial neural networks
C.N	Construction Number
ESAL	Cumulative Equivalent Single Axle Load
AADTT	Annual Average Daily Truck Traffic
AADT	Annual Average Daily Traffic
SPSS	Statistical Package for the Social Sciences
MLR	Multiple Linear Regressions
R^2	Coefficient of Determination
RMSE	Root Mean Square Error
MAE	Mean Absolute Error
Tem Avg	Temperature average
Wind average.	Wind average
Total ann precip	Total average annual precipitation

Chapter1: Introduction

1.1 Introduction

Around 93% of the world's paved roads are surfaced with asphalt. These pavements, better known as flexible pavements, consist of several layers of asphalt materials placed over granular material layers or treated subgrade. Each layer plays a role in supporting traffic loads. The layers also limit the impact of the environment (e.g., freezing and thawing) on the road. However, the life cycle of pavement is influenced by numerous distresses. These include rutting, fatigue cracking, block cracking, transverse cracking, potholes, patching, and thermal cracking.

In the first few years of a road's usage, distresses initially form as micro-sized fissures. After the pavement has been exposed to traffic, distresses form and the process continues, resulting in a series of cracks. The functional condition is mainly concerned with the surface texture or quality of the ride. In contrast, the structural condition is concerned with the pavement's structural ability and capability to maintain certain traffic volume, as determined by deflection, layer thickness, and material characteristics. Technically, road damage means that roads cannot deliver the best possible service to users and passengers and require maintenance work. Many factors influence the service life of road, such as (1) structure and material parameters, (2) volumetric properties of the mixture, (3) environmental conditions, and (4) traffic volume (AASHTO R30, 2002). These pavement distress forms have continually been a challenge for pavement engineers aiming to build roads with long life and good performance.

1.2 Problem Statement

Highways is a major contributor to national and local economic and social well-being. In the U.S, Canada, and other countries worldwide, government transportation departments spend a

significant portion of their annual budgets on road repair. Therefore, major efforts have been made in recent decades to improve prediction models by understanding the mechanisms underlying the variables that influence pavement performance. Deterioration of pavements is caused by the increasing volume of traffic, repeated loads, asphalt concrete layer properties, coupled with weather conditions.

The active pavement management system assures that pavement sections are maintained at high levels of service, structurally sound conditions, and with a minimum budget and resources.

Predicting pavement performance and enhancing the realism and accuracy of performance prediction models continues to be challenging for the following reasons:

- Pavement predictions concerning various distresses are achieved through mathematical approaches. Nevertheless, pavement performance assessment is still challenging, as these approaches can only be applied effectively under similar conditions and often entail continuous calibration.
- Precisely predicting the distresses of asphalt pavement, such as fatigue cracking, permanent deformation (rutting), patching, potholes, transverse cracking, ravelling, and longitudinal cracking, may be problematic due to the highly complicated behaviour of asphalt pavement material under different environmental conditions.
- Predicting pavement performance is linked to the evaluation of road conditions and the level of serviceability, along with factors such as operation function, location, traffic volume, type of soil, and economic conditions.

1.3 Research Objectives

The primary motivation of the research was the Modeling asphalt pavement performance indices in four climate regions, introducing performance prediction models that can accurately predict pavement conditions and service life based on the effect of internal and external parameters on pavement performance. Research Specific objectives can be summarized as follows:

- Modeling the relationship between asphalt pavement performance indices.
- To study and define parameters that significantly impact pavement indices by conducting a comprehensive investigation of the effects of three fundamental parameters and relevant performance models.
- Modeling of asphalt pavement performance indices using conventional techniques in four climate regions.
- Modeling of asphalt pavement performance indices using soft computing techniques in four climate regions.

1.4 Research Scope

To fulfil all the research objectives, the scope of the study was divided into six phases, as follows:

- **<u>Phase A</u>: Modeling of Asphalt Pavement Performance Indices Using (FIS)**

This research proposes using a fuzzy inference system (FIS) to estimate pavement indices (PCI and IRI), taking the severity and level of the other pavement distress as input parameters. It should be noted that FIS is one of the most common techniques used for classification problems.

- **<u>Phase B:</u> Modeling the Relationship Between Asphalt Pavement Performance Indices**

This research work modeling the relationship between two asphalt pavement performance indicators (PCI and IRI) for climate regions in the U.S. and Canada.

- **<u>Phase C</u>: Modeling of Asphalt Pavement Performance Indices Using (MLR)**

The multiple linear regression (MLR)method was used to modeling asphalt pavement performance indices (PCI & IRI).

- **<u>Phase D</u>: Modeling of Asphalt Pavement Performance Indices Using (ANN)**

The fourth phase proposed modeling asphalt pavement performance indices using (ANN). The ANNs method effectively investigates and analyzes the data. This technique could recognize data patterns that are not easily detected by traditional statistical.

- **<u>Phase E:</u> Comparison and validation between (MLR) and (ANNs) models**

  The performance of the MLR models was compared with the performance of the ANNs models to evaluate the accuracy of the models in predicting pavement performance based on pavement distress parameters. R^2, RMSE and MAE values were used to measure and compare the performance of the models.

- **<u>Phase F:</u> Case Study**

  The case study focuses on studying the effect of pavement distress on determining pavement condition. St. John's, the capital of Newfoundland and Labrador-Canada is the case study's site. These include the determination of PCI, IRI, and PSR of flexible pavement and developing reliable prediction models for St. John's roads using soft computing techniques.

Research Scope Limited

The research focused on only flexible asphalt pavement data with no maintenance or rehabilitation.

Method Analysis:

The study relies on three different techniques to achieve its objectives, as follows:

1- Machine learning (FIS) technique using MATLAB software.
2- Multiple linear regression (MLR) method using statistical product and service solutions (IBM SPSS software).
3- Machine learning (ANNs) technique using MATLAB software.

1.5 Dissertation Structure

This thesis is comprised of eight chapters as follow:

Chapter 1: Introduction

This chapter introduced the concept of pavement management and asset management. Also included are the research objective, scope of the study.

Chapter 2: Literature Review

This chapter presented a review of the pavement management system. The chapter also presented a review of pavement condition evaluation, previous studies on pavement performance modelling, and types of distress. Finally, the chapter reviewed all parameters that influence pavement performance.

Chapter 3: Research Methodology

This chapter presented the research methodology for Modeling of Asphalt Pavement Performance Indices. The chapter also briefly explained the principle of the three soft computing techniques used in later chapters.

Chapter 4: Modeling of Asphalt Pavement Performance Indices Using FIS

This chapter presented the modeling of asphalt pavement performance indices using a fuzzy inference system (FIS).

Chapter 5: Modeling the Relationship Between Asphalt Pavement Performance Indices (PCI&IRI)

This chapter focused on studying the correlation between PCI and IRI using different mathematical methods.

Chapter 6: Modeling of Asphalt pavement performance Indices Using (MLR) and (ANNs) Techniques

This chapter discussed different pavement performance prediction models and the significant factors affecting PCI and IRI models. This chapter also discussed the asphalt pavement performance indices modeling using different techniques.

Chapter 7: A Case Study

This chapter described a simple case study for 37 road sections in St. John's, Newfoundland, Canada. It summarized of significant findings of the study.

Chapter 8: Conclusions and Recommendations

This chapter considered with summarizes the conclusions and suggestions for future work.

Chapter2: Literature Review

2.1 Pavement Management System

Pavement performance can be generally defined as the change in their condition or function concerning age. It can also indicate the ability of pavement to carry the intended traffic and satisfy the environment during the design life, both functionally and structurally. The United States and Canada face a broad range of challenges due to their harsh climates, road safety issues, environmental concerns, and vast land size. These challenges increase the government's responsibility for maintaining an effective road transport system to sustain both countries' competitiveness in the global economy. Economic and financial conditions are driving governments to explore new and creative ways to finance transportation projects.

The prediction model is an essential method for implementing efficient maintenance strategies. Pavement network management agencies need to consider such a strategy to realize cost-efficient management of pavements for long-term service life.

This chapter summarises the methods, main observations, and knowledge gaps in using these pavement performance methods and prediction models. The chapter also reviews previous studies conducted concerning the objectives of the present work. A systematic literature review also highlights studies that use the PMS, PCI, and IRI when studying flexible pavement.

2.1 History of Test Roads in North America (US and Canada)

In the early 1920s, the American Association of State Highway Officials (AASHO) began conducting a significant series of road tests, with the last important experiment performed in the late 1950s (AASHTO, 1972). These comprehensive studies were intended to determine the extent to which load traffic leads to the deterioration of the pavement. Canadian transportation agencies

noticed the empirical studies being carried out in the United States and decided to use local materials and conditions to perform similar experiments.

Early in 1965, the Ministry of Transportation Ontario (MTO) started to collect data on 36 newly designed pavement test sections in the province of Ontario. These test parts were located near Brampton, on Highway 10. The key objectives of the experiments were to: compare the results of the AASHO Road Test with the materials and conditions of Ontario; measure the performance of standard pavement designs; and record the performance of different base materials (Kamel et al., 1973). An empirical study was the primary feature of the AASHO Road Test, in which a specific vehicle type and weight were used to repeat the loading of each road segment. A total of six 2-lane test loops were constructed. Loops 2 to 6 were exposed to different truck traffic combinations. It should be noted that loop 1 was used as a section of control to test environmental impact, so it was not part of the loading tests. The main drawback of this empirical study is that such approaches can only be applied effectively under local conditions and often entail continuous calibration.

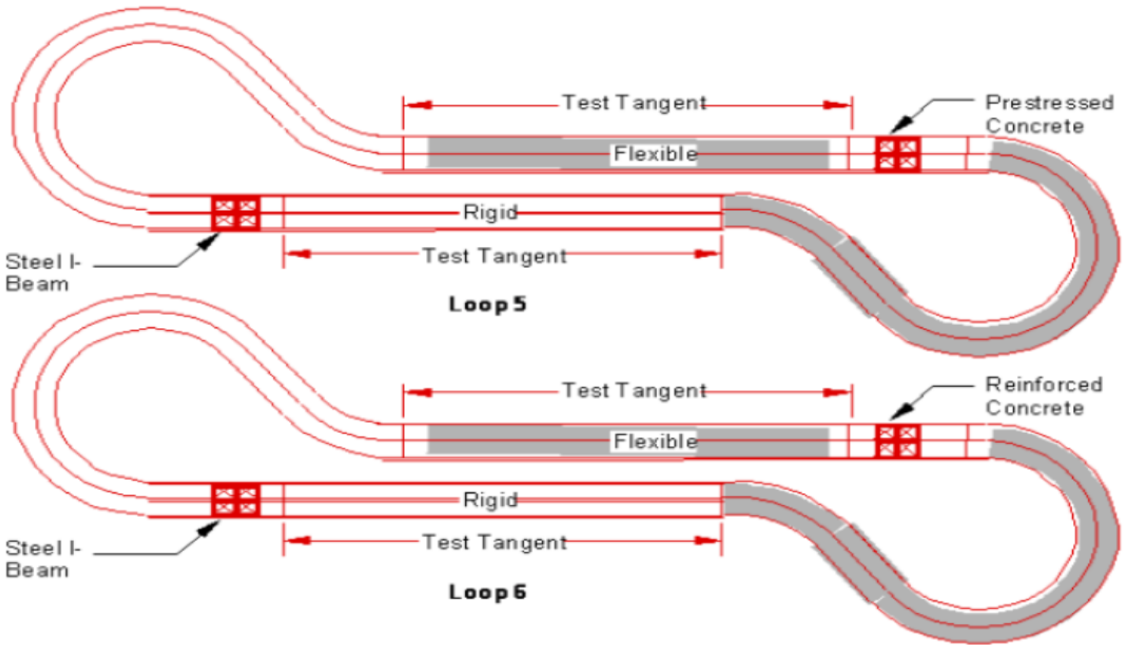

Figure 2-1: The AASHO road test configuration (1962).

One of the most significant drawbacks of empirical studies is related to the limitations of the Road Test experiment. The data obtained from this experiment are highly related to the constraints associated with the experiment's location. Data were collected on one type of subgrade soil and road construction material under specific environmental and traffic conditions (NCHRP, 2004). C-SHRP initiated additional research in the late 1980s to study the effects of climate conditions on roadway efficiency. The main objectives of that study were to record paving practices in Canada; and better understand asphalt concrete (AC) properties that affect the efficiency of low temperatures (Gavin et al., 2003). In three separate locations across Canada – Lamont, Alberta; Hearst, Ontario; and Sherbrooke, Quebec – three C-SHRP test sites were built. However, only one test site was a full-study experiment (the one near Lamont), whereas the other two sites were used as smaller-scale satellite experiments (Gavin et al., 2003).

2.2 Pavement Management Systems

A Pavement Management System (PMS) for pavement rehabilitation can be defined as "a system that will produce a multi-layer program for pavement rehabilitation to utilize available finds most cost-effectively" (Hudson et al., 1979). PMSs are becoming essential resources in the decision-making process to maintain and preserve pavement networks. The PMS program is ideal for keeping all paved road sections under satisfactory structural conditions and serviceability. Nevertheless, it should not have any significant adverse effects on the environment, traffic, or social and community activities(Fwa et al, 2000) .

Numerous PMSs, ranging from the complex to the simplistic, have been established. However, many of these systems suffer from mismanagement. Dewan (2004) reported on the main issues confronting pavement management efforts, with the author highlighting the components that are crucial for the inclusion of ineffective management strategies.

Several different management systems have been developed, applied, and studied across the U.S. In Pennsylvania, Kilareski and Churilla (1983) built a PMS that was suitable for a highly industrialised state and large highway network. Their PMS was then implemented in a few other states and monitored using two modules: a distress progression survey, and a network serviceability inventory. The distress progression survey was intended to gather data related to repair decision optimization and prioritizing, as well as budget estimations (Kilareski & Churilla, 1983). In a similar project, Sachs and Suede (1996) looked at modifications in a PMS implemented in Washington. The authors developed a procedure that identified five kinds of distresses, then applied it to a look-up Table charting three severity levels for alligator cracking across various percentage ranges (Sachs & Suede, 1996). In other related work, several different types of PMSs have been applied at the project and network levels. Gharaibeh et al. (1999) presented a management system in Illinois that integrated data, analytical procedures, geographical information system (GIS), and presentation methods. The developed system was used in five highway infrastructure components (i.e., intersections, bridges, culverts, traffic signs, and pavement). The authors employed an integrated network-level system to carry out a trade-off analysis on feasible maintenance options for the five components mentioned above. The analysis aimed to prioritize the minimizing of traffic disruptions (Gharaibeh et al, 1999).

Sebaaly et al. (1996), in similar work, also proposed developing a PMS in Nevada at the project and network levels. Their developed system integrated performance models that considered life-cycle cost analysis (LCCA) and traffic and environmental impacts. Another key consideration in their study was network optimisation methods that dealt with maintenance and rehabilitation prioritisation. At the project level, the authors performed pavement evaluations using non-destructive deflection testing (sebaaly et al., 1996).

A few years later, Rasdorf et al. (2000) developed a PMS to implement in the North Carolina Department of Transportation (NCDOT). This system was intended to highlight the needs and challenges of developing a comprehensive information management system. The PMS enabled an environment that permitted data format standardisation and data sharing and reduced the need for training. The key contribution of the developed database was the application of geographic information system (GIS) and the linear reference method (LRM) (Rasdorf et al., 2000).

In Portugal, Golabi and Pereira (2003) investigated how the Portuguese pavement management system (PPMS) was being developed and implemented. The authors noted that the main modules in the system were GIS, a database, a model that evaluated pavement quality, and pavement rehabilitation and strategic improvement model (PRISM). The authors also reported that the Mov modelling method, which applied probabilistic prediction models for assigning state transition probabilities using knowledge and experience, was being employed to further develop optimisation models with predictive capabilities (Golabi & Pereira, 2003).The average age of the highways and roads in Canada is 15.4 years (Gagnon et al., 2008), with a high percentage of the network length being more than 10 years old and requiring regular maintenance and rehabilitation. Table (2-1) presents the ages of highways and roads across Canada.

In-service overlay performance investigation and assessment over the years significantly supports the potential decisions of provincial transportation ministries regarding design variables such as type of pavement, asphalt mixture, pavement structure and construction parameters. In fact, in both the U.S. and Canada, a large portion of the transportation departments' annual budgets are allocated to road repair and maintenance. Alberta Transportation, for instance, spends around 50% of its annual budget repairing and maintaining the highway network in Alberta(Government of Alberta, 2011).

Table 2-1: Ages of highways and roads in all provinces of Canada.

Canada/Province	**Age of Highway and roads(year)**
Newfoundland and Labrador	14.9
Prince Edward Island	16.4
Nova Scotia	13.9
New Brunswick	16.3
Newfoundland and Labrador	15.2
Quebec	15.2
Ontario	13.9
Manitoba	17.1
Saskatchewan	16.7
Alberta	14.4
British Columbia	15.8

Road maintenance programs have developed rapidly over the past 30 years. One study from the late 1900s reports on road work done in western Canada. In May 1990, the SPS-5 sections in Alberta joined the LTPP programme, and the overlay building was completed in September 1990 (although the control section did not receive an overlay). After completing the overlay building, each of the eight sections underwent different maintenance, depending on their circumstances. Crack sealing and pothole patching were the most common treatments applied. The researchers report that two of the sections (502 and 509) came to an end in 2006, after only 16 years of service life (Norouzi et al., 2014).

In another study that looked at all SPS-5 sections across North America, Hall et al. (2003) applied the newly revised IRI measurements. The researchers found no noticeable difference between recycled asphalt pavement (RAP) and virgin long-term IRI or between milled and non-milled overlays. The influence of pre-overlay IRI, overlay age and average annual temperature on long-term IRI was significant (Kathleen T. Hall et al., 2003).

Rajagopal and George (1991) conducted parametric studies to estimate appropriate maintenance timing and select the most suitable level for three treatments (surface treatment and thin and thick overlays). The researchers found that the underlying structural condition directly impacted the immediate effect of maintenance work and that early maintenance treatment decreased future costs (Rajagopal & George, 1991).

Several studies were conducted on SPS 5 sections across sixteen states in the U.S. and two provinces in Canada to evaluate the influence of various overlay strategies on pavement performance. West et al. (2011) used the latest reported data to compare the statistical distress found for the nine sections. The authors concluded in their analysis that both mixture type and milling before overlay construction would significantly affect pavement output in terms of fatigue cracking, transverse cracking, and longitudinal cracking. Their research also showed no significant impact of overlay thickness on longitudinal cracking (West et al., 2011).

2.3 Parameters Affecting Pavement Performance

Predicting pavement performance is considered a difficult task since several variables affect the pavement's performance. A number of different parameters have identified the research as affecting pavement performance. Janno and Shepherd (2000) investigated how seasonal variations impact pavement material properties. They found that moisture and temperature have the most

significant impacts overall, but that long-term performance is highly dependent on pavement layer properties and the subgrade soil. There is a need to determine and investigate the different potential parameters that influence pavement performance. As presented in Figure (2-2), the most crucial factors are materials and construction, Traffic volume, climate, and performance.

These factors were especially influential in regions where wide seasonal fluctuations were the norm (Janno and Shepherd 2000). Even so, given the changes in climate across different regions, including closely neighbouring ones developing accurate prediction models based on a "one-size-fits-all" approach is very challenging.

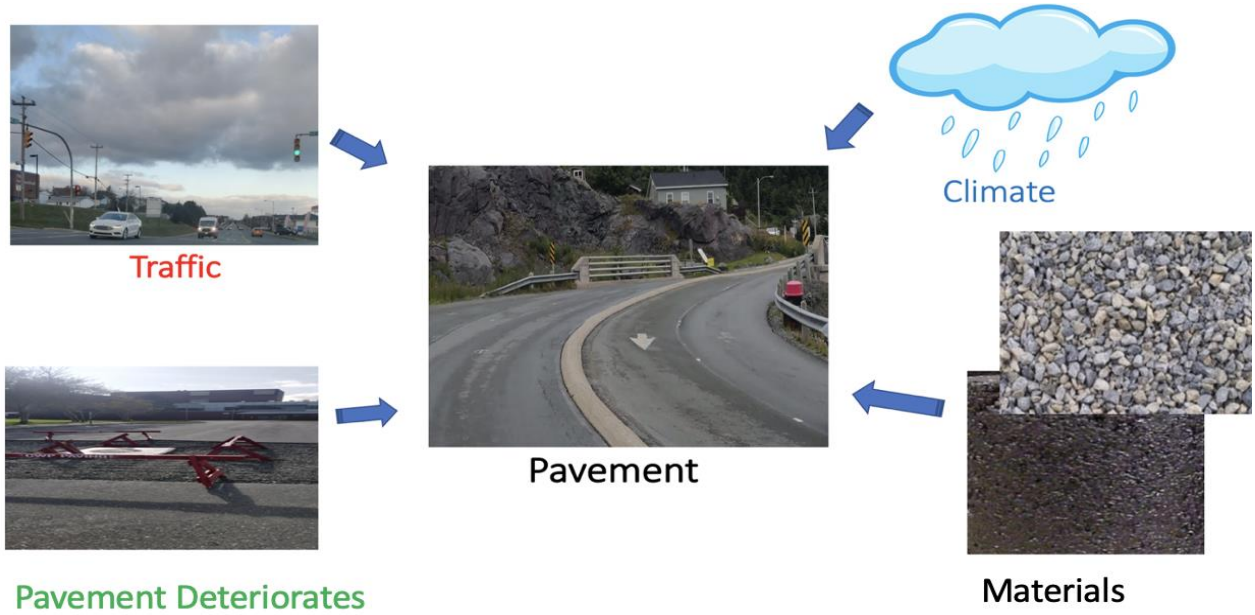

Figure 2-2: Parameters affecting pavement performance.

Despite the inherent difficulties in creating such a model, there is widespread consensus that such a model is needed for predicting various aspects of planning and budgeting in, for instance, transportation departments. The hope is that accurately predicting the impact of local and regional environments might enhance pavement performance and lead to decreased maintenance costs. A broad range of environmental factors has been reported to impact pavement performance (Mrawira

and Wile 2000) strongly. The most critical are temperature, the freeze/thaw cycle, overall moisture content, and the Ground Water Table (GWT). At the same time, seasonal weather variations contribute to changes in pavement material properties, thus affecting performance through secondary effects resulting from the factors mentioned above.

2.4 Pavement Deterioration

The extent and types of distress need to be identified and the reasons underlying the deterioration before a proper repair strategy is chosen to remedy the distressed pavement. Common causes of deterioration include harsh climate, heavy traffic loading, low-quality materials, deficient drainage, and construction flaws. The most typical causes of pavement distresses are ageing and traffic repetition, but distress may also be compounded simply through time, when, for instance, a crack can permit the intrusion of water to the pavement and eventually results in a pothole or stripping. Therefore, timely maintenance is critically essential. Deteriorates can be classified into several types as follow:

Cracking

Cracks are fractures that occur on the pavement surface in various ways forms. The causes of cracks are many, including fatigue, shrinkage, deformation, and climate impact (temperature, snow, wind..., etc.). Table (2-2) shows the most common crack types in flexible pavement. Four fundamental types of cracking have been described as mentioned in this section.

Fatigue Cracking (Alligator Cracking)

Fatigue cracking is one of the main modes of distress in flexible pavements along with rutting and thermal cracking. Fatigue cracking includes a single crack and series of interconnected multi cracks leading to create small, nonuniform zones on the pavement, fatigue cracking due to

primarily dependent on 3 main reasons, repeated traffic loads, vehicle speed, and temperature of the pavement (Langlois et al., 1999).

The linear distance in square metres of the impacted wheel path or fatigue cracking area is measured. Each area is categorized based on the severity level. If there are two distress in the same place, such as fatigue cracking and rutting, each distress must be dealt with separately (Miller & Bellinger, 2003) (FHWA 2009).

(a)Low Severity

(b) Medium Severity

(c) High Severity

Figure 2-3: Severity levels for fatigue cracking in asphalt pavement.

Block cracking

Block cracking may be defined as the development of interconnected cracks across areas that have not been subjected to heavy traffic load. These cracks demarcate rectangular shaped blocks on the pavement. The size of the blocks typically ranges between 30 x 30 cm and 300 x 300 cm (ACRP, 2016; DOT, 2010; Federal Highway Administration 2009). This form of distress develops across the width of the pavement (i.e., including wheel paths). However, on hot-mix asphalt (HMA) surfaces, they tend to extend a short distance only. An example of block cracking is given in Figure (2-4).

Figure 2-4: Block cracking in asphalt pavement.

The main causes of block cracking are hardening, shrinking, and inadequate compaction of the mix (FHWA 2009, FDOT 2015). Options include low, medium, and high. At low (L) severity levels, the cracks are tight and feature little spalling. The average width of these cracks is up to 6 mm (Hall et al. 1993). At medium (M) severity levels, crack widths measure greater than 6 mm but less than 12 mm. At high (H) severity levels, the cracks have an average width 12 mm or greater, and there is severe spalling as well as either moderate or severe parallel cracking occurring

near the crack intersections. Note that this cracking is typically randomized (Hall et al. 1993). The best approach is to measure the area(s) affected either by square meters or by the entire pavement length. Block cracking of low severity can be remedied by constructing a thin wearing course, while block cracking that is medium or high may require recycling or overlays, and base problems may need pavement reconstruction or reclamation (Adlinge & Gupta, 2013).

Longitudinal cracking

Longitudinal cracking may be defined as the presence of long cracks parallel with the centerline. Cracking at the exact lane center is referred to as center-of-lane cracking. This form of cracking may occur from the centre line to the wheel path's outer edge, as depicted in Figure 2-5 (a, b). Note that the positioning of these cracks (i.e., wheel path/non-wheel path) in large part determines their severity.

(a) (b)

Figure 2-5: Longitudinal cracking in asphalt pavement.

The main causes of longitudinal cracks are construction-related failures, i.e., poor technique or low compaction, as well as heavy loads and frost heaving occurring between lanes. Additional causes are sub-surface crack development and low temperatures that lead to surface shrinkage

(Scott et al., 2012). Options include low, medium, and high. Low (L) severity levels of longitudinal cracking involve issues such as cracks that are not on the wheel path and which have only minor spalling. At L severity, the crack width measures a maximum of 6 mm (FHWA 2009). Medium (M) severity levels in longitudinal cracking are indicated by moderate spalling that features filled cracks less than 6 mm wide and non-filled cracks between 6 mm and 19 mm (Miller et al., 2003). High (H) severity levels of longitudinal cracking are indicated by crack widths 19 mm or greater.

For each severity level (L, M and H), the affected areas are measured linearly in meters. Longitudinal cracking may be repaired using spray patching or other similar applied treatment.

Transverse cracking

Transverse cracking may be defined as cracks which develop perpendicular to a road's centerline. This form of cracking is typically regularly spaced and begins as hairline (narrow) cracks that grow wider over time (Miller et al., 2003). Transverse cracking may form at any surface location and grow deeper over time. The main causes of transverse asphalt cracking are low temperatures that lead to surface shrinkage. This form of cracking may also be caused by a paving lane joint being poorly constructed, or by reflective cracks that have been induced by sub-surface cracking (Hall et al.,1993). Options include low, medium, and high. In low (L) severity levels of transverse cracking, tight cracks appear with widths measuring around 6 mm, accompanied by slight spalling. In medium (M) severity levels of transverse cracking, the cracks measure between 6 mm and 19 mm and are randomly placed (FHWA 2009). In high (H) levels of severity for this form of cracking, the cracks are greater than 19 mm, with severe spalling around the cracks (Miller et al. 2003). Examples of transverse cracking are shown in Figure 2-6 (a, b).For each severity level (L, M and H), the measurement of transverse cracks includes length and number of cracks. If the

severity level of the distress for this form of cracking is rated L or M, sealing of cracks is the best option. However, for transverse cracking rated as H, an overlay should be applied.

(a) (b)

Figure 2-6: Transverse cracking in asphalt pavement.

Rutting

Rutting may be defined as vertical deformations in pavements that cause surface depressions in the direction of the wheel path. Depressions may develop across wide expanses, mostly in the direction of the wheel path. Figure 2-7(a, b) illustrates abrasive and structural rutting in St. John's, Newfoundland, Canada. Rutting represents a critically important form of distress that occurs in flexible pavements. Shearing may then form as a result of the rutting, damaging the road's top surface and thus significantly impacting the ride quality of motorists (Kandhal et al., 2003; Miljkovic et al., 2011).

Options include low, medium, and high. In the low (L) degree, the rut depth measures between 6 and 12 mm. In the medium (M) severity degree, the rut depth is greater than 3 mm but less than 25 mm, while a high (h) degree of severity measures above 26 mm (ODOT 2010).

(a) Abrasive rutting (b) Structural rutting

Figure 2-7: Rutting in asphalt pavement.

To measure the depth of ruts, recording implements such as a straightedge or a profilometer may be used. Another option is using a data collection vehicle (DCV) (ODOT 2010).

If a surface rut is categorized as minor, it likely can be filled. However, ruts with a deeper profile need to be treated with an overlay on top of the affected surface. In cases of unstable asphalt, recycling is an option, whereas in cases where inconsistencies are found in the sub-grade, the best approach is either reconstruction or reclamation, both of which require extensive work (Adlinge et al., 2009).

Potholes

Potholes may be defined as localized distress that form as bowl-shaped holes that range in size. The primary location of potholes is an area of poor drainage that is characterized as having heavy slow-moving traffic. Classic examples of water-filled potholes are given in Figure 2-8 (a, b). The formation of potholes occurs when pavement depressions deteriorate over time as the result of inadequate strength in the pavement layer. Potholes may also be caused by fatigue cracking. In either of these cases, tiny pavement fragments are incrementally removed, leading to progressive distress that eventually propagates within the pavement's lower layers.

(a) (b)

Figure 2-8: Potholes in asphalt pavement.

Options include low, medium, and high. Pothole that are considered to be low (L) severity have a depth of 25 mm or less, while those considered to have medium (M) severity range in depth between (25-&50) mm. High (H) severity potholes feature depths of 50 mm or more. For each severity level (L, M and H), the potholes are counted, and the pothole area is measured in square meters. Pothole repair options include excavation, patching and/or rebuilding. The most common approach is to patch the hole on a regular basis (i.e., seasonally). Patching must be done correctly, however, or the unevenness of the road may cause further driver discomfort.

Delamination

Delamination may be defined as the removal of a portion of the asphalt surface as the result of the surface's improper bonding to the layer underneath. Delamination distress decreases the pavement's serviceability due to peeling and slipping of the layers as well as cracking in the wheel paths. Delamination primarily occurs along the shoulder or wheel path, as illustrated in Figure 2-9 (a, b, c, d). The main causes of delamination are heavy traffic loads, water percolation, and inadequate interfacial bonding of the layers. This form of pavement distress has no severity degree

measurement, as any delamination that extends to depths below the top two layers leads to surface distress in high traffic. Moreover, delamination may vary in size from a few square centimetres to dozens of square meters. Surface or sub-surface delamination is primarily measured using non-destructive test strategies, including strain gages or Ground Penetrating Radar.

Delamination is usually repaired either by placing a thin overlay of asphalt on top of the affected area, milling off the affected surface layers, or replacing the wearing course (Celaya et al., 2011).

(a)

(b)

(b)

(d)

Figure 2-3: Delamination in asphalt pavement.

For flexible pavements, Hicks (1999) provided a logical approach to determine the most effective preventive maintenance treatment for distress as shown in Table (2-2) (Miller & Bellinger, 2003) (Miller & Bellinger, 2003). Moreover, materials play a significant role in determining the life of pavements. Change of structure, chemical composition, and surface tension properties of asphalt varies with the ageing of asphalt, making the asphalt cement stiffer and more vulnerable to moisture damage. Moreover, some other significant binding characteristics include temperature susceptibility, adhesion cohesion and hardening & ageing (Miller & Bellinger, 2003).

Based on the information published by Gupta et al. (2011), IRI is typically influenced by four factors, namely: The California Bearing Ratio (CBR) of the subgrade soil, the thickness of the pavement, the traffic volume on the road, and the age of the pavement. Researchers used ANNs and MLR to develop deterioration models and observed that prediction accuracy with the regression equation was less than that with an ANNs model(Gupta et al., 2011).

2.4.1 Materials and Constructions Parameters

The material parameters needed for the design phase are divided into three fundamental classes, pavement model material inputs, material-related criteria for pavement distress, and other properties of materials. The following independent variables are considered to develop the IRI performance deterioration prediction equations:

- Age, the age is selected since it reflects the impacts of the season and the environment.
- structural number (SN) is an important Independent Variable (input variable). It represents the overall structure constructed to ensure load road carrying capacity to the frequent traffic loads over the service life. The SN considers structural parameters of layer, layer thickness and drainage parameters of the base and the sub-base.,

- Equivalent Single Axle Load.

Table 2-2: Flexible pavement distress types.

Distress Categorised	Unit	Potential causes	Severity Level		
			L	M	H
Fatigue Crack(W*P)	mm^2	Repeated traffic loading.	W≤6 P≤32.8	6≤W ≤19 32.8≤P≤150	W≥19
Block Crack	mm^2	1-Asphalt concrete shrinkage. 2-Daily temperature cycling.	W≤6	6≤W ≤12	W≥12
Longitudinal & Transverse Crack	mm	1-Asphalt concrete surface shrinkage. 2-A poor joint between pavement lanes. 3-The reflection of the joint in the underlying layer.	W≤6	6≤W ≤12	
Edge Crack	mm	1-Repeated traffic loading. 2-Frost-weakened base.		-----	
Rutting (rut depth)	mm^2	1-The inadequate thickness of the surface of the pavement. 2-Rise moisture content. 3-Poor compaction.	(6-12)	(13-25)	≥ 26
Patching	mm^2	Lack of serviceability structural capacity in the surface pavement.		------	
Potholes	mm^2	1-From a surface loss. 2-Base layer material is weak due to water leaking the pavement layer through cracks.	25	25 – 50	≥50
Ravelling	mm^2	Loss of asphalt and aggregate particles dislodging.	------		
Bleeding	mm^2	Excess bituminous material.			
Delamination	mm	1-Water leaks and heavy loads. 2-Poor interfacial bonding between various courses.	30 square centimeters to tens of square meters		

***W is width of crack. **P is cracks forming a complete pattern.**

Some sections of some years the data are not available the cumulative equivalent single axle load (ESAL) for in the LTPP database. The ESAL values for the missing data are estimated using following Equation:

$$\mathbf{ESALs_y = ESALs_{y-1} - X(1 + AARG)} \qquad \textbf{2-1}$$

Where, Y is the year of the measured or interpolated IRI and PCI, the latest ESAL value depends on calculate the ESAL of the previous year multiplied by the Average Annual Rate of Growth (AARG).

2.4.2 Environmental Parameters

The environmental effect is one of the important parameters contributing to pavement deterioration. This includes temperature, precipitation quantities and freeze-thaw cycles, temperatures in all asphalt layers, Pavement's structural performance can be gauged through observation and measurement of pavement deflection, and it has been shown that stiff asphalt layers are sometimes too brittle for winter conditions like Canada. Asphalt layers should be stiff enough to limit the permanent deformation in the summertime, but it should be flexible enough in the wintertime to the long-term performance of pavement structure was showed to strongly depend on the properties of the pavement layer(s) and the subgrade soil. There influences were especially strong in regions where there were seasonal weather fluctuations (Janno & Shepherd, 2000). Such regional changes in climatic conditions, along with variations within those regions, can make the development of prediction models extremely difficult, particularly when the models need to have a "one-size-fits-all" solution. Therefore, developing a model that is able to predict regional environmental impacts while also incorporating seasonal variabilities in pavement materials will

contribute immensely to the improvement of pavement performance. It will also reduce costs related to maintenance.

Various environmental factors have been reported in the literature as having substantial impacts on pavement performance and strength (Mrawira & Wile, 2000).

A pavement's structural performance is usually measured by pavement deflection as well as by observation. For flexible pavement, layer moduli and surface deflection can be significantly impacted by asphalt concrete temperature, along with asphalt concrete layer stiffness. The latter factor has a strong effect on the structural capacity of the pavements. Increases in temperature cause the asphalt to decrease in stiffness, leaving it vulnerable to heavy loads. Furthermore, as the asphalt concrete stiffness decreases, higher stress levels are being transmitted both to the base and the subgrade layers.

2.4.3 Traffic Volume Parameters

Traffic loading-induced fatigue is a key parameter that leads to significantly shortened pavement life. This type of fatigue results in compression that occurs at the top layer and tension on the bottom. When these stress states persist over a long period of time, the usually result in the formation of surface cracks that permit moisture to enter the pavement sub-layers (i.e., the base and sub-grade layers). Repeated traffic loading with the presence of these stresses and deteriorating conditions cause furthermore serious cracking and ultimately pavement failure. Common traffic-induced stresses are traffic volume, truck type, load application time, tire pressure, and ESAL (specifically, the number of equivalent single axle loads).

Additionally, material pavement layers employed in roadway construction are critical factors toward the future performance of the pavement. Asphalt mixes need to have appropriate blending

properties suitable for the environment to resist cracking. The aggregate used in the base and sub-base should have sufficient stiffness to avoid deformation caused by repeated traffic. These properties are obtainable when properly performed compaction processes are applied.

A crucial parameter for describing the strength of pavement is the sub-grade resilient modulus, given that the since the sub-grade forms the foundation. Hence, the use of sub-grade materials appropriate to the environmental and load conditions will likely yield pavement that is strong and enjoys a lengthy operational life. Several studies (Tarefder et al., 2008) demonstrate the connection between a suitable sub-grade and longer pavement life.

2.4.4 Additional Parameters

Additional parameters include construction quality (e.g., construction joints and roughness level); construction and design factors (e.g., surface and maintenance properties); and geometric features (e.g., drainage facilities provision, longitudinal and cross slope, and horizontal /vertical alignment, etc.). All of these parameters are well-known to affect the performance of the pavement. However, because they typically have only a slight or indirect effect, they will not be heavily weighted in the models' classification and development process.

2.5 Pavement Performance Measures

Pavement performance is defined as the ability of pavement to serve traffic over time satisfactorily serve traffic over time (AASHTO, 2003). Pavement performance measures are ratings for a pavement section representing the pavement condition and are used to help manage a pavement network.

A pavement condition index can help provide paving rehabilitation alternatives, estimate maintenance and rehabilitation costs, and track different pavement types of performance. There

are various popular types of performance systems. Still, the most popular ones and will be described in more detail are Pavement Condition Index (PCI), the International Roughness Index (IRI), and the Present Serviceability Index (PSI). The adopted condition rating generally numerically scales based on good or poor pavement results (Pavement Interactive, 2007).

2.5.1 International Roughness Index (IRI)

One of the key factors determining pavement serviceability is roughness. American society for testing and materials (ASTM E867-06) defines pavement roughness as a "deviation of a surface from the true planar surface with characteristic dimensions that affect vehicle dimensions and ride quality" (ASTM International 2012). The roughness of a pavement can be determined using the International Roughness Index (IRI), which is a measurement devised in 1982 by the International Road Roughness Experiment (IRRE) in Brazil, with sponsorship from the World Bank. The aim of the IRRE in developing the IRI was to create a stable standard that was globally recognized (Sayers 1995).

Road roughness needs to be properly measured in order to apply suitable repair and maintenance procedures. Its measurement is also important for improving traffic safety, decreasing dynamic loads on pavement structures, and enhancing ride comfort levels. As mentioned, the IRI represents a consensus model for a standard parameter which describes a vehicle's vertical movement along a road characterized as 'non-smooth'. The idea of an IRI was initially presented in a report (National Cooperative Highway Research Program), after which the World Bank solicited for researchers to devise the index on a universal scale (Gillespie et al., 1980). Today, the IRI is used the world over as a standard measurement of road roughness.

The IRI uses simulations to determine roughness responses in vehicles moving 80 km/hr. It is represented as the ratio of a quarter car model's accumulated suspension motion to the travelled distance and typically ranges in value between 1 to 5 m/km for a paved stretch of highway, with low values of IRI denoting a smooth surface. In current usage, the U.S. Federal Highway Administration classifies high-speed pavements that have IRI values exceeding 2.7 m/km as being in "poor" condition (U.S. Department of Transportation 2010). Table (2-3) presents five main pavement ride quality categories, based on the IRI's measured values as standards.

In recent research, pavement roughness has been found to be synonymous with pavement serviceability. Kavianipour et al., (2015) reported in their findings that pavement roughness significantly impacted traffic safety. The relationship between pavement distress and the IRI was also investigated in earlier studies (Perera & Kohn, 2006; Prozzi and Madanat, 2004). The findings generally show that because the IRI provides such an accurate reflection of pavement performance, changes in a pavement's life cycle essentially mirror changes in IRI levels.

Numerous factors may determine the degree of a pavement's roughness. These include climatic conditions, material properties, rehabilitation and design parameters, and traffic loading. The distress's extent and severity are also a contributing factor. Perera and Kohn (2001), when measuring roughness traits in a road's test areas, noted strong associations between environmental conditions and pavement performance. More specifically, the authors noted patterns in roughness progression occurring between distinct environmental areas that were characterized by, for instance, dry Freeze/dry no-freeze, or by wet-freeze/wet no-freeze. The patterns appeared dependent on pavement thickness in total, which included the base, sub-base and sum of the surface, as well as freezing indices, number of fines in base layers, number of wet days, and annual precipitation (Perera & Kohn, 2006).

In both Canada and the U.S., nearly all monitoring of roughness at the network level is conducted with accelerometer sensors, along with infrared, acoustic, and/or laser sensors (Ong et al., 2010). Smartphones integrate a number of sensors, such as accelerometers and Global Positioning System (GPS). Accelerometers measure accumulative vertical displacement caused by pavement roughness, while GPS sensors determine distance travelled (Zang et al., 2018). Both of these values are used in formulating the IRI. In the present study, the smartphone-based application TotalPave is employed for determining the IRI (TotalPave Inc. 2018). TotalPave streams unprocessed sensor data from the smartphone to the cloud for IRI conversion. According to the U.S. Department of Transportation, pavement ride quality based on IRI can be categorized into five groups, as shown in Table (2-3) (Islam et al., 2014).

The IRI can also be used as a statistic index for summarizing surface deviations of a single wheel track by using the quarter car system to create a profile. Figure (2-10) illustrates a quarter car comprising a sprung mass (i.e., the portion of the vehicle body with the user) and an unsprung mass (i.e., wheels and suspension). The sprung mass connects with the unsprung mass via suspension, as simulated using a spring and a damper. Another spring is used to bring the sprung mass and the real pavement into contact with each other (Arellano et al., 2006).

Table 2-3: Pavement ride quality based on roughness.

Category	**IRI Rating (m/Km), by Highway Type**		**Interstate and Noninterstate Ride Quality**
	Interstate	**Noninterstate**	
Very good	<1	<1.0	Acceptable 0–2.0
Good	1.0-1.5	1.0-1.50	
Fair	1.5-1.90	1.50-2.70	
Poor	1.9-2.70	2.70-3.50	-
Very poor	>2.70	>3.5	Less than acceptable >2.70

The quarter car system moves through the longitudinal pavement profile at 80 km/hr (~50 mph) in the simulation. As the car moves through the simulated pavement roughness, dynamic excitation occurs in the system. These create varying vertical speeds (Z_S) and accelerations (Z_U) in the sprung/unsprung masses, thus producing relative movement between the simulated vehicle's axle and chasses. The following equation can be used to calculate a given section length's IRI value (Arellano 2006):

$$\boldsymbol{IRI = \frac{1}{L}\int_0^{\frac{X}{V}} |Z_S - Z_U|\, dt} \qquad \textbf{2-2}$$

where:

IRI= International Roughness Index (mm/m or m/km), L= length of section (m)

X= longitudinal distance (m) ,V= speed of the quarter-car model (m/s) , $\frac{X}{V}$ = time it takes the model to run a certain distance x , dt= time increment , Z_S= vertical speed of the sprung mass

Z_U= vertical speed of the unsprung mass.

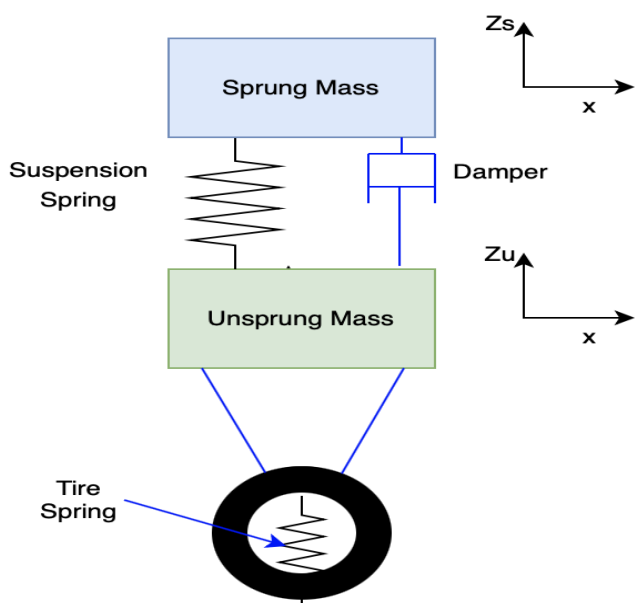

Figure 2-4: The quarter car comprising a sprung mass.

In 2002, the U.S. Federal Highway Administration (FHWA) deemed roads with an IRI of maximum 170 inches/mile to be categorized as “acceptable” with regard to roads in the national highway system (NHS) (Shahin, 1994).

A few years later, FHWA defined roads with an IRI of 95 inches/mile or less to be “good”. Nowadays, specifications to obtain an IRI are being set by ASTM International (2008) in accordance with 15 ASTM Standard E1926-08. So, for instance, the IRI of a right wheel track right international roughness index (RIRI) denotes the roughness measurement of a road surface as specified by the FHWA and in accordance with the administration’s highway performance monitoring system (HPMS).

Various researchers have investigated roughness trends over the past few decades. (Khazanovich et al. (1998) analyzed JPC (i.e., GPS-3) sections by classifying them as “good”, “normal” and “poor” according to IRI vs. time performance. In the study, a pavement section was deemed “good” under the following IRI conditions:

$$\boldsymbol{IRI < 0.631 + 0.0631 \times age} \qquad \textbf{2-3}$$

Where IRI is denoted in m/km, and age represents the age of the pavement (in years). Similarly, a pavement section was deemed “normal” under the following IRI conditions:

$$\boldsymbol{IRI > 1.263 + 0.0947 \times age} \qquad \textbf{2-4}$$

Where IRI is referenced in m/km, and age indicates the age of the pavement (in years).

Note that pavement sections were categorized as "normal" if their performance fell between "good" and the cut-off limit for "poor."

It is worth mentioning that 71% of the sections deemed "poor" Khazanovich et al.'s (1998) study were situated along wet-freeze zones, while only 24% were located in dry-freeze areas, 6% in wet

no-freeze zones and 0% were found in dry no-freeze locations. The authors also found that higher IRI values were correlated with higher numbers of freeze-thaw cycles, higher numbers of annual days below 0 °C, and higher freeze index values. They also reported that increased moisture levels that persisted over time (as determined by the annual average number of wet days) resulted in higher roughness levels. Accordingly, pavements located in more moderate climates generally showed lower IRI values.

Another important correlation reported by Khazanovich et al. (1998) was the no relationship existing between the type of sub-grade and the pavement performance. For example, around 70% of road sections that were built over sub-grade that was fine-grained gave "poor" performance measurements on the IRI. In contrast, only 33% of road sections constructed over coarse-grained soils showed poor performance. Interestingly, the authors found no trend between IRI and traffic loadings (Khazanovich et al. 1998).

Meanwhile, sections of the studied roadways that had stabilized bases (18%) showed lower levels of IRI in comparison to road sections that had granular bases (82%). In fact, the road sections that had asphalt-stabilized bases showed an IRI that was lower than every other base. In their study, Khazanovich et al. (1998) applied linear regression strategies in order to estimate the initial roughness (i.e., at the time of construction) as a means to find the rate of increase for roughness. Their calculations determined that the poorest performing road sections demonstrated higher average rates of increasing roughness compared to all other types, whereas those sections whose performance was deemed “good” demonstrated much lower rates. At the same time, poorly performing road sections consistently showed back-casted initial roughness that was much higher in comparison to sections whose performance was considered either “good” or “normal” (Khazanovich et al. 1998).

In a study done by Perera et al. (1998), the authors discovered that jointed reinforced concrete pavements (JRCP) (i.e., GPS-4) pavements with high values of IRI shared similar features, such as thicker slabs, longer joint spacing, higher portland cement concrete (PCC) modulus values, higher sub-grade moisture content, and lower water/cement ratios.

Khazanovich et al. (1998) investigated jointed reinforced concrete pavements (JRCP) sections by applying a method similar to their general pavement studies (GPS-3) section analysis approach. The authors found that JRCP built over coarse-grained soil generally gave better performance compared to JRCP built over sub-grade characterized as fine-grained (Khazanovich et al. 1998). The IRI boundary for new and rebuilt roads in Canadian provinces and several countries is presented in Table (2-4), with many national guidelines identifying different thresholds to approve new and rebuilt roads. IRI frontier values are primarily a function of:

- Functional classification of the road such as principal roads, minor roads, and highways,
- surface type (flexible pavement, rigid pavements),
- speed design of the road,
- road section length, and
- average annual daily traffic (AADT).

Generally, 4 out of 10 reported countries (Belarus, Slovakia, Spain, and Australia) represented IRI specifications as a road functional classification function. For example, Australia classified practical road levels into “highways and principal roads” based on vehicle speed (Gaspard, 2014; Múčka, 2017; Puppala & Chittoori, 2012).

Table 2-4: IRI limit specifications for reconstructed roads.

Country	Road type	Evaluation length (m)	IRI (mm/m)
Belarus	AC/PCC – new roads (highways and first-class roads)	N/A	1.5
	AC/PCC – reconstructed (highways and first-class roads) AC/PCC – Second- and third-class roads		2
	Third class roads – cold AC and crushed stone – reconstruction		2
	Fourth and fifth class roads – cold AC and crushed stone – reconstruction		2.5
Slovakia	AC/PCC – highways and expressways – acceptance	20	1.9
	AC/PCC – primary and secondary roads – acceptance	-	1.9
	AC/PCC – third class roads and local roads –acceptance	-	3.3
	Highways and expressways – during the warranty period (1–5 years)	-	2.2 -3
Spain	AC – highways (50,80, and 100) %	100	1.5, 1.8, and 2
	AC – other roads (50,80, and 100) %	100	1.5, 2, and 2.5
	AC – highways – after rehabilitation (>10 cm) (50,80, and 100) %	100	1.5, 1.8, and 2
	AC – highways – after rehabilitation (<10 cm) (50,80, and 100) %	100	1.5 ,2 and 2.5
	AC – other roads – after rehabilitation (>10 cm) (50,80, and 100) %	100	1.5 ,2 and 2.5
	AC – other roads – after rehabilitation (<10 cm) (50,80, and 100) %	10	1.5 ,2 and 2.5
	Note: IRI limits are defined as three percentiles		
Australia	AC/PCC – freeways	500	1.6
	AC/PCC-highways and main roads (<80 km/h)		1.9
	AC/PCC-highways and main roads (100 km/h)		1.9
Bosnia and Herzegovina	AC/PCC – new road – acceptance (AADT > 2000 and medium or heavy traffic loading (>80 equivalent standard axle loads (ESALs) of 82 KN/day)) (AADT < 2000 and lighter traffic loading (up to 80 ESALs of 82 KN/day)) *Limit value, **threshold value	20	2.0*, 2.6** 4.0*, 4.6**
	AC/PCC – new road – acceptance (AADT > 2000, ESAL > 80) (AADT < 2000, ESAL < 80) *Limit value, **threshold value	100	1.2*, 1.8** 3.8*, 4.6**
	AC/PCC – new road – the end of the warranty period (Five years from construction) (AADT > 2000, ESAL > 80) (AADT < 2000, ESAL < 80)	100	1.8*, 2.5** 4.5*, 4.6**

Country	Road type	Evaluation length (m)	IRI (mm/m)
Canada – Alberta	AC – Schedules I, II and III, acceptance (full pay)	100	(0.71–1.04), (0.81–1.20) and (0.81–1.54)
	AC – Schedules I, II and III, corrective work	100	1.55, 1.55 and 1.85
	AC – localised roughness	7.62	2.8
Canada – Quebec	AC – acceptance (full pay) (70%), and (100%)	100/1000	(1.2–1.3) and <1.4
	AC – rejection, remedial action is specified.		1.8
Canada – British Columbi	AC – acceptance (full pay)	100	1.1–1.2
	AC – corrective work	100	1.8
Canada – Ontario	AC – acceptance (full pay)	100	0.65–1
	AC – rejection (corrective work)	100	1.25
	AC – localised roughness	7.62	3.4
Canada – Nova Scotia	AC – Categories A, B and C, acceptance (full pay)	100	(0.8, 1) and 1.1
	AC – Categories A, B and C, optional corrective work	100	(1.8–3), (2.3–3) and (2.4–3)
	AC – Categories A, B and C, acceptance	10	(1.1, 1.4) and 1.5
	AC – Categories A, B and C, corrective work	10	3

2.5.2 Pavement Condition Index (PCI)

The PCI was developed in the 1980s to estimate a road's general condition. This index determines the condition by counting and weighing various distress types of distress based on either imagery or physical inspection data. The PCI was initially created by the U.S. Army's Engineering Corps as a means to gauge the condition of airfield pavement. Today, several transportation agencies rely solely on PCI data to make decisions around the construction, repair, and maintenance of airfields, roads and parking lots around the world. Arhin et al. (2015) investigated the similarities and differences between IRI and PCI by studying data from the U.S. and Canada.

PCI uses visual survey results (whether through imagery or field site inspections) to identify the quantity, type, and severity of the pavement distress. The field inspection method has consistently shown that PCI is good at determining the condition and integrity of the structure under study. It has also been shown to be a reliable index for gauging both current and future performance solely by considering traffic conditions, without the need for testing structural capacity, skid resistance, or roughness (Al-Suleiman & Shiyab, 2003; Shahin & Walther, 1990). In fact, PCI is currently in use globally by public and private highway agencies. In comparison to other indexes, the PCI takes into consideration every kind of distress, including quantity and severity, while also providing a good indication of a network's functional and structural conditions. For these reasons, PCI is the strategy chosen for the present work.

The program "TotalPave" was used for gathering and extracting IRI and PCI data. Test site locations comprised sections of roads from a variety of climatic regions in Canada and the United States. In Canada, the test sites were located in the provinces of Ontario, Quebec, and Prince Edward Island, while in the U.S., the sites were situated in New York, New Jersey, Virginia, Vermont, and Maryland. A simplistic model was developed for the study in order to relate the IRI method with the PCI. The formula is given in Equation (2-5) below:

$$\mathbf{Log(PCI) = 2 - 0.4361 log\ (IRI)} \qquad \textbf{2-5}$$

Optimization strategies are typically used for developing correlations. Some of these techniques include genetic programming (GP) and Artificial neural networks(ANNs), both of which may be used for evaluating PCI data in relation to other pavement indexes (except for IRI), according to the various forms of distress and their severity (Shahnazari et al. 2012). Utilizing PCI data derived from a total of 1,250 km of roadway, Shahnazari et al. (2012) devised a regression-based model that employed an ANNs framework. Then, in order to evaluate the PCI, the authors used a GP-

based root-mean-square error (RMSE) fitness function. They discovered that the field-investigated PCI values were highly similar to those generated by the GP and ANNs approaches. More specifically, in the GP-based model, RMSE and R-squared showed 1.79, 2.63 and 0.98, respectively, while in the ANNs-based models, RMSE and R-squared showed 0.99, and 0.996, respectively.

A model that was developed for use with IRI as a PCI function was employed as a way to evaluate pavement management system user benefits. In the model, the R-squared value is 0.53 with a 28% coefficient of variation. Real and predicted IRI rates are then graphically correlated in order to illustrate the data dispersion and validate the model. Equation (2-6) expressed the model (note that the IRI appears as m/km) (Arhin et al. 2015):

$$\boldsymbol{IRI = 0.017(153 - PCI)} \qquad \textbf{2-6}$$

PCI is a pavement condition number rating of 0 to 100, the worst-case rating is 0, and the best-case condition is 100, as shown in Table (2-5). (Morova et al., 2012; Salama et al., 2006).

Table 2-5: Pavement condition index (PCI).

PCI	0-10	10-25	25-40	40-55	55-70	70-85	85-100
Rating	Failed	Very poor	Poor	Fair	Good	Very good	Excellent

The method of calculation for the flexible paving PCI- system (Fwa, 2006) is as follows:

Phase 1: Assess the intensity and extent of each type of distress. The level of severity is represented by three clusters: low, medium and high. Whereas the extent is quantified by linear or square metres is measured according to the form of distress.

Phase 2: Calculate the density of pavement distress by.

Phase 2-a: Obtain distress extent is measured following equation

$$\boldsymbol{Density} = \frac{\boldsymbol{Distress\ area\ (m^2)}}{\boldsymbol{Section\ area (m^2)}} \times \mathbf{100} \qquad \textbf{2-7}$$

Phase 2-b: Calculate distress extent is measured by linear metres

$$\boldsymbol{Density} = \frac{\boldsymbol{Distress\ amount\ in\ the\ linear\ (m^2)}}{\boldsymbol{Sample\ unit\ area\ in\ (m^2)}} \times \mathbf{100} \qquad \textbf{2-8}$$

Phase 2-c: Calculate distress extent is measured by number of potholes

$$\boldsymbol{Density} = \frac{\boldsymbol{Number\ of\ potholes}}{\boldsymbol{Sample\ unit\ area\ in\ (m^2)}} \times \mathbf{100} \qquad \textbf{2-9}$$

Phase 3: Determine deduct points (DP) from standard deduct value curves for each distress type.

Phase 4: Calculate total deduct value (TDV) for all distress of each section.

Phase 5: Adjust total deduct value (TDV) by calculating corrected deduct value (CDV).

Phase 6: Compute (PCI) for each part by subtracting (CDV) from 100.

2.5.3 Present Serviceability Rating (PSR)

After the 1950s, measuring indicators such as roughness, skew and slip resistance began to appear, which could be used to measure road performance. The current level of service (PSR) is based on personal observation after creating the AASHO Road Test (AASHO 1962).

In the AASHO road test, a useful tool was devised for characterizing road surface conditions according to the driver's comfort level, namely the Pavement Serviceability Rating (PSR). To use the PSR, drivers submit their opinions based on a scale (0 to 5), with 0 indicating poor pavement conditions and 5 indicating excellent conditions. It explains the road's roughness because the PSR relies on the rider's interpretation of the ride quality. Table (2-6) presents a typical PSR rating form obtained from the AASHO road test protocol (US DOT 2000). The need for a non-board-based

system is that the PSR is a level of ride quality that requires a certain number of monitors, which is unrealistic for large networks.

Table 2-6: Present serviceability rating.

PSR	Rating	Description
4.0–5.0	Excellent	Only new (or nearly new) pavements that are smooth enough and distress free. Constructed/resurfaced during the data year.
3.0–4.0	Good	Not quite as smooth but provide a first-class ride and few visible distresses (initial signs of rutting and fine random cracks).
2.0–3.0	Fair	Riding quality is noticeably inferior and barely tolerable for high-speed traffic. Rutting, map cracking and heavy patching is seen.
1.0–2.0	Poor	Heavily damaged to affect speed of free-flow traffic. Large potholes, raveling, cracking, rutting on 50% or more of the surface.
0.0–1.0	Very poor	Extremely deteriorated condition. Pavements are passable only at reduced speed and considerable ride discomfort. Large potholes and deep cracks exist. Distresses over 75% or more of the surface.

2.6 Finding Connections Between PCI, IRI, and PSR

Several studies have investigated the possibility that specific relationships may exist between different pavement condition indexes. Initial efforts investigated connections between IRI and PSR, since both parameters provide an indication of pavement surface roughness as it potentially relates to ratings such as rideability (Al-Omari and Darter 1994). In other work, Loprencipe et al. (2017) created a regression model based on IRI and PCI. Their aim was to calculate Vehicle Operating Costs (VOC) by employing technically advanced distress evaluation strategies for airports and highways, and visual surveys for urban roadways. The researchers found that PCI correlated to other indexes that applied automated surveys in their calculations. A few of the highway agencies' jurisdictions also utilized PCI and/or IRI models, as pavement distress (PCI) had an impact on pavement smoothness (IRI). A firm correlation between IRI and PCI was found in Arhin et al.'s (2015) study conducted in urban areas. These authors used the least squares

method to predict PCI from IRI, which led to the development of statistically notable regression models.

Another group of researchers who investigated IRI and PCI as predictor variables were Park et al. (2007). These authors created a power regression model that showed a disappointing 59% efficiency. From their results, they conceded that IRI is unfeasible as a unique predictor for pavement condition ratings, A few years later, Shah et al. (2013) worked on devising the Overall Pavement Condition Index (OPCI), which included distress factors such as longitudinal cracking, transverse cracking, and alligator cracking, as well as skid resistance, structural capacity, and roughness. The latter factor was determined through ride quality rating (RQR) and IRI.

Overall, reasonably extensive research has been carried out with the goal of determining the extent of the relationship (if any) between and among various pavement performance indexes. Most of the studies, however, have been conducted in areas characterized by moderate climates. In contrast, the present work attempts to find the interrelationships of performance indexes in regions characterized by cold and harsh climatic conditions.

Finding connections between PCI and IRI

Several studies have investigated the possibility that specific relationships may exist between different pavement condition indices. Initial efforts explored connections between IRI and PCI, since both parameters indicate pavement surface roughness and pavement condition.

Dewan and Smith (2002) later found the relationship between PCI and IRI. Their proposed model resulted in the formulation:

$$\boldsymbol{PCI = 153 - (58.48 \times IRI)} \qquad \textbf{2-10}$$

The R^2value of this model was determined to be **28%**.

Another group of researchers, Park et al. (2007), investigated IRI and PCI as predictor variables. The model they proposed gave the following equation:

$$\boldsymbol{log_{PCI} = -0.115(log_{IRI}) + 2.13} \qquad \textbf{2-11}$$

The R^2value here was determined to be **59%**.

Furthermore, a strong correlation between IRI and PCI was found in a study by Arhin et al. (2015), which was conducted in urban areas. These authors used linear scheduling method (LSM) to predict PCI from IRI, which led to the development of statistically notable regression models. Three models proposed by the researchers led to the following equations:

1- Model proposed for Asphalt:

$$\boldsymbol{PCI = -0.224 \times IRI + 120.02} \qquad \textbf{2-12}$$

The R^2value of this model was determined to be **82%**.

2- Model proposed for Composite:

$$\boldsymbol{PCI = -0.203 \times IRI + 113.73} \qquad \textbf{2-13}$$

The R^2value of this model was determined to be **75%**.

3- Model proposed for Concrete:

$$\boldsymbol{PCI = -0.172 \times IRI + 111.01} \qquad \textbf{2-14}$$

The R^2value of this model was determined to be **72%.**

In another study, developed IRI regression models considering pavement age as the input parameter where describing the relationship between IRI and pavement age by deriving an exponential relationship(Psalmen Hasibuan & Sejahtera Surbakti, 2019). Equation (2-15) below presents their proposed model:

$$\text{IRI} = 16.07 \times exp^{(-0.269 * PCI)} \quad \text{2-15}$$

The R^2value of this model was determined to be **59%.**

In related work, Elhadidy et al. (2019) found that PCI correlated to other indices that applied automated surveys in their calculations. A few of the highway agencies' jurisdictions also utilized PCI and or IRI models, as pavement distress (PCI) had an impact on pavement smoothness (IRI). Their proposed model is presented in Equation (2-16) below:

$$PCI = \frac{1}{0.048} \times ln\left(\frac{79.933}{IRI} - 14.061\right) \quad \text{2-16}$$

The R^2value of this model was determined to be **93%.**

Piryonesi et al. (2019) found a low correlation between IRI and PCI values despite having a larger sample size. Their proposed model is shown in Equation (2-17) below:

$$IRI = -0.012PCI + 2.064 \quad \text{2-17}$$

The R^2value of this model was determined to be **30.2%.**

2.7 Modelling Pavement Deterioration

Effective pavement management, whether at the network or project level, requires the development of a deterioration model that is sufficiently accurate to minimize prediction errors. Thus, reducing overall costs related to maintenance. Ideally, an optimal deterioration model would incorporate contributions from variables like traffic, pavement structure, and the effects of climate and weathering on the deterioration process. At the network level, predicting deterioration of pavements enables appropriate resource allocation as well as plan prioritization, while at the project level, good prediction enables the relevant authorities overseeing the project to be informed of the best maintenance actions to take well in advance (Lytton, 1987; Prozzi and Madanat, 2004).

Considering the importance of the above, highway authorities around the world have been involved in the development of several pavement deterioration models which they apply to their respective pavement management systems. These models are invaluable because they can forecast various distress types and range from being quite simplistic and project-specific to being quite comprehensive and applicable to numerous situations across multiple projects (Lytton, 1987).

Al-Omari and Darter. (1994) developed a linear regression model between IRI and pavement rut depth. The model proposed in work led to the following equation:

$$\boldsymbol{IRI = 57.56 \times rut\ depth - 334.28} \qquad \textbf{2-17}$$

The R^2value of the model was determined to be **93%.**

Farias and Souza. (2002) also examined a linear regression model between IRI and Root Mean Square of the vertical acceleration values were determined for 1 and 3.5-meter base lengths. Their work proposed a model resulting in the equation 2-19.

$$\boldsymbol{IRI = 0.04 + 0.45 \times RMSVA1.0 + 1.66 \times RMSVA3.5} \qquad \textbf{2-18}$$

Where RMSVA: Root Mean Square of the vertical acceleration.

The R^2value of the model was determined to be **95.8%.**

In another researchers, Adams and Bahia. (2004) applied a model between IRI and asphalt concrete properties. Their a model presents in the equation 2-20.

$$\boldsymbol{IRI = 4.08 - 0.616 \times SN - 4.51 \times AC + 7.79x\ P200 \times AC - 3.78 \times P200 + 0.709 \times ESAL - 0.489 \times Thick} \qquad \textbf{2-20}$$

where AC, Asphalt Concrete, P200, the percent passing no. 200 seize,

The R^2value of the model was determined to be **71.4%.**

Garber et al. (2011) studied relationship among PCI and various parameters. Age, ADT, and Structure Number. The model shows in the equation 2-21.

$$\mathbf{PCI = 98.87 - 2.18\times age + 0.02\times ADT + 0.28\times Structure\ Number} \qquad \mathbf{2\text{-}21}$$

where ADT, average daily traffic in 1000 Vah/day.

The R^2value of the model was determined to be **97.3%**

Mahmood (2015) studied the relationship among PCI and various parameters. Cracking area, Maintenance effect Longitudinal, and ESAL. The model shows in the equation 2-22.

$$\boldsymbol{PCI = 98.86 - 0.407 \times age - 0.24 \times Cracking\ area - 0.065 \times Longitudinal + 3.404 \times Maintenance\ effect - 0.003 \times ESAL} \qquad \mathbf{2\text{-}22}$$

The R^2value of the model was determined to be **79%.**

Castelló et al. (2020) studied relationship among PCI and the influence of traffic load. Their a model presents in Equation 2-23.

$$\mathbf{PCI = 121.96 - 5.80\times age - 0.0296\times ESAL} \qquad \mathbf{2\text{-}23}$$

The R^2value of the model was determined to be **55%.**

In the same study, Castelló et al. (2020) studied the influence of the pavement structure. Their proposed model is presented in Equation (2-24) below:

$$\mathbf{PCI = 99.44 - 5.54\times age + 1.27\times Structure\ Number} \qquad \mathbf{2\text{-}24}$$

The R^2value of the model was determined to be **49%.**

Zeiada et al. (2020) investigated the impact of pavement design factors on pavement performance in hot climates. Their proposed model is presented in Equation (2-25) below:

$$\mathbf{IRI = 0.4406 \times Initial\ IRI + 0.0003 \times E - 0.0015 \times P - 0.0024 \times MAT + 0.0037 \times ARH + 0.0446 \times MAWV + 1.0688 \times ALD - 0.1555 \times SSH + 0.5318 \times AE - 0.1274 \times SCI} \quad \text{2-25}$$

where E is the evaporation, P is the precipitation, MAT is the mean annual temperature, ARH is the annual relative humidity, MAWV is the mean annual wind velocity, ALD is the average albedo, SSH is the sunshine percentage, AE is the average emissivity, and SCI is the Structural Capacity Index.

The R^2value of the model was determined to be **38%.**

2.8 Summary of Reviewed

This chapter has reviewed the literature related to PMS characterization and performance assessment using predicted-based approaches and numerical modelling. The literature review showed some of the MPS' difficulties and challenges in planning and building modern pavement. Furthermore, the standard prediction methods available are insufficient to fully understand the study of all influence variables on pavement performance networks. Developing an approach to PMS can provide an enhanced prediction modelling of pavement performance to combat one distress but ignore other distresses. Therefore, the motivation for this study was to provide different enhanced modelling approaches that help predict pavement performance in different climate conditions while working on how to determine and minimize any adverse impact on pavement performance.

Chapter3: Research Methodology

3.1 Soft Computing Techniques

In pavement engineering, the application of soft computing techniques has been growing in popularity due to the efficiency of the data storage and management, as well as the fast data processing speeds and impressive learning/adaptability of the systems. In real life, engineering decisions must be made in highly dynamic, ever-changing environments, which means that the tools used by engineers must be likewise readily adaptable to change and suitable for various levels of expertise.

In general terms, soft computing strategies are logic-based information processing tools used to solve complex problems related to performance evaluation and prediction (Chattopadhyay, 2006). The two most common soft computing approaches are Artificial Neural Networks (ANNs) and - Fuzzy Inference Systems (FIS). The present chapter provides a short overview of the main features of ANNs and FIS, showing how these techniques are beneficial to pavement engineering in relation to planning, scheduling, condition monitoring, forecasting, classification, and trend analysis.

3.2 Multiple Linear Regression

Multiple Linear Regression (MLR) is typically used to research the relationship between independent and dependent variables. The conventional regression method is a powerful and comprehensive means for evaluating relationships between independent and dependent parameters. Some regression assumptions must be considered in developing regression models. For example, Sousa et al. (2007) reported that error values are assumed to be independent across observations since collinearity between variables can lead to incorrect predictions.

Developing regression models requires some consideration of regression assumptions. According to(Sousa et al., 2007) , have been reported that predictions are inaccurate if the error values are not independent across observations due to the possibility of collinearity between variables causing incorrect predictions. A study by(Smith, 1999) found the error term distribution to be a normal distribution N (o,σ^2) and the relationship between the response variable (Y_i) and the explanatory variables to be linear. As one of the commonest and oldest of all statistical techniques, linear regression has been used extensively in research (Guisan et al., 2000). The classical linear regression model is formulated as follows:

$$\boldsymbol{Y} = \boldsymbol{\alpha} + \boldsymbol{X^T\beta} + \boldsymbol{\varepsilon} \qquad \textbf{3-1}$$

where Y stands for the dependent variable, α indicates a constant called the intercept, X = (x_1 , x_2,…, , x_n) denotes an explanatory variable vector, β = {β_1,…, β_n} expresses a regression coefficient vector (i.e., one for every explanatory variable), and ε is random measured errors and all other variations that are not explained using the linear model. Note that in calibrating regression models, the aim is minimizing unexplained variations through the use of estimation strategies like the least squares algorithm (Guisan et al. 2000). In the present work, the statistical software SPSS is employed for developing MLR models.

The R^2 value is a method used to estimate the accuracy of a model by calculating correlation between observed and predicted values. R^2values range between 0 and 1, where the closer to (1) represents that the observed and predicted values are the stronger the relationship, and 0 indicates no relationship between them. RMSE and MAE values represent used to measure the differences between observed and predicted values. Good prediction models should have a high R^2 and a low

RMSE and MAE. R^2, RMSE, and MAE values were determined using Equations (3-2) to (3-4), respectively.

$$\boldsymbol{R^2 = 1 - \frac{\sum_i (t_i - o_i)^2}{\sum_i (o_i)^2}} \qquad \textbf{3-2}$$

$$\textbf{RMSE}=\sqrt{\frac{\sum_i (t_i - o_i)^2}{n}} \qquad \textbf{3-3}$$

$$\textbf{MAE}=\frac{1}{n}\sum_i^n |t_i - o_i| \qquad \textbf{3-4}$$

o_i= actual value observation i;

t_i = predicted value of observation i

and n = number of observations.

3.3 Fuzzy logic

Zadeh (1965) proposed the fuzzy set theory in 1965. The main reason it was developed was to serve as a tool that could provide efficient solutions to complicated problems. When used in a model, fuzzy logic incorporates linguistic (qualitative) and numerical (quantitative) data. Since its introduction, fuzzy set theory has been applied to a broad range of fields, including design, scheduling, planning, decision-making, structural damage assessment, and automatic control, for disciplines as diverse as transportation, anthropology, and real estate. Figures (3-1) and (3-2) representation of a crisp of a fuzzy set.

Zadeh (1965), in developing fuzzy set theory, defined a fuzzy set as an extension of a crisp (classical) set that permits either full membership or no membership only as elements.

In a crisp set.

If x is an element of set A then $\mu_A(x) = 1$,

x is not an element of set A then $\mu_A(x) = 0$

$\mu_A(x_1) = 1, \mu_A(x_2) = 1, \mu_A(x_3) = 1,$

$\mu_A(x_4) = 0, \mu_A(x_5) = 0,$

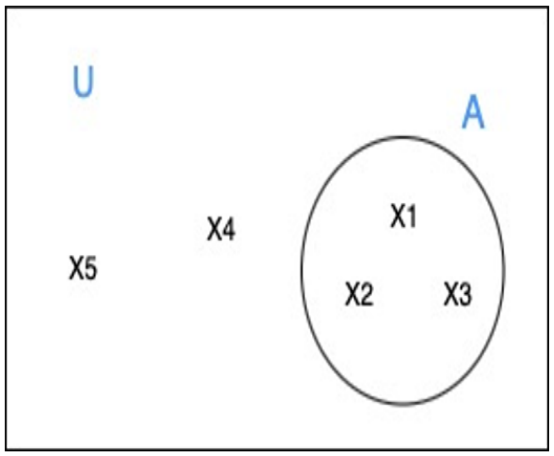

Figure 3-1: Representation of a crisp (classical) set.

Fuzzy set theory is a further extension of this concept by permitting the inclusion of partial membership in a set. Hence, according to Selvi (2009), fuzzy set *A* in a discourse universe *U* may be characterized as having a membership $\mu_A(x)$ which assumes values at an interval [0, 1]

In a fuzzy set;

$\mu_A(x_1)=1.0$

$\mu_A(x_2)=0.9$

$\mu_A(x_3)=0.6$

$\mu_A(x_4)=0.1$

$\mu_A(x_5)=0.0$

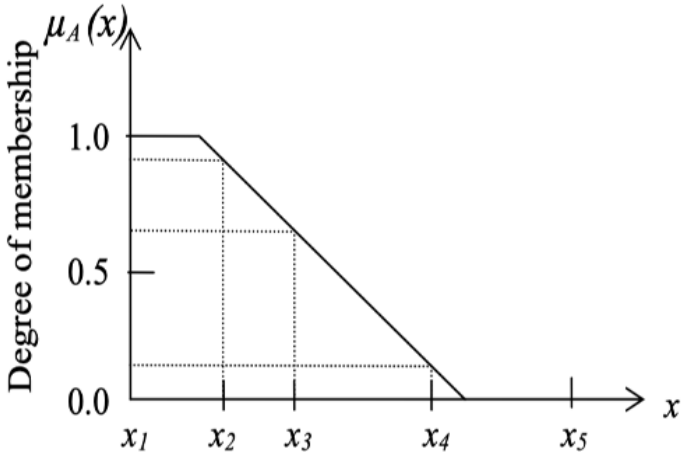

Figure 3-2: Representation of a fuzzy set.

In classical fuzzy logic theory, a challenge arises in that any object belonging in a single set may get rejected. The latter approach proposes partial belonging of an object in a variety of subsets within a universal set (Tayfur et al. 2003).

3.4 Fuzzy inference system (FIS)

The FIS considers all fuzzy rules belonging to a specified rule base and then learns to transform an input set into corresponding outputs. This process involved five distinct sub-processes, as listed below:

1. Fuzzification layer: containing the input variables.
2. Product (Rule layer): This layer composed of several fuzzy If-Then rules.
3. Normalization: In this step, control rules are combined with membership functions (MFs) to derive outputs.
4. Defuzzification: Finally, every aggregated fuzzy output set is converted to single values.
5. Overall Output layer: This layer representative the dependents variables.

Overall, fuzzification consists of two processes: the creation of MFs as input/output data, and their representation in the form of linguistic labels. Note that fuzzy sets generally provide simplistic linguistic labels (e.g., poor-good-excellent, low-medium-high, etc.). Further, fuzzy rules present as an IF-THEN sequence format as input parameters, which then proceeds to algorithms that define the output label (e.g., low-medium-high). Figure (3-3) illustrated the flowchart of the methodology used to develop a model built for pavement classification utilizing a fuzzy inference system.

3.4.1 Membership Functions Generation

In conventional mathematics, a single numerical rating might be assigned to each descriptive term. This number might represent the mean value, for example, when some range of values might all

be classified with that same number in reality. Fuzzy sets can be used to describe this uncertainty (Elton & Juang, 1988).

Tigdemir et al. three following guidelines were considered really useful in developing any fuzzy logic system (Tigdemir et al., 2002).

1. The fuzzy system operates effectively when it is possible to define the rules connecting outputs to inputs precisely.

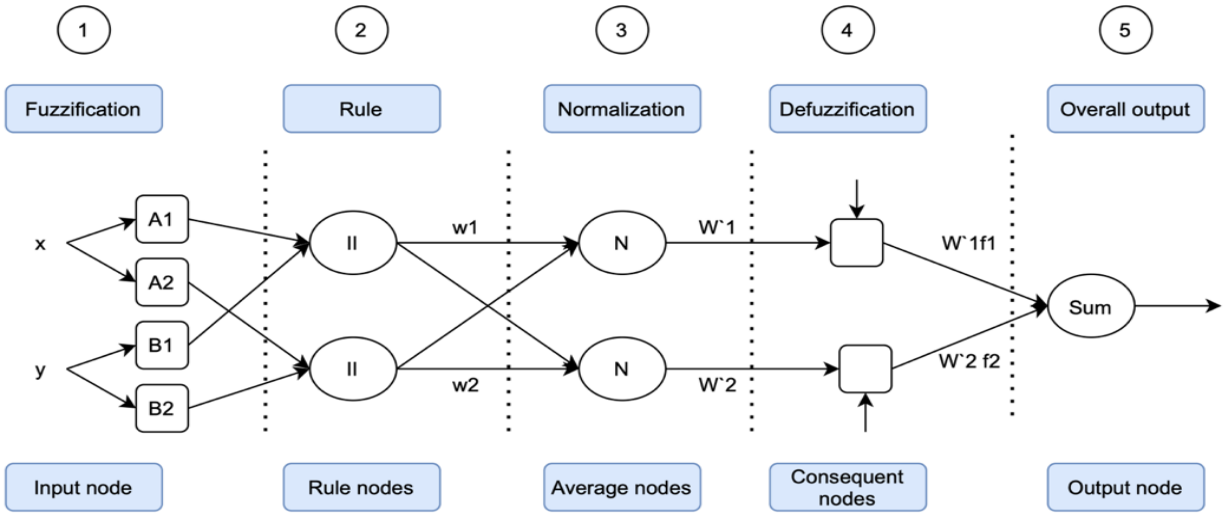

Figure 3-3: Schematic diagram of a fuzzy inference system.

2. Sets of rules can be obtained via the fuzzy inference method from operating data, but these weren't quite as strong as those extracted from specific results. Even so, they can be strengthened by providing greater weight to inputs with larger membership functions and integrating from relevant specifically from experience.

3. The system is Table. Certain rules may be left out or may contain errors without significantly sacrificing performance. When collecting pavement condition data and the international roughness index data, two forms of uncertainty are inherent in each distress's magnitude, density, and weighting factors. The level of preparation and accuracy between evaluators (Tighe et al., 2008)

affects the magnitude and density of distress data. However, can be dealt with by these complexities and contradictions associated with the subjectively evaluated. Functions are added to denote a value that would be a member of the set with a number between [0 1], reflecting its actual membership degree. Therefore, a degree of (0) indicates that the related value is not in the set, while a value of (1) is wholly representative of the set value. (Golroo & Tighe, 2009).

The simplest and sufficient function to represent severity, density, and weighting factors is Triangular Fuzzy Numbers (TFN). Equation. (3-5) to (3-9) Explain the concept of TFN:

$$\boldsymbol{\mu(x) = 0; x < l} \qquad \textbf{3-5}$$

$$\boldsymbol{\mu(x) = \frac{x-l}{m-l}; l < x < m} \qquad \textbf{3-6}$$

$$\boldsymbol{\mu(x) = 1; x = 1} \qquad \textbf{3-7}$$

$$\boldsymbol{\mu(x) = \frac{u-x}{u-m}; m < x < u} \qquad \textbf{3-8}$$

$$\boldsymbol{\mu(x) = 0; x > u} \qquad \textbf{3-9}$$

where: $\mu(x)$=Membership function, l and u =lower and upper domains, respectively., m =value which its corresponding membership measure is equal to 1.

The fuzzy method provides convenient tools to combine subjective analysis and uncertainty in international roughness index, pavement condition index, and maintenance-needs evaluation.

The two most common types of fuzzy rules are Takagi-Sugeno and Mamdani (Mehran 2008). Also known as “Sugeno”, the Takagi-Sugeno type of fuzzy rules is more widely used than the other type, as it clearly defines output in the rules as being a function of all the input variables. The Takagi-Sugeno fuzzy rules may be formulated as:

If x_1 is M_1 and x_2 is M_2 and x_3 is M_3 THEN u_1 = f (x_1 , x_2 , x_3), u_{12} = g (x_1 , x_2 , x_3) where: x_1 , x_2 , x_3 : input parameters, u_1 , u_2: Outputs, M_1, M_2 , M_3 : fuzzy sets; f (x) and g (x) indicated any type of function.

3.5 Artificial Neural Networks (ANNs)

Artificial neural networks have demonstrated their usefulness in solving complex problems quickly and efficiently. Below is a short summary of ANNs models, with information mostly obtained from the work of Gershenson (2003). Viewed from their most basic aspect, ANNs comprise inputs multiplied by weights that are representations of the relevant input's strength. Using a mathematical function, these inputs are processed to calculate a neuron's activation. An additional computational function is needed to find the artificial neuron's output(s), with the ANNs then combining the artificial neurons as a means to process information.

In this network process, weights play a pivotal role in describing the input, such that a higher weight for an artificial network indicates a more influential input. Furthermore, because weights have an integral impact on neuron computation, the weights in an ANN require adjusting to obtain the desired output. This process is relatively straight-forward with only a few neurons, but more neurons added to the mix means greater complexity in weight adjustment. To remedy this situation, algorithms are used in a process known as "training" (or "learning"). Backpropagation is frequently used for training neuron weights (Mcclelland and Rumelhart 1986). In an ANN network that is organised by layers, the process of backpropagation sends a forwarding signal, after which the error gets propagated backwards. Neurons in the input layers supply the network with inputs, while neurons in the output layers supply the ANN with outputs. Note that there is one (or more) hidden layer located between the output and input and layers.

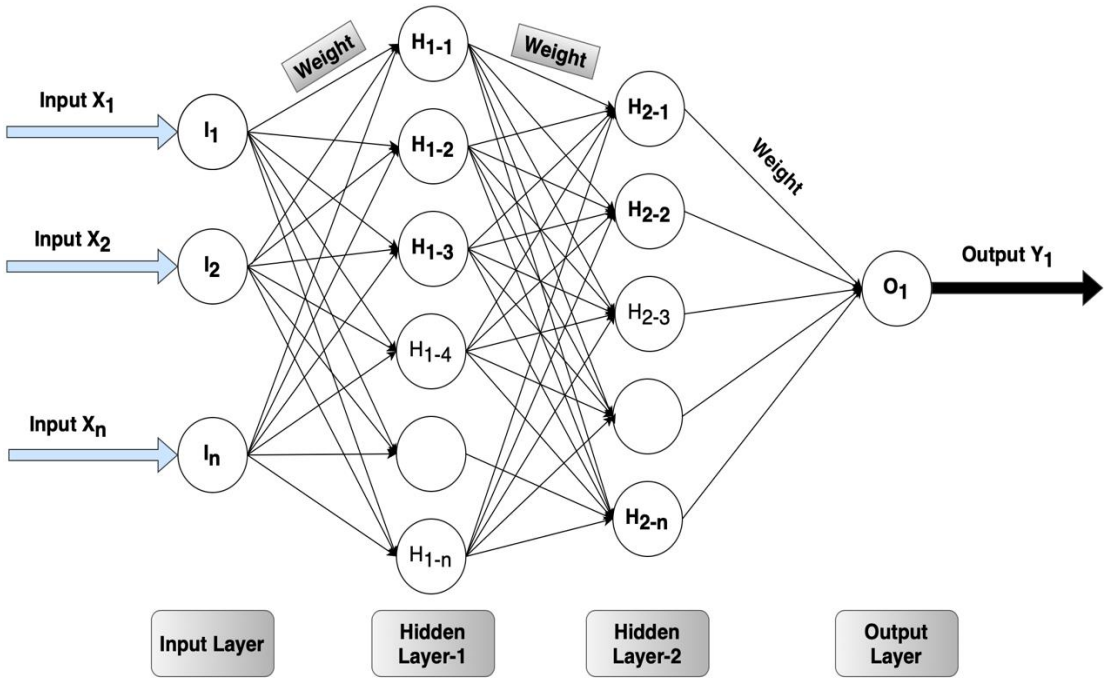

Figure 3-4: Typical structure of ANN.

Additionally, backpropagation functions through supervised learning, where the network obtains from the user examples of inputs/outputs the network should determine. Based on these provided examples, the error can be computed, i.e., the difference between predicted and real results. The whole point of backpropagation is minimizing this error while the ANN learns the training data. The process of training an ANN typically begins using random weight values, which are later these adjusted and the error subsequently reduced. In other words, ANNs are created in such a way as to learn based on supplied information (Ceylan et al. 2009; Zaman et al. 2010).

3.6 Applying ANNs and FIS to Pavement Studies

Roberts and Attoh-Okine (1998) conducted a comparison of two different ANNs models for their efficacy in predicting roughness according to traffic load and pavement condition. Their study employed 105 data points that were characterized as different kinds of variables (e.g., block

cracking, transverse cracking, fatigue cracking, rutting, equivalent axle loads, etc.). In this approach, the IRI was used as a target variable to the problem, while the rest were used as input counterparts. In total, 75 examples were extracted from the dataset for the training process and 30 were used for validation purposes.

In many transportation departments worldwide, the pavement distress evaluation method has significant problems due to subjectivity and inconsistency in pavement distress manifestations.

Develop an expert system to organize pavement distress manifestations to provide consistency to the process and minimize subjectivity (Tsao et al. 1994; Abaza et al. 2001; Labi and Shiha 2005). The expert system, which can process information in qualitative grades, e.g., minimal, moderate, etc., can be developed using fuzzy logic (Pedersen 1989; Li et al. 2005). Expert systems help nonexperts of engineers to solve or diagnose problems and learn about situations (Zimmermann., 1991).

According to Slatter (1987); Zimmermann (1991), expert systems are soft computing techniques that depend more on the heuristics of experts rather than logical problem-solving procedures and can eliminate inconsistency, reduce subjectivity, and deal with uncertainty in any decision process. Tigdemir et al. (2002) utilized fuzzy set theory to categorize pavement distress into minimal, moderate, and severe levels under uncertainty and fuzzy logic. A fuzzy logic approach can be used to define the classifiers, which are symbolic representations of distress. Mahmood (2015) applied fuzzy logic theory for PCI models for 180 and 291 sections of the measured deterioration.

A BP-based 10-5-1 multilayer perceptron (MLP) is another proposed neural net whose comparison model comprises a quadratic function ANNs. This tool utilizes both supervised and unsupervised (i.e., self-organized) learning and has feedforward functioning in its generalized adaptive architecture. Moreover, it employs an evolutionary mechanism for problem-fitting and does not

need a certain layer or node number to be specified by the modeller. The researchers demonstrated that the latter model (R^2 = 0.74) easily out performed a conventional MLP network (R^2 = 0.57) (Roberts and Attoh-Okine, 1998). A study carried out by Ghanizadeh and Fakhri (2014) presented an ANN model that aimed to predict transverse and longitudinal stresses under an asphalt layer. The data for their work came from the analysis of 5,000 flexible pavement sections; the analysis was conducted by employing the layered elastic theory, which stipulates 3,000 for training, 500 for cross-validation, and 1,500 for testing (Ghanizadeh and Fakhri 2014). The authors' levenberg–marquardt (LM) -based 7-15-4 MLP network model was then demonstrated in the study as being highly accurate (R^2=0.999) (Ghanizadeh and Fakhri 2014).

In an earlier work, Choi et al. (2004) utilized a BP-based 6-10-1 MLP network to develop an ANN that could predict IRI values. The researchers designed a series of nets in order to determine whether or not the network topology would give acceptable performance. The nets employed hidden nodes that increased 1 by 1, starting at 1 and going to 15. For the learning portion, 92 data points were used, with 25 of these being set aside to test validation. The results showed that the authors' proposed network was effective when used for purposes of predicating pavement performance (Choi et al. 2004). Within the same research field, Solhmirzaei et al. (2012) designed a model that was highly accurate in predicting pavement profiles. The authors used a BP-based x-15-4 Wavelet Neural Network (WNN) in their study, with inputs comprising vehicle acceleration on a road and outputs comprising vertical displacement profiles for the moving wheels.

In a recent study, Tigdemir (2014) presented two BP-based 7-20-1 MLP NNs with the same input variables. The author's goals were, firstly, to predict AASHTO-based design life, and secondly, to predict correlations (if any) between AASHTO-based design and real-life design, with regard to lifespan of pavement using ESAL. The study used 234 road sections overall, while the training

dataset used 164 random sections from this sample. The rest were equally divided for testing and validation. Tigdemir (2014) found that although the first model performed excellently (R^2= 0.999), the second model gave only accepTable results in the training and testing datasets (R^2 > 0.90). Even worse, significant errors occurred during validation. In the same line of research, Tigdemir (2014) presented a BP-based 7-20-2 MLP net integrating the previously mentioned output variables and retaining the same inputs. The author reported good correlations in each output variable of R^2 was 97%, and 94%. Fathi et al. (2019) predicted the alligator deterioration index (ADI) index using a hybrid car training method that combined random forests (RF) and ANN methods. Nitsche et al. (2014) attempted to predict weighted longitudinal profile (WLP) indices. Researchers were primarily interested in evaluating the effectiveness of these techniques for predicting range and standard deviation.

In another study, some researchers employed image processing techniques to characterize laboratory-made asphalt concrete samples (Nejad et al.,2015). The same research used an ANN technique to characterize laboratory-made samples asphalt concrete samples (Nejad et al.,2015). Fujita et al. (2017) applied the Support Vector Machine (SVM) technique to detect asphalt pavement cracks.

Hoang et al. (2019) investigated and identified pavement cracks using various machine learning (ML) techniques in several studies, such as support vector machine (SVM), artificial neural network (ANN), random forests (RF) mm, radial basis function neural network (RBFNN), naive Bayesian classifier (NBC), and classification tree (CT), as well as image processing techniques.

According to Karballaeezadeh et al. (2020) three techniques were used for determining structural capacity in Coatings flexible pavements: Gaussian process regression (GPR), tree and random forest. Some researchers applied ANN and SVM methods to model acoustic longevity where

maximum aggregate size, binder content, air void content, vehicle speed, and thickness were input variables (Cao et al.,2020).

Zeiada et al. (2019) applied four ML techniques (GPR, SVM, Ensemble, ANN) to simulate pavement performance in warm climates. Inkoom et al. (2019) attempted to predict highway pavement conditions using ML methodologies. They used methods such as bootstrap forest, gradient boosted trees, K nearest neighbours, Nave Bayes, and multivariable linear regression. Nabipour et al. (2019) predicted the remaining service life (RSL) of pavement using SVM and genetic expression programming (GEP) methods.

In a more recent study conducted by Leiva-Villacorta et al. (2017), ANN models were developed that were able to accurately predict pavement layer moduli. The authors generated a database by utilizing layered-elastic analysis of a multi-layered (3 layers in this case) flexible pavement structure. In all, 100,000 data points per ANN were generated. The authors then applied these results to developing a BP-based 13-20-20-3 MLP network that was subsequently demonstrated to give estimations that were highly correlated ($R^2 \geq 0.99$) (Leiva-Villacorta et al., 2017).

In related work, Ziari et al. (2015) proposed developing an ANN that could predict IRI values for flexible pavements both over the long and short terms. The authors employed sensitivity analysis utilizing a range of LM-based MLP networks and parameterizing the hidden layer number (1 - 3) and nodes (3-100) as a means to determine the optimal model for their purposes. The learning databank had 205 data points; of these, 154 were used for training, 41 for validation, and 10 for testing. Based on their findings, the authors were satisfied that the ANN models could predict future pavement conditions with satisfactory accuracy both for the short and long terms. The best short-term performance was yielded in the topology 9-80-50-30-1, while for structure, the topology 9-3-1 gave the best performance. For long-term performance, the 9-8-1 layout resulted

in the best performance, while for the testing sets, the layouts 9-5-1, 9-7-1, 9-20-1 and 950-1 yielded mean absolute percentage error (MAPE) < 10% and R^2 > 0.9 (Ziari et al., 2015).

Meanwhile, Zofka and Yut (2012) considered whether it would be feasible to use three ANNs in predicting the compliance of hot mix asphalt creep in relation to the compliance of binder creep, and vice-versa. The network dataset for the three ANNs had 594, 594, and 600 points each. These were randomly separated into subsets designated for training (60%), validation (20%) and testing (20%). The authors' proposed nets comprised BP-based 11-20-6, 15-20-6 and 12-20-6 MLPs. According to the study results, extremely high correlation (~98%) was shown in comparison to the targeted counterpart (Zofka and Yut., 2012).

Yousefzadeh et al. (2010) proposed an LM-based X-6-6-4 RNN (input node number unclear) to predict pavement profiles for four vehicle wheels, i.e., four outputs. Both the profiles themselves and the vehicle acceleration were used as inputs for network feedback. The results indicated reasonably good estimation of pavement profiles by the ANNs (Yousefzadeh et al., 2010). A similar study (Ngwangwa et al., 2014) also investigated ANNs-based predictions for road profiles. The authors created an LM-based 3-50-50-2 MLP network that was trained using around 4,000 data points, with validation conducted utilizing measured data. The authors' results indicated correlations they described as very good, including for discrete obstacles (Ngwangwa et al. 2014).

In a study conducted by Singh et al. (2013), the authors used an ANN to predict asphalt mixture dynamic modulus according to aggregate parameter shape. An automated aggregate image measurement system was employed to determine the shape parameters (e.g., sphericity, texture, angularity, etc.) of the fine and coarse aggregates. A 4-layer feedforward neural network was for model construction and a backpropagation algorithm was employed for data training. The input variables for the shape parameters were air voids, asphalt viscosity, and loading frequency (Singh

et al., 2013). Mirzahosseini et al. (2013) looked at the feasibility of applying ANNs models for predicting rutting performance in dense asphalt mixtures. Six input parameters were used by the authors in the proposed network, namely filler, air voids, bitumen, viscosity modifying admixture (VMA), coarse aggregate percentage, and Marshall Quotient. Additionally, statistical measures were employed as a means for evaluating the predictive tool's efficiency. The authors reported that the ANN-based model gave excellent performance in predicting asphalt mixture flow number, which is defined as a measure for repeated load deformation (Mirzahosseini et al., 2013).

ANN was also used in a study by Shafabakhsh et al. (2015) to predict deformation in asphalt concrete mixtures that had been modified using nano-additives, giving good results (Shafabakhsh et al., 2015). Other researchers investigated the predictive quality of ANN in Marshall tests on dense bituminous mixtures that were polypropylene-modified (Tapkin et al., 2010).

3.7 Research Plan

Based on this research's literature review and objectives, there is a clear need to analyze an extensive data set and a series of tasks designed for various road sections in the U.S. and Canada. The present study considers three different key parameters, as follows:

- Pavement distresses (performance parameters).
- Environmental parameters.
- Traffic volume parameters.

The primary purpose of this research was to introduce a practical approach for the Modeling asphalt pavement performance indices (PCI and IRI) under different climate regions and different parameters. In this study were used three different techniques were (FIS), (MLR), and (ANNs). The research methodology is illustrated in Figure (3-5). The research plan includes seven principal areas as follows:

- Data aggregation of study,
- Modeling of asphalt pavement performance indices using (FIS),
- Modeling the relationship between asphalt pavement performance indices (PCI&IRI),
- Modeling of asphalt pavement performance indices using (MLR),
- Modeling of pavement performance indices using (ANNs),
- Comparison and validation between (MLR) and (ANNs) models, and
- Case study.

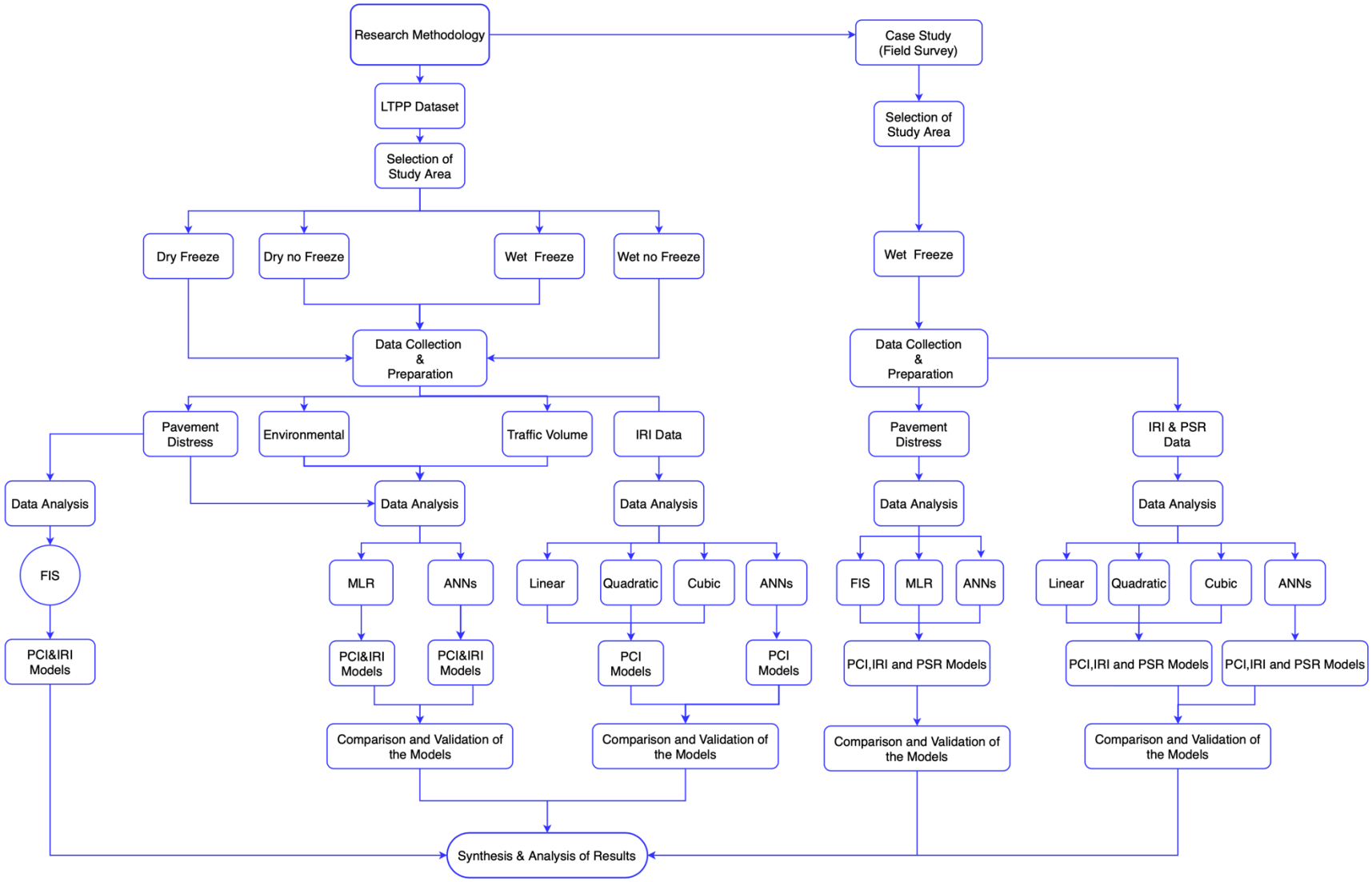

Figure 3-5: Schematic diagram of research methodology.

3.8 Data Aggregation of Study

Data are the basis for establishing stable predictive models, so obtaining correct and high-quality data is important. Two data resources were used for this study as follows:

- The Long-Term Pavement Performance (LTPP) dataset.
- The Field Survey of the city St. John's -Newfoundland- Canada.

The Long-Term Pavement Performance (LTPP) program is a significant resource for data collection about pavement conditions. The data include four climatic zones in the U.S. and Canada. The study considers three key parameters: pavement distress, environmental, and traffic volume parameters. The preprocessing of data is essential to provide homogeneity to the data, improve the networks' output, and improve the predictive models. Figure 3-6 shows the LTPP climatic regions (FHWA2014).

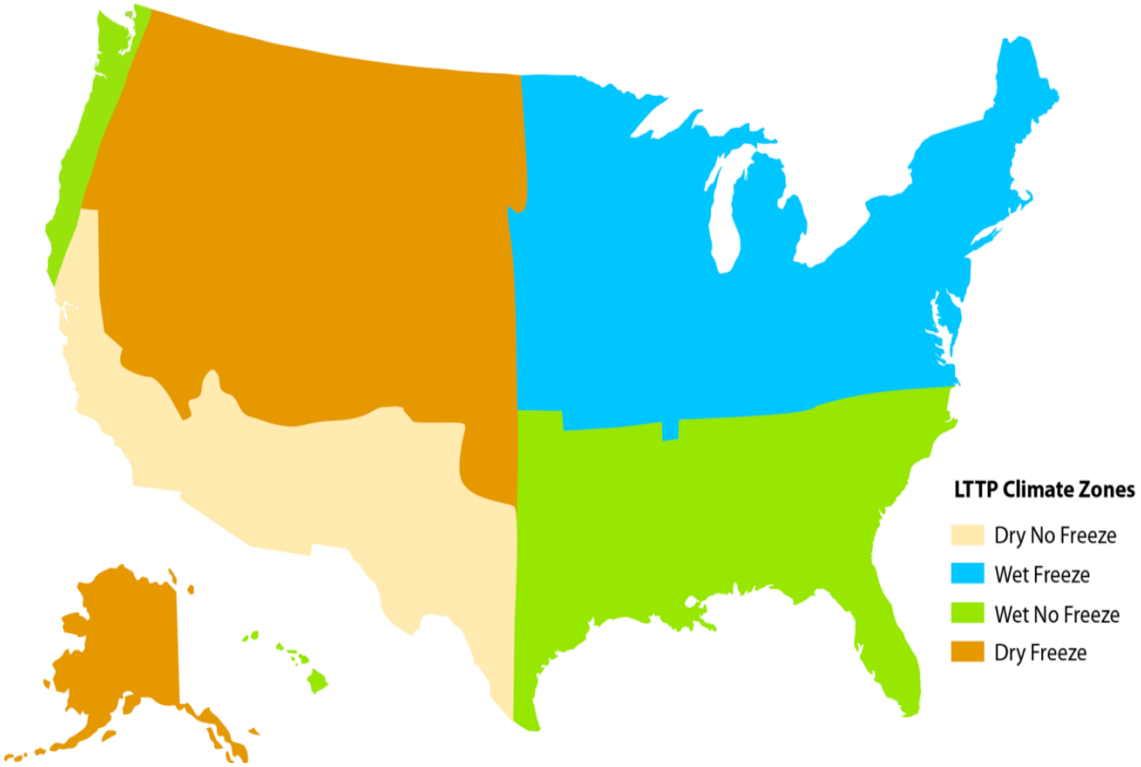

Figure3-6: LTPP climatic regions.

3.9 Modeling of Asphalt Pavement Performance Indices

This study utilized three techniques to achieve its primary goals: Multiple Linear Regression (MLR), Fuzzy Inference System (FIS), and Artificial Neural Networks (ANNs).These techniques were used to build models of asphalt pavement to predict the asphalt pavement performance and evaluate the level of their applicability to the performance models available.

3.10 Modeling of Asphalt Pavement Performance Indices Using (FIS)

The LTPP was selected as the data source for constructing a fuzzy rule-based system for pavement section classification. Nine distress types were input parameters (Rutting, fatigue cracking, block cracking, longitudinal cracking, transverse cracking, patching, potholes, bleeding, and ravelling). Each distress type was represented by three triangular membership functions representing its severity level (Minimal, Moderate, and Severe), creating seven membership functions of output PCI and five triangular membership functions of output IRI.

3.11 Modeling of Asphalt Pavement Performance Indices Using (MLR)

This study used the statistical computer software SPSS 27 to regression analysis to predict the value of pavement performance from data collected from the LTPP data. Equations (3-10) to (3-12) showed basic formulations equations of the prediction models to find the correlation between PCI and IRI. Equations (3-13) to (3-18) presented the prediction models' basic formulations to discover the influence of pavement distress, environmental data, and traffic parameters on PCI and IRI values.

$$\mathbf{PCI}=\boldsymbol{C}+\boldsymbol{a_1}\times(\boldsymbol{IRI}) \qquad \textbf{3-10}$$

$$\mathbf{PCI}=\boldsymbol{C}+\boldsymbol{a_1}\times(\boldsymbol{IRI})+\boldsymbol{a_2}\times(\boldsymbol{IRI})^{\mathbf{2}} \qquad \textbf{3-11}$$

$$\text{PCI}=C + a_1 \times (IRI) + a_2 \times (IRI)^2 + a_3 \times (IRI)^3 \quad \text{3-12}$$

$$\text{PCI}=C + a_1X_{age} + a_2X_1 + a_3X_2 + a_4X_3 + a_5X_4 + a_6X_5 + a_7X_6 + a_8X_7 + a_9X_8 + a_{10}X_9 + a_{11}X_{10} \quad \text{3-13}$$

$$\text{IRI}=C + a_1X_{age} + a_2X_1 + a_3X_2 + a_4X_3 + a_5X_4 + a_6X_5 + a_7X_6 + a_8X_7 + a_9X_8 + a_{10}X_9 + a_{11}X_{10} \quad \text{3-14}$$

$$\text{PCI}=C + a_1X_{age} + a_2\mathcal{W}_1 + a_3\mathcal{W}_2 + a_4\mathcal{W}_3 + a_5\mathcal{W}_4 + a_6\mathcal{W}_5 + a_7\mathcal{W}_6 + a_8\mathcal{W}_7 \quad \text{3-15}$$

$$\text{IRI}=C + a_1X_{age} + a_2\mathcal{W}_1 + a_3\mathcal{W}_2 + a_4\mathcal{W}_3 + a_5\mathcal{W}_4 + a_6\mathcal{W}_5 + a_7\mathcal{W}_6 + a_8\mathcal{W}_7 \quad \text{3-16}$$

$$\text{PCI}=C + a_1X_{age} + a_2X_{ESAL} + a_3X_{AADTT} + a_4X_{ADTT} \quad \text{3-17}$$

$$\text{IRI}=C + a_1X_{age} + a_2X_{ESAL} + a_3X_{AADTT} + a_4X_{ADTT} \quad \text{3-18}$$

where PCI = Pavement Condition Index, IRI = International Roughness Index, C= Constant, $\mathbf{X}_{age}$ = Age of pavement, $\mathbf{X}_1$ =Rutting, $\mathbf{X}_2$ = Fatigue Cracking, $\mathbf{X}_3$ = Block Cracking, $\mathbf{X}_4$ = Longitudinal Cracking, $\mathbf{X}_5$ = Transverse Cracking, $\mathbf{X}_6$ = Patching, $\mathbf{X}_7$ = Potholes, $\mathbf{X}_8$ = Bleeding, $\mathbf{X}_9$ = Ravelling, $\mathbf{X}_{10}$ = Delamination, $\mathbf{X}_{ESAL}$ = Annual ESAL, $\mathbf{X}_{AADTT}$ = Annual average daily truck traffic Trucks, $\mathbf{X}_{AADT}$ = Annual average truck traffic, $\mathcal{W}_1$ = Temperature average, $\mathcal{W}_2$ = Freeze index year, $\mathcal{W}_3$ = Number of freeze days, $\mathcal{W}_4$ = Total precip, $\mathcal{W}_5$ = Total snowfall year, $\mathcal{W}_6$ = Wind average, $\mathcal{W}_7$ = Humidity, $a_1, a_2, a_3 \ldots\ldots\ldots\ldots a_{11}$ = Coefficients.

3.12 Modeling of Asphalt Pavement Performance Indices Using (ANNs)

Artificial neural networks were applied to train and test data to create models in various fields. In the present thesis, ANNs have been used to address regression modelling limitations. This study's techniques to predict pavement performance were based on ANNs methods. These numerical analysis provide a possible explanation for the underlying correlation between the independent and dependent parameters identified as relevant for evaluating pavement performance. Moreover, ANNs work to demonstrate each variable's influence on pavement performance and the influence of interactions of the variables.

The backpropagation method is a well-known supervised learning algorithm used for training and adjusting the artificial network by reducing the error between the network's performance and that of the target output. The network training process begins with a random number of weights and biases, after which inputs are introduced to the system. The error is then measured as the difference between the network output and output values propagated backwards over the artificial neural network. The weights of each layer are adjusted to reduce errors during the next round. This operation continues until a minimum error is reached. The present study divides the data into three phases, giving 70% of the data for training, 15% for testing, and 15% for validation.

The network outputs PCI and IRI can be calculated using Equations (3-19) and (3-20). A hyperbolic tangent sigmoid transfer function (tansig) is applied as a transfer function for the hidden and output layers. This method is one of the best ways to simulate an ANNs. Figure (3-7) presented an architecture of an ANNs processing of the backpropagation algorithm (Svozil et al. 1997).

$$\text{IRI=PCI}=\boldsymbol{f}\circ\{\boldsymbol{O_O}+\sum_{i=1}^{n}\boldsymbol{W_i}\,\boldsymbol{f_h}[\boldsymbol{H_l}+\sum_{k=1}^{z}\boldsymbol{W_{kl}}\,\boldsymbol{f_h}\,][\boldsymbol{H_k}+\sum_{j=1}^{s}\boldsymbol{W_{jk}}\,\boldsymbol{f_h}(\,\boldsymbol{H_j}+\sum_{i=1}^{v}\boldsymbol{W_{ij}}\,\boldsymbol{I_i})]\} \quad \textbf{3-19}$$

$$f_{o,h}(T) = \frac{2}{1+e^{-2T}} - 1 \qquad \textbf{3-20}$$

where , O_O = bias for the output layer, l= subscript for hidden layer 3, k = subscript for hidden layer 2,

j = subscript for hidden layer 1, i = subscript for the input layer, n = number of nodes in hidden layer 3, z = number of nodes in hidden layer 2, s = number of nodes in hidden layer 1,

v = number of nodes in the input layer, W_l = weight factors for the output layer (size: 1 × z),

W_{kl} = weight factors for hidden layer 3 (size: n × z), W_{jk} = weight factors for hidden layer 2 (size: k ×j), W_{ij} = weight factors for hidden layer 1 (size: j ×i), H_l = bias for hidden layer 3 (size: n × 1), H_k = bias for hidden layer 2 (size: z × 1), H_j = bias for hidden layer 1 (size: s × 1), f_o = transfer function for the output layer, f_h = transfer function for the hidden layers.

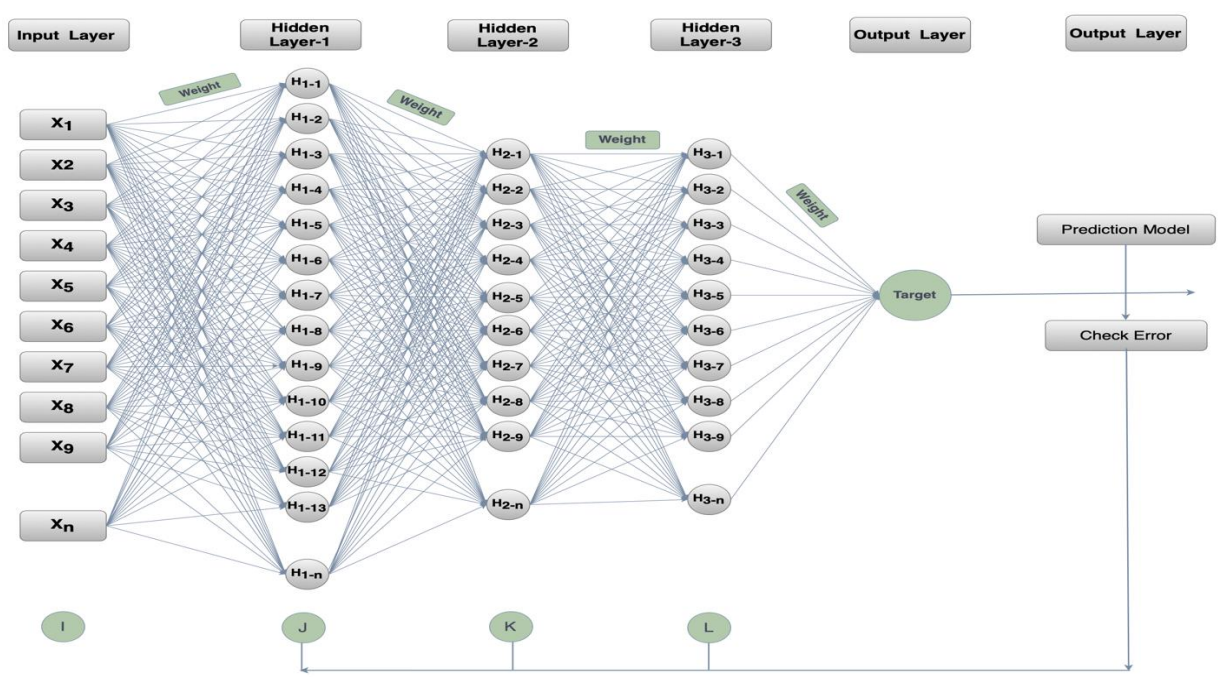

Figure 3-7: Architecture of (ANN) processing of backpropagation algorithm.

3.13 Comparison and validation between (MLR) and (ANNs) models

The performance of the MLR models was compared with the performance of the ANNs models to evaluate the accuracy of the models in predicting pavement performance based on pavement distress parameters. R^2, RMSE and MAE values were used to measure and compare the performance of the models.

3.14 Case study

The case study focuses on studying the effect of pavement distress on determining pavement conditions. St. John's, the capital of Newfoundland and Labrador-Canada, is the case study's site. This study includes the determination of PCI, IRI, and PSR of flexible pavement and developing reliable prediction models for St. John's roads.

Chapter4: Modeling of Asphalt Pavement Performance Indices Using (FIS)

4.1 Introduction

This chapter's main objectives are to present a classification for flexible pavement based on severity and density distress. The research study presented two indices for predictions of the distress values: The Fuzzy Pavement Condition Index (FPCI) and the Fuzzy International Roughness Index (FIRI). These two measurements offer quantitative indicators for the entire pavement network to assess pavement segment degradation. Mahmood (2015) utilized fuzzy logic theory for PCI models for 180 and 291 sections of the measured deterioration.

4.2 Methodology and Data Collection

This study selected (120) and (150) test sections from the LTPP dataset to create the fuzzy rules. These sections have nine distress types (rutting, fatigue cracking, block cracking, longitudinal cracking, transverse cracking, patching, potholes, bleeding, and ravelling). Each severity level (Minimal, Moderate, and Severe) was extracted and calculated. Table (4-1) presents the descriptive statistics for 120 and 150 sections of the measured deterioration.

The system was evaluated for two datasets sections (120) and (150). This technique creates membership functions and rules by measuring fuzzy pavement classification efficiency. The coefficients of determination (R^2), (RMSE), and (MAE) were used as the performance indicator metrics in the evaluation of the performance (FPCI &IRI) of analytical models and the comparison among four methods, Centroid, Bisector, Som, and Lom. Figure (4-1) showed that Structure of fuzzy logic approach of PCI and IRI.

Table 4-1: Descriptive statistics for 120 and 150 sections of the measured deterioration.

Parameters	Min Statistic	Maxi Statistic	Mean Statistic	Mean Std. Error	Std Statistic
PCI	5.00	100.00	59.07	2.78	32.34
IRI	0.74	4.04	1.54	0.06	0.72
Age	4.00	23.00	13.01	0.40	4.60
Rutting	0.0	135.9	23.6	3.1	37.7
Fatigue Cracking	0.00	377.90	38.59	6.58	76.48
Block Cracking	0.00	557.60	5.80	4.30	50.01
Longitudinal	0.00	325.60	66.88	7.77	90.29
Transverse	0.00	192.30	30.63	3.74	43.50
Patching	0.00	45.80	1.52	0.67	7.73
Potholes	0.00	0.00	0.00	0.00	0.00
Bleeding	0.00	350.80	18.95	6.12	70.32
Ravelling	0.00	564.30	44.98	10.62	122.05

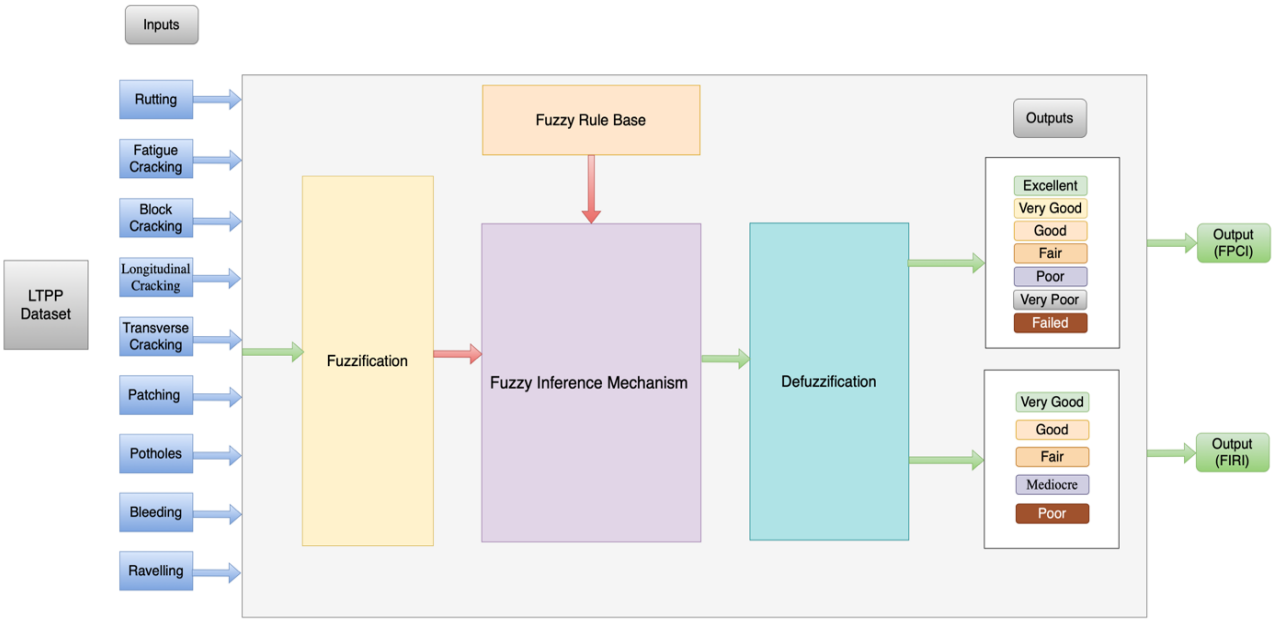

Figure 4-1: Structure of fuzzy logic approach of PCI and IRI.

4.3 Fuzzy Inference System

4.3.1 Model Formulation and Fuzzy Rule-Based System

The research study presents two models estimating the Fuzzy Pavement Condition Index (FPCI) and Fuzzy International Roughness Index (FIRI). A pavement classification system was built by considering the density of Rutting, fatigue cracking, block cracking, longitudinal cracking, transverse cracking, patching, potholes, bleeding, and ravelling as inputs. These models were created using MATLAB 2020b.

4.4 Constructing the Fuzzy Logic Model

4.4.1 Data Pre-Processing and Feature Selection

The fuzzy model used nine independent variables as inputs and one dependent variable as output (FPCI or FIRI). After extracting and revising data from the LTPP data set, the fuzzy model was prepared with nine independent parameters of distress types. Triangular membership function (time) was selected to fuzzy the crisp values of inputs variables, and various numbers of memberships functions (MF) were specified for each input and output variable. Distress types and the number of membership functions to evaluate PCI and IRI are described in Table (4-2).

4.4.2 Membership Function

In evaluating the pavement distress performance using fuzzy logic, the membership functions for input variables of distress severity levels were classified into three classes: minimal, moderate, and severe. The output variables have seven PCI membership functions classified as: Failed, Very Poor, Poor, Fair, Good, Very Good, and Excellent. Similarly, the output variables have five IRI membership functions classified as: Poor, Mediocre, Fair, Good. and Very Good (ASTM International D6433-18). In this technique, for each input and output (FPCI and FIRI).

Table 4-2: Distress types and number of membership functions to evaluate PCI and IRI.

Distress of type	Category	Number of MF	Description
Rutting	Input	3	Extremely important
Fatigue Cracking	Input	3	Relatively important
Block Cracking	Input	3	Relatively important
Longitudinal Cracking	Input	3	Important
Transverse Cracking	Input	3	Important
Patching	Input	3	Moderately important
Potholes	Input	3	Moderately important
Ravelling	Input	3	Relatively important
Bleeding	Input	3	Relatively important
PCI	Output	7	Extremely important
IRI	Output	5	Extremely important

4.4.3 Fuzzy Rule Generation

Generating the rules is the second phase of this approach. Tables (4-3) and (4-4) present rules generation FIS for FPCI and FIRI, respectively.

4.4.4 Defuzzification methods

This study used four deduzzification methods :

1- Centroid method

Sugeno (1985) developed this widely used technique. A centroid defuzzification method can be expressed as follows:

$$\boldsymbol{Z_C = \frac{\int \mu_A(Z) Z dx}{\int \mu_A(Z) dx}} \qquad \textbf{4-1}$$

Where Z_C is the crisp output, $\mu_A(Z)$ is the aggregated membership function and z is the output variable.

2- Bisector Method

Essentially, a bisector is a vertical line dividing an area into two equal zone subregions. Sometimes it coincides with the centroid line, but not always. A bisector defuzzification method can be expressed as follows:

$$\boldsymbol{Z_B = \int_{Z_B}^{\beta} \mu_A(Z) dx} \qquad \textbf{4-2}$$

where Z_B is the crisp output.

3- Largest of Maximum

Largest of maximum takes the largest amongst all z that belong to $[Z_1, Z_2]$ as the crisp value called Z_{Lom} .

4- Smallest of Maximum

This selects the smallest output with the maximum membership function as the crisp value Z_{Som}. In other words, in Smallest of Maximum chooses the smallest among all z that belong to $[Z_1, Z_2]$.

Table 4-3: Fuzzy rules for PCI.

Rule No	Distress type (Input)									FPCI (Output)
	Rutting	**Fatigue Cracking**	**Block Cracking**	**Longitudinal Cracking**	**Transverse Cracking**	**Patching**	**Potholes**	**Bleeding**	**Ravelling**	
1	Minimal	Minimal	Minimal	Minimal	Minimal	Minimal	Minimal	Minimal	Minimal	Excellent
2	Minimal	Minimal	Minimal	Moderate	Minimal	Minimal	Minimal	Minimal	Minimal	Excellent
3	Minimal	Minimal	Minimal	Severe	Minimal	Minimal	Minimal	Minimal	Moderate	Very Good
4	Minimal	Minimal	Minimal	Minimal	Severe	Minimal	Minimal	Minimal	Minimal	Good
5	Minimal	Severe	Minimal	Moderate	Minimal	Minimal	Minimal	Minimal	Minimal	Good
6	Minimal	Moderate	Minimal	Minimal	Severe	Minimal	Minimal	Minimal	Minimal	Good
7	Minimal	Moderate	Minimal	Minimal	Minimal	Minimal	Minimal	Minimal	Minimal	Good
8	Minimal	Minimal	Minimal	Minimal	Minimal	Minimal	Minimal	Minimal	Moderate	Good
9	Minimal	Moderate	Minimal	Moderate	Severe	Minimal	Minimal	Moderate	Minimal	Good
10	Minimal	Moderate	Minimal	Moderate	Minimal	Minimal	Minimal	Minimal	Severe	Fair
11	Minimal	Minimal	Minimal	Moderate	Moderate	Minimal	Minimal	Minimal	Minimal	Fair
12	Moderate	Severe	Minimal	Minimal	Minimal	Minimal	Minimal	Moderate	Minimal	Fair
13	Moderate	Minimal	Minimal	Minimal	Minimal	Minimal	Minimal	Minimal	Severe	Poor
14	Minimal	Severe	Minimal	Minimal	Moderate	Minimal	Minimal	Minimal	Minimal	Poor
15	Moderate	Moderate	Minimal	Minimal	Minimal	Moderate	Minimal	Minimal	Minimal	Poor
16	Minimal	Minimal	Minimal	Moderate	Severe	Minimal	Minimal	Minimal	Minimal	Poor
17	Minimal	Minimal	Minimal	Moderate	Moderate	Minimal	Minimal	Minimal	Minimal	Very Poor
18	Moderate	Moderate	Minimal	Minimal	Moderate	Minimal	Minimal	Moderate	Minimal	Very Poor
19	Moderate	Moderate	Minimal	Moderate	Severe	Minimal	Minimal	Moderate	Moderate	Very Poor
20	Minimal	Minimal	Minimal	Minimal	Moderate	Minimal	Minimal	Minimal	Severe	Very Poor
21	Minimal	Severe	Minimal	Severe	Severe	Minimal	Minimal	Moderate	Minimal	Very Poor
22	Moderate	Moderate	Minimal	Moderate	Moderate	Minimal	Minimal	Minimal	Moderate	Very Poor
23	Minimal	Minimal	Minimal	Severe	Severe	Minimal	Minimal	Minimal	Minimal	Very Poor
24	Minimal	Moderate	Minimal	Minimal	Moderate	Minimal	Minimal	Minimal	Minimal	Failed
25	Moderate	Severe	Minimal	Moderate	Severe	Minimal	Minimal	Minimal	Minimal	Failed
26	Severe	Moderate	Minimal	Moderate	Severe	Minimal	Minimal	Minimal	Minimal	Failed
27	Severe	Severe	Minimal	Moderate	Moderate	Minimal	Minimal	Moderate	Minimal	Failed

Table 4-4: Fuzzy rules for IRI.

Rule No	Distress type (Input)									FIRI (Output)
	Rutting	**Fatigue Cracking**	**Block Cracking**	**Longitudinal Cracking**	**Transverse Cracking**	**Patching**	**Potholes**	**Bleeding**	**Ravelling**	
1	Minimal	Minimal	Minimal	Minimal	Minimal	Minimal	Minimal	Minimal	Minimal	Very Good
2	Minimal	Minimal	Minimal	Minimal	Severe	Minimal	Minimal	Minimal	Minimal	Very Good
3	Minimal	Minimal	Minimal	Minimal	Moderate	Minimal	Minimal	Minimal	Minimal	Very Good
4	Moderate	Moderate	Minimal	Minimal	Minimal	Minimal	Minimal	Minimal	Minimal	Good
5	Minimal	Minimal	Minimal	Minimal	Moderate	Minimal	Minimal	Moderate	Minimal	Good
6	Moderate	Moderate	Minimal	Moderate	Minimal	Minimal	Minimal	Minimal	Moderate	Fair
7	Minimal	Moderate	Minimal	Moderate	Minimal	Minimal	Minimal	Minimal	Severe	Fair
8	Minimal	Minimal	Minimal	Severe	Moderate	Minimal	Minimal	Minimal	Minimal	Fair
9	Moderate	Moderate	Minimal	Moderate	Moderate	Minimal	Minimal	Minimal	Minimal	Mediocre
10	Minimal	Minimal	Minimal	Severe	Minimal	Minimal	Minimal	Minimal	Moderate	Mediocre
11	Minimal	Minimal	Minimal	Severe	Minimal	Minimal	Minimal	Minimal	Minimal	Mediocre
12	Severe	Severe	Minimal	Minimal	Moderate	Minimal	Minimal	Minimal	Minimal	Poor
13	Severe	Moderate	Minimal	Severe	Moderate	Minimal	Minimal	Moderate	Minimal	Poor
14	Severe	Severe	Minimal	Severe	Severe	Minimal	Minimal	Moderate	Minimal	Poor
15	Severe	Severe	Minimal	Severe	Severe	Minimal	Minimal	Moderate	Minimal	Poor

4.5 The Results of Pavement Section Classification

4.5.1 Fuzzy Pavement Condition Index (PCI)

Table (4-5) displays the level of agreement of the (FPCI) values for 120 and 150 sections, respectively. The performance was evaluated by the (R^2) (RMSE) and (MAE) for FPCI. Comparison of the goodness of fit statistics of the 120 sections versus the 150 sections in Table (4-5) provides the following conclusions:

- **Centroid method**: The results indicated that the R^2, RMSE, and MAE values were Improvements; the improvement values were 1.03%, 6.12%, and 8.10%, respectively.

- **Bisector method**: The results indicated that the R^2, RMSE, and MAE values were improvements; the Improvement values were 0.62%, 7.01%, and 0.372%, respectively

Table 4-5: Assessment various fuzzy inference systems' configurations for FPCI.

Inference	**Number of sections**	**Defuzzification**	**Statistical Error Measures (PCI)**			**Improvement (%)**		
			R^2	**RMSE**	**MAE**	R^2	**RMSE**	**MAE**
Mamdani (Triangular)	**120**	Centroid	97.3*	5.28*	4.617*	-	-	-
		Bisector	96.3	5.916	5.367	-	-	-
		Lom	95.4	8.096	6.185	-	-	-
		Som	95.8	6.696	5.567	-	-	-
	150	Centroid	98.3*	4.957*	4.243*	+1.03	+6.12	+8.10
		Bisector	96.9	5.499	5.347	+0.62	+7.01	+0.372
		Lom	98.2	5.042	4.487	+2.85	+37.72	+27.45
		Som	97.6	5.465	4.92	+1.84	+18.38	+11.6

*Indicates the best results for each fuzzy system in the column.

- **Lom method:** The results indicated that the R^2, RMSE, and MAE values were Improvements; the improvement values were 2.85%,37.72%, and 27.45%, respectively.
- **Som method:** The results indicated that the R^2, RMSE, and MAE values were Improvements; the improvement values were 1.84%,18.38%, and 11.6%, respectively.

The results illustrated the centroid method yields a more accurate result (R^2= 98.3%, RMSE =4.957%, and MAE=4.243%) compared to other methods. The Lom method has the most significant Improvement among methods (R^2= 2.85%, RMSE =37.72% and MAE=27.45%). This means that the accuracy of models was enhanced by increasing the number of sections.

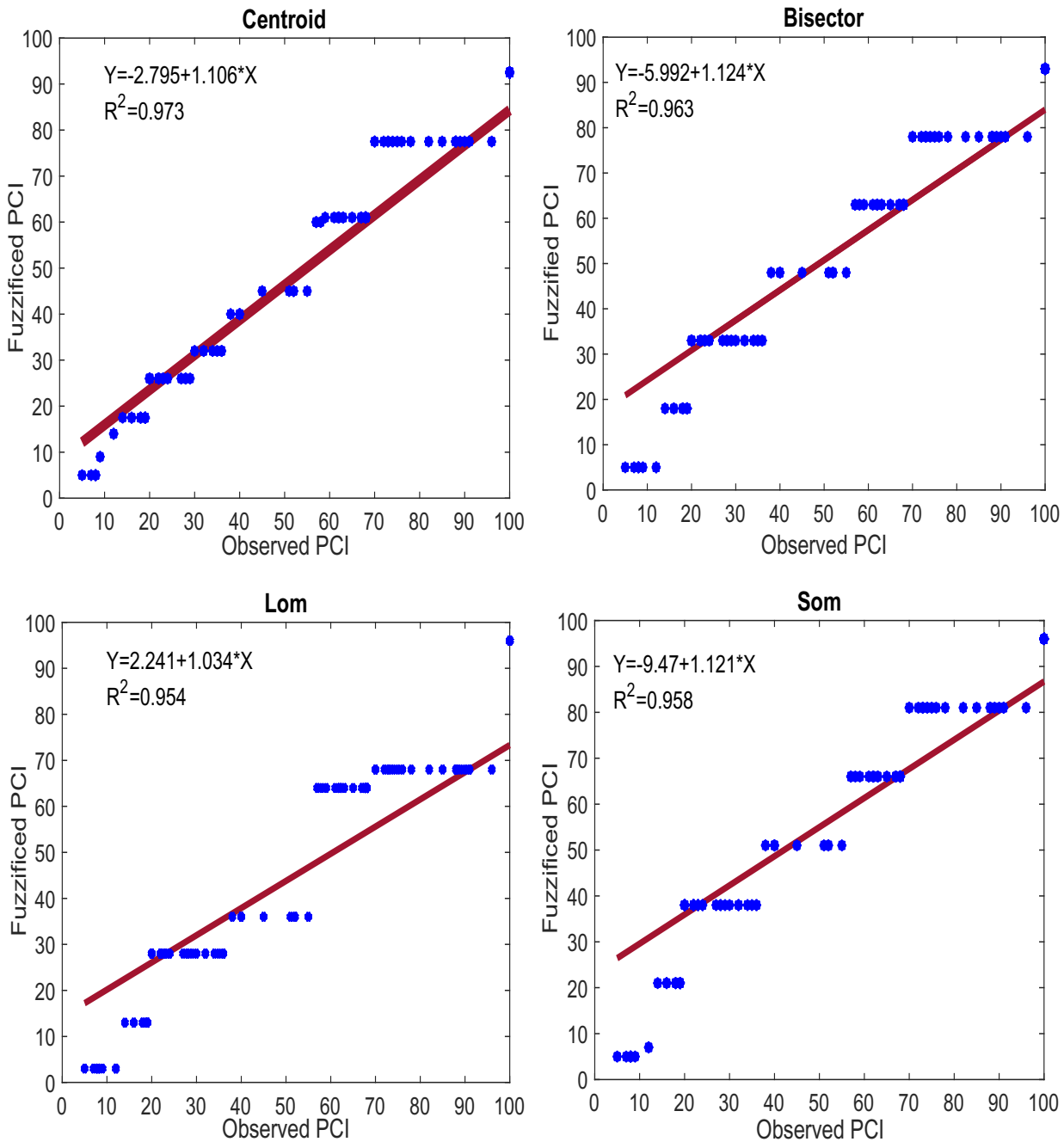

Figure 4-2: Fuzzy inference system for PCI (120 sections).

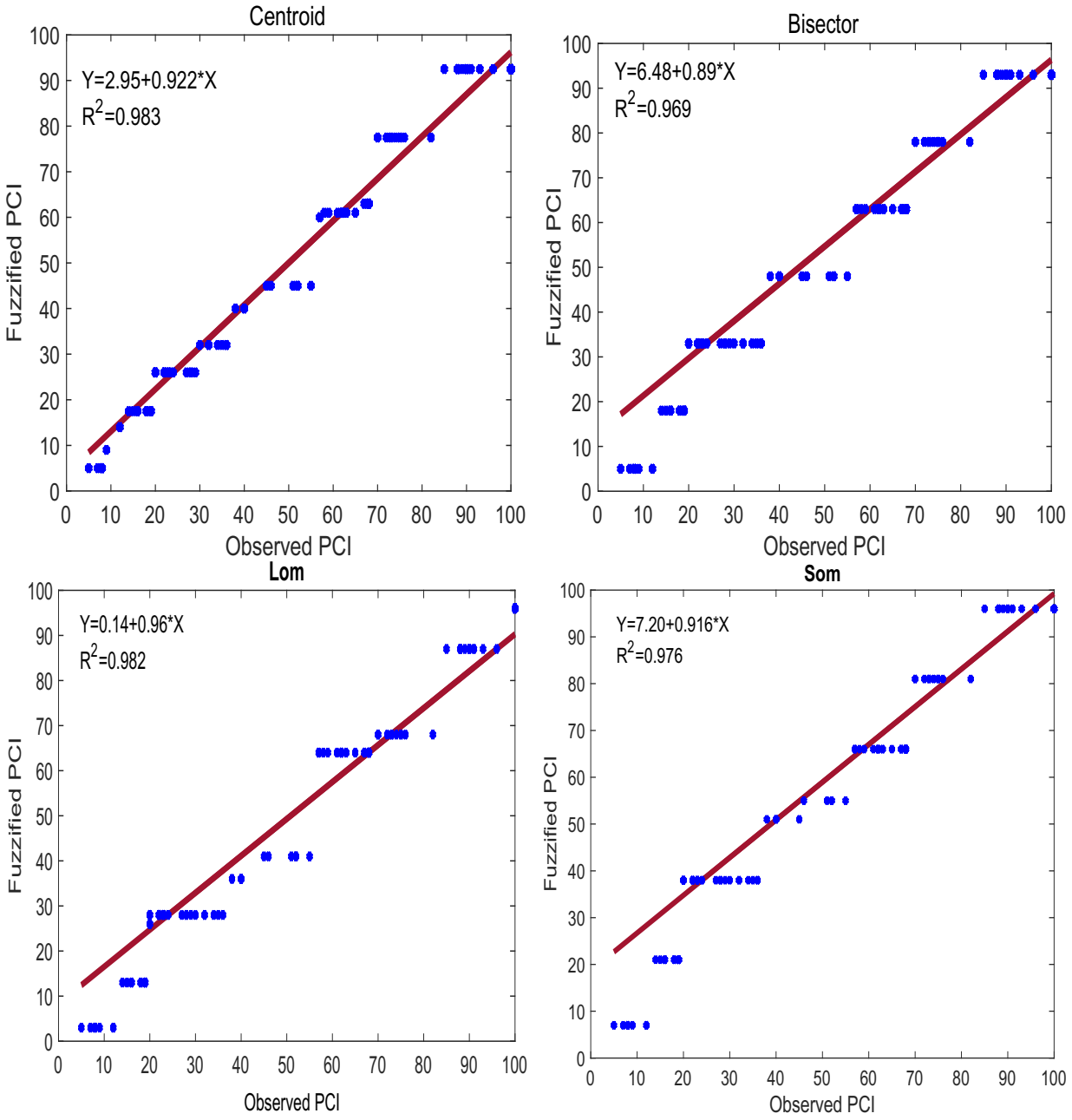

Figure 4-3: Fuzzy inference system for PCI (150 sections).

Although the Improvement was relatively slight, it still showed that the accuracy level improved with an increase in the number of sections. Figures (4-2) and (4-3) show the relation between the observed PCI and fuzzified FPCI and use four methods of analysis for 120 and 150 sections, respectively.

4.5.2 Fuzzy International Roughness Index (IRI)

Table (4-6) presents the level of agreement of the (FIRI) values for 120 and 150 sections, respectively.

Table 4-6: Assessment various fuzzy inference systems' configurations for FIRI

Inference	**Number of sections**	**Defuzzification**	**Statistical Error Measures (IRI)**			**Improvement (%)**		
			R^2	**RMSE**	**MAE**	R^2	**RMSE**	**MAE**
Mamdani (Triangular)	**120**	Centroid	90.3*	0.318*	0.26*	-	-	-
		Bisector	89.9	0.319	0.261	-	-	-
		Lom	89.3	0.412	0.314	-	-	-
		Som	88.3	0.345	0.278	-	-	-
	150	Centroid	92.9*	0.285*	0.227*	+2.78	+10.37	+12.70
		Bisector	92.7	0.286	0.233	+3.02	+10.34	+10.73
		Lom	91.9	0.33	0.249	+2.83	+19.90	+20.7
		Som	91.5	0.345	0.277	+3.5	0	+0.36

*Indicates the best results for each fuzzy system in the column.

The performance was evaluated by the R^2, RMSE, and MAE for FIRI. Comparison of the goodness of fit statistics of the 120 sections versus the 150 sections in Table (4-6) provides the following conclusions:

- **Centroid method:** The results indicated that the R^2, RMSE, and MAE values were Improvements; the improvement values were 2.78%, 10.37%, and 12.70%, respectively.
- **Bisector method:** The results indicated that the R^2, RMSE, and MAE values were Improvements; the Improvement values were 3.02%, 10.34%, and 10.73%, respectively.
- **Lom method:** The results indicated that the R^2, RMSE, and MAE values were Improvements; the improvement values were 2.83%,19.90%, and 20.70%, respectively.

- **Som method:** The results indicated that the R^2, RMSE, and MAE values were Improvements; the improvement values were 3.5%,0%, and 0.36%, respectively.

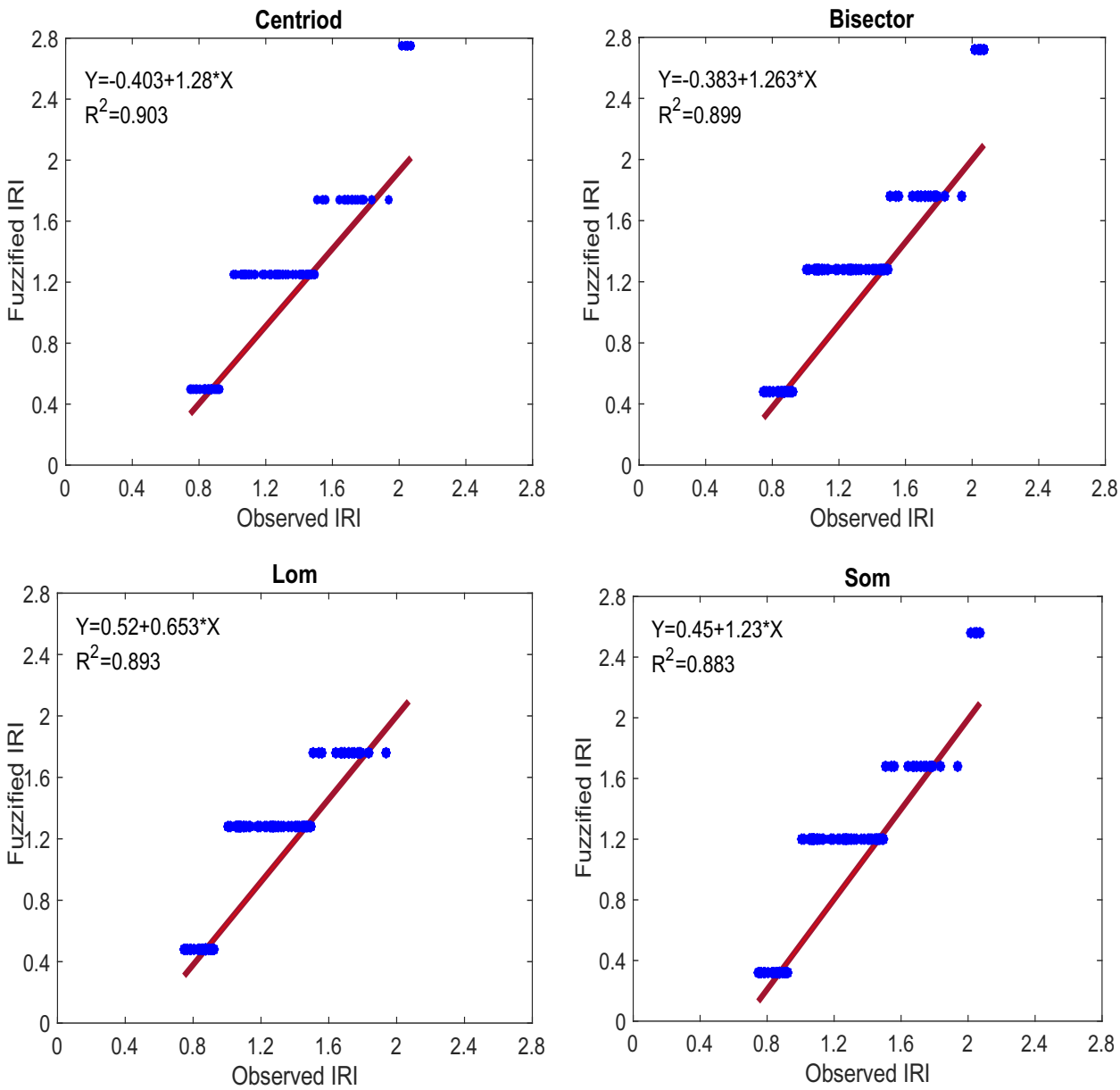

Figure 4-4: Fuzzy inference system for FIRI (120 sections).

The results illustrated the centroid method yields a more accurate result (R^2= 92.9%, RMSE =0.285%, and MAE=0.227%) than other methods. The Lom method has the most significant

Improvement among methods (R^2= 2.83%, RMSE =19.90% and MAE=20.70%). This means that the accuracy of models was enhanced by increasing the number of sections.

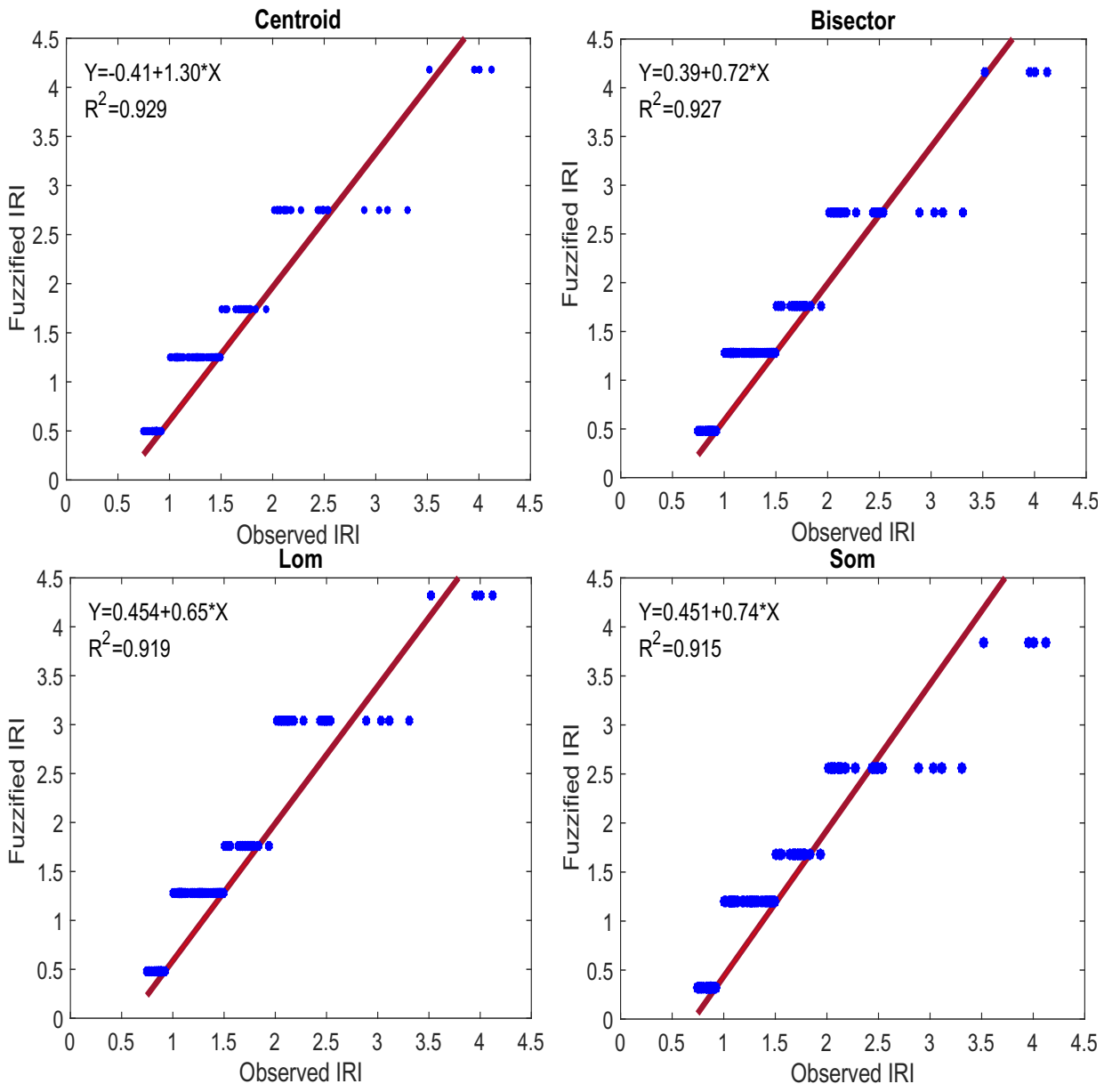

Figure 4-5: Fuzzy inference system for FIRI (150 sections).

Although the improvement was relatively slight, but it was indicated that accuracy improved as the number of sections increased. Figures (4-4) and (4-5) show the relation between the observed IRI and fuzzified FIRI and use four methods of analysis for 120 and 150 sections, respectively.

4.5.2.1 Sensitivity of Pavement Distress Types Using the FIS

The FPCI and FIRI models were created through several steps. The first step was the fuzzy partition generation for inputs and outputs for the 120 and 150 sections of pavement. The second step was the generation of fuzzy rules from numerical data. The third step was the FPCI and FIRI model development of a pavement classification model, which used nine variables as FIS inputs: rutting, fatigue cracking, block cracking, longitudinal and transverse cracking, patching and potholes, bleeding, and ravelling.

The effect of input parameters on the efficiency of the fuzzy pavement categorization system in the computation of output parameters (FPCI and FIRI) was investigated using a sensitivity analysis. The sensitivity analysis was carried out by creating the FIS model and analysing the influence of each input on output.

Table (4-7) summarizes a sensitivity analysis to determine the effects of input variables on the efficacy of PCI and IRI evaluation models. This analysis generated empirical models by considering the individual independent input impact (one by one) and neglecting the other independent input impacts. R^2 was used as the index to evaluate the correlation strength between independent and dependent input variables.

Figure (4-6) presents the sensitivity analysis for FPCI. Compared to other variables, the analysis showed that rutting has the most significant impact on FPCI fuzzified classification, and transverse, fatigue, and longitudinal cracking have some effects on FPCI. In contrast, block cracking, and patching slightly influence the classification model.

Figure (4-7) shows the sensitivity analysis for FIRI. Compared to other variables, this analysis showed that rutting has the most significant impact on FIRI fuzzified classification and patching

and fatigue cracking have some effects on FIRI fuzzified classification. Other variables have minor effect on FIRI fuzzified classification.

Table 4-7: Sensitivity analysis of prediction models for FPCI and FIRI.

Independent Variable	R^2			
	PCI		IRI	
	120	150	120	150
Rutting	45.1	46.5	12.4	14.2
Fatigue	27.9	28.4	58	63
Block Cracking	0. 1	0. 2	0. 1	-
Longitudinal Cracking	26.6	26.6	0. 1	1.4
Transverse Cracking	35.5	39.9	1.7	1.6
Patching	5.1	0.6	9.6	0. 1
Potholes	-	-	-	0. 1
Bleeding	9.6	7.2	12	0. 6
Ravelling	6.5	7.1	0. 1	0. 2

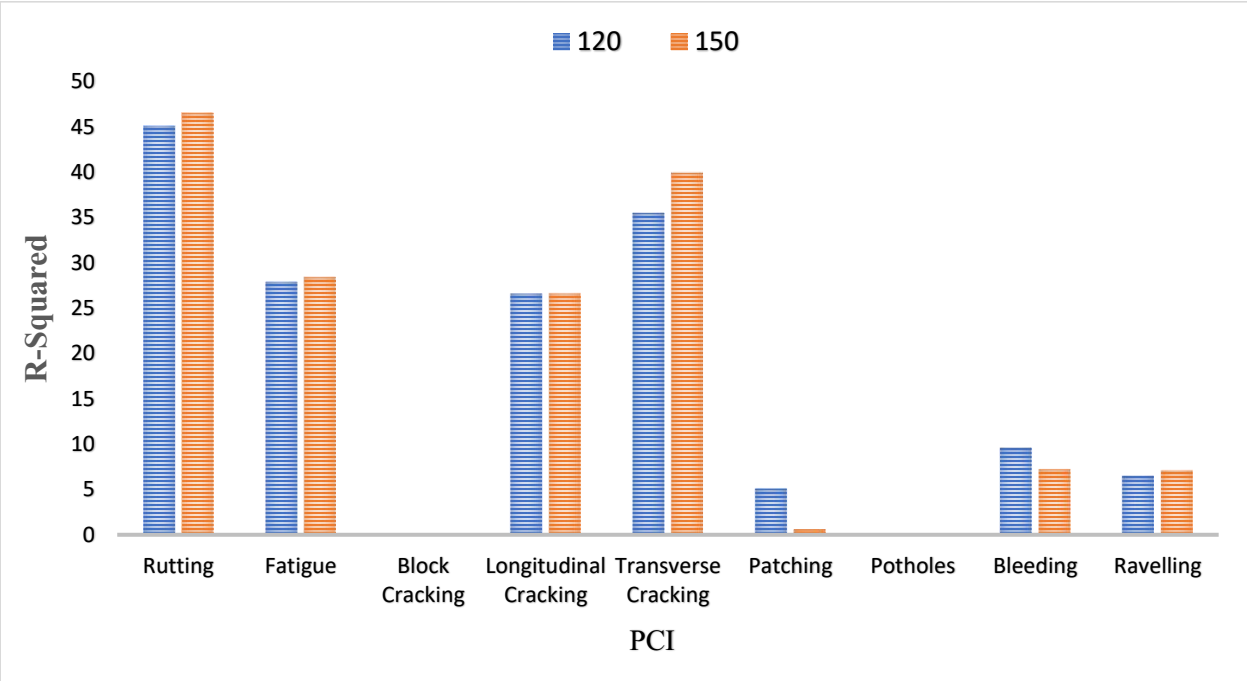

Figure 4-6: Sensitivity analysis of input variables on prediction for FPCI.

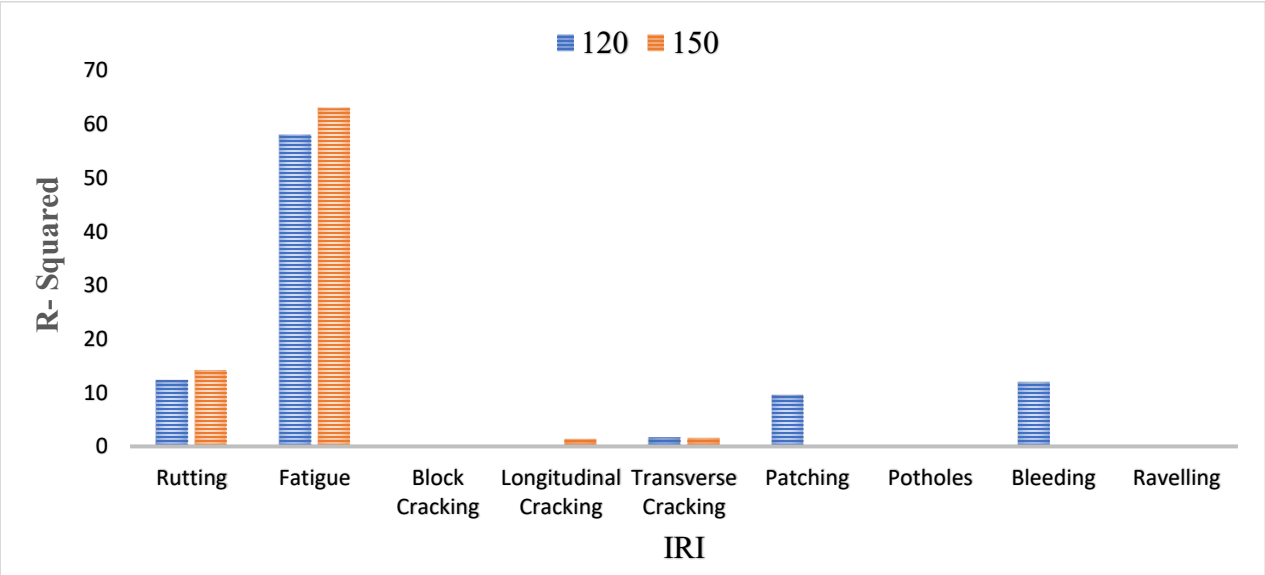

Figure 4-7: Sensitivity analysis of input variables on prediction for FIRI.

4.6 Summary

This study used two sets of pavement distress data extracted from the LTPP database. Data sets were used to develop a PCI and IRI prediction model using the fuzzy inference algorithm. The membership function parameter was determined by a set of input and output data defined via a hybrid optimization algorithm. Drafting the structure of the FIS model by trial and error was a method adopted for constructing the optimal FIS. The nine density types of pavement distress coefficients (rutting, fatigue cracking, block cracking, longitudinal cracking, transverse cracking, patching, potholes, bleeding, and ravelling) were input variables. And IRI and PCI were considered as the target parameters. Two data sets were collected from the LTPP data set for FIS modelling, with (120) and (150) sections.

Several important advantages were drawn from FIS technique, as follows:

- Although the FIS technique does not provide an equation for the prediction of PCI and IRI, the model can correlate with pavement distress. Based on the R^2 values, it was evident that the four methods have good accuracy, as their R^2values exceed 89%.
- Based on the sensitivity analysis, it is concluded that the rutting has most influence on the FPCI calculation, and transverse cracking, longitudinal cracking, and fatigue cracking have some influence on the FPCI calculation, while patching, bleeding, and ravelling have minor effects on the FPCI calculation.
- Based on the sensitivity analysis, it is concluded that the rutting has most influence on the FIRI calculation patching and fatigue cracking have some influence on the FIRI, while transverse cracking, longitudinal cracking, bleeding, and ravelling have only minor effects on the FIRI.

- Incorporating additional sections with different distresses and various severities improves the model results, which helps the programme to learn and develop additional rules.
- Results indicated that the performance of developed models was enhanced by increasing the number of sections.

Chapter5: Modeling the Relationship Between Asphalt Pavement Performance Indices (PCI and IRI)

5.1 Introduction

The IRI and the PCI are widely used pavement performance indicators in many countries. These indicators are important in determining the effectiveness of pavement rehabilitation and treatment programs. This chapter sought to clarify the relationship between these two performance indicators using the LTPP data for four climate regions in the U.S. and Canada. Figure (5-1) shows the research methodology of examining and developing the relationship between asphalt pavement performance indices.

5.2 Pavement Condition Index Calculation

After collecting the pavement distress data and IRI values from the LTPP database for four climate regions in the U.S. and Canada, PCI values were calculated for 53 road sections with 408 observations using the ASTM D6433-18 standard. Based on these data, three mathematical methods (linear, quadratic, and cubic) and ANNs techniques were developed for prediction models. Table (5-1) presents a brief description of the specification of the IRI and PCI dataset.

Table 5-1: Gathered pavement distress data for four climate regions.

Parameters	Unit	Climate Regions			
		Dry Freeze	Dry no Freeze	Wet Freeze	Wet no Freeze
PCI	%	52-80	50-100	8-100	8-100
IRI	(m/km)	0.89-1.69	0.68-2.66	0.72-4.04	0.62-3.76

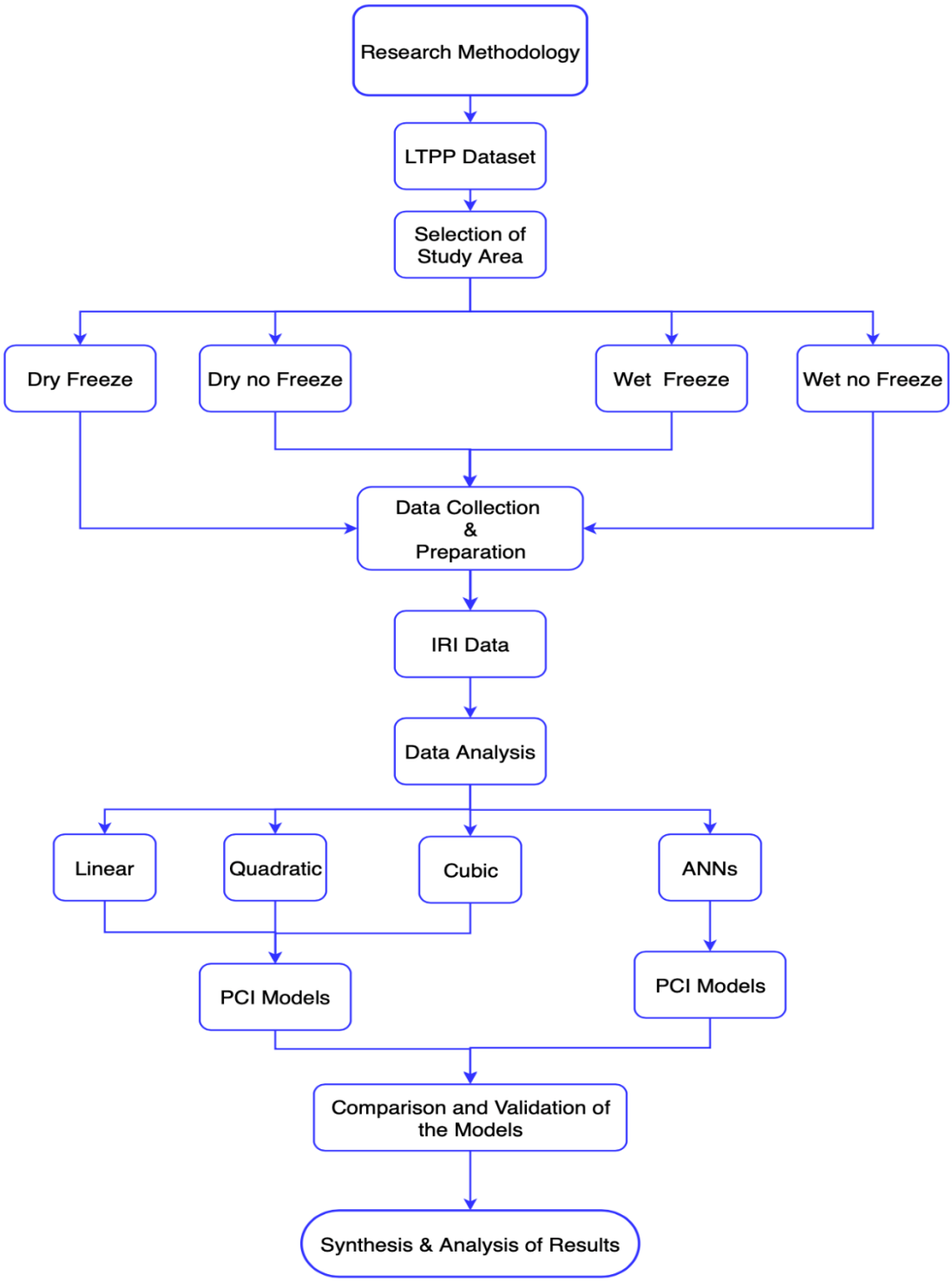

Figure 5-1: Research methodology of the examining and Modeling the relationship between asphalt pavement performance indices.

5.3 Modeling the Relationship Between Asphalt Pavement Indices (PCI and IRI) Using Mathematical Methods

Three mathematical methods (linear, quadratic, and cubic) were used to develop a correlation between the two indicators PCI and IRI. Analysis was carried out by the SPSS programme to determine the correlation between the PCI and IRI. The correlation between the PCI and IRI was conducted based on the LTPP dataset, and the correlation was assessed using R^2 values, RMSE, and MAE. Equations from (5-1) to (5-12) summarised the regression models and presented the relation between (PCI& IRI) for four climate regions as follows:

1-Dry Freeze:

Regression analysis was carried out to determine the correlation between the PCI and IRI. Equations (5-1), (5-2), and (5-3) represent the correlation between the PCI and IRI and used the linear, quadratic, and cubic methods, respectively.

$$\boldsymbol{PCI = 97.363 - 27.92(IRI)} \qquad \textbf{5-1}$$

The correlation coefficient (R^2) of this relationship is **87.7%.**

$$\boldsymbol{PCI = 143.83 - 108.270(IRI) + 31.88(IRI)^2} \qquad \textbf{5-2}$$

The correlation coefficient (R^2) of this relationship is **92.3%.**

$$\boldsymbol{PCI = 143.83 - 108.270(IRI) + 31.88(IRI)^2} \qquad \textbf{5-3}$$

The correlation coefficient (R^2) of this relationship is **92.3%.**

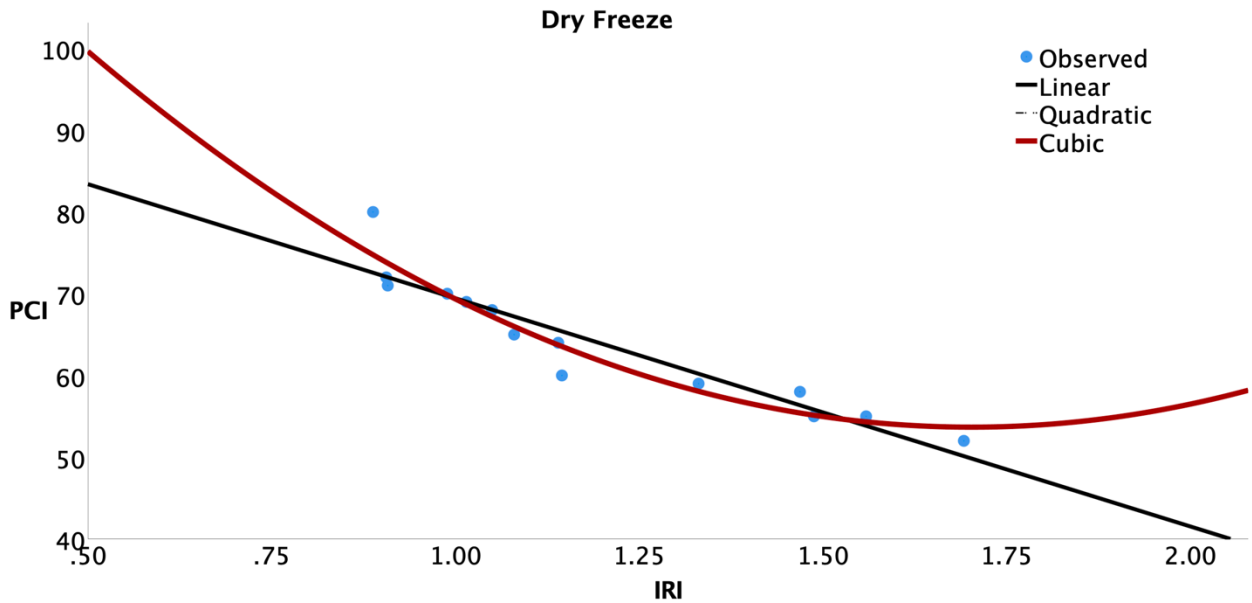

Figure 5-2: PCI versus IRI plot for dry freeze.

The previous three equations showed that the dependant variable PCI was negatively correlated with the independent variable (IRI), which was to be expected, since the roughness of roads causes PCI values to decrease. Figure (5-2) presented the relationship between PCI and IRI for the dry freeze region, and the Figure showed the relationship between PCI and IRI by three mathematical methods, linear, quadratic, and cubic.

2-Dry no Freeze:

Regression analysis was carried out to determine the correlation between the PCI and IRI. Equations (5-4), (5-5), and (5-6) represent the correlation between the PCI and IRI and used the linear, quadratic, and cubic methods, respectively.

$$\boldsymbol{PCI = 115.012 - 29.72(IRI)} \qquad \textbf{5-4}$$

The correlation coefficient (R^2) of this relationship is **89%.**

$$\boldsymbol{PCI = 128.7 - 57.3(IRI) + 11.44(IRI)^2} \qquad \textbf{5-5}$$

The correlation coefficient (R^2) of this relationship is **92%.**

$$\boldsymbol{PCI = 128.7 - 57.3(IRI) + 11.44(IRI)^2} \qquad \textbf{5-6}$$

The correlation coefficient (R^2) of this relationship is **92%.**

As observed in equation (5-4), the regression analysis (linear method) showed that the PCI variable was negatively correlated with IRI. R^2 for equation (5-4) was 86 %. While R^2 for equations (5-5) and (5-6) were 92 % for the quadratic and cubic methods, respectively. Figure (5-3) presents the relationship between PCI and IRI for the dry no freeze region using three mathematical methods: linear, quadratic, and cubic.

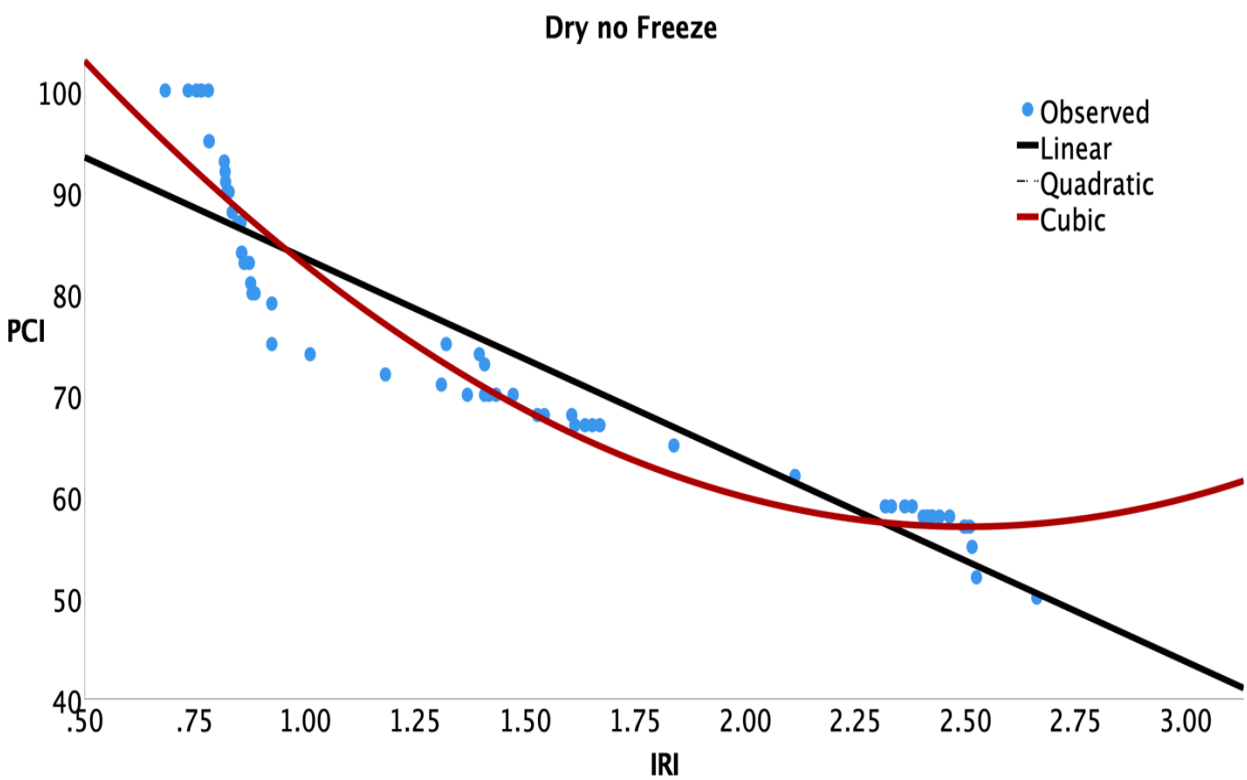

Figure 5-3: PCI versus IRI plot for dry no freeze.

3-Wet Freeze:

Three regression models were developed to predict PCI from IRI data. Equations (5-7), (5-8), and (5-9) represents the correlation between the PCI and IRI, using the linear, quadratic, and cubic methods, respectively.

$$\boldsymbol{PCI = 115.012 - 29.72(IRI)} \qquad \textbf{5-7}$$

The correlation coefficient (R^2) of this relationship is **82.1%.**

$$\boldsymbol{PCI = 121.6 - 38.23(IRI) + 2.11(IRI)^2} \qquad \textbf{5-8}$$

The correlation coefficient (R^2) of this relationship is **82.5%.**

$$\boldsymbol{PCI = 97.97 + 8.11(IRI) - 24.36(IRI)^2 + 4.31(IRI)^3} \qquad \textbf{5-9}$$

The correlation coefficient (R^2) of this relationship is **83.5 %.**

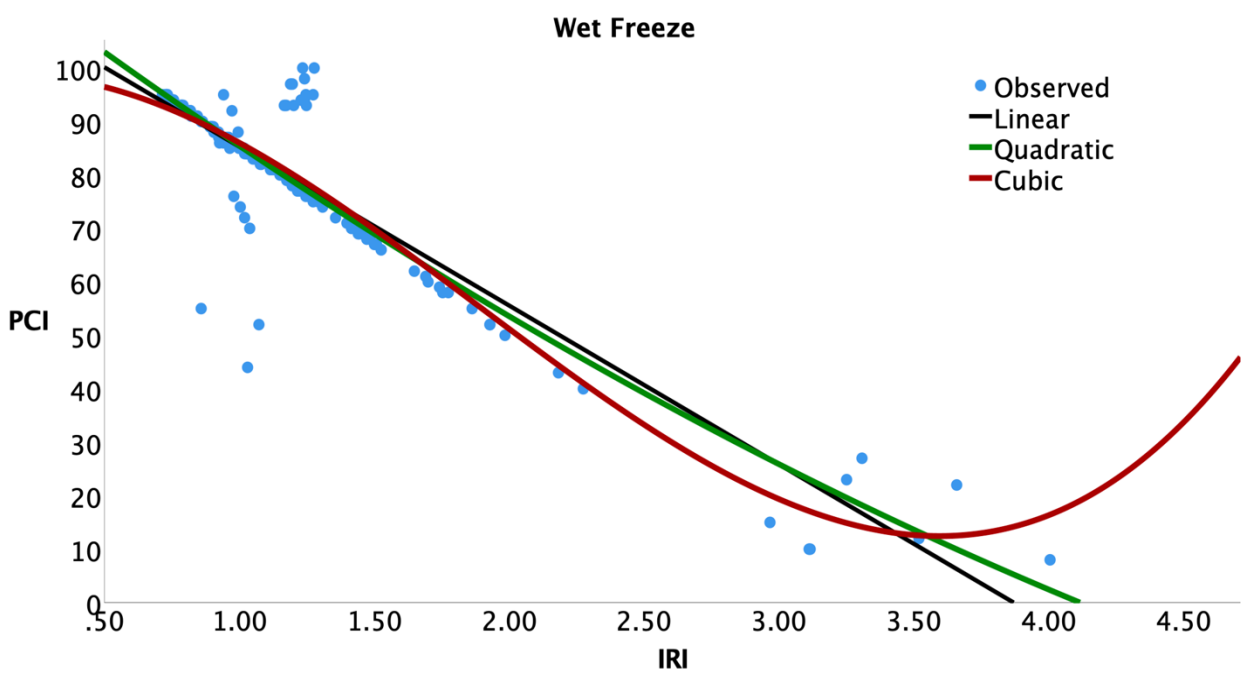

Figure 5-4:PCI versus IRI plot for wet freeze.

As observed in equations (5-7), (5-8), and (5-9), R^2 values were 82.1 %, and 82.5 %, and 83.5%, respectively. This indicates that using the IRI data in a wet freeze climate model it challenging to predict PCI value. Figure (5-4) presents the relationship between PCI and IRI for the wet freeze region using three mathematical methods: linear, quadratic, and cubic.

4-Wet no Freeze:

Three regression models were developed to predict PCI from IRI data. Equations (5-10), (5-11), and (5-12) represented the correlation between the PCI and IRI, and used the linear, quadratic, and cubic methods, respectively.

$$\mathrm{PCI}=136.508-45.923(\mathrm{IRI}) \qquad \textbf{5-10}$$

The correlation coefficient (R^2) of this relationship is **92.7%.**

$$\mathrm{PCI}=161.51-79(\mathrm{IRI})+9.23(\boldsymbol{IRI})^2 \qquad \textbf{5-11}$$

The correlation coefficient (R^2) of this relationship is **94.4%.**

$$\boldsymbol{PCI} = \mathbf{133.465} - \mathbf{27.21}(\boldsymbol{IRI}) - \mathbf{18.71}(\boldsymbol{IRI})^2 + \mathbf{4.60}(\boldsymbol{IRI})^3 \qquad \textbf{5-12}$$

The correlation coefficient (R^2) of this relationship is **94.8%.**

Equations (5-10), (5-11) and (5-12) showed that the R^2 were 92.7 %, 94.4 % and 94.8 %, respectively. Based on this, IRI data in the wet no freeze climate can easily predict PCI value. Figure (5-5) presents the relationship between PCI and IRI for the wet no freeze region using three mathematical methods: linear, quadratic, and cubic.

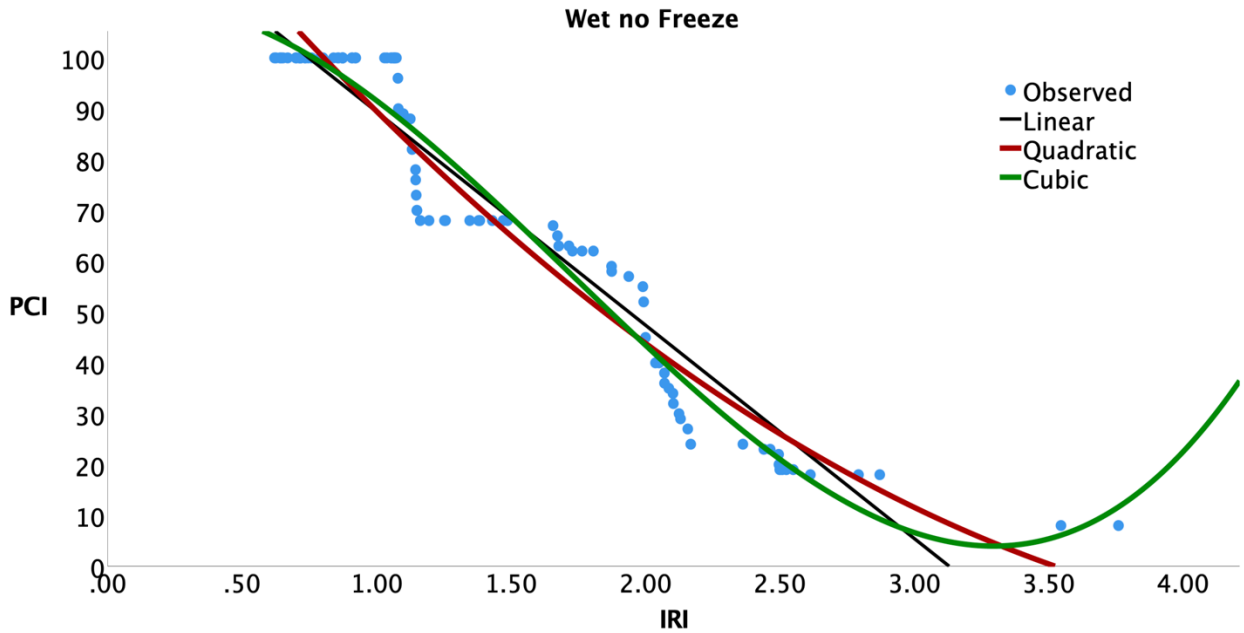

Figure 5-05: PCI versus IRI plot for wet no freeze.

5.4 Comparison and validation of the mathematical models

The R^2, RMSE, and MAE three statistical error measures were used for validating the developed regression model for the three mathematical methods mentioned above. Results showed that the $R^2$was good, while the RMSE and the MAE values in all cases were low, as shown in Table (5-2).

Table 5-2: Summary of correlation between IRI & PCI.

Climate Regions	Statistical Error Measures								
	R^2			RMSE			MAE		
	Linear	Quadratic	Cubic	Linear	Quadratic	Cubic	Linear	Quadratic	Cubic
Dry Freeze	87.7	92.3	92.3	2.704	2.132	2.132	1.764	1.563	1.563
Dry no Freeze	86	92	92	5.274	3.999	3.999	4.401	2.974	2.974
Wet Freeze	82.1	82.5	83.5	8.387	8.301	8.055	4.708	4.09	4.045
Wet no Freeze	92.7	94.4	94.8	8.173	7.137	6.940	6.354	5.763	5.348

According to Table (5-2), several conclusions can be drawn:

- **Dry Freeze:** The results indicated that the R^2, RMSE, and MAE values of the cubic models improved by 4.9%, 21.15%, and 11.39% compared to the linear models.
- **Dry no Freeze:** The results indicated that the R^2, RMSE, and MAE values of the cubic models improved by 6.52%, 24.17%, and 32.42% compared to the linear models.
- **Wet Freeze:** The results indicated that the R^2, RMSE, and MAE values of the cubic models improved by 1.68%, 1.20%, 3.96%,2.96%, 14.08%, and 1.10% compared to the linear models and quadratic model, respectively.
- **Wet no Freeze:** The results indicated that the R^2, RMSE, and MAE values of the cubic models improved by 2.22%, 15.09%, 15.83%, 0.42%, 2.76%, 7.20% compared to the linear models and quadratic model, respectively.

The results obtained from the regression analysis showed that the cubic regression models could be used for estimating the PCI values from the IRI. Cubic model results provided the best fit in all cases, with less error between the observed and predicted values compared to linear and quadratic methods. This result is consistent with some previous research. For example, Park et al. (2007) conducted a regression model and reported R^2=59%. AASHTO (2008a) used the M-E model to predict IRI values, the R^2 was 56%, by Arhin et al. (2015), R^2 = 82%, Psalmen Hasibuan & Sejahtera Surbakti, 2019), R^2 = 59%, Elhadidy et al. (2019), R^2 = 93%, and Timm (2015), R^2 = 63%. Despite following the ASTM standard, there remains a certain amount of uncertainty related to the correlation between PCI and IRI of flexible pavements owing to factors such as:

- the survey team estimates (human errors),
- the data collection devices, and
- the maintenance record of the road.

Table (5-1) shows PCI and IRI values for four climate regions. For example, PCI values for the dry no freeze region ranged between 52 and 100; these values were classified as fair to excellent. In contrast, IRI values were rated as very good to poor, and ranged between 0.68 and 2.66 (m/km). The results demonstrated that the same section of the road could have a good PCI but a poor IRI, even though IRI and PCI were strongly correlated. To understand these differences, the impact of pavement distress type was investigated with two road performance indicators. Some pavement distress, like potholes and bleeding, substantially reduce the PCI values but insignificantly influences the IRI values. However, the patching significantly affects the IRI values but insignificantly influences the PCI values.

5.5 Modeling the Relationship Between Asphalt Pavement Indices (PCI and IRI) Using Artificial Neural Network (ANNs) Technique

Artificial neural networks have been used to develop effective and accurate models. These models aim to predict the relationship between the PCI and IRI obtained from the LTPP datasets for four climate regions in the U.S. and Canada. The architecture of the designed network consists of one input layer with one variable, three hidden layers, and an output layer. 53 flexible pavement sections with 408 observations have been chosen within the four climatic regions. Figure (5-6) displays the architecture of the ANNs. The model's performance was assessed using the three common methods of R^2value, RMSE, and MAE. Figure (5-7) presents the ANN prediction results for PCI models for four climate regions. According to Table (5-3), several conclusions can be drawn:

- **Dry Freeze:** The R^2value was 99.7%, while the RMSE and MAE values were 0.89% and 0.89%.

- **Dry no Freeze:** The R^2 value was 98.5%, while the RMSE and MAE values were 0.39% and 0.336%.

Table 5-3: Performance of PCI models by using ANNs technique based on IRI values.

Climate Regions	Statistical Error Measures(%)		
	R^2	RMSE	MAE
Dry Freeze	99.7	0.89	0.89
Dry no Freeze	98.5	0.39	0.336
Wet Freeze	99.8	0.661	0.484
Wet no Freeze	99.8	0.827	0.601

- **Wet Freeze:** The R^2 value was 99.8%, while the RMSE and MAE values were 0.661% and 0.484%.
- **Wet no Freeze:** The R^2 value was 99.8%, while the RMSE and MAE values were 0.827% and 0.601%.

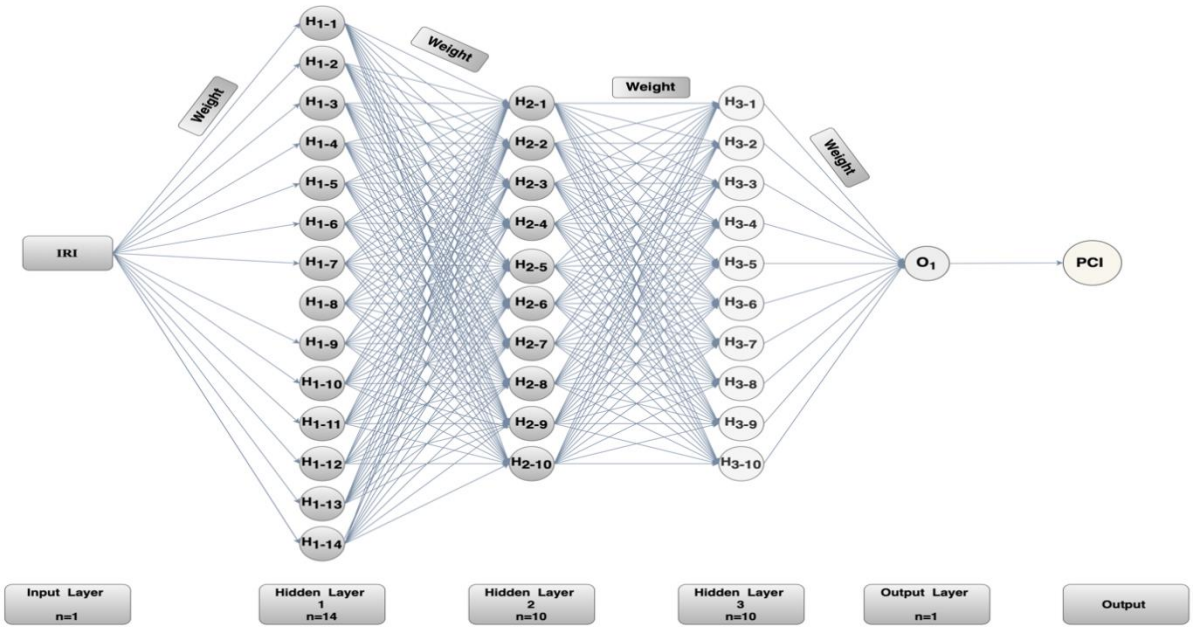

Figure 5-6: Architecture of ANN model for PCI.

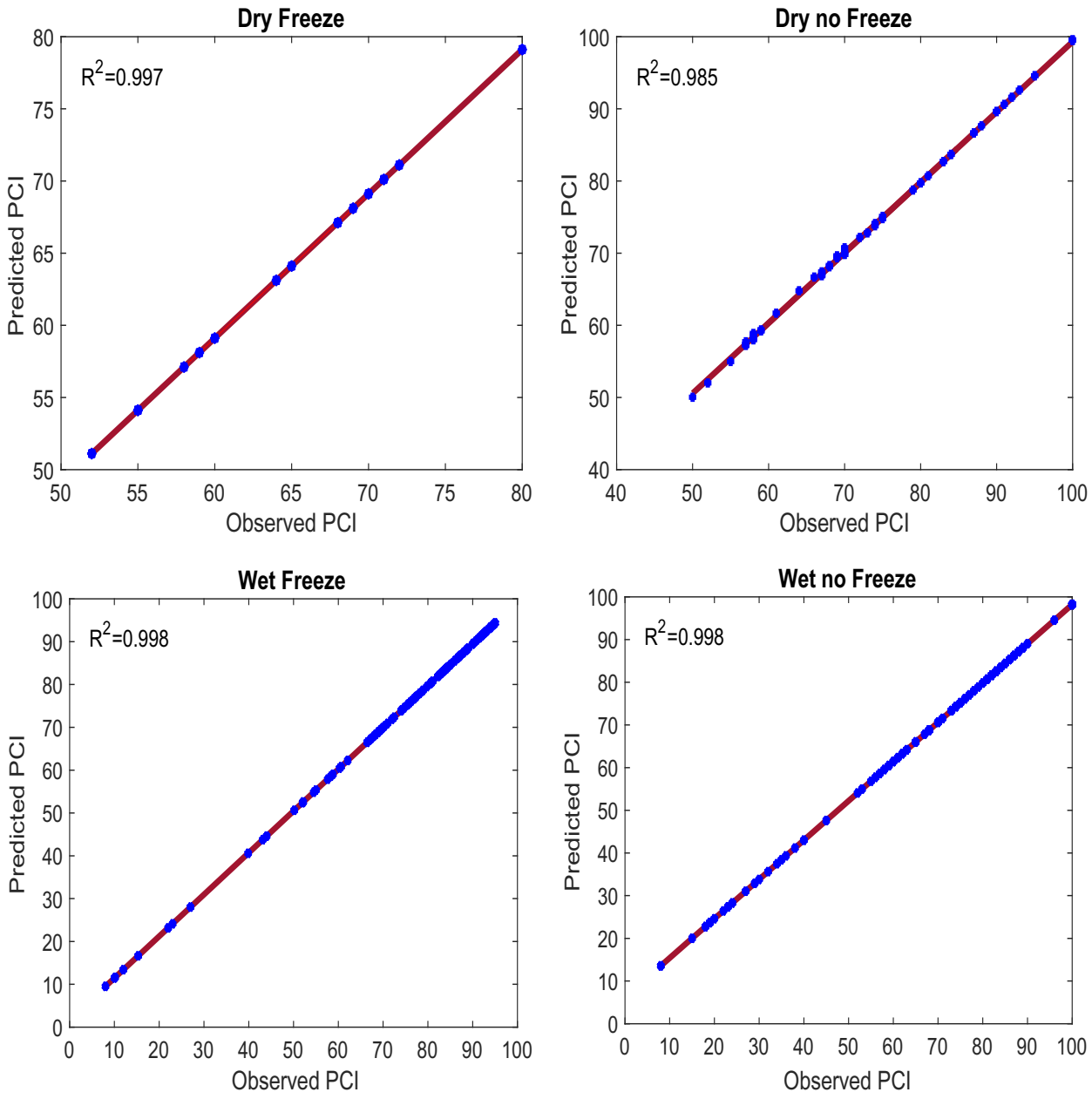

Figure 5-7: Performance of the ANNs for predicting PCI models for four climate regions.

5.6 Comparison and validation of the models

To validate the prediction models developed in this chapter, the R^2, RMSE, and MAE methods were adopted to validate the cubic and ANNs techniques. The R^2 was used to evaluate the relationship strength between the input and output variables. The RMSE and MAE were used to

determine whether if there were any significant differences between observed and prediction errors' values. In all cases, the calculated R^2 were strong, and RMSE and MAE values were found to be low, as shown in Table (5-4). Figures (5-8) and (5-9) present the comparison between the cubic method and the ANNs technique. Table (5-4) provided a promising approach to compare the cubic models to ANNs models. A summary of the findings is as follows:

This study presented good models for accurate PCI prediction for flexible pavement for four climate regions. The model's input variables were evaluated and assessed to produce an accurate and strong model.

Table 5-04: Comparison of the cubic models to the ANNs models.

Climate Region	**Statistical Error Measures**								
	Cubic Generated			**ANNs Generated**			**Improvement (%)**		
	R^2	**RMSE**	**MAE**	R^2	**RMSE**	**MAE**	R^2	**RMSE**	**MAE**
Dry Freeze	92.3	2.132	1.563	99.7	0.89	0.89	+7.42	+58.26	+43.06
Dry no Freeze	92	3.999	2.974	98.5	0.39	0.336	+6.60	+90.25	+88.70
Wet Freeze	83.5	8.055	4.045	99.8	0.661	0.484	+16.33	+91.79	+88.03
Wet no Freeze	94.8	6.940	5.348	99.8	0.827	0.601	+5.01	+88.08	+88.76

- The results indicated that the $R^2$of the ANNs models improved by 7.42%, 6.60%, 16.33 %, and 5.01%, compared to the cubic models, for dry freeze, dry no freeze, wet freeze, and wet no freeze, respectively.
- The results indicated the RMSE value of the ANNs models was reduced by 58.26%, 90.25%, 91.79%, and 88.08% compared to the cubic models, for dry freeze, dry no freeze, wet freeze, and wet no freeze, respectively.

- The results indicated the MAE value of the ANNs models was reduced by 43.06%, 88.70%, 88.03%, and 88.76%, compared to the cubic models, for dry freeze, dry no freeze, wet freeze, and wet no freeze, respectively.
- According to the results, the cubic models could estimate the PCI values from the IRI with reasonable accuracy. Results showed that the ANNs technique has the best fit and high accuracy in all cases with less error between observed and predicted values than the cubic method.

5.7 Summary

Several important conclusions can be drawn from this chapter, as follow:

- The LTPP data were used in this study to determine correlations between the PCI and IRI of flexible pavement. The results indicate that all methods were able to predict models by using IRI data.
- The results indicated that the most accurate models were the cubic models, compared to linear and quadratic models, in all cases.
- The results indicated that the ANNs models were more accurate than cubic models in all cases.
- Finally, when comparing the MLR and the ANN data, it was observed that the ANNs models showed more strong correlations between the PCI and IRI.

Chapter6: Modeling of Asphalt Pavement Performance Indices Using (MLR) and (ANNs) Techniques

6.1 Introduction

The pavement performance prediction models are essential for pavement management and effectively prioritize allocating resources, where pavement redesign and maintenance costing are conducted with these models. This section provides the research methodology used to model performance prediction indices (PCI and IRI) and investigates the potential impact of various fundamental parameters on pavement performance. This is critical to understanding potential relationship types and calculating correlations between input and output variables.

The methodology for this chapter is based on the several following steps:

1. Collecting data from the LTPP dataset for four climate regions.
2. Modeling of asphalt pavement performance indices using (MLR) technique.
3. Modeling of asphalt pavement performance indices using (ANNs) technique.
4. Comparison and validation of the MLR and ANNs models.
5. Specifically, the following three parameters are analyzed to determine study their effect on asphalt pavement performance indices (PCI &IRI) prediction models:
    - Effect of pavement distress (performance parameters),
    - effect of environmental parameters, and
    - effect of traffic parameters.

Figure 6-1 presents the research methodology of the Modeling asphalt pavement performance indices.

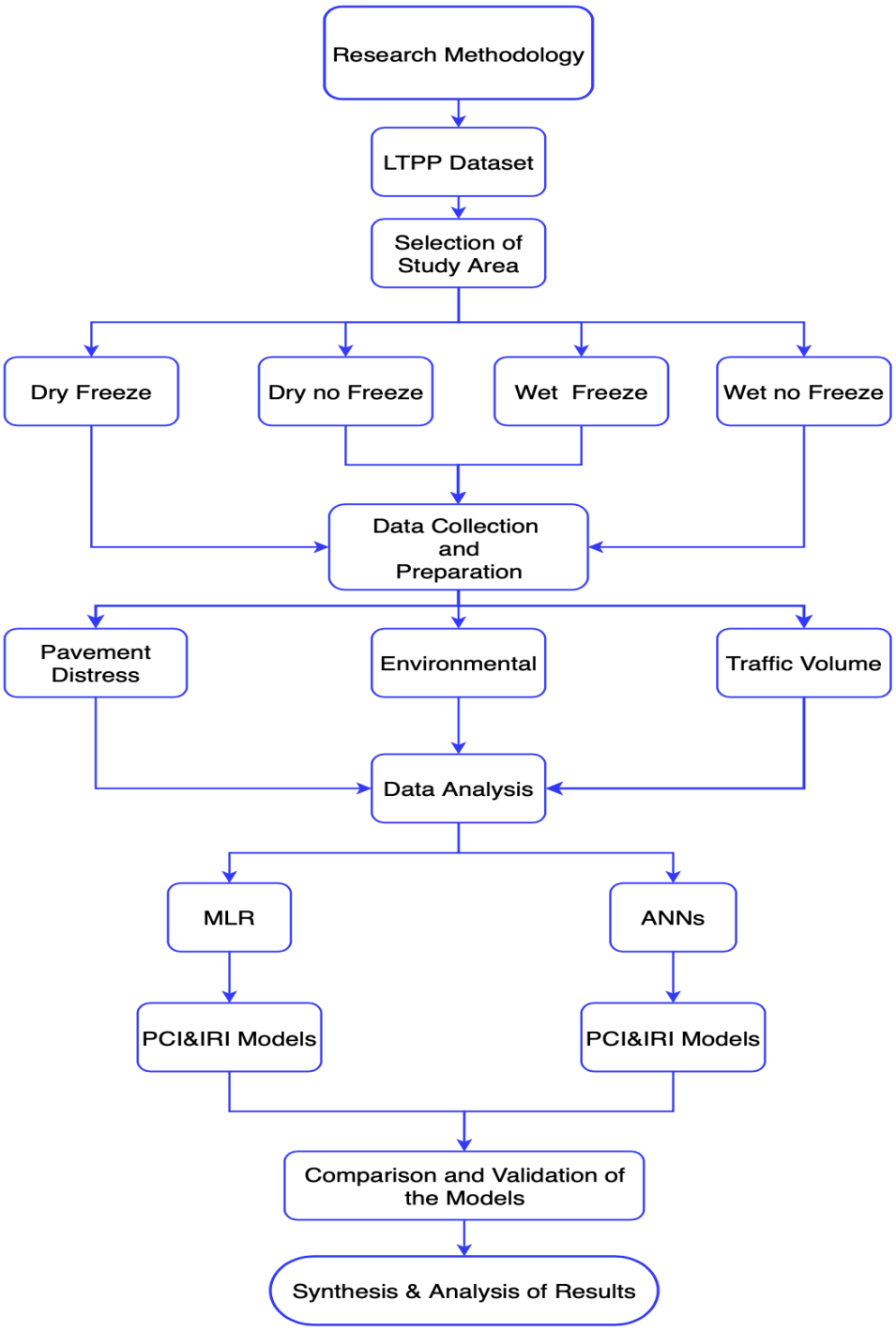

Figure 6-1: The research methodology of the modeling asphalt pavement performance indices.

6.2 Effect of Pavement Distress on Indices Values

This section focused on modeling asphalt pavement performance indices (PCI and IRI) based on pavement distress variables and studying the effect of these variables on asphalt pavement performance indices for four climate regions in the U.S. and Canada. The relevant data were collected on the pavement distress parameters of 53 road sections with 408 observations from the LTPP dataset, and distributed to four climate regions (dry freeze, dry no freeze, wet freeze, wet no freeze). The present study was divided into three phases as follows:

- Modeling of asphalt pavement performance indices using (MLR) technique.
- Modeling of asphalt pavement performance indices using (ANNs) technique.
- Comparison and validation of the MLR and ANNs models.

Ten pavement distress variables were assessed and used to predict the PCI and IRI for each climate region, including age, rutting, fatigue cracking, block cracking, longitudinal cracking, transverse cracking, potholes, patching, bleeding, and ravelling.

Note that both the surface type of asphalt concrete pavement (ACP) and type of subgrade (coarse-grained) are constant for all data regions. Table (6-1) briefly describes the selected dataset of pavement distress specification.

Table 6-1: Gathered pavement distress data from four climate regions.

Parameters	Unit	Climate Regions			
		Dry Freeze	Dry no Freeze	Wet Freeze	Wet no Freeze
PCI	%	52-80	50-100	8-91	8-100
IRI	(m/km)	0.89-1.69	0.68-2.66	0.79-4.04	0.75-3.76
Number of data samples	Number	14	61	144	189
Age	Year	6-18	3-34	3-33	1-31
Rutting	Mm	0-10	0-16	0-29	0-22
Fatigue Cracking	m^2	0-170	0-304.8	0-218.7	0-377.90
Block Cracking	m^2	0	0	0	0
Longitudinal Cracking	M	128.9-378.5	0-306	0-319	0-377.1
Transverse Cracking	M	22-65	0-140	0-293	0-193
Patching	m^2	0	0-1.5	0	0-46
Potholes	(Count)	0	0	0	0
Bleeding	m^2	0	0	0-350.80	0-275
Ravelling	m^2	0	0-76.3	0-564.3	0-564

6.2.1 Modeling of Asphalt Pavement Performance Indices Using (MLR) Technique

Research in this part focuses on using pavement distress variables to model asphalt pavement performance indices (PCI and IRI). Pavement distress parameters were input variables, and pavement performance indices (PCI and IRI) were output parameters. Eight prediction models were developed using (MLR) technique from the collected data. The PCI and IRI regression models are shown in Tables (6-2) and (6-3).

The PCI regression analysis results illustrated in Table (6-2) indicate that the R^2 values were 77%, 91.6%, 86.6%, and 89.3% for dry freeze, dry no freeze, wet freeze, and wet no freeze, respectively.

Based on the R^2 values, it was evident that all models have good accuracy, as their R^2values exceed 77%.

Table 6-2: PCI models summary based on pavement distress.

Model	PCI			
	Dry Freeze	**Dry no Freeze**	**Wet Freeze**	**Wet no Freeze**
R^2	77	91.6	86.8	89.4
Constant	82.2	104.94	116.52	113.33
Age	0.067	-0.492	-2.74	-3.087
Rutting	0.232	0.048	0.178	0.205
Fatigue Cracking	-0.095	0.04	–0.018	0.007
Block Cracking	-	-	-	-
Longitudinal Cracking	-0.096	-0.011	0.001	-0.004
Transverse Cracking	0.054	0.104	0.024	-0.045
Patching	-	-2.793	-	0.021
Potholes	-	-	-	-
Bleeding	-	-	0.01	0.005
Ravelling	-	-0.053	0.008	-0.004

The IRI regression analysis results illustrated in Table (6-3) indicate that the R^2 values were 70.7%, 90.3%, 77.7%, and 89.4% for dry freeze, dry no freeze, wet freeze, and wet no freeze, respectively. Based on the R^2 values, all models had a good correlation, as their R^2 values exceed 70%.

Table 6-3: IRI models summary based on pavement distress.

Model	IRI			
	Dry Freeze	**Dry no Freeze**	**Wet Freeze**	**Wet no Freeze**
R^2	70.7	90.6	77.7	89.3
Constant	2.273	0.063	0.155	0.365
Age	-0.126	0.088	0.081	0.074
Rutting	0.083	0.011	-0.007	-0.004
Fatigue Cracking	-0.003	-0.002	0.001	-0.0001
Block Cracking	-	-	-	-
Longitudinal Cracking	-0.007	-	-	-0.0001
Transverse Cracking	0.035	-	-0.001	-0.001
Patching	-	0.043	-	-
Potholes	-	-	-	-
Bleeding	-	-	-	-
Ravelling	-	-0.002	-	-

Equations from (6-1) to (6-8) summarised the regression models for four climate regions as follows:

1- <u>Dry Freeze</u>

Table (6-2) presents the regression analysis result for PCI for the dry freeze area. The PCI model was negatively correlated with fatigue and longitudinal cracking, and positively correlated with age, rutting, and transverse cracking. Equation (6-1) described the relationship between the PCI and pavement distress as follows:

$$\boldsymbol{PCI = 82.2 + 0.067X_{age} + 0.232X_1 - 0.095X_2 - 0.096X_4 + 0.054X_5} \qquad \textbf{6-1}$$

The correlation coefficient (R^2) of this relationship is **77%.**

Table (6-3) presents the regression analysis result of the IRI for the dry freeze area. The IRI model had a positive relationship with rutting and transverse cracking. The IRI model had a negative relationship with age, fatigue cracking, and longitudinal cracking, Equation (6-2) described the relationship between the IRI and pavement distress as follows:

$$\boldsymbol{IRI = 2.273 - 0.126X_{age} + 0.083X_1 - 0.003X_2 - 0.007X_4 + 0.035X_5} \qquad \textbf{6-2}$$

The correlation coefficient (R^2) of this relationship is **70.7 %.**

2- <u>Dry no Freeze</u>

The regression analysis result of the PCI model for the dry no freeze area is shown in Table (6-2). The PCI model was positively correlated with fatigue and transverse cracking. The PCI model was negatively correlated with age, rutting, fatigue cracking, longitudinal cracking, patching, and ravelling. Equation (6-3) described the relationship between the PCI and pavement distress as follows:

$$\boldsymbol{PCI = 104.94 - 0.492X_{age} + 0.048X_1 + 0.04X_1 - 0.011X_4 + 0.104X_5 - 2.793X_6 - 0.053X_9} \qquad \textbf{6-3}$$

The correlation coefficient (R^2) of this relationship is **91.6 %.**

The regression analysis result of the IRI model for the dry no freeze area is presented in Table (6-3). The IRI model was negatively correlated with fatigue cracking and ravelling. The IRI model had a positive relationship correlated with age, rutting, and patching. Equation (6-4) described the relationship between the IRI and pavement distress as follows:

$$\mathbf{IRI = 0.063 + 0.088X_{age} + 0.011\,X_1 - 0.002\,X_2 + 0.043X_6 - 0.002\,X_9} \qquad \text{6-4}$$

The correlation coefficient (R^2) of this relationship is **90.6%.**

3- Wet Freeze

Table (6-2) presents the regression analysis results for the PCI model for the wet freeze area. The PCI model was negatively correlated with age and fatigue cracking. The PCI model was positively correlated with rutting, longitudinal cracking, transverse cracking, bleeding, and ravelling. Equation (6-5) described the relationship between the PCI and pavement distress as follows:

$$\boldsymbol{PCI = 116.52 - 2.74X_{age} + 0.178X_1 - 0.018X_2 + 0.001X_4 + 0.024X_5 + 0.010X_8 + +0.008X_9} \qquad \textbf{6-5}$$

The correlation coefficient (R^2) of this relationship is **86.8%.**

Table (6-3) presents the regression analysis results for the IRI model for the wet freeze area. The IRI model was negatively correlated with rutting and transverse cracking. The IRI model was positively correlated with age, and fatigue cracking. Equation (6-6) described the relationship between the IRI and pavement distress as follows:

$$\mathbf{IRI = 0.155 + 0.081X_{age} - 0.007X_1 + 0.001X_2 - 0.001X_5} \qquad \textbf{6}\text{-6}$$

The correlation coefficient (R^2) of this relationship is **77.7%.**

4- Wet no Freeze

The regression analysis result of the PCI model for the wet no freeze area is presented in Table (6-2). The PCI model was negatively correlated with age, transverse cracking, longitudinal cracking, and ravelling. The PCI model was positively correlated with rutting, fatigue cracking, patching, and bleeding. Equation (6-7) describes the relationship between the PCI, and pavement distress as follows:

$$\boldsymbol{PCI = 113.33 - 3.078X_{age} + 0.205X_1 + 0.007X_2 - 0.004X_4 - 0.045X_5 + 0.021X_6 + 0.005X_8 - 0.004X_5} \quad \textbf{6-7}$$

The correlation coefficient (R^2) of this relationship is **89.3%.**

The regression analysis result of the IRI model for the wet no freeze area is presented in Table (6-3). The IRI model was negatively correlated with rutting, fatigue cracking, longitudinal cracking, and transverse cracking. Equation (6-8) described the relationship between the IRI and pavement distress as follows:

$$\boldsymbol{IRI = 0.365 + 0.074X_{age} - 0.004X_1 - 0.0001X_2 - 0.0001X_4 - 0.001X_5} \quad \textbf{6-8}$$

The correlation coefficient (R^2) of this relationship is **89.4 %.**

6.2.1.1 Validation of MLR Models

Models Validation was applied to determine how accurately the PCI and IRI models can forecast. In this study used cross validation method to evaluating models performance. 80 % of the data samples for each category were randomly selected to construct deterioration models. The remaining 20 % of the data samples were used to test the empirical models' accuracy(Field. 2009; Mahmood. 2014). Figures (6-2) to (6-5) show the linear relations in each climate area for PCI and IRI. Tables (6-4) and (6-5) illustrate the reduction in R^2, RMSE, and MAE values for all sections in the four climate regions.

- **Models Validation of PCI Models**

After the validation test, Table (6-4) illustrates the reduction in R^2, RMSE, and MAE values for all sections in the four climate regions.

Table 6-4: Validation of PCI models based on pavement distress.

Climate Regions	Statistical Error Measures (PCI)								
	MLR			Validation			Reduction % (±)		
	R^2	RMSE	MAE	R^2	RMSE	MAE	R^2	RMSE	MAE
Dry Freeze	77.0	5.468	4.361	75.4	3.816	2.777	-2.078	-30.212	-36.322
Dry no Freeze	91.6	4.247	3.2	89.4	4.583	3.537	-2.402	+7.331	+9.528
Wet Freeze	86.8	7.195	5.616	77.4	7.495	6.001	-10.83	+4.003	+6.416
Wet no Freeze	89.3	7.324	5.79	92.6	8.909	6.16	+3.5	+17.791	+6.006

Based on Table (6-4), Figures (6-2), and (6-3), the following conclusions can be drawn:

- **Dry Freeze:** The results indicated that the reduction in R^2, RMSE, and MAE values was insignificant; the accuracy reductions were 2.078 %, 30.212 %, and 36.322 %, respectively. Thus, the MLR method's ability to predict PCI models of pavement distress was accurate.
- **Dry no Freeze:** The results indicated that the reduction in R^2, RMSE, and MAE values was insignificant; the accuracy reductions were 2.402 %, 7.331 %, and 9.528%, respectively. Thus, the MLR method's ability to predict PCI models of pavement distress was accurate.
- **Wet Freeze:** The results indicated that the reduction in R^2, RMSE, and MAE values was insignificant; the accuracy reductions were 10.83%, 4.003%, and 6.416%, respectively. Thus, the MLR method's ability to predict PCI models of the pavement distress was good.
- **Wet no Freeze:** The results indicated that the reduction in R^2, RMSE, and MAE values was insignificant; the accuracy reductions were 3.5%, 17.791%, and 6.006%, respectively. Thus, the MLR method's ability to predict PCI models of the pavement distress was good.

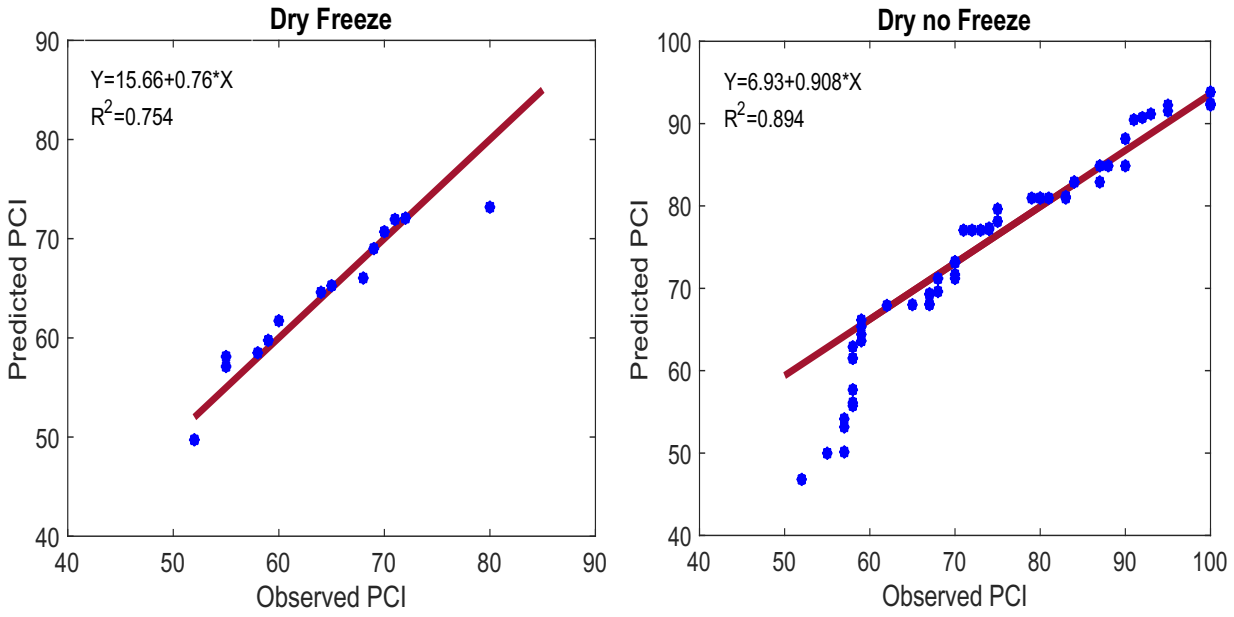

Figure 6-2*:* MLR model for the dry freeze and dry no freeze regions based on pavement distress.

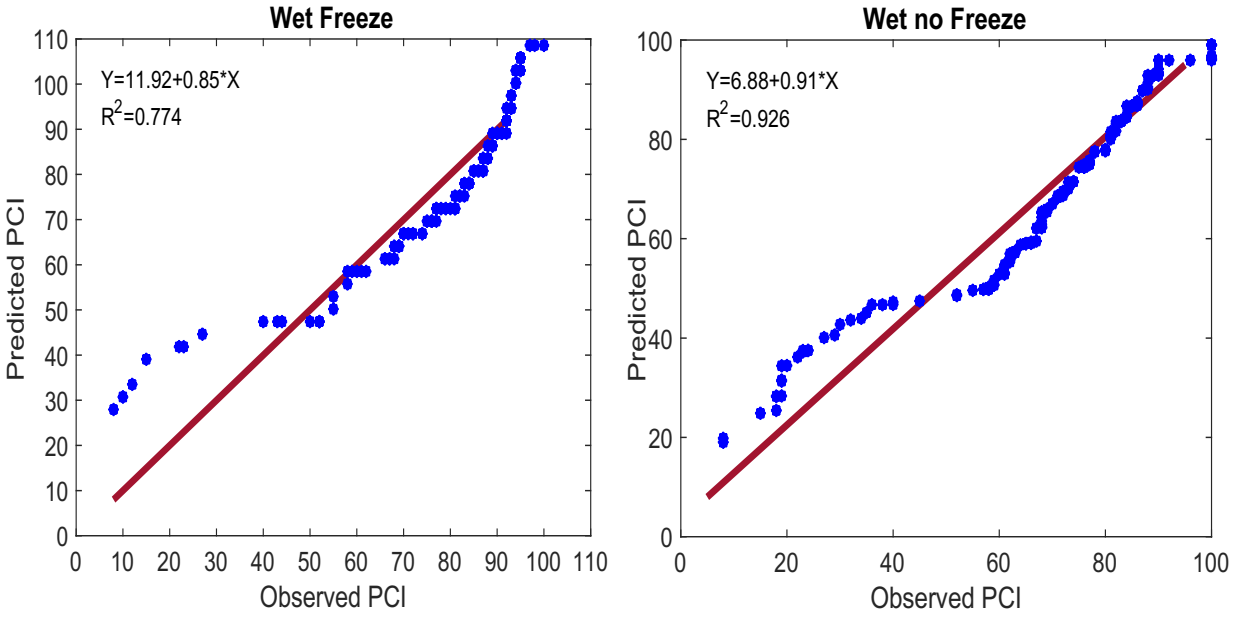

Figure 6-3: MLR model for the wet freeze and wet no freeze regions based on pavement distress.

- **Models Validation of IRI**

After the validation test, Table (6-5) illustrates the reduction in R^2, RMSE, and MAE values for all sections in the four climate regions.

Table 6-5: Validation of IRI models based on pavement distress.

Climate Regions	Statistical Error Measures (IRI)								
	MLR			Validation			Reduction % (±)		
	R^2	RMSE	MAE	R^2	RMSE	MAE	R^2	RMSE	MAE
Dry Freeze	70.7	0.144	0.099	60.6	0.178	0.113	-14.29	-19.10	-12.39
Dry no Freeze	90.6	0.213	0.164	89.1	0.221	0.173	-1.656	+3.182	+5.202
Wet Freeze	77.7	0.286	0.204	76.0	0.297	0.212	-2.19	+3.704	+3.774
Wet no Freeze	89.4	0.178	0.092	88.4	0. 295	0.113	-1.12	+39.661	+18.584

Based on Table (6-5), Figures (6-4), and (6-5), the following conclusions can be drawn:

- **Dry Freeze:** The results indicated that the reduction of R^2 was insignificant, while RMSE and MAE values was insignificant; the accuracy reductions were 14.29%, 19.10%, and 12.39 %, respectively. Thus, the MLR method's ability to predict IRI models of pavement distress was accurate.
- **Dry no Freeze:** The results indicated that the reduction in R^2, RMSE, and MAE values was insignificant; the accuracy reductions were 1.656%, 3.182%, and 5.202%, respectively. Thus, the MLR method's ability to predict IRI models of pavement distress was accurate.

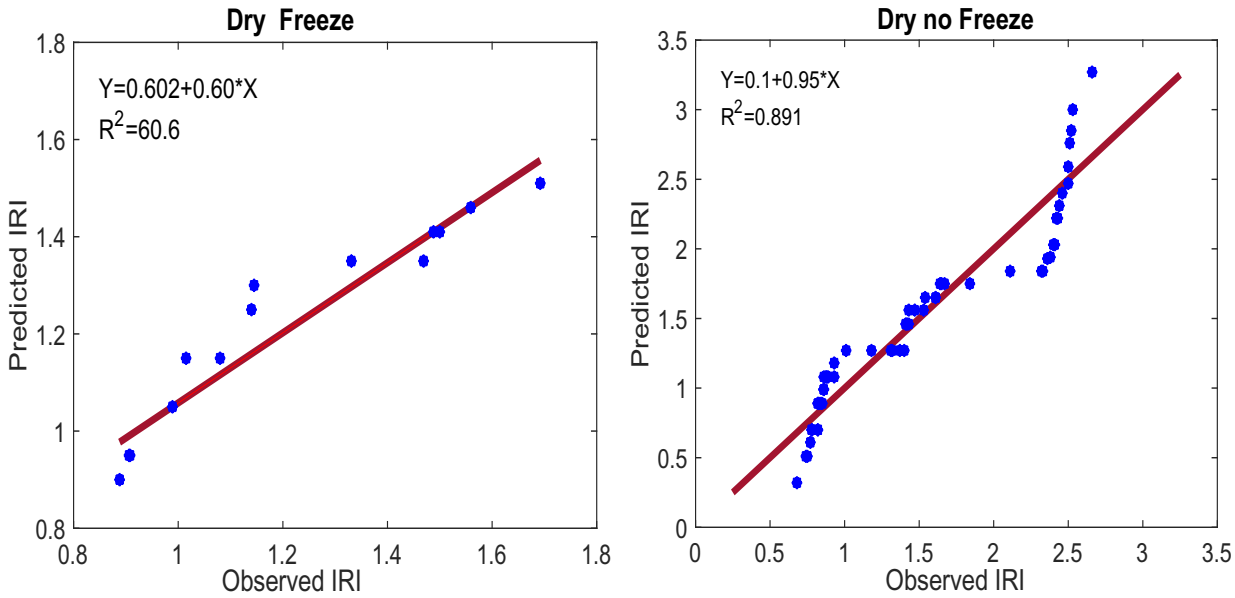

Figure 6-4: MLR model for the dry freeze and dry no freeze regions based on pavement distress.

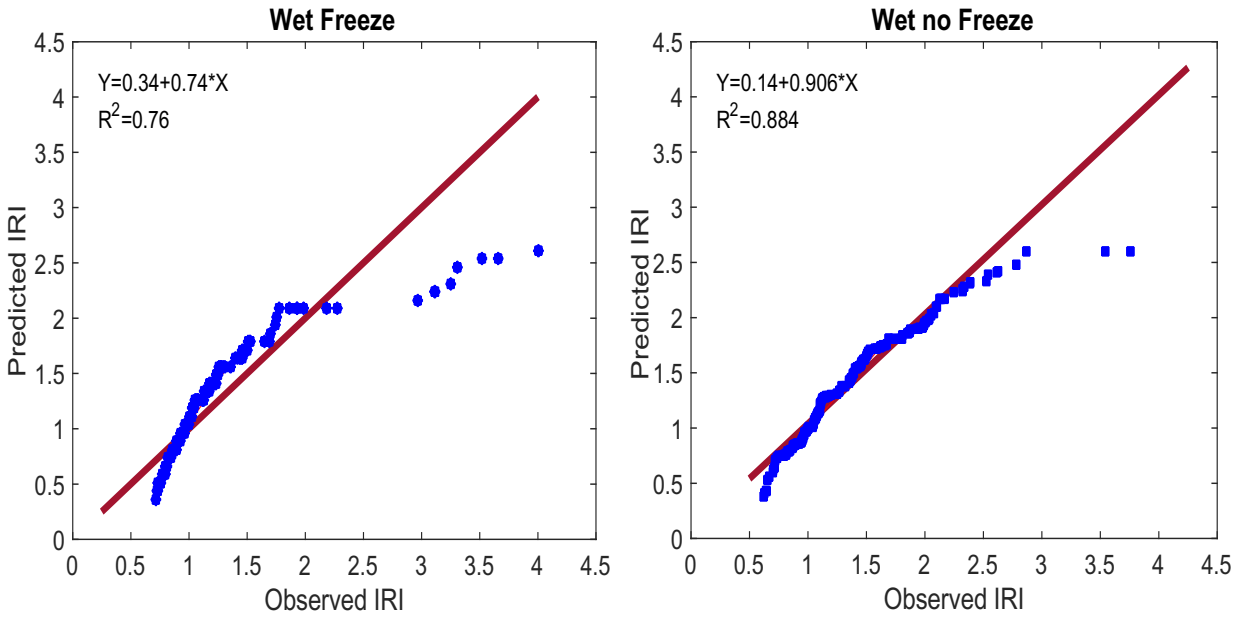

Figure 6-5: MLR model for the wet freeze and wet no freeze regions based on pavement distress.

- **Wet Freeze:** The results indicated that the reduction in R^2, RMSE, and MAE values was insignificant; the accuracy reductions were 2.19%, 3.704%, and 3.774%, respectively. Thus, the MLR method's ability to predict IRI models of pavement distress was reasonable.

- **Wet no Freeze:** The results indicated that the reduction in R^2, RMSE, and MAE values was insignificant; the accuracy reductions were 1.12%, 39.661%, and 18.584%, respectively. Thus, the MLR method's ability to predict IRI models of pavement distress was acceptable.

6.2.1.2 MLR Model Sensitivity Analysis for PCI and IRI

The PCI and IRI evaluations include a sensitivity analysis to determine the effect of input variables on the statistical prediction models' effectiveness. A multiple regression was performed, the Backward elimination approach to determine the predictor's type (pavement distress) that has significant effects on the dependent variables (PCI& IRI). The model starts with all dependent variables included, and the least important variables are eliminated. The operation ends when there are no significant variables in the model.

- **MLR Model Sensitivity Analysis for PCI**

A sensitivity analysis was conducted to determine the effects of input variables on the efficacy of the prediction models (PCI). The results of the sensitivity analysis for PCI were presented in Table (6-6) and Figure (6-6).

Based on Table (6-6) and Figure (6-6), the following conclusions can be drawn:

Dry Freeze: Compared with other variables, longitudinal cracking is the most significant factor affecting the prediction model. Age, fatigue cracking, and transverse cracking have some impacts on the prediction model. While rutting has a minor impact on the prediction model. Other parameters have no influence on the prediction model.

Table 6-6: Sensitivity analysis of prediction models for PCI based on pavement distress.

Independent Variable	R^2			
	Dry Freeze	**Dry no Freeze**	**Wet Freeze**	**Wet no Freeze**
Age	7.9	85.9	85.9	89
Rutting	1.6	8.5	2.3	-
Fatigue Cracking	10.3	6.3	15.5	0.8
Block Cracking	-	-	-	-
Longitudinal Cracking	49.1	8.0	0.3	4
Transverse Cracking	16.2	2.0	7.9	6.6
Patching	-	-		-
Potholes	-	-	-	-
Bleeding	-	-	-	-
Ravelling	-	-	-	-

Dry no Freeze: Compared with other variables, age is the most significant factor affecting the prediction model. Rutting, fatigue cracking, longitudinal cracking, and transverse cracking have some and minor impacts on the prediction model. Other parameters have no influence on the prediction model.

Wet Freeze: Compared with other variables, age is the most significant impact variable on the prediction model. Fatigue has some impact on the prediction model. While rutting, longitudinal, and transverse cracking have minor impacts on the prediction model. Other parameters have no influence on the prediction model.

Wet no Freeze: Compared with other variables, age is the most significant factors affecting the prediction model. Fatigue cracking, longitudinal and transverse cracking have some minor effects on the prediction model. Other parameters have no influence on the prediction model.

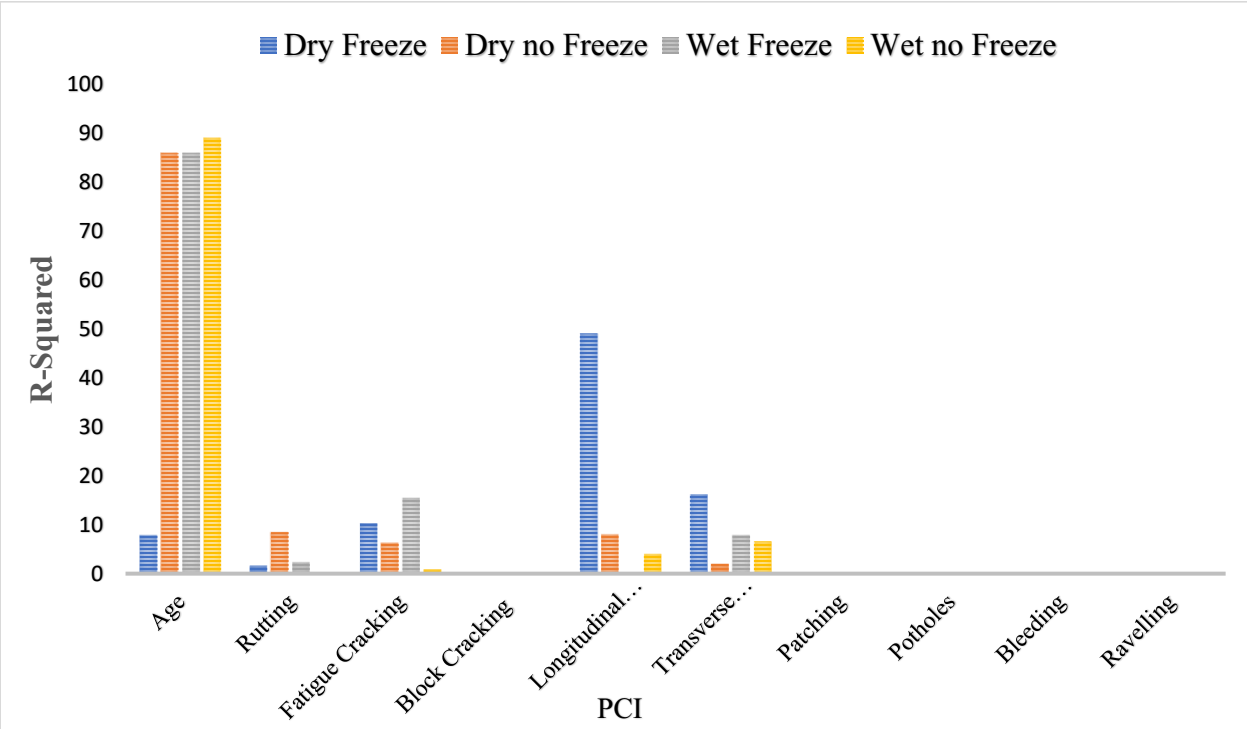

Figure 6-6: Sensitivity analysis of MLR for PCI based on pavement distress.

- **MLR Model Sensitivity Analysis for IRI**

A sensitivity analysis was conducted to determine the effects of input variables on the efficacy of prediction models (IRI). The results of the sensitivity analysis for IRI are presented in Table (6-7) and Figure (6-7).

Table (6-7) and Figure (6-7) showed the following conclusions:

Dry Freeze: Compared with other variables, age is the most significant factor affecting the prediction pavement performance model. Fatigue cracking, transverse cracking, and rutting have some impacts on the prediction model. While Longitudinal cracking has a minor effect on the prediction model. Conversely, block cracking, patching, potholes, bleeding, and ravelling do not have a statistical significance influence on pavement condition.

Table 6-7: Sensitivity analysis of prediction models for IRI for pavement distress.

Independent Variable	R^2			
	Dry Freeze	**Dry no Freeze**	**Wet Freeze**	**Wet no Freeze**
Age	79.8	88.2	76	89.3
Rutting	18.9	10.1	17	0.2
Fatigue Cracking	59	7.1	13.2	1.1
Block Cracking	-	-	-	-
Longitudinal Cracking	1.3	1.6	3.0	4.1
Transverse Cracking	50.7	1.2	5.4	7.7
Patching	-	0.1	-	-
Potholes	-	-	-	-
Bleeding	-	-	-	-
Ravelling	-	-	-	-

Dry no Freeze: Compared with other variables, age is the significant impact variable on the prediction model. Rutting has some impact on the prediction model. While fatigue cracking, longitudinal cracking, transverse cracking, and patching have minor impacts on the model. Conversely, block cracking, potholes, bleeding, and ravelling do not have a statistical significance influence on pavement condition.

Wet Freeze: Compared with other variables, age is the significant impact variable on the prediction model. Rutting and fatigue cracking have some effects on the prediction model, while longitudinal and transverse cracking have minor effects on the model. Conversely, block cracking, patching, potholes, bleeding, and ravelling do not have a statistical significance influence on pavement condition.

Wet no Freeze: Compared with other variables, age is the significant impact variable on the prediction model. Fatigue cracking, rutting, Longitudinal and transverse cracking have minor effects on the prediction model. Conversely, block cracking, patching, potholes, bleeding, and ravelling do not have a statistical significance influence on pavement condition.

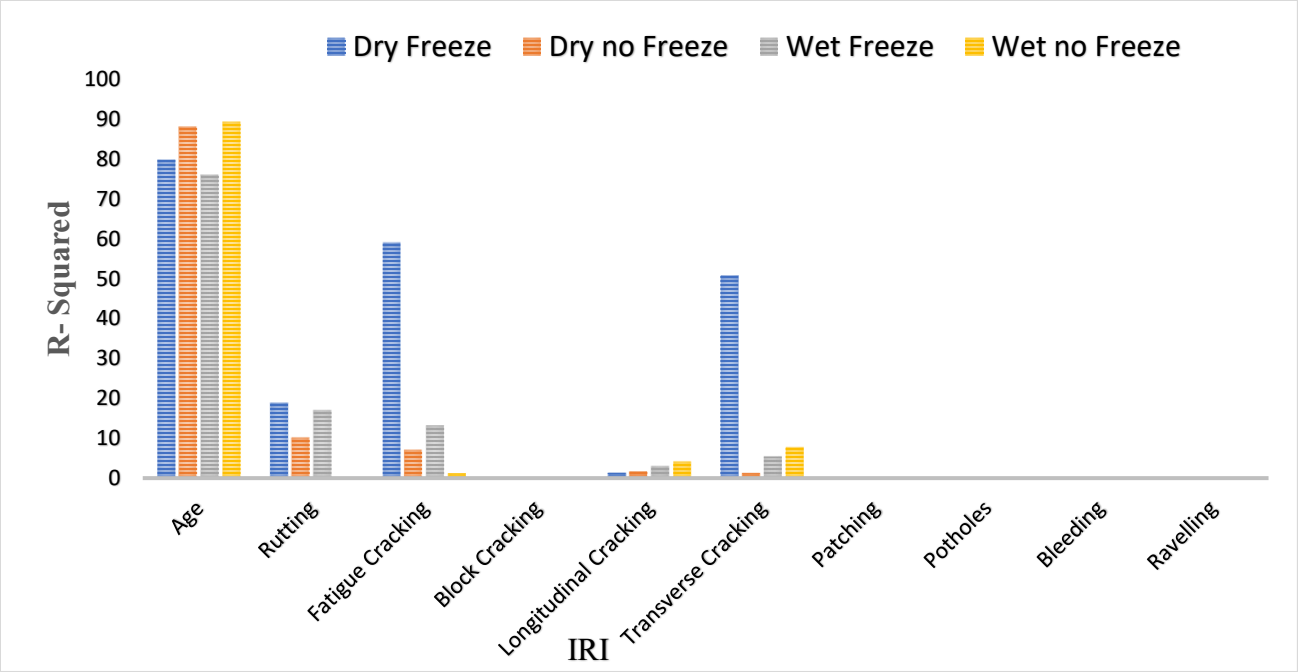

Figure 6-7: Sensitivity analysis of MLR for IRI based on pavement distress.

6.2.2 Modeling of Asphalt Pavement Performance Indices Using (ANNs) Technique

The artificial neural network has been used to train the data presented in Table (6-1). The ANNs technique aimed to model asphalt pavement performance indices (PCI and IRI) based on the age and nine pavement distress parameters as input variables for four climate regions. The inputs used were rutting, fatigue cracking, block cracking, longitudinal, transverse, patching, potholes, bleeding, and ravelling. The architecture of the designed network consists of one input layer with ten parameters, three hidden layers, and an output layer. Figure (6-8) illustrates the architecture of

the ANN. The ANNS models' performance was assessed using the three standard methods of R^2 value, RMSE, and MAE.

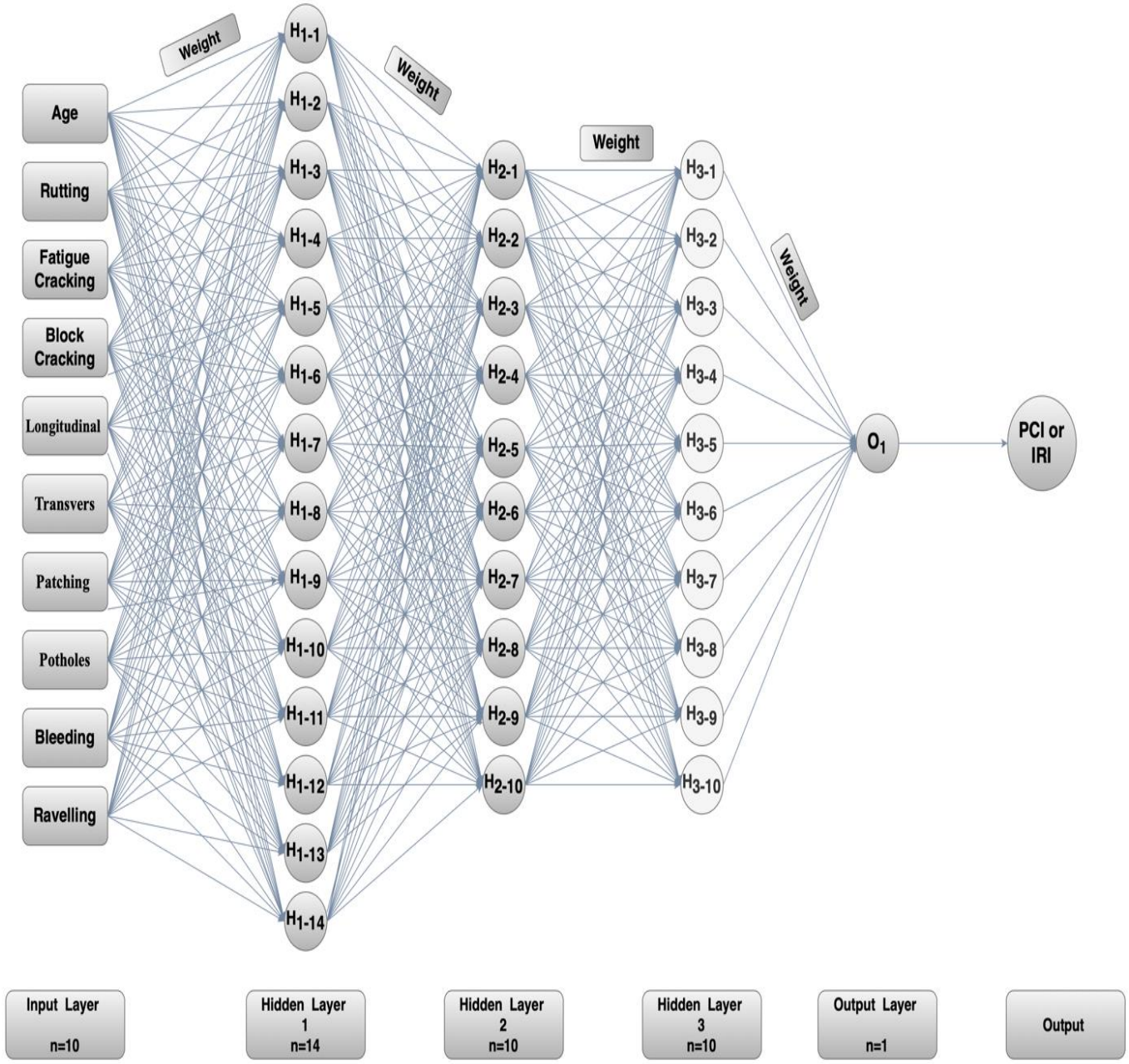

Figure 6-8: Architecture of ANN model based on pavement distress.

6.2.2.1 Modeling of Asphalt Pavement Performance Index (PCI)

Table (6-8) illustrates a summary of the PCI models by using ANNs technique based on pavement distress for four climate regions.

Table 6-8: Performance of PCI models by using ANNs technique based on pavement distress.

Climate Regions	**Statistical Error Measures (PCI)**		
	R^2	**RMSE**	**MAE**
Dry Freeze	99.1	1.425	1.417
Dry no Freeze	99.2	0.585	0.499
Wet Freeze	99.8	0.44	0.44
Wet no Freeze	98.3	1.413	1.022

Table (6-8) and Figure (6-9) showed the following conclusions:

- **Dry Freeze:** The R^2value was 99.1%, while the RMSE and MAE values were 1.425% and 1.417%.
- **Dry no Freeze:** The R^2value was 99.2%, while the RMSE and MAE values were 0.585% and 0.499%.
- **Wet Freeze:** The R^2value was 99.8%, while the RMSE and MAE values were 0.44% and 0.44%.
- **Wet no Freeze:** The R^2value was 98.3% while the RMSE and MAE values were 1.413% and 1.022%.

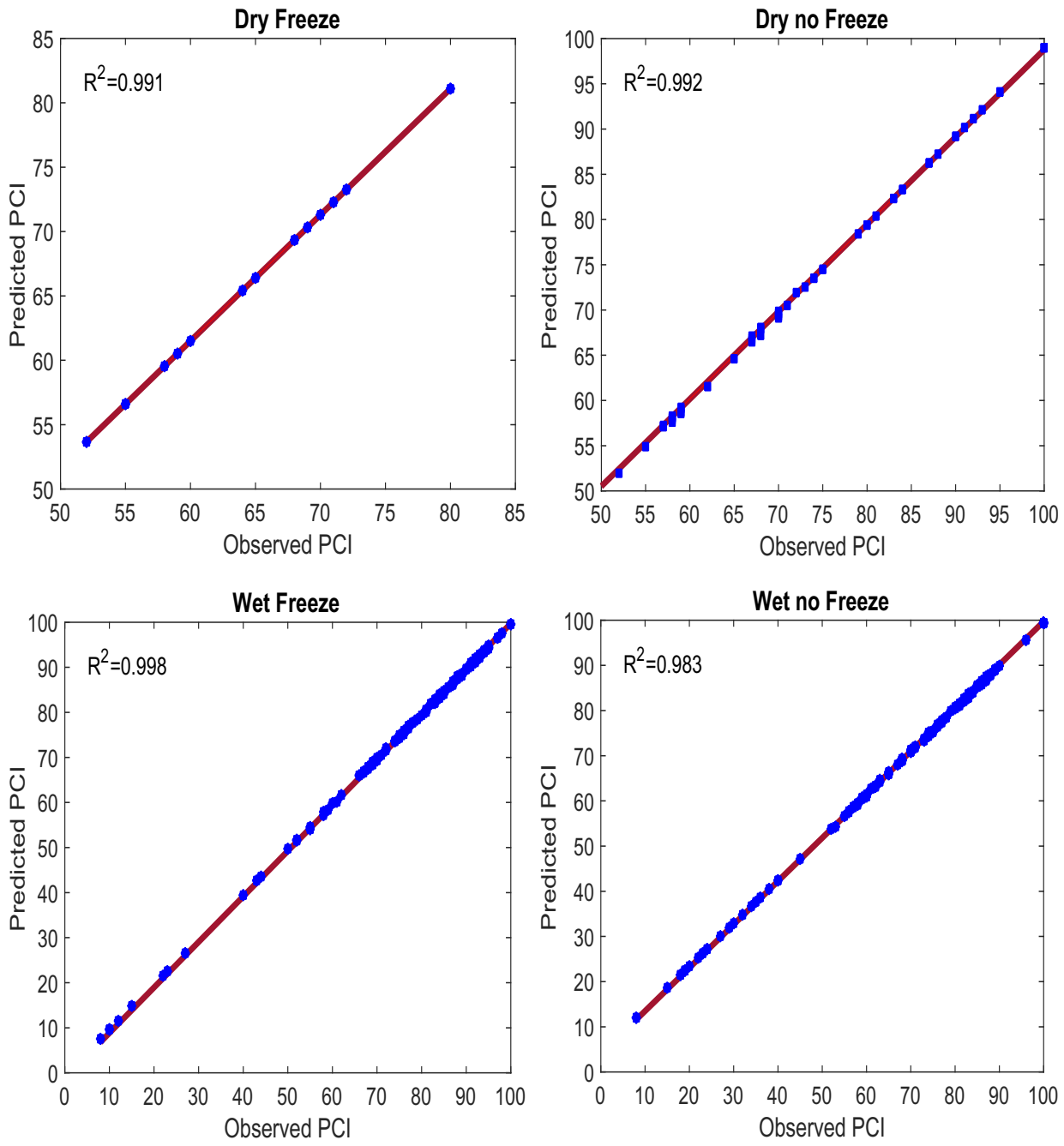

Figure 6-9: ANNs model goodness-of-fit results for PCI values based on pavement distress.

6.2.2.2 Modeling of Asphalt Pavement Performance Indices (IRI)

Table (6-9) illustrates a summary of the IRI models by using ANNs technique, based on pavement distress for four climate regions.

Table 6-9:Performance of IRI models by using ANNs technique based on pavement distress.

Climate Regions	**Statistical Error Measures (IRI)**		
	R^2	**RMSE**	**MAE**
Dry Freeze	99.8	0.008	0.007
Dry no Freeze	99.5	0.006	0.005
Wet Freeze	99.1	0.021	0.021
Wet no Freeze	97.5	0.028	0.023

Based on Tables (6-9), and Figure (6-10), the following conclusions can be drawn:

- **Dry Freeze:** The R^2value was 99.8%, while the RMSE and MAE values were 0.008% and 0.007%.
- **Dry no Freeze:** The R^2value was 99.5%, while the RMSE and MAE values were 0.006% and 0.005%.
- **Wet Freeze:** The R^2value was 99.1%, while the RMSE and MAE values were 0.021% and 0.021%.
- **Wet no Freeze:** The R^2value was 97.5%, while the RMSE and MAE values were 0.028% and 0.023%.

Larger values of R^2 and lower values of RMSE and MAE suggest that a strong correlation exists between the predicted and the measured IRI values.

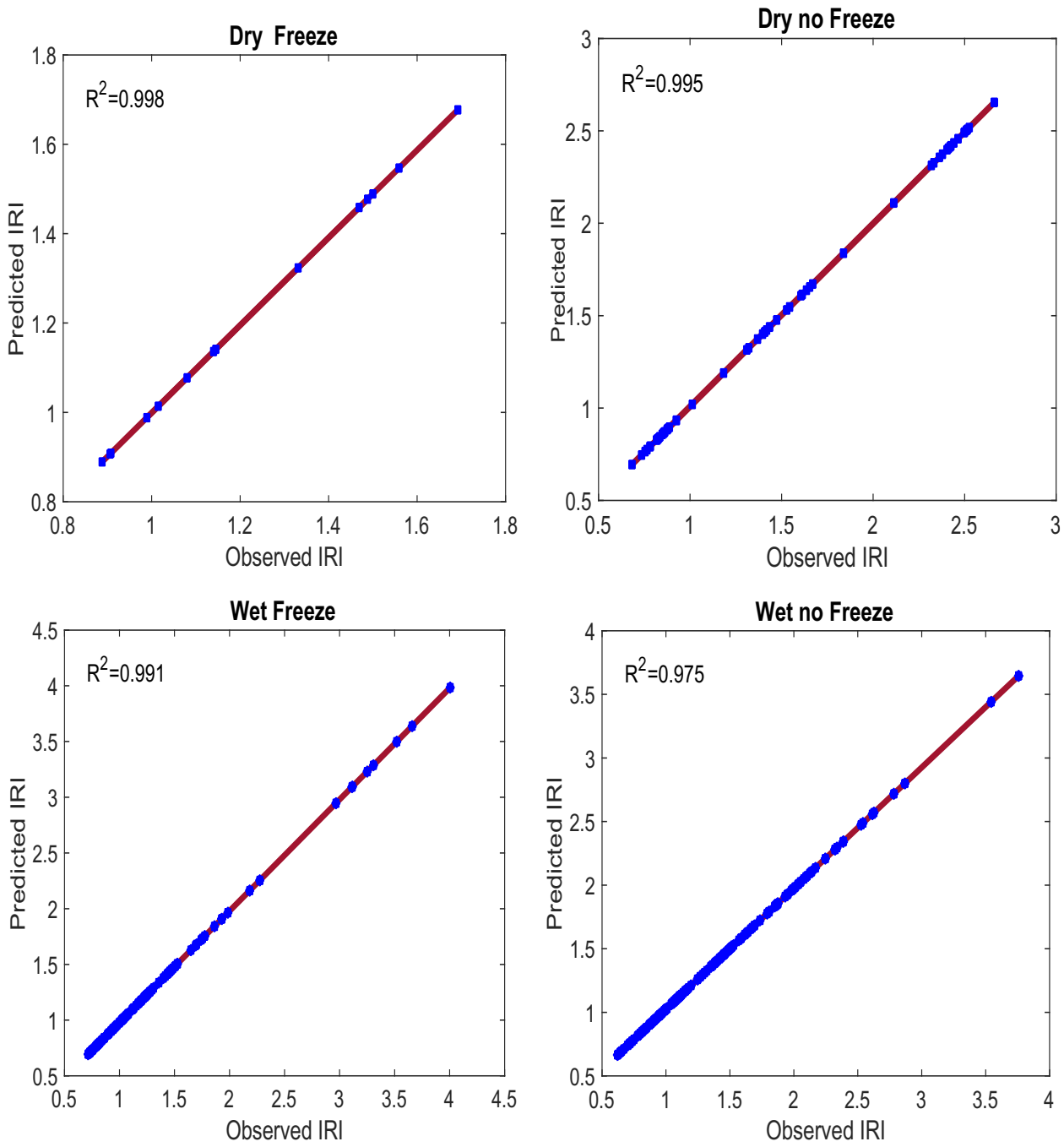

Figure 6-10: ANNs model goodness-of-fit results for IRI values based on pavement distress.

6.2.3 Validation of ANN Models

A total of 408 observations have been chosen from the LTPP dataset for four climate regions investigations were used in ANNs modeling, where 70% of the data set was used for training, 15% for testing, and 15% for validation (checking) the network. Tables (6-10) and (6-11) show the results of the models for the validation dataset.

- **Validation of PCI Models**

The statistical error measures R^2 and RMSE were used to evaluate the performance of the ANNs models. Based on the R^2values, all models had a strong correlation, as their R^2values exceeded 98%, while with RMSE values, all models had a low error, as their error did not exceed 1.515%. Thus, the ANNs technique's ability to predict PCI models of pavement distress was accurate. Table (6-10) illustrates Validation of PCI models for all sections in the four climate regions.

Table 6-10: Validation of PCI models based on pavement distress.

Climate Regions	**Statistical Error Measures (PCI)**					
	R^2			**RMSE**		
	Traning	Testing	Validation	Traning	Testing	Validation
Dry Freeze	98.6	99.7	99.3	1.361	0.792	1.425
Dry no Freeze	99.1	99.4	100	0.308	0.930	0.959
Wet Freeze	99.9	99.6	99.8	0.275	0.873	1.515
Wet no Freeze	98.4	98.6	98.4	1.994	4.174	0.964

- **Validation of IRI Models**

The statistical error measures $R^2$and RMSE were used to evaluate the performance of the ANNs models. Based on the R^2 values, all models had a strong correlation, as their R^2 values exceeded 99%, while for RMSE values, all models had minor errors. Thus, the ANNs technique's ability to predict IRI models of pavement distress was accurate. Table (6-11) illustrates Validation of IRI models for all sections in the four climate regions.

Table 6-11: Validation of IRI models based on pavement distress.

Climate Regions	**Statistical Error Measures (IRI)**					
	R^2			**RMSE**		
	Traning	Testing	Validation	Traning	Testing	Validation
Dry Freeze	99.6	99.8	99.8	0.009	0.026	0.037
Dry no Freeze	99.7	100	100	0.024	0.062	0.04
Wet Freeze	99.9	99.9	99.6	0.027	0.002	0.009
Wet no Freeze	99.4	99.6	99.1	0.044	0.019	0.102

6.2.4 Comparison of the Models

To validate the developed models in this part, all models were evaluated by comparing MLR and ANNs techniques based on pavement distress for four climate regions, as shown in Tables (6-12) and (6-13).

6.2.4.1 Comparison of MLR and ANNs Models for PCI

The performance of the MLR models was compared with the performance of the ANNs models to evaluate the accuracy of the models in predicting pavement performance based on pavement

distress parameters. R^2, RMSE and MAE values were used to measure and compare the performance of the models. Table (6-12) and Figures (6-12) and (6-13) present the comparison of the MLR models to the ANNs models for PCI.

Table 6-12: Comparison of the MLR and ANNs models for PCI based on pavement distress.

Climate Regions	**Statistical Error Measures (PCI)**								
	MLR Generated			**ANNs Generated**			**Improvement (%)**		
	$\boldsymbol{R^2}$	**RMSE**	**MAE**	$\boldsymbol{R^2}$	**RMSE**	$\boldsymbol{MAE}$	$\boldsymbol{R^2}$	**RMSE**	$\boldsymbol{MAE}$
Dry Freeze	77	5.468	4.361	99.1	1.425	1.417	+22.30	+73.94	+67.51
Dry no Freeze	91.6	4.247	3.2	99.2	0.585	0.499	+7.66	+86.23	+84.41
Wet Freeze	86.8	7.195	5.616	99.8	0.44	0.44	+13.03	+93.88	+92.17
Wet no Freeze	89.3	7.324	5.79	98.3	1.413	1.022	+9.16	+80.71	+82.35

ANNs and MLR models for PCI were compared in Table (6-12). Accordingly, the following conclusions can be drawn:

- The statistics indicated R^2values from the ANNs models were higher than its MLR counterpart by 22.30%, 7.66%, 13.03%, and 9.16% for dry freeze, dry no freeze, wet freeze, and wet no freeze, respectively.
- The RMSE values of the ANNs models were less than its MLR counterparts by 73.94%, 86.23%, 93.88%, and 80.71% for dry freeze, dry no freeze, wet freeze, and wet no freeze, respectively.
- The MAE values of the ANNs models were less than its MLR counterparts by 67.51%, 84.41 %, 92.17 %, and 82.35 % for dry freeze, dry no freeze, wet freeze, and wet no freeze, respectively.

- Larger values of R^2 and lower values of RMSE and MAE suggest that a strong correlation exists between the predicted and the measured PCI values.

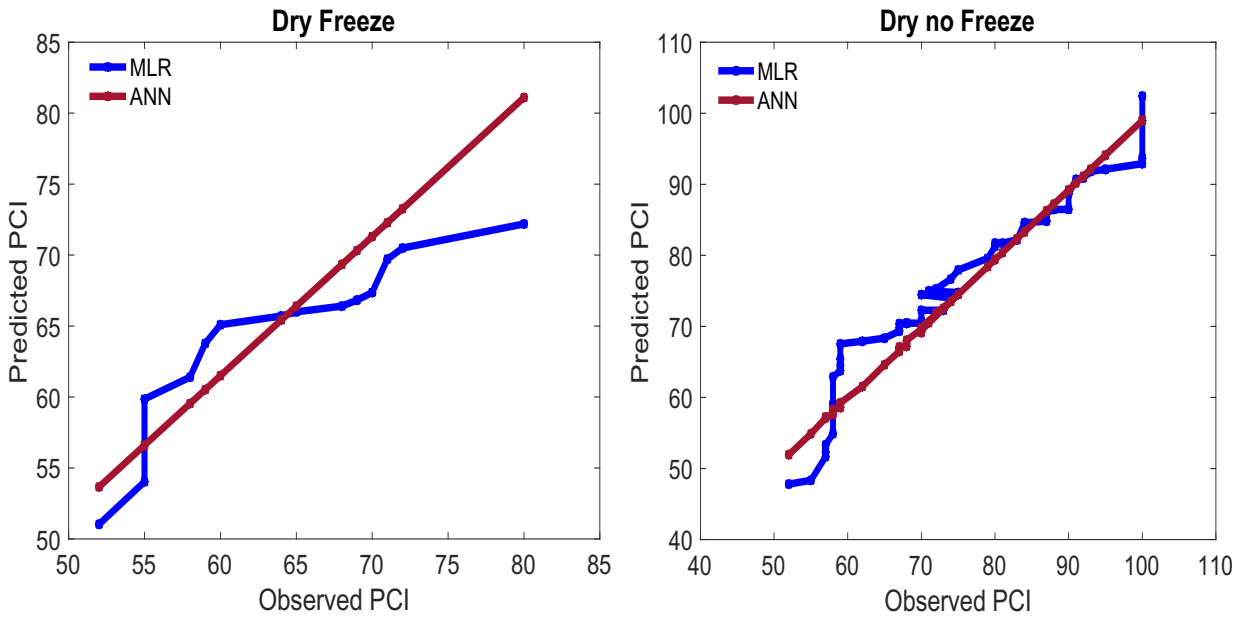

Figure 6-11: Fitness of MLR and ANNs models to PCI prediction based on pavement distress data from two climate regions: (left) dry freeze; (right) dry no freeze.

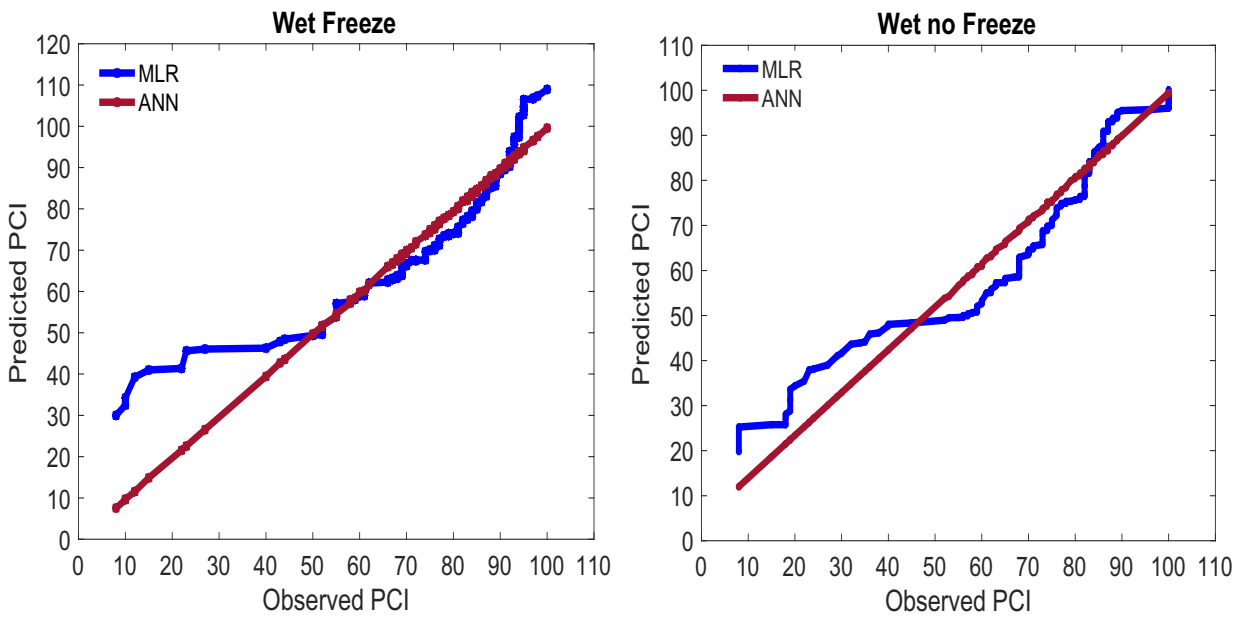

Figure 6-12: Fitness of MLR and ANNs models to PCI prediction based on pavement distress data from two climate regions: (left) wet freeze; (right) wet no freeze.

Several conclusions can be drawn from Figures (6-11) and (6-12):

- The MLR approach had a slight corrugation while ANNs had a straight line, which explains why ANNs models tend to be more accurate.
- Figures clearly showed that the ANNs prediction models provided more accuracy than the MLR models under different climate conditions.

Table (6-12), Figures (6-11), and (6-12) showed that the MLR and ANNs models have an actual ability to the predict PCI. In addition, the ANNs technique can predict the PCI with higher accuracy than the MLR technique in all cases.

6.2.4.2 Comparison of ANNs and MLR Models for IRI

The performance of the MLR models was compared with the performance of the ANNs models to evaluate the accuracy of the models in predicting pavement performance based on pavement distress parameters. R^2, RMSE and MAE values were used to measure and compare the performance of the models. Table (6-13) and Figures from (6-13) and (6-14) present the comparison of the MLR models to the ANNs models for IRI.

Table 6-13: Comparison of the MLR and ANNs models for IRI based on pavement distress.

Climate Regions	**Statistical Error Measures (IRI)**								
	MLR Generated			**ANNs Generated**			**Improvement (%)**		
	R^2	**RMSE**	**MAE**	R^2	**RMSE**	MAE	R^2	**RMSE**	MAE
Dry Freeze	70.7	0.144	0.099	99.8	0.008	0.007	+29.16	+94.44	+92.29
Dry no Freeze	90.6	0.213	0.164	99.5	0.006	0.005	+9.94	+97.18	+96.95
Wet Freeze	77.7	0.286	0.204	99.1	0.021	0.021	+21.59	+92.66	+89.71
Wet no Freeze	89.4	0.178	0.092	97.5	0.028	0.023	+8.31	+84.30	+75.00

According to Table (6-13), several conclusions can be drawn:

- The statistics indicated R^2values from the ANNs models were higher than the R^2values of the MLR models by 29.16%, 9.94%, 21.59%, and 8.31% for dry freeze, dry no freeze, wet freeze, and wet no freeze, respectively.
- The RMSE values of the ANN models were less than the RMSE values of the MLR models by 94.44%, 97.18%, 92.66%, and 84.30%, for dry freeze, dry no freeze, wet freeze, and wet no freeze, respectively.
- The MAE values of the ANNs models were less than the MAE values of the MLR models by 92.29 %, 96.95 %, 89.71 %, and 75 %for dry freeze, dry no freeze, wet freeze, and wet no freeze, respectively.

Table (6-13), and Figures (6-13) and (6-14) showed that the MLR and ANNs models have an ability to perform the prediction of IRI models. In addition, the ANNs technique can predict the IRI models with higher accuracy than the MLR technique in all cases. This result is consistent with some previous research. For example, Chandra et al. (2012) compared the performance of ANN and MLR models in predicting pavement roughness from various types of distress. They found that the ANN model is significantly more accurate than the MLR model, with a mean square error of 18% lower.

Alharbi (2018) compared the performance of ANN and MLR models in riding, cracking, and rutting indices. The R^2 values from the MLR models were lower than the R^2 values of the ANN models by 61.40%, 48.15%, and 48.15% for riding, cracking, and rutting index, respectively.

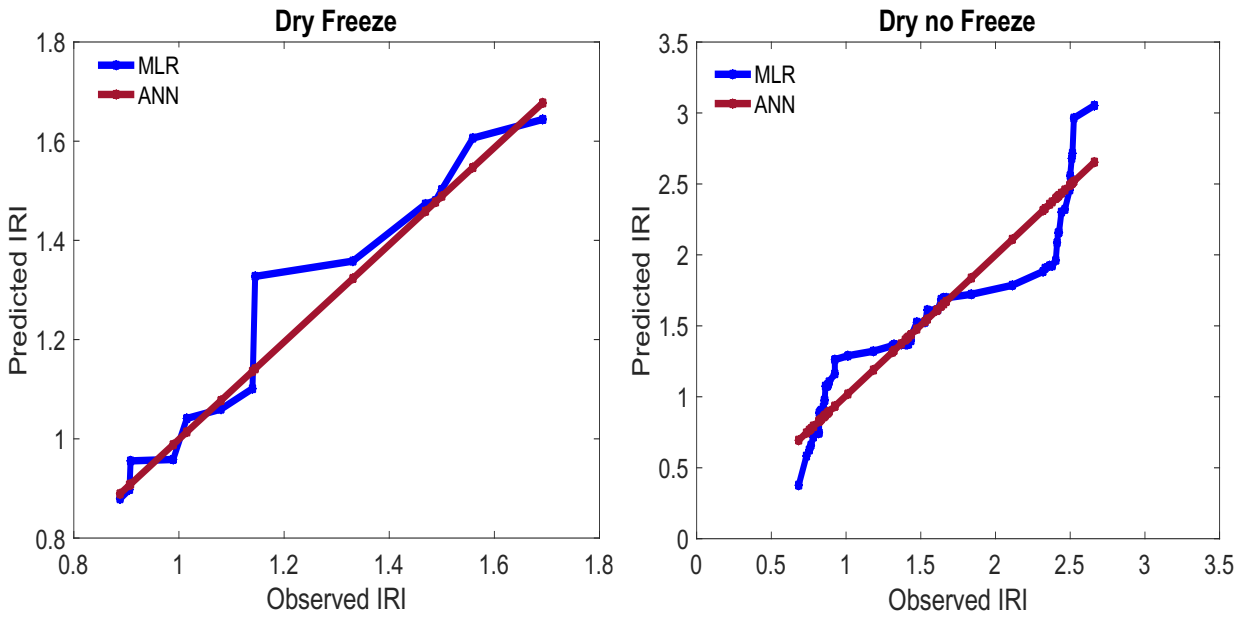

Figure 6-13: Fitness of MLR and ANNs models to IRI prediction based on pavement distress data from two climate regions: (left) dry freeze; (right) dry no freeze.

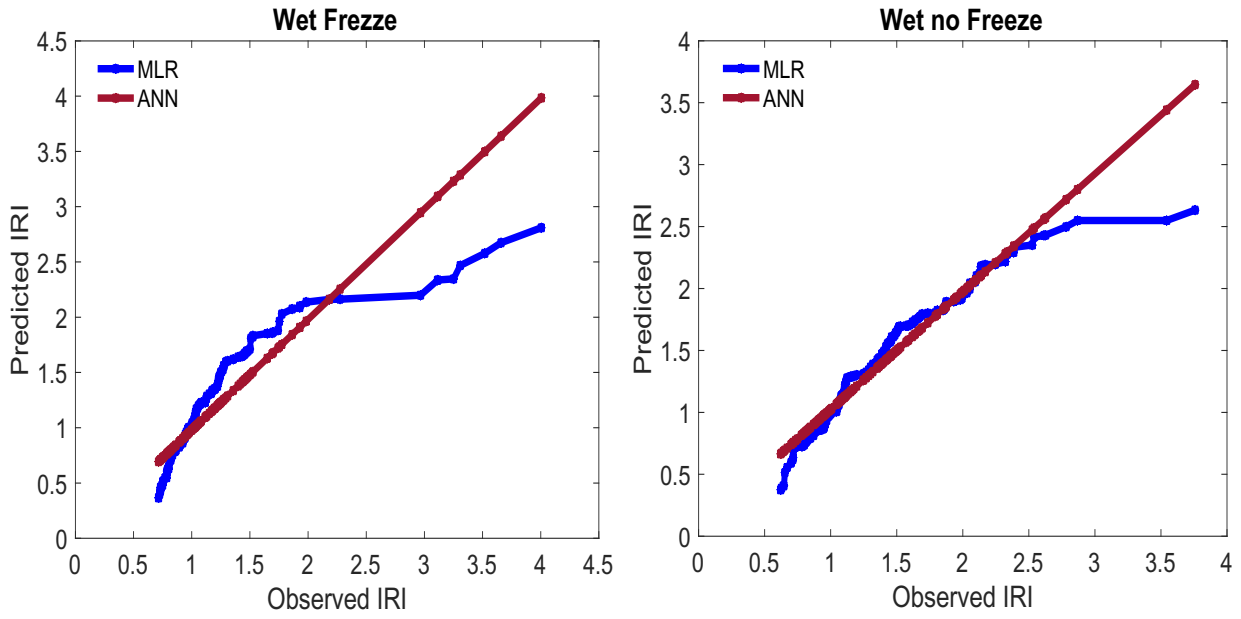

Figure 6-14: Fitness of MLR and ANNs models to IRI prediction based on pavement distress data from two climate regions: (left) wet freeze; (right) wet no freeze.

6.2.5 Summary

This part of the research focused on modeling asphalt pavement performance indices (PCI and IRI) based on pavement distress variables and studying the effect of these variables on asphalt pavement performance indices for four climate regions in the U.S. and Canada. Several important advantages were drawn from the MLR and the ANNs technique, as follows:

- Nine pavement distress variables and the age of the pavement were included for four climate regions. Rutting, fatigue cracking, block cracking, transverse cracking, patching, potholes, bleeding, and ravelling were considered independent variables in developing the models to predict PCI and IRI.
- The MLR and ANNs models have an ability to perform the prediction of PCI and IRI models. In addition, the ANNs prediction models provided more accuracy than the MLR models under four climate regions.
- Even though the ANN technique does not provide equations for predicting PCI and IRI as the MLR technique, the models can be used to forecast pavement distress with high accuracy. The approach has good accuracy since itsR^2values exceed 97 %, as evidenced by the R^2 values.
- There is a considerable reduction in error value when using the ANNs technique for each climate region compared to the MLR technique.
- Modelling of distress parameters is helpful for predicting pavement destress. Incorporating additional sections with different distresses and various severities improves the model results, which helps the programme to learn and develop models. The present study uses nine distress parameters for predicting the (PCI) and IRI. Future studies may include some more parameters like construction number, corrugation, slippage cracks, depression, polished aggregate, shoving to further improve these models.

6.3 Effect of Environmental Parameters on IRI and PCI Values

This section focused on modeling asphalt pavement performance indices (PCI and IRI) based on environmental variables and studying the effect of these variables on asphalt pavement performance indices for four climate regions in the U.S. and Canada. The relevant data were collected on the environmental parameters of 53 road sections with 408 observations from the LTPP dataset and distributed to four climate regions (dry freeze, dry no freeze, wet freeze, wet no freeze). The present study was divided into three phases as follows:

- Modeling of asphalt pavement performance indices using (MLR) technique.
- Modeling of asphalt pavement performance indices using (ANNs) technique.
- Comparison and validation of the MLR and ANNs models.

Eight environmental variables were assessed effect and used to predict the PCI and IRI for each climate region, including the age of pavement, the annual average freezing temperature, the average freeze index, the number of freeze days, the average annual precipitation, the average total snowfall, average speed wind, and humidity average.

Note that both the type of asphalt concrete pavement (ACP) and subgrade (coarse-grained) were constant for all data regions. Table (6-14) briefly describes the selected dataset of environmental.

Table 6-14: Gathered environmental data from four climate regions.

Parameters	Unit	Climate Regions			
		Dry Freeze	Dry no Freeze	Wet Freeze	Wet no Freeze
PCI	%	52-80	50-100	8-91	8-100
IRI	(m/km)	0.89-1.69	0.68-2.66	0.79-4.04	0.75-3.76
Number of data samples	Number	14	61	144	189
Age	Year	6-18	3-34	3-33	1-31
Temperature average	° C	4.95-9.9	10.5-25.2	4.1-14.1	12.1-25.6
Freeze Index	° C/day	86.4-726	1-182	65-1759	0-185
Number of freeze Days	Number	82-133	45-83	78-143	0-87
Total average annual precipitation	(mm)	345-702.6	50.7-737.3	349.9-1881.2	357.5-4917
Total Snowfall	(%)	425-2371	0-184	561-10325	0-916
Wind average	Km/h	4-5.5	3.5-7.2	3.3-7.25	2.4-7.8
Humidity	%	57.5-86	53.5-71	42.5-82	37-77.5

6.3.1 Modeling of Asphalt Pavement Performance Indices Using (MLR) Technique

Research in this part focuses on studying the influence of environmental factors on the road condition indicator values PCI and IRI across four climate regions in the U.S. and Canada. Eight prediction models were developed using multiple regression analysis techniques from the collected data. The PCI and IRI regression models are shown in Tables (6-15) and (6-16). Eight prediction models were developed using multiple regression analysis techniques from the collected data. Environmental data collected for each section of asphalt pavement included eight input variables. The PCI regression analysis results illustrated in Table (6-15) indicate that the R^2 values were 71.4%, 91.8%, 87.3%, and 89.5% for dry freeze, dry no freeze, wet freeze, and wet no freeze, respectively.

Table 6-15: PCI models summary based on environmental parameters.

Model	PCI			
	Dry Freeze	**Dry no Freeze**	**Wet Freeze**	**Wet no Freeze**
R^2	71.4	91.8	87.3	89.5
Constant	133.91	144.75	108.40	118.43
Age	-0.784	– 1.993	-2.71	–3.053
Temperature average	-8.044	0.043	–0.89	-0.244
Freeze Index	-0.035	-0.047	0.004	-0.088
Number of freeze Days	0.12	-0.041	-0.088	0.19
Total average annual precipitation	0.003	- 0.004	0.001	0.001
Total Snowfall	0.005	-0.001	-	0.006
Wind average	-11.24	-1.10	0.101	0.054
Humidity	0.837	-0.52	0.107	-0.103

Table 6-16: IRI models summary based on environmental parameters.

Model	IRI			
	Dry Freeze	**Dry no Freeze**	**Wet Freeze**	**Wet no Freeze**
R^2	74	90.2	81	89.6
Constant	0.324	0.552	0.508	0.059
Age	0.015	0.086	0.077	0.073
Temperature average	0.177	-0.14	-0.054	0.006
Freeze Index	-	-0.002	-	-
Number of freeze Days	-0.003	0.001	0.004	-
Total average annual precipitation	$-3.9x10^{-5}$	0.000021	$3.8x10^{-5}$	$2.53x10^{-5}$
Total Snowfall	$-4.8x10^{-5}$	0.001	$-2.5x10^{-5}$	$-7.788x10^{-5}$
Wind average	0.26	0.036	-0.016	0.009
Humidity	-0.027	-0.005	-0.002	0.001

The IRI regression analysis results illustrated in Table (6-16) indicate that the R^2 values were 74%, 90.2%, 81%, and 89.6% for dry freeze, dry no freeze, wet freeze, and wet no freeze, respectively. Equations from (6-9) to (6-16) summarised the regression models for four climate regions as follows:

1- **Dry Freeze**

Table (6-15) presents the regression analysis results for PCI for the dry freeze area. The PCI model was negatively correlated with age, temperature average, freeze index, and wind average. The PCI model was positively correlated with number of freeze days, total average annual precipitation, total snowfall, and humidity. Equation (6-9) described the relationship between the PCI and environmental parameters as follows:

$$\boldsymbol{PCI = 133.91 - 0.784\, X_{age} - 8.044\, W_1 - 0.035\, W_2 + 0.12\, W_3 + 0.003\, W_4 + 0.005\, W_5 - 11.24\, W_6 + 0.837\, W_7} \qquad \textbf{6-9}$$

The correlation coefficient (R^2) of this relationship is **71.4%.**

Table (6-16) presents the regression analysis result of IRI for the dry freeze area. The IRI model was positively correlated with age, temperature average, and wind average. The IRI model was negatively correlated with number of freeze days, total average annual precipitation, total snowfall, and humidity. Equation (6-10) described the relationship between the IRI and environmental parameters as follows:

$$\boldsymbol{IRI = 0.324 + 0.015X_{age} + 0.177\, W_1 - 0.003\, W_3 - 3.9x10^{-5} W_4 - 4.8X10^{-5} W_5 + 0.26W_6 - 0.027\, W_7} \qquad \textbf{6-10}$$

The correlation coefficient (R^2) of this relationship is **74%.**

2- **Dry no Freeze**

The regression analysis result of the PCI model for the dry no freeze area is shown in Table (6-15). The PCI model was negatively correlated with age, freeze index, number of freeze days, total average annual precipitation, total snowfall, wind average, and humidity. The PCI was positively correlated with temperature average. Equation (6-11) described the relationship between the PCI and environmental parameters as follows:

$$\boldsymbol{PCI = 144.75 - 1.993X_{age} + 0.043\,W_1 - 0.047\,W_2 - 0.041\,W_3 - 0.004\,W_4 - 0.001\,W_5 - 1.10W_6 - 0.52\,W_7} \qquad \textbf{6-11}$$

The correlation coefficient (R^2) of this relationship is **91.8%.**

The regression analysis result of the IRI model for the dry no freeze area is presented in Table (6-16). The IRI model was negatively correlated with temperature average, freeze index, total average annual precipitation, and humidity. The IRI model was positively correlated with age, number of freeze days, total snowfall, and wind average. Equation (6-12) described the relationship between the IRI and environmental parameters as follows:

$$\boldsymbol{IRI = 0.552 + 0.086X_{age} - 0.14W_1 - 0.002W_2 + 0.001W_3 - 0.000021\,W_4 + 0.001W_5 + 0.036W_6 - 0.005\,W_7} \qquad \textbf{6-12}$$

The correlation coefficient (R^2) of this relationship is **90.2%.**

3- **Wet Freeze**

The regression analysis result of the PCI model for the wet freeze area is presented in Table (6-15). The PCI model was negatively correlated with age, temperature average, and number of freeze days. The PCI model was positively correlated with freeze index, total average annual

precipitation, wind average, and humidity. Equation (6-13) described the relationship between the PCI and environmental parameters as follows:

$$\mathbf{PCI=108.4-2.71}X_{age}\mathbf{-0.89}W_1\mathbf{+0.0044}W_2\mathbf{-0.088}\,W_3\mathbf{+0.001}\,W_4\mathbf{+0.101}\,W_6\mathbf{+0.107}\,W_7 \qquad \textbf{6-13}$$

The correlation coefficient (R^2) of this relationship is **87.3%.**

The regression analysis result of the IRI model for the wet freeze area is presented in Table (6-16). The IRI model was negatively correlated with temperature average, total snowfall, wind average, and humidity. The IRI model was positively correlated with age, number of freeze days, and total average annual precipitation. Equation (6-14) described the relationship between the IRI and environmental parameters as follows:

$$\boldsymbol{IRI = 0.508 + 0.077}X_{age}\boldsymbol{- 0.054}W_1\boldsymbol{+ 0.004}W_3\boldsymbol{+ 3.8x10^{-5}}W_4\boldsymbol{- 2.5 \times 10^{-5}}W_5\boldsymbol{-}$$
$$\boldsymbol{0.016}\,W_6\boldsymbol{- 0.002}W_7 \qquad \textbf{6-14}$$

The correlation coefficient (R^2) of this relationship is **81%.**

4- <u>Wet no Freeze</u>

The regression analysis result of the PCI model for the wet no freeze area is presented in Table (6-15). The PCI model was negatively correlated with age, temperature average, freeze index, and humidity. The PCI model was positively correlated with number of freeze days, total average annual precipitation, total snowfall, wind average. Equation (6-15) described the relationship between the PCI and environmental parameters as follows:

$$\boldsymbol{PCI = 118.43 - 3.053X_{age} - 0.244W_1 - 0.008W_2 + 0.19\,W_3 + 0.001W_4 + 0.006\,W_5 + 0.054W_6 - 0.013W_7} \quad \textbf{6-15}$$

The correlation coefficient (R^2) of this relationship is **89.5%.**

The regression analysis result of the IRI model for the dry no freeze area is presented in Table (6-16). The IRI was negatively correlated with total snowfall. The IRI was positively correlated with age, temperature average, total average annual precipitation, wind average, and humidity. Equation (6-16) described the relationship between the IRI and environmental parameters as follows:

$$\boldsymbol{IRI = 0.059 + 0.073X_{age} + 0.06W_1 + 2.53 \times 10^{-5}W_4 - 7.788 \times 10^{-5}W_5 + 0.009W_6 + 0.001\,W_7} \quad \textbf{6-16}$$

The correlation coefficient (R^2) of this relationship is **89.6%.**

6.3.1.1 Validation of MLR Models

- **Validation of PCI Models**

After the validation test, Table (6-17) illustrates the reduction in R^2, RMSE, and MAE values for all sections in the four climate regions.

Based on Table (6-17), Figures (6-15), and (6-16), the following conclusions can be drawn:

- **Dry Freeze:** The results indicated that the reduction in R^2, RMSE, and MAE values was insignificant; the accuracy reductions were 23.81%, 24.96%, and 7.57%, respectively. Thus, the MLR method's ability to predict PCI models of environmental parameters was accurate.

Table 6-17: Validation of PCI models based on environmental parameters.

Climate Regions	Statistical Error Measures (PCI)								
	MLR			Validation			Reduction % (±)		
	R^2	RMSE	MAE	R^2	RMSE	MAE	R^2	RMSE	MAE
Dry Freeze	71.4	4.114	3.482	54.4	5.483	3.767	-23.81	+24.96	+7.57
Dry no Freeze	91.8	6.586	4.194	88.2	5.162	3.786	-3.92	-21.62	-9.73
Wet Freeze	87.3	7.057	5.642	85.8	7.468	5.85	-1.72	+5.50	+3.56
Wet no Freeze	89.5	6.606	5.481	72.0	7.532	5.946	-19.55	+12.29	+7.82

- **Dry no Freeze:** The results indicated that the reduction of R^2 , RMSE, and MAE was insignificant; the accuracy reductions were 3.92%, 21.62%, and 9.73%, respectively. Thus, the MLR method's ability to predict PCI models of the environmental parameters with was accuracy.
- **Wet Freeze:** The results indicated that the reduction in R^2, RMSE, and MAE values was insignificant; the accuracy reductions were 1.72%, 5.50%, and 3.56%, respectively. Thus, the MLR method's ability to predict PCI models of environmental parameters was good.
- **Wet no Freeze:** The results indicated that the reduction of R^2, RMSE, and MAE was insignificant, while; the accuracy reductions were 19.55%,12.29%, and 7.82%, respectively. Thus, the MLR method's ability to predict PCI models of environmental parameters was accuracy.

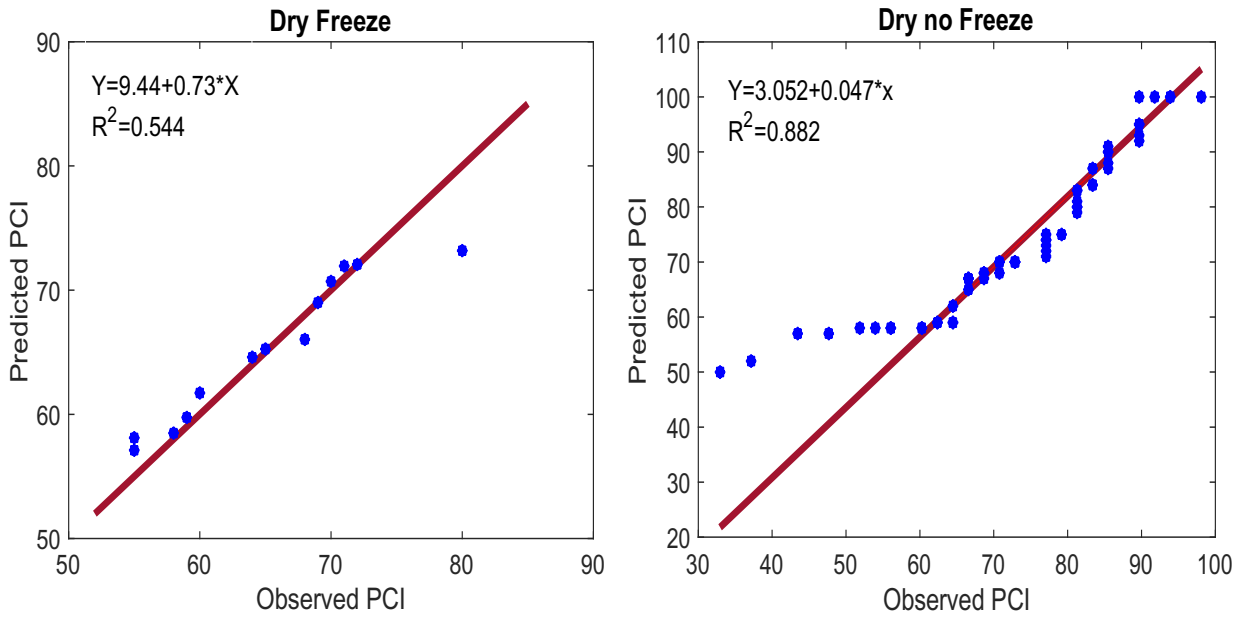

Figure 6-15: MLR model for the dry freeze and the dry no freeze region based on environmental.

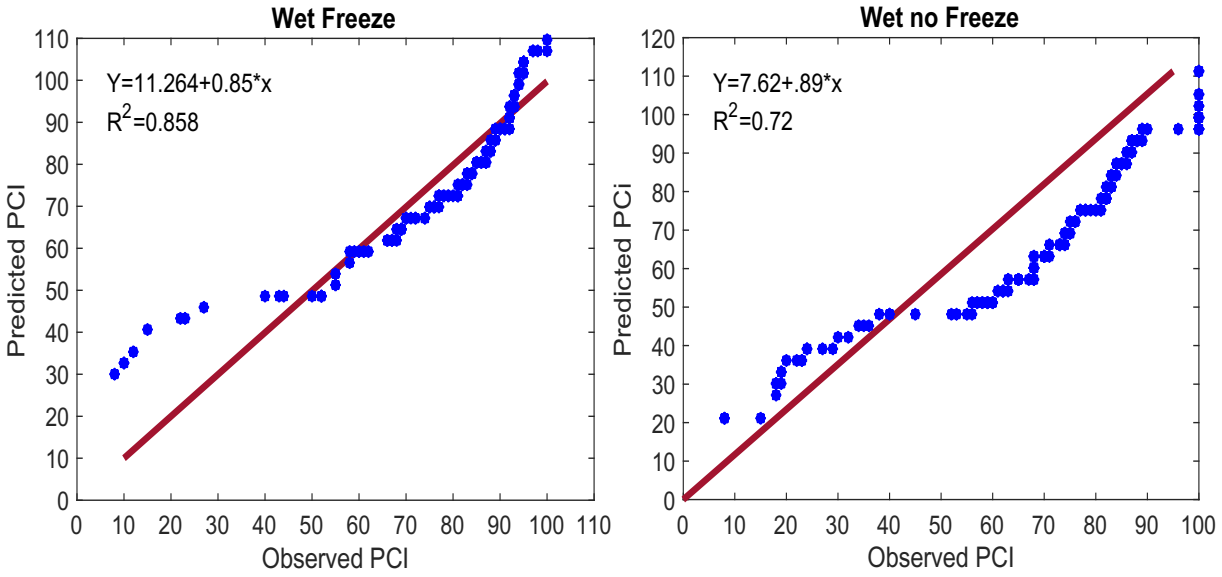

Figure 6-16: MLR model for the wet freeze and the wet no freeze region based on environmental.

- **Validation of IRI Models**

After the validation test, Table (6-18) illustrates the reduction in R^2, RMSE, and MAE values for all sections in the four climate regions.

Table 6-18: Validation of PCI models based on environmental parameters.

Climate Regions	Statistical Error Measures (IRI)								
	MLR			Validation			Reduction % (±)		
	R^2	RMSE	MAE	R^2	RMSE	MAE	R^2	RMSE	MAE
Dry Freeze	74	0.136	0.116	61.5	0.165	0.132	-16.89	+17.58	+12.12
Dry no Freeze	90.2	0.294	0.184	89.0	0.224	0.172	-1.33	-23.81	-6.52
Wet Freeze	81.0	0.264	0.202	76.0	0.297	0.215	-6.17	+11.11	+6.05
Wet no Freeze	89.6	0.177	0.093	88.9	0.181	0.095	-0.78	+2.21	+2.11

Based on Table (6-18), Figures (6-17), and (6-18), the following conclusions can be drawn:

- **Dry Freeze:** The results indicated that the reduction in R^2, RMSE, and MAE values was insignificant; the accuracy reductions were 16.89 %, 17.58%, and 12.12%, respectively. Thus, the MLR method's ability to predict IRI models of environmental parameters was accurate.
- **Dry no Freeze:** The results indicated that the reduction in R^2, RMSE, and MAE values was insignificant; the accuracy reductions were 1.33%, 23.81%, and 6.52%, respectively. Thus, the MLR method's ability to predict IRI models of environmental parameters was accurate.

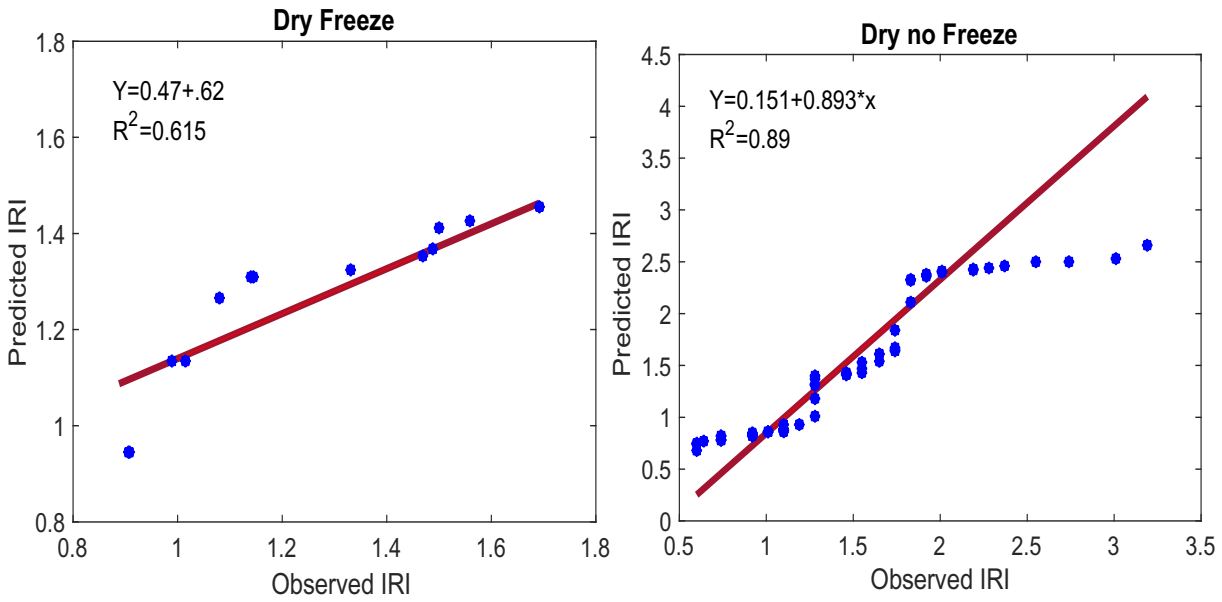

Figure 6-17: MLR model for the dry freeze and the dry no freeze region based on environmental.

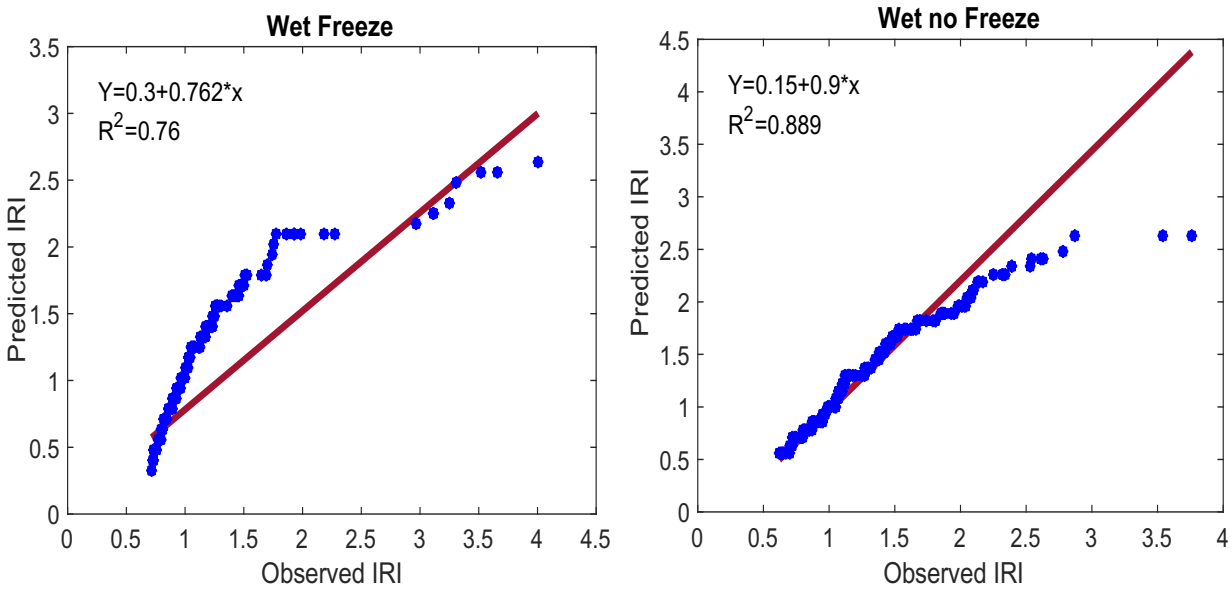

Figure 6-18 : MLR model for the wet freeze and the wet no freeze region based on environmental.

- **<u>Wet Freeze:</u>** The results indicated that the reduction in R^2, RMSE, and MAE values was insignificant; the accuracy reductions were 6.17%,11.11%, and 6.05%, respectively. Thus, the MLR method's ability to predict IRI models of environmental parameters was accurate.

- **Wet no Freeze:** The results indicated that the reduction in R^2, RMSE, and MAE values was insignificant; the accuracy reductions were 0.78%, 2.21%, and 2.11%, respectively. Thus, the MLR method's ability to predict IRI models of environmental parameters was accurate.

6.3.1.2 MLR Model Sensitivity Analysis for PCI and IRI

- **MLR Model Sensitivity Analysis for PCI**

A sensitivity analysis is conducted to determine the effects of input variables on the efficacy of the prediction models (PCI). A multiple regression was performed the Backward elimination approach to determine the predicator's type (environmental parameters) that have major effects on the dependent variables (PCI& IRI). The results of the sensitivity analysis for PCI were presented in Table (6-19) and Figure (6-19).

Table 6-19: Sensitivity analysis of prediction models for PCI based on environmental parameters.

Independent Variable	R^2			
	Dry Freeze	**Dry no Freeze**	**Wet Freeze**	**Wet no Freeze**
Age	7.7	87.6	85.5	89
Temperature average	46.1	2.6	2.5	1.0
Freeze index	23.0	6.2	4.9	4.0
Number of freeze days	15.5	1.5	2.7	4.8
Total average annual precipitation	2.0	3.6	15.3	1.1
Total snowfall	70.1	6.4	2.0	3.0
Wind average	19.3	9.0	13.3	2.2
Humidity	36.2	2.8	4.2	1.0

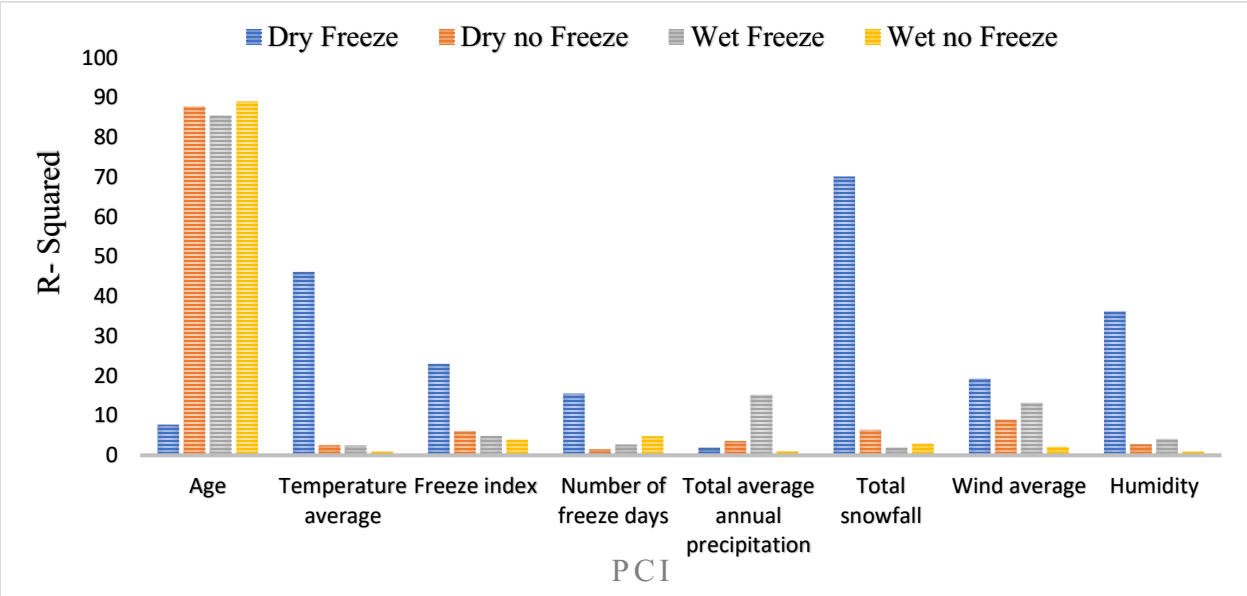

Figure 6-19: Sensitivity analysis of MLR for PCI based on environmental parameters.

Based on Table (6-19) and Figure (6-19), the following conclusions can be drawn:

Dry Freeze: Compared with other variables, total snowfall is a significant factor affecting the prediction model. Temperature average, humidity, freeze index, wind average, and number of freeze days have some effects on the prediction model; the impact values were 46.1%,36.2%, 23%, 19.3%, and 15.5%, respectively. While total average annual precipitation has minor effect on the model.

Dry no Freeze: Compared with other variables, age is the most significant impact variable affecting the prediction model. Temperature average, freeze index, number of freeze days, total average annual precipitation, total snowfall, wind average, and humidity have minor effects on the model; the impact values were 2.6%, 6.2%, 1.5%, 3.6%, 6.4%, 9%, 2.8%, respectively.

Wet Freeze: Compared with other variables, age is the most significant impact variable affecting the prediction model. Temperature average, freeze index, number of freeze days, total average

annual precipitation, total snowfall, wind average, and humidity have some and minor effects on the model; the impact values were 2.5%, 4.9%, 2.7%, 15.3%, 2%, 13.3%, 14.2%, respectively.

Wet no Freeze: Compared with other variables, age is the most significant impact variable affecting the prediction model. Temperature average, freeze index, number of freeze days, total average annual precipitation, total snowfall, wind average, and humidity have minor effects on the model; the impact values were 1.0%, 4.0%, 4.8%, 1.1%, 3.0%, 2.2%, 1.0%, respectively.

- **MLR Model sensitivity analysis for IRI**

A sensitivity analysis was conducted to determine the effects of input variables on the efficacy of prediction models (IRI). The results of the sensitivity analysis for IRI are presented in Tables (6-20) and Figure (6-20).

Table 6-20: Sensitivity analysis of prediction models for IRI based on environmental parameters.

Independent Variable	R^2			
	Dry Freeze	**Dry no Freeze**	**Wet Freeze**	**Wet no Freeze**
Age	79.1	88.2	76	89.3
Temperature average	-	6.6	5.1	2.0
Freeze index	3.2	1.6	4.6	8.0
Number of freeze days	21.7	1.90	3.7	6.5
Total average annual precipitation	1.1	6.4	14	2.3
Total snowfall	21.6	9.3	7	13
Wind average	10.8	11	10.9	2.5
Humidity	3.9	15.2	4.2	1.0

Based on Table (6-20) and Figure (6-20), the following conclusions can be drawn:

Dry Freeze: Compared with other variables, age is a significant factor affecting the prediction model. Number of freezes days, total snowfall, and wind average have some effects on the prediction model. Other parameters have minor statistical significance impacts on the prediction model.

Dry no Freeze: Compared with other variables, age is the most significant impact variable affecting the prediction model. Humidity has some effect on the prediction model, while temperature average, freeze index, number of freeze days, total average annual precipitation, total snowfall, and average wind have minor effects on the prediction model.

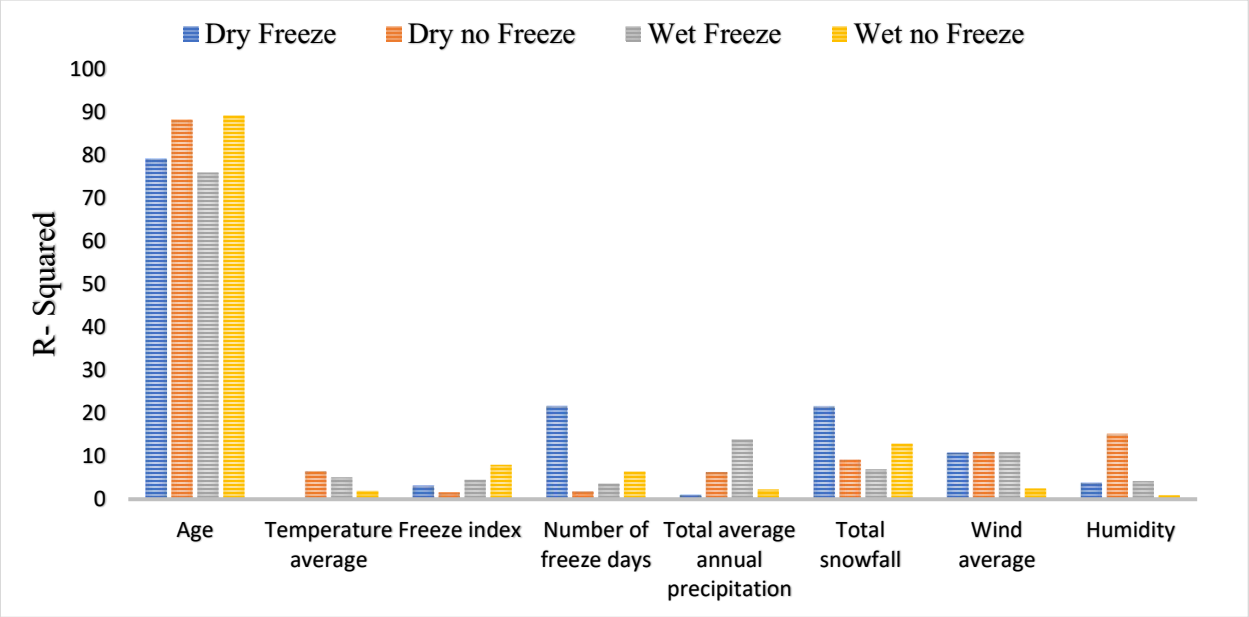

Figure 6-20: Sensitivity analysis of MLR for IRI based on environmental parameters.

Wet Freeze: Compared with other variables, age has the most significant variable impact on the prediction model. Total average annual precipitation and average wind have some effects on the prediction model, while temperature average, freeze index, number of freeze days, total snowfall, and humidity have minor effects on the prediction model.

<u>Wet no Freeze</u>: Compared with other variables, age is the most significant factor affecting the prediction model. Total snowfall has some impact on the IRI models. While other parameters have minor impacts on the prediction model.

6.3.2 Modeling of Asphalt Pavement Performance Indices Using (ANNs) Technique

Th artificial neural network has been used to train the data presented in Table (6-14). The ANNs technique aimed to model asphalt pavement performance indices (PCI and IRI) based on age and seven environmental parameters as input variables for four climate regions. The inputs used were age of pavement, the annual average freezing temperature, the average freeze index, the number of freeze days, the average annual precipitation, the average total snowfall, average speed wind, and humidity average. The architecture of the designed network consists of one input layer with eight parameters, three hidden layers, and an output layer. Figure (6-21) illustrates the architecture of the ANN.

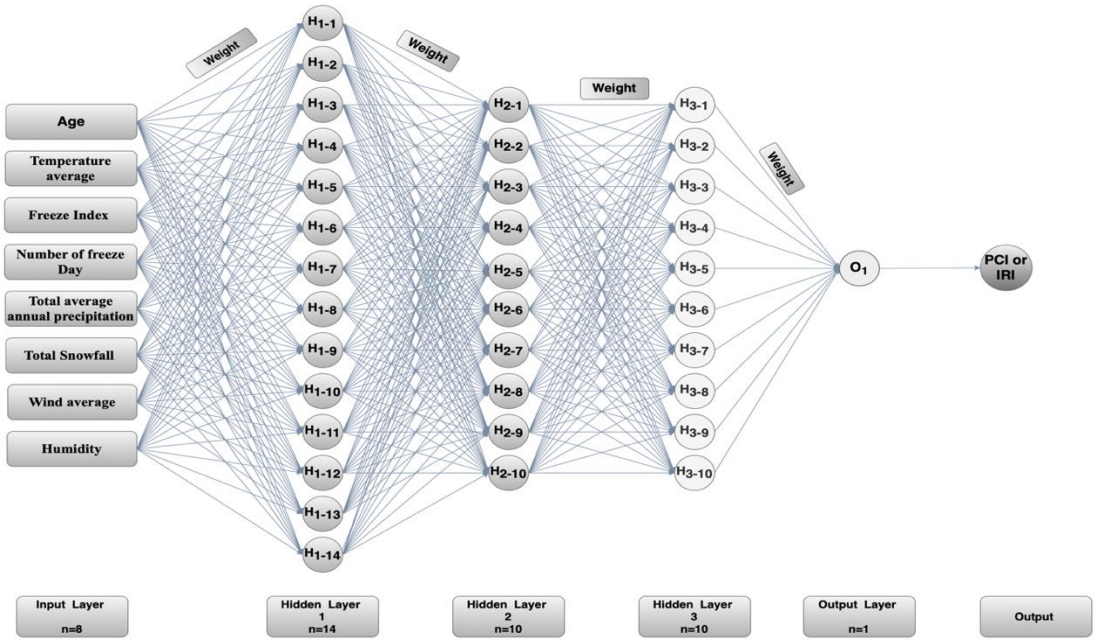

Figure 6-21: Architecture of ANN model for PCI and IRI based on environmental parameters.

6.3.2.1 Modeling of Asphalt Pavement Performance Index (PCI)

Table (6-21) illustrates a summary of the PCI models by using an ANNs technique based on environmental parameters for four climate regions.

Table 6-21: Performance of PCI models by using ANNs technique based on environmental parameters.

Climate Regions	**Statistical Error Measures (PCI)**		
	R^2	**RMSE**	**MAE**
Dry Freeze	99.8	1.112	0.945
Dry no Freeze	99.1	0.636	0.542
Wet Freeze	98.7	0.558	0.478
Wet no Freeze	99.8	0.75	0.553

Based on Table (6-21) and Figure (6-22), the following conclusions can be drawn:

- **Wet Freeze:** The R^2 value was 99.8%, while the RMSE and MAE values were 1.112% and 0.945%.
- **Wet no Freeze:** The R^2 value was 99.1%, while the RMSE and MAE values were 0.636% and 0.542%.
- **Wet Freeze:** The R^2 value was 98.7%, while the RMSE and MAE values were 0.558% and 0.478%.
- **Wet no Freeze:** The R^2 value was 99.8%, while the RMSE and MAE values were 0.75%, and 0.553%.

6.3.2.2 Modeling of Asphalt Pavement Performance Index (IRI)

Table (6-22) illustrates a summary of the IRI models by using an ANNs technique, based on environmental parameters for four climate regions.

Table 6-22: Performance of IRI models by using ANNs technique based on environmental parameters.

Climate Regions	**Statistical Error Measures (IRI)**		
	R^2	**RMSE**	**MAE**
Dry Freeze	99.7	0.008	0.007
Dry no Freeze	98.9	0.007	0.006
Wet Freeze	99.9	0.012	0.008
Wet no Freeze	99.6	0.028	0.021

Based on Table (6-22) and Figure (6-23), the following conclusions can be drawn:

- **Wet Freeze:** The R^2value was 99.7%, while the RMSE and MAE values were 0.008% and 0.006%.
- **Wet no Freeze:** The R^2value was 98.9%, while the RMSE and MAE values were 0.007% and 0.006%.
- **Wet Freeze:** The R^2value was 99.9% while the RMSE and MAE values were 0.012% and 0.008%.
- **Wet no Freeze:** The R^2value was 99.6%, while the RMSE and MAE values were 0.028% and 0.021%.

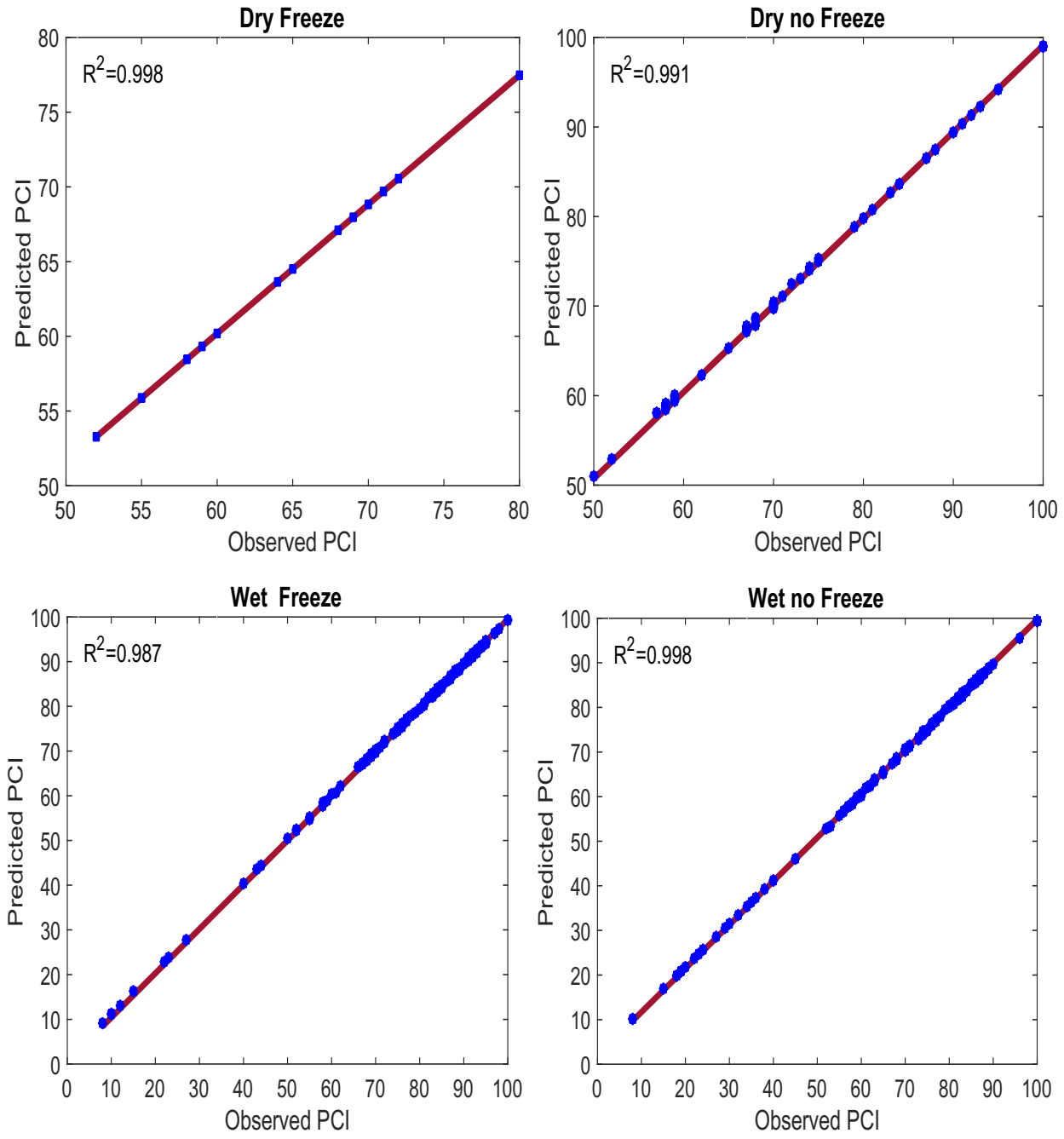

Figure 6-22: ANNs model goodness-of-fit results for PCI values based on environmental parameters.

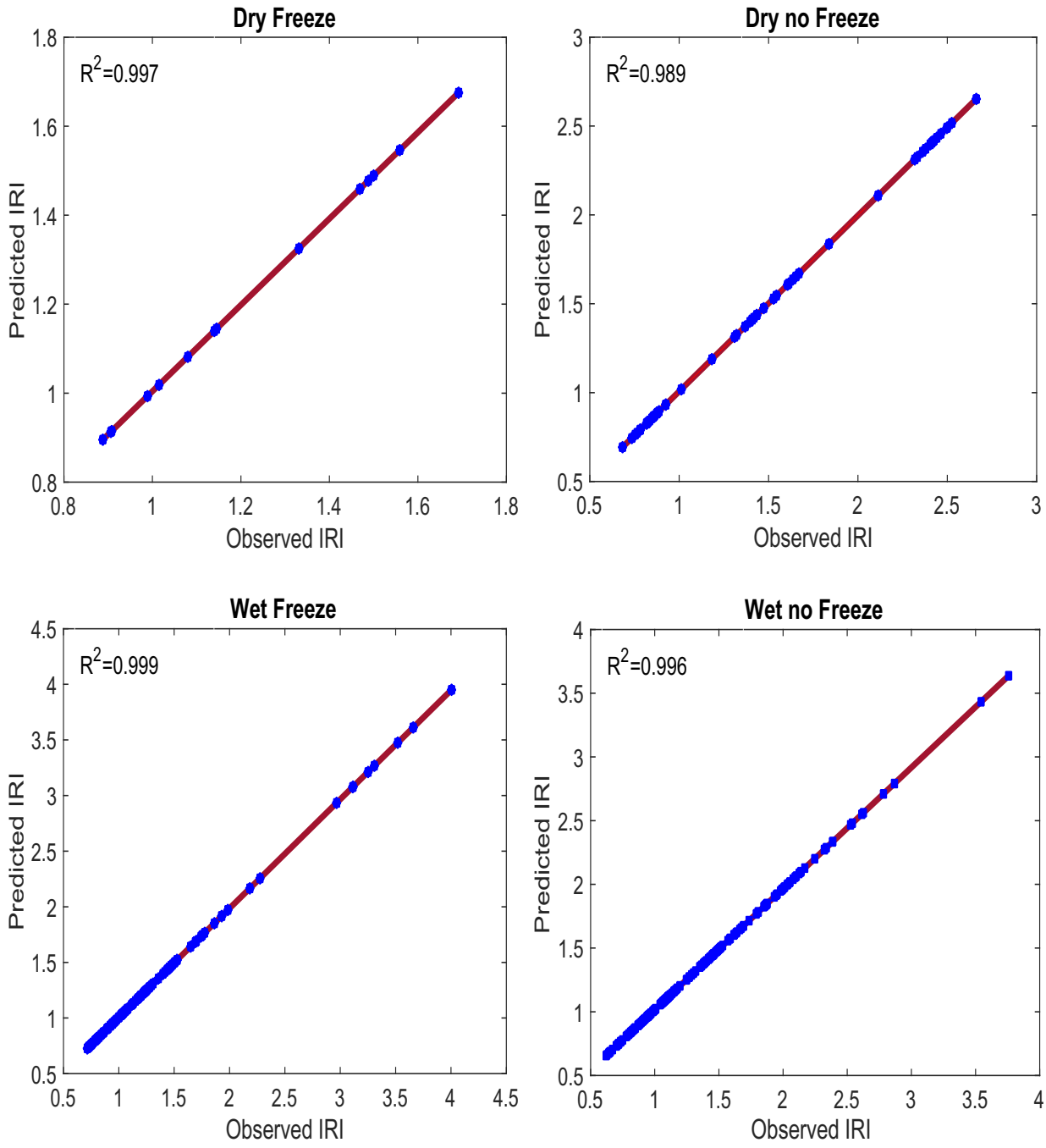

Figure 6-23: ANNs model goodness-of-fit results for IRI values based on environmental parameters.

6.3.3 Validation of ANNs Models

A total of 408 observations obtained from the LTPP dataset for four climate regions investigations were used in ANNs modeling. The models were 70% of the data set was used for training, 15% for testing, and 15% for validation (checking) the network. Tables (6-23) and (6-24) shows the results of the models for the validation dataset.

- **Validation of PCI Models**

The statistical error measures R^2 and RMSE were used to evaluate the performance of the ANNs models. Based on the R^2values, all models had a strong correlation, as their R^2values exceeded 98%, while with RMSE values, all models had a low error, as their error did not exceed 1.71%. Thus, the ANNs technique's ability to predict PCI models of environmental parameters was accurate. Table (6-23) illustrates Validation of PCI models for all sections in the four climate regions.

Table 6-23: Validation of PCI models based on environmental parameters.

Climate Regions	**Statistical Error Measures (PCI)**					
	R^2			**RMSE**		
	Traning	Testing	Validation	Traning	Testing	Validation
Dry Freeze	97.6	100	100	0.262	0.778	1.161
Dry no Freeze	99.1	100	100	0.448	0.959	0.937
Wet Freeze	99.9	99.6	99.8	0.756	0.471	0.97
Wet no Freeze	98.4	98.6	98.1	2.30	4.174	1.71

- **Validation of IRI Models**

The statistical error measures $R^2$and RMSE were used to evaluate the performance of the ANNs models. Based on the R^2 values, all models had a strong correlation, as their R^2 values exceeded 98%, while for RMSE values, all models had minor errors. Thus, the ANNs technique's ability to predict IRI models of environmental parameters was accurate. Table (6-24) illustrates Validation of IRI models for all sections in the four climate regions.

Table 6-24: Validation of IRI models based on environmental parameters.

Climate Regions	**Statistical Error Measures (IRI)**					
	R^2			**RMSE**		
	Traning	Testing	Validation	Traning	Testing	Validation
Dry Freeze	99.6	100	99.8	0.011	0.034	0.045
Dry no Freeze	98.6	99.3	100	0.013	0.013	0.015
Wet Freeze	99.9	100	99.5	0.259	0.264	0.259
Wet no Freeze	99.4	100	99.1	0.003	0.107	0.017

6.3.4 Comparison of the Models

To validate the developed models in this part, all models were evaluated by comparing MLR and ANNs techniques based on environmental parameters for four climate regions, as shown in Tables (6-25) and (6-26).

6.3.4.1 Comparison of ANNs and MLR Models for PCI

The performance of the MLR models was compared with the performance of the ANNs models to evaluate the accuracy of the models in predicting pavement performance based on environmental

parameters. R^2, RMSE and MAE values were used to measure and compare the performance of the models. Table (6-25) and Figures (6-24) and (6-25) present the comparison the MLR models to the ANNs models for PCI.

Table 6-25: Comparison of the MLR and ANNs models for PCI based on environmental parameters.

Climate Regions	**Statistical Error Measures (PCI)**								
	MLR Generated			**ANNs Generated**			**Improvement (%)**		
	$\boldsymbol{R^2}$	**RMSE**	**MAE**	$\boldsymbol{R^2}$	**RMSE**	$\boldsymbol{MAE}$	$\boldsymbol{R^2}$	**RMSE**	$\boldsymbol{MAE}$
Dry Freeze	71.4	4.114	3.482	99.8	1.112	0.945	+28.46	+72.97	+72.86
Dry no Freeze	91.8	6.586	4.194	99.1	0.636	0.542	+7.37	+90.34	+87.08
Wet Freeze	87.3	7.057	5.642	98.7	0.558	0.478	+11.55	+92.09	+91.53
Wet no Freeze	89.5	6.606	5.481	99.8	0.75	0.553	+10.32	+88.65	+89.91

According to Table (6-25), several conclusions can be drawn:

- The statistics indicated R^2values from the ANNs models were higher than its MLR counterpart by 28.46%, 7.37%, 11.55%, and 10.32% for dry freeze, dry no freeze, wet freeze, and wet no freeze, respectively.
- The RMSE values of the ANNs models were less than its MLR counterparts by 72.97%, 90.34%, 92.09%, and 88.65% for dry freeze, dry no freeze, wet freeze, and wet no freeze, respectively.
- The MAE values of the ANNs models were less than the MAE values of the MLR models by 72.86%, 87.08%, 91.53%, and 89.91% for dry freeze, dry no freeze, wet freeze, and wet no freeze, respectively.
- ANNs models provided more accurate predictions than MLR models.

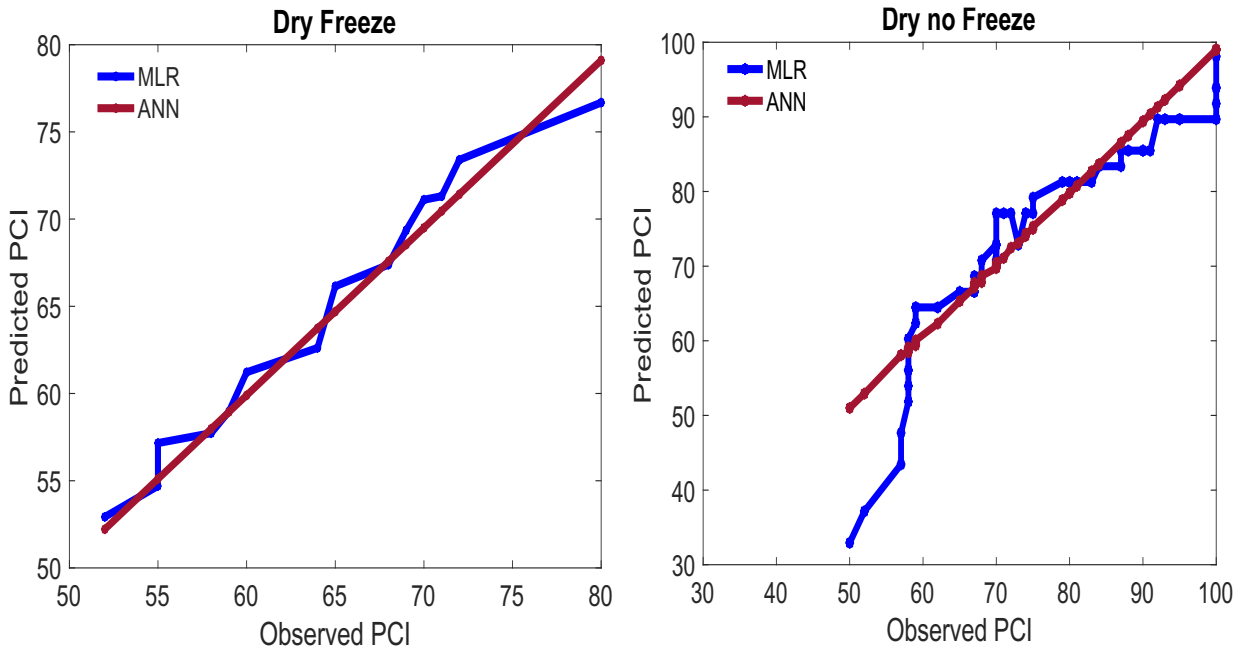

Figure 6-24: Fitness of MLR and ANNs models to PCI prediction based on environmental data from two climate regions: (left) dry freeze; (right)dry no freeze.

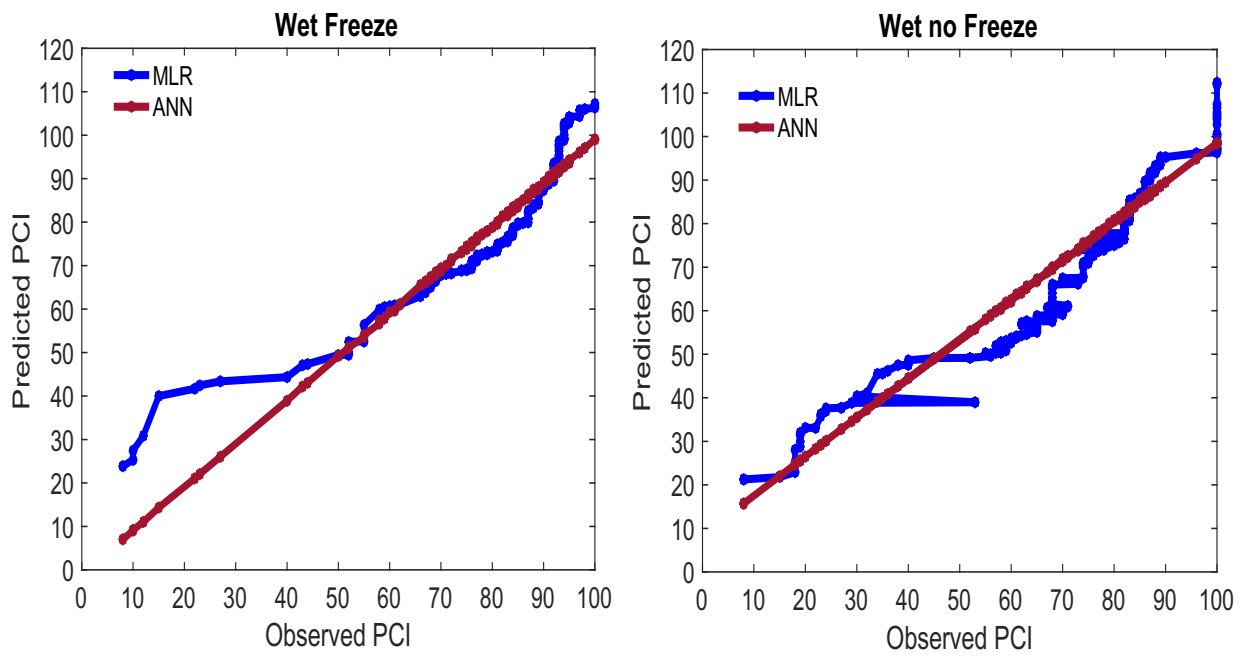

Figure 6-25: Fitness of MLR and ANNs models to PCI prediction based on environmental data from two climate regions: (left) wet freeze; (right)wet no freeze.

According to Figures (6-24) and (6-25), several conclusions can be drawn:

- The MLR strategy has a corrugation, but the ANNs approach has a straight line, explaining why ANNs models are more accurate.
- The graphs clearly illustrated that the ANNs prediction models were more accurate under various climate conditions than the MLR prediction models.

Table (6-25), Figures (6-24), and (6-25) showed that the MLR and ANNs models have an ability to perform the prediction PCI models. In addition, the ANNs technique can predict the PCI models with higher accuracy than the MLR technique in all cases.

6.3.4.2 Comparison of ANNs and MLR Models for IRI

The performance of the MLR models was compared with the performance of the ANNs models to evaluate the accuracy of the models in predicting pavement performance based on environmental parameters. R^2, RMSE and MAE values were used to measure and compare the performance of the models. Table (6-26) and Figures from (6-26) and (6-27) present the comparison the MLR models to the ANNs models for IRI.

Table 6-26: Comparison of the MLR and ANNs models for IRI based on environmental parameters.

Climate Regions	**Statistical Error Measures (IRI)**								
	MLR Generated			**ANNs Generated**			**Improvement (%)**		
	R^2	**RMSE**	**MAE**	R^2	**RMSE**	**MAE**	R^2	**RMSE**	**MAE**
Dry Freeze	74	0.136	0.116	99.7	0.008	0.007	+25.78	+94.12	+93.97
Dry no Freeze	90.2	0.294	0.184	98.9	0.007	0.006	+8.80	+96.20	+96.74
Wet Freeze	81.0	0.264	0.202	99.9	0.012	0.008	+18.92	+94.06	+96.04
Wet no Freeze	89.6	0.177	0.093	99.6	0.028	0.021	+10.04	+69.89	+77.42

According to Table (6-26), several conclusions can be drawn:

- ANNs models provided more accurate predictions than MLR models.
- The statistics indicated R^2 values from the ANNs models were higher than its MLR counterpart by 25.78%, 8.80%, 18.92%, and 10.04% for dry freeze, dry no freeze, wet freeze, and wet no freeze, respectively.
- The statistics indicated RMSE values from the ANNs models were higher than its MLR counterpart by 94.12%, 96.20%, 94.06%, and 69.89% for dry freeze, dry no freeze, wet freeze, and wet no freeze, respectively.
- The statistics indicated MAE values from the ANNs models were higher than its MLR counterpart by 93.97%, 96.74%, 96.04%, and 77.42%for dry freeze, dry no freeze, wet freeze, and wet no freeze, respectively.

Based on Figures from (6-26) and (6-27), several conclusions can be drawn:

- The MLR approach has a slight corrugation while ANNs exhibits a straight line, which explains why ANN models tend to be more accurate.
- Figures clearly showed that the ANNs prediction models provided more accuracy than the MLR prediction models under different climate conditions.

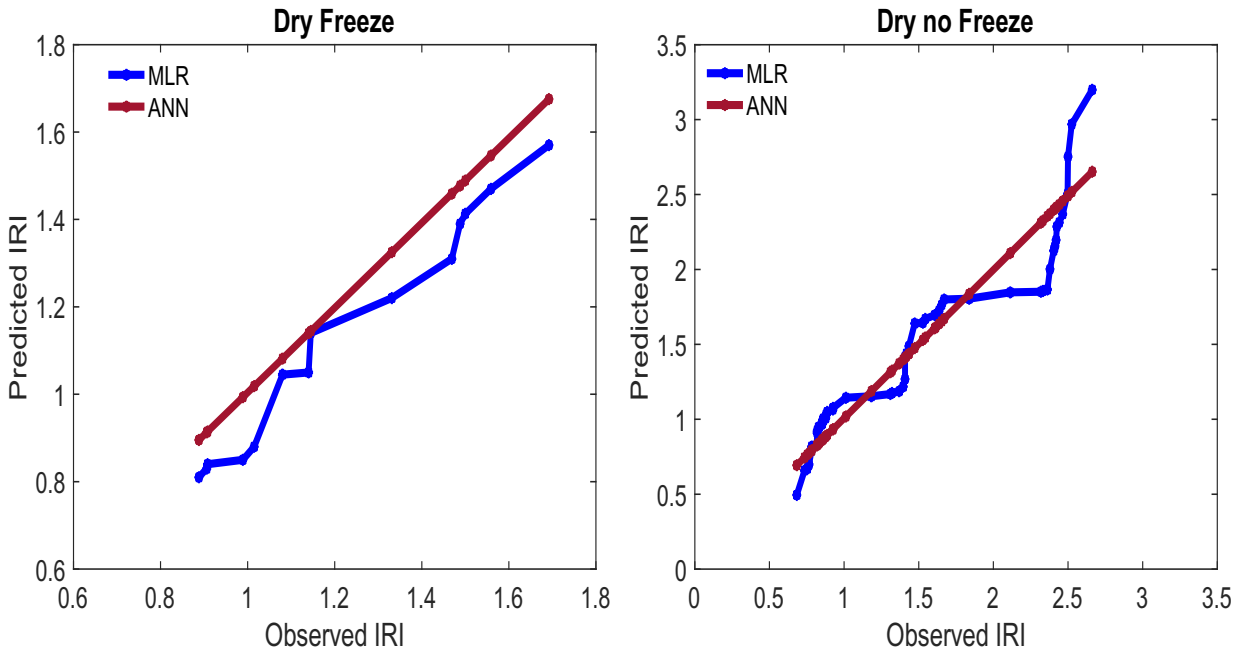

Figure 6-26: Fitness of MLR and ANNs models to IRI prediction based on environmental data from two climate regions: (left) dry freeze; (right)dry no freeze.

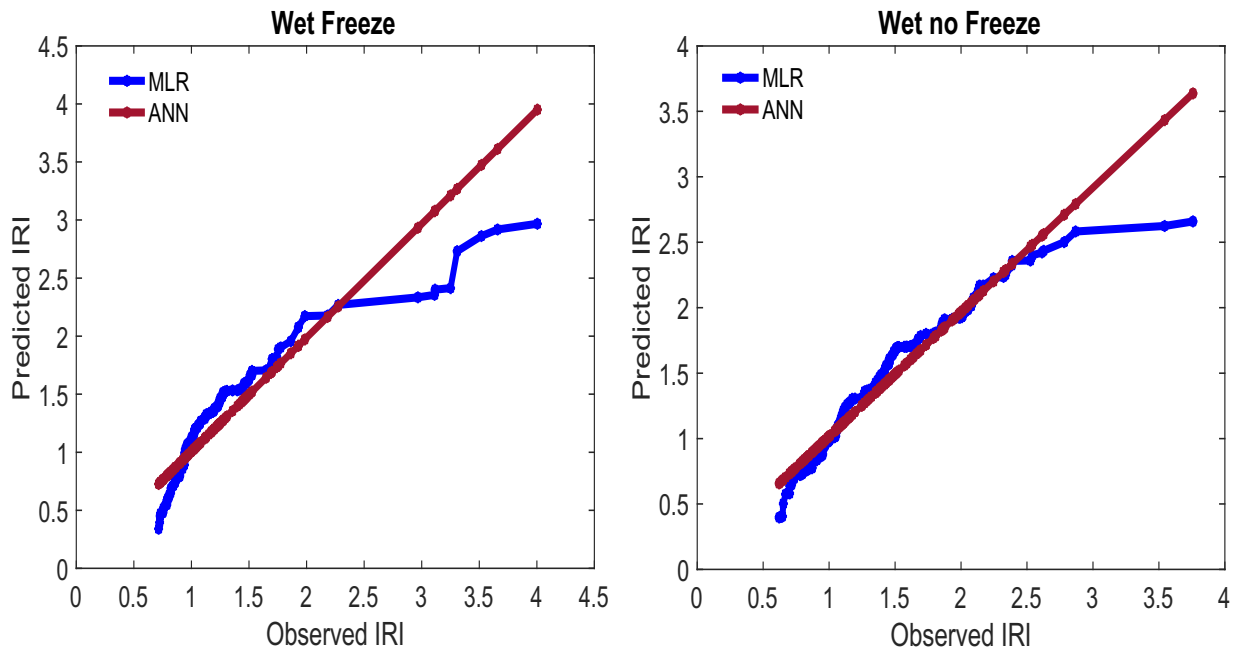

Figure 6-27: Fitness of MLR and ANNs models to IRI prediction based on environmental data from two climate regions: (left) wet freeze; (right)wet no freeze.

- Table (6-26), Figures (6-26), and (6-27) showed that the MLR and ANNs models have an ability to perform the prediction IRI models. In addition, the ANNs prediction models provided more accuracy than the MLR models under all climate conditions.
- The results of this study are consistent with some of the previous studies. For example, Hossain et al. (2017) studied the performance of ANN and MLR models in predicting pavement roughness based on environmental parameters. They found the ANN model more accurate than the MLR model, with a RMSE of 2% lower for four climate regions. Zeiada et al. (2020) compared the performance of ANN and MLR models in predicting pavement roughness based on environmental parameters. They found that the ANN model is significantly more accurate than the MLR model, with a R^2 of 56% lower.

6.3.5 Summary

This part of the research focused on modeling asphalt pavement performance indices (PCI and IRI) based on environmental variables and studying the effect of these variables on asphalt pavement performance indices for four climate regions in the U.S. and Canada. Several important advantages were drawn from the MLR and the ANNs technique, as follows:

- The pavement's age and seven different environmental variables were included for the four studied climate regions, namely temperature average, freeze index, number of freeze days, total average annual precipitation, total snowfall, wind average, and humidity. These were considered independent variables in developing the models to predict future PCI and IRI.
- The MLR and ANNs models have the ability to perform the prediction of PCI and IRI models. In addition, the ANNs prediction models provided more accuracy than the MLR models under four climate regions.

6.4 Effect of Traffic Volume Parameters on IRI and PCI Values

This section focused on modeling asphalt pavement performance indices (PCI and IRI) based on traffic volume variables and studying the effect of these variables on asphalt pavement performance indices for four climate regions in the U.S. and Canada. The relevant data were collected on the traffic volume parameters of 53 road sections with 408 observations from the LTPP dataset and distributed to four climate regions . Table (6-27) briefly describes the selected dataset of traffic volume. The present study was divided into three phases as follows:

- Modeling of asphalt pavement performance indices using (MLR) technique.
- Modeling of asphalt pavement performance indices using (ANNs) technique.
- Comparison and validation of the MLR and ANNs models.

Table 6-27: Gathered traffic volume data from four climatic regions.

Parameters	Unit	Climate Regions			
		Dry Freeze	Dry no Freeze	Wet Freeze	Wet no Freeze
PCI	%	52-80	50-100	8-91	8-100
IRI	(m/km)	0.89-1.69	0.68-2.66	0.73-4.04	0.62-3.76
Number of data samples	Number	14	61	144	189
Age	Year	6-18	3-34	3-33	1-31
ESAL	-	5044-47803	4851-1085824	15432-579222	5880-797000
AADTT	Track/day	41-183	11-3538	78-1914	54-3219
AADT	Track/year	6466-66978	4015-1294908	21756-698610	12555-1107775

6.4.1 Modeling of Asphalt Pavement Performance Indices Using (MLR) Technique

Research in this part focuses on using traffic volume variables to model asphalt pavement performance indices (PCI and IRI). Traffic volume parameters were input variables, and pavement performance indices (PCI and IRI) were output parameters. Eight prediction models were developed using (MLR) technique from the collected data. The PCI and IRI regression models are shown in Tables (6-28) and (6-29).

Table 6-28: PCI models summary based on traffic volume.

Model	**PCI**			
	Dry Freeze	**Dry no Freeze**	**Wet Freeze**	**Wet no Freeze**
R^2	76.4	87.7	85.7	88.1
Constant	78.43	100.53	112.08	114.1
Age	-0.82	- 1.724	- 2.45	- 3.0
ESAL	-	$1.77\ x\ 10^{-6}$	$-1.55\ x\ 10^{-5}$	$1.65\ x\ 10^{-5}$
AADTT	-0.037	-0.001	0.004	-0.003
AADT	-	$1.87\ x\ 10^{-6}$	$6.82\ x\ 10^{-6}$	$-2.80\ x\ 10^{-6}$

The PCI regression analysis results illustrated in Table (6-28) indicate that the R^2 values were 76.4%, 87.7%, 85.7%, and 88.1% for dry freeze, dry no freeze, wet freeze, and wet no freeze, respectively.

The IRI regression analysis results illustrated in Table (6-29) indicate that the R^2 values were 78.4%, 94.7%, 75%, and 89.4% for dry freeze, dry no freeze, wet freeze, and wet no freeze, respectively.

Table 6-29: IRI models summary based on traffic volume.

Model	IRI			
	Dry Freeze	**Dry no Freeze**	**Wet Freeze**	**Wet no Freeze**
R^2	78.4	94.7	75	89.4
Constant	0.767	0.20	0.274	0.342
Age	0.07	0.084	0.071	0.073
ESAL	$7.34\ x\ 10^{-5}$	$-3.9\ x\ 10^{-7}$	$-5.75\ x\ 10^{-5}$	$-1.82\ x\ 10^{-7}$
AADTT	-0.025	$6.75\ x\ 10^{-7}$	-	$4.52\ x\ 10^{-5}$
AADT	$1.95\ x\ 10^{-5}$	$2.68\ x\ 10^{-7}$	$-2.07x10^{-7}$	$-2.73\ x\ 10^{-8}$

Equations from (6-17) to (6-24) summarised the regression models for four climate regions as follows:

1- <u>Dry Freeze</u>

The PCI model for the dry freeze region is presented in Table (6-28). The PCI model was negatively correlated with age and AADTT. Equation (6-17) described the relationship between PCI and traffic volume as follows:

$$\boldsymbol{PCI = 78.43 - 0.82\, X_{age} - 0.037 X_{AADTT}} \qquad \textbf{6-17}$$

The correlation coefficient (R^2) of this relationship is **76.4%.**

Table (6-29) presents the regression analysis result of IRI for the dry freeze area. The IRI model was negatively correlated with AADTT. The IRI model was positively correlated with age, ESAL and AADT. Equation (6-18) described the relationship between the IRI and traffic volume as follows:

$$\boldsymbol{IRI = 0.767 + 0.07\, X_{age} + 7.34 \times 10^{-5} X_{ESAL} - 0.025 X_{AADTT} - 1.95 \times 10^{-5} X_{AADT}} \qquad \textbf{6-18}$$

The correlation coefficient (R^2) of this relationship is **78.4%.**

2- **Dry no Freeze**

Table (6-28) presents the PCI model for the dry no freeze area. The PCI model was negatively correlated with the age and AADTT. The PCI model was positively correlated with ESAL and AADT. Equation (6-19) described the relationship between the PCI and traffic volume as follows:

$$\boldsymbol{PCI = 100.53 - 1.724X_{age} + 1.77 \times 10^{-6}X_{ESAL} - 0.001X_{AADTT} + 1.87 \times 10^{-6}X_{AADT}} \quad \textbf{6-19}$$

The correlation coefficient (R^2) of this relationship is **87.7%.**

Table (6-29) presents the IRI model for the dry no freeze area. The IRI value was negatively correlated with ESAL. The IRI model was positively correlated with age, AADTT and AADT. Equation (6-20) described the relationship between the IRI and traffic volume as follows:

$$\boldsymbol{IRI = 0.20 + 0.084X_{age} - 3.90 \times 10^{-7}X_{ESAL} + 6.75 \times 10^{-7}X_{AADTT} + 2.68 \times 10^{-7}X_{AADT}} \quad \textbf{6-20}$$

The correlation coefficient (R^2) of this relationship is **94.7%.**

3- **Wet Freeze**

The regression analysis result of the PCI model for the dry no freeze area is presented in Table (6-28). The PCI model was negatively correlated with age and ESAL. The PCI model was positively correlated with AADT and AADTT. The (6-21) described the relationship between PCI and traffic volume as follows:

$$\boldsymbol{PCI = 112.08 - 2.45\,X_{age} - 1.55 \times 10^{-5}X_{ESAL} + 0.004X_{AADTT} + 6.82 \times 10^{-6}X_{AADT}} \quad \textbf{6-21}$$

The correlation coefficient (R^2) of this relationship is **85.7%.**

Table (6-29) presents the regression analysis results for IRI model for the wet freeze area. The IRI value was negatively affected with AADT. The IRI was positively correlated with age and ESAL. Equation (6-22) described the relationship between the IRI and traffic volume as follows:

$$\boldsymbol{IRI = 0.274 + 0.071X_{age} + 5.75 \times 10^{-5}X_{ESAL} - 2.07 \times 10^{-7}X_{AADT}} \qquad \textbf{6-22}$$

The correlation coefficient (R^2) of this relationship is **75%.**

4- <u>Wet no Freeze</u>

The regression analysis result of the PCI model for the dry no freeze area is presented in Table (6-28). The PCI model was negatively correlated with age, AADT and AADTT, and positively correlated with ESAL. Equation (6-23) described the relationship between the PCI and traffic volume as follows:

$$\textbf{PCI} = \mathbf{114.1 - 3.0}\ \boldsymbol{X_{age}} \mathbf{+ 1.65\times 10^{-5}}\boldsymbol{X_{ESAL}} \mathbf{- 0.003}\boldsymbol{X_{AADTT}} \mathbf{-2.80\times 10^{-5}}\boldsymbol{X_{AADT}} \qquad \textbf{6-23}$$

The correlation coefficient (R^2) of this relationship is **88.1%.**

The regression analysis result of the IRI model for the dry no freeze area is presented in Table (6-29). The IRI value was negatively correlated with ESAL and AADT. The IRI was positively correlated with age and AADTT. Equation (6-24) described the relationship between the IRI and traffic volume as follows:

$$\boldsymbol{IRI = 0.34 + 0.073\ X_{age} - 1.82 \times 10^{-7}X_{ESAL} + 4.52 \times 10^{-5}X_{AADTT} - 2.73 \times 10^{-8}X_{AADT}} \qquad \textbf{6-24}$$

The correlation coefficient (R^2) of this relationship is **89.4%.**

6.4.1.1 Validation of MLR Models

- **Validation of PCI Models**

After the validation test, Table (6-30) illustrates the reduction in R^2, RMSE, and MAE values for all sections in the four climate regions.

Table 6-30: Validation of PCI models based on traffic volume.

Climate Regions	Statistical Error Measures (PCI)								
	MLR			Validation			Reduction % (±)		
	R^2	RMSE	MAE	R^2	RMSE	MAE	R^2	RMSE	MAE
Dry Freeze	76.4	3.738	2.793	60.8	5.136	3.874	-20.42	+27.220	+27.92
Dry no Freeze	87.7	4.935	4.281	87.1	4.963	4.241	-0.684	+0.564	+0.934
Wet Freeze	85.7	7.486	5.631	85.1	7.613	5.821	-0.700	+1.668	+3.264
Wet no Freeze	88.1	7.458	5.939	89.4	7.503	6.053	+1.454	+0.600	+1.883

Based on Table (6-30), Figures (6-28), and (6-29), the following conclusions can be drawn:

- **Dry Freeze:** The results indicated that the reduction in R^2, RMSE, and MAE values was insignificant; the accuracy reductions were 20.42%, 27.22%, and 27.92%, respectively. Thus, the MLR method's ability to predict PCI models of the traffic volume was accurate.
- **Dry no Freeze:** The results indicated that the reduction of R^2 ,RMSE and MAE values was insignificant; the accuracy reductions were 0.684%,0.564%, and 0.934%, respectively. Thus, the MLR method's ability to predict PCI models of the traffic volume was accurate.
- **Wet Freeze:** The results indicated that the reduction of R^2 , RMSE, and MAE values was insignificant; the accuracy reductions were 0.7%,1.668%, and 3.264%, respectively. Thus, the MLR method's ability to predict PCI models of the traffic volume was accurate.

- **<u>Wet no Freeze:</u>** The results indicated that the reduction in R^2, RMSE, and MAE values was insignificant; the accuracy reductions were 1.454%, 0.60%, and 1.883%, respectively. The MLR method's ability to predict PCI models of the traffic volume was accurate.

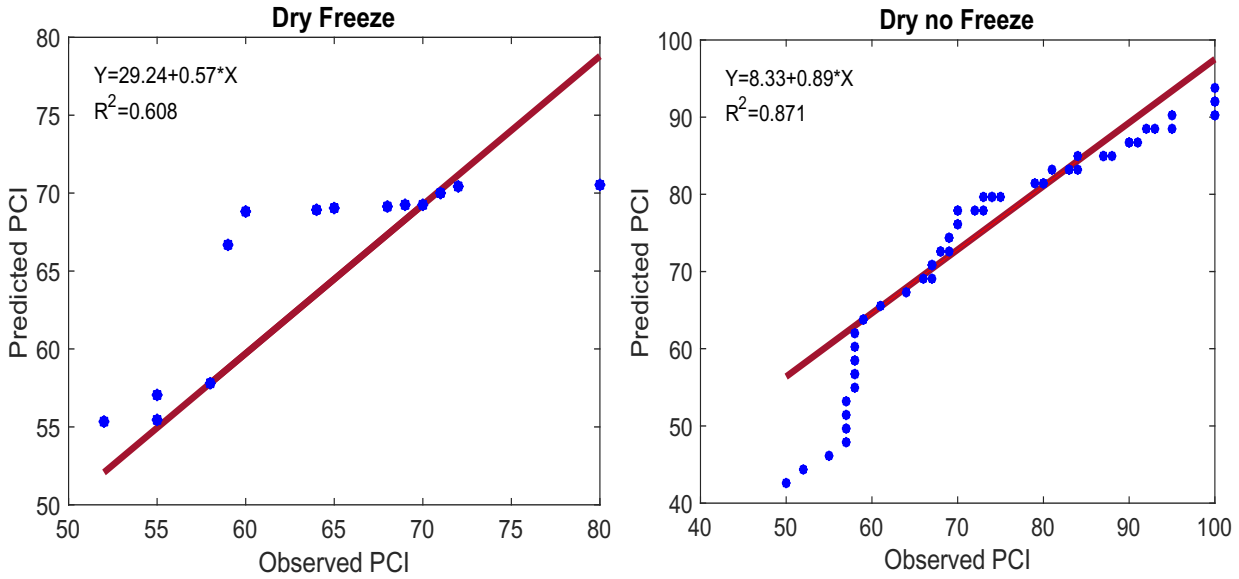

Figure 6-28: MLR model for the dry freeze and the dry no freeze region based on traffic volume.

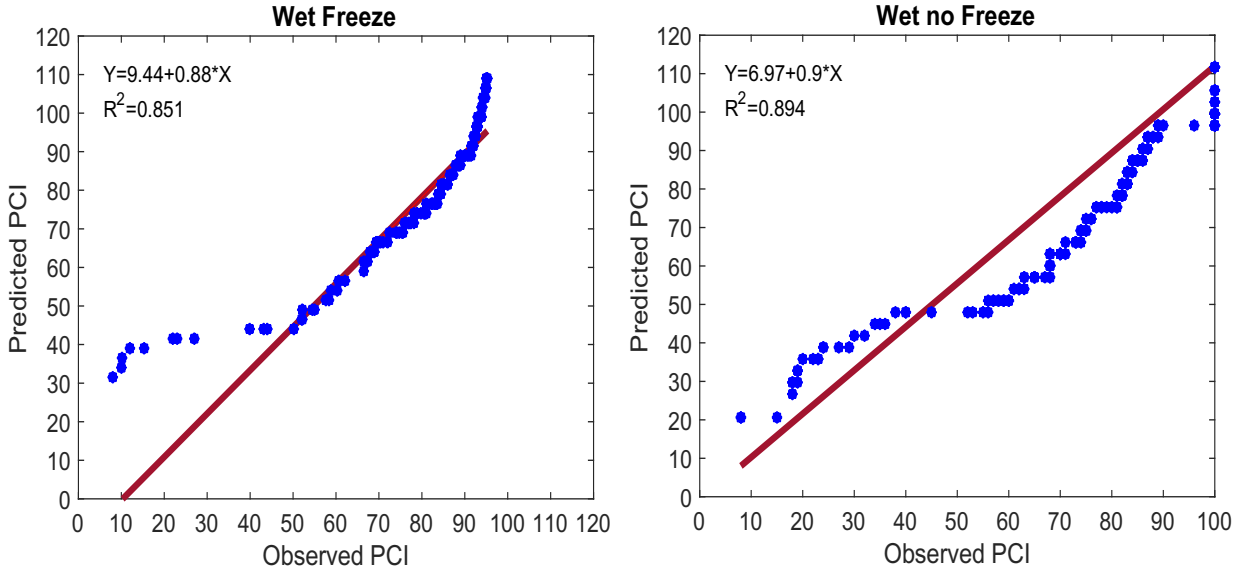

Figure 6-29: MLR model for the wet freeze and the wet no freeze region based on traffic volume.

- **Validation of IRI Models**

After the validation test, Table (6-31) illustrates the reduction in R^2, RMSE, and MAE values for all sections in the four climate regions.

Table 6-31: Validation of IRI models based on traffic volume

Climate Regions	Statistical Error Measures (IRI)								
	MLR			Validation			Reduction % (±)		
	R^2	RMSE	MAE	R^2	RMSE	MAE	R^2	RMSE	MAE
Dry Freeze	78.4	0.123	0.082	73.4	0.095	0.071	-6.30	-22.76	-13.41
Dry no Freeze	94.7	0.15	0.118	94.1	0.162	0.125	-0.634	+7.407	+5.600
Wet Freeze	75.0	0.304	0.216	74.7	0.308	0.222	-0.400	+1.299	+2.703
Wet no Freeze	89.4	0.18	0.093	89.0	0.18	0.094	-0.447	0.000	+1.064

Based on Table (6-31), Figures (6-30), and (6-31), the following conclusions can be drawn:

- **Dry Freeze:** The results indicated that the reduction in R^2, RMSE, and MAE values was insignificant; the accuracy reductions were 6.30%, 22.76%, and 13.41%, respectively. Thus, the MLR method's ability to predict IRI models of the traffic volume was accurate.
- **Dry no Freeze:** The results indicated that the reduction in R^2, RMSE, and MAE values was insignificant; the accuracy reductions were 0.634%, 7.407%, and 5.60%, respectively. Thus, the MLR method ability to predict IRI models of the traffic volume was accurate.
- **Wet Freeze:** The results indicated that the reduction in R^2, RMSE, and MAE values was insignificant; the accuracy reductions were 0.40%,1.299%, and 2.703%, respectively. Thus, the MLR method's ability to predict IRI models of the traffic volume was accurate.

- **<u>Wet no Freeze:</u>** The results indicated that the reduction of R^2 ,RMSE, and MAE values was insignificant; the accuracy reductions were 0.447%, 0.0%, and 1.046%, respectively.

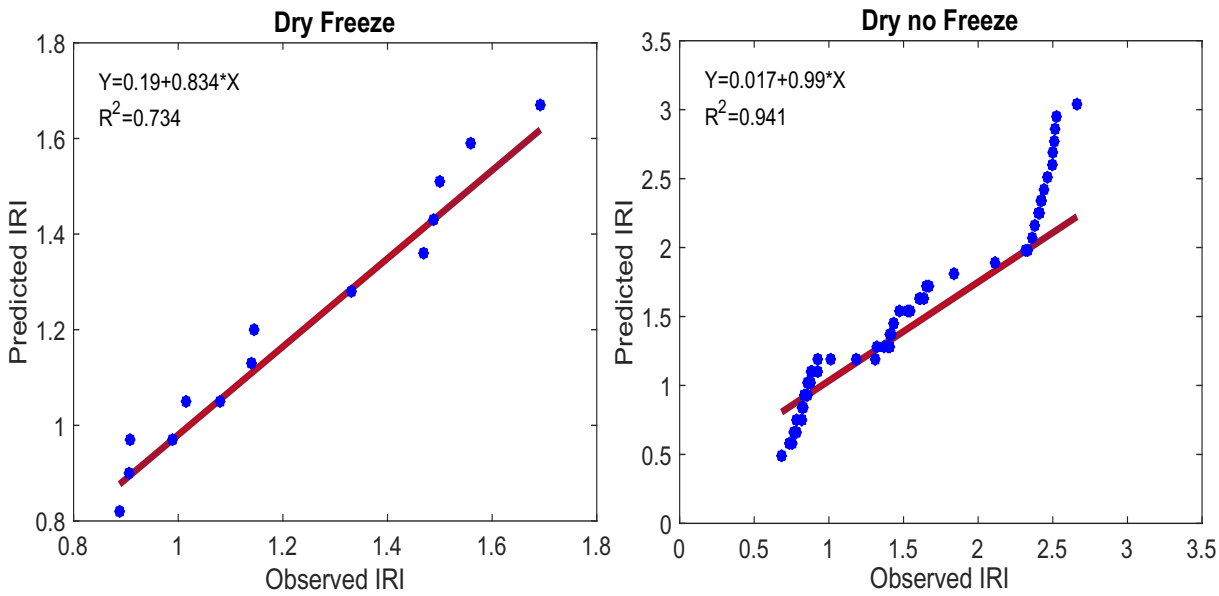

Figure 6-30: MLR model for the dry freeze and the dry no freeze region based on traffic volume.

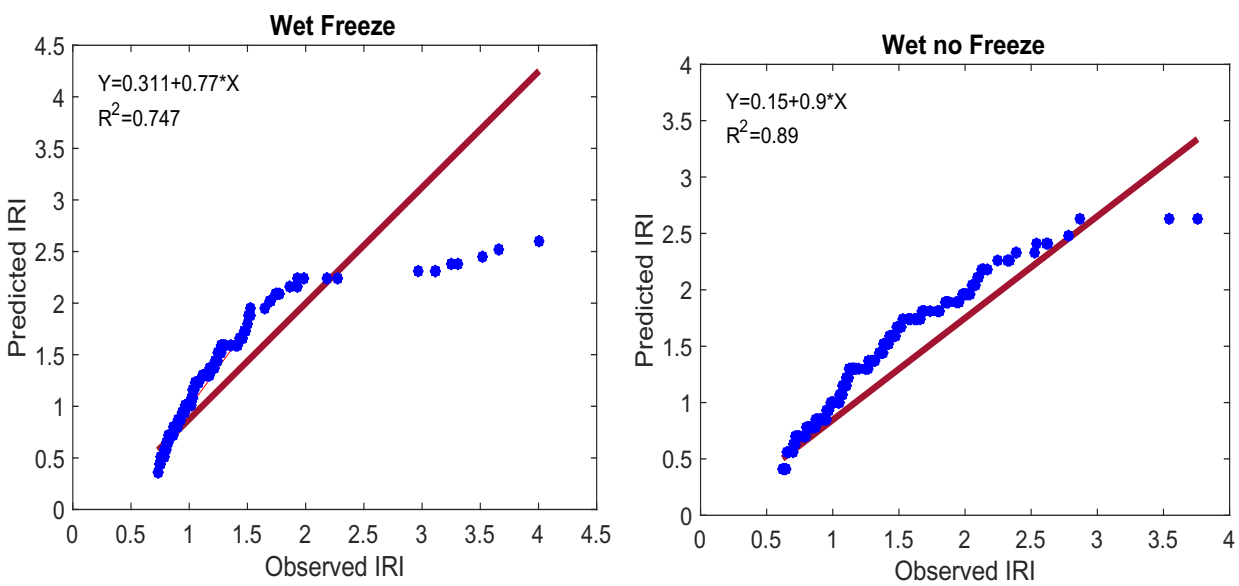

Figure 6-31: MLR model for the wet freeze and the wet no freeze region based on traffic volume.

6.4.1.2 MLR Model Sensitivity Analysis for PCI and IRI

- **MLR Model Sensitivity Analysis for PCI**

A sensitivity analysis was conducted to determine the effects of input variables on the efficacy of the statistical prediction models in the PCI evaluation. The results of the sensitivity analysis for PCI are presented in Table (6-32) and Figure (6-32).

Based on Table (6-32) and Figure (6-32), the following conclusions can be drawn:

Dry Freeze: Compared with ESAL and AADTT are the most significant factors affecting on the prediction model, and AADT has some effect on the model. While age has a minor effect on the prediction model.

Dry no Freeze: Compared with other variables, age is the most significant factor affecting on the prediction model. AADTT and AADT have minor impacts on the prediction model, while ESAL has no a statistical significance effect on the prediction model.

Table 6-32: Sensitivity analysis of prediction models for PCI based on traffic volume.

Independent Variable	R^2			
	Dry Freeze	Dry no Freeze	Wet Freeze	Wet no Freeze
Age	5.2	87.5	85.2	89
ESAL	56.5	-	6.0	-
AADTT	55.1	5.0	2.0	2.0
AADT	28.6	4.0	1.0	-

Wet Freeze: Compared with other variables, age is the most significant factor affecting on the prediction model. ESAL, AADTT and AADT have minor effects on the prediction model.

Wet no Freeze: Compared with other variables, age is the most significant factor affecting on the prediction model. AADTT has a minor impact on the prediction model. While ESAL and AADT do not have a statistical significance influence on the PCI model.

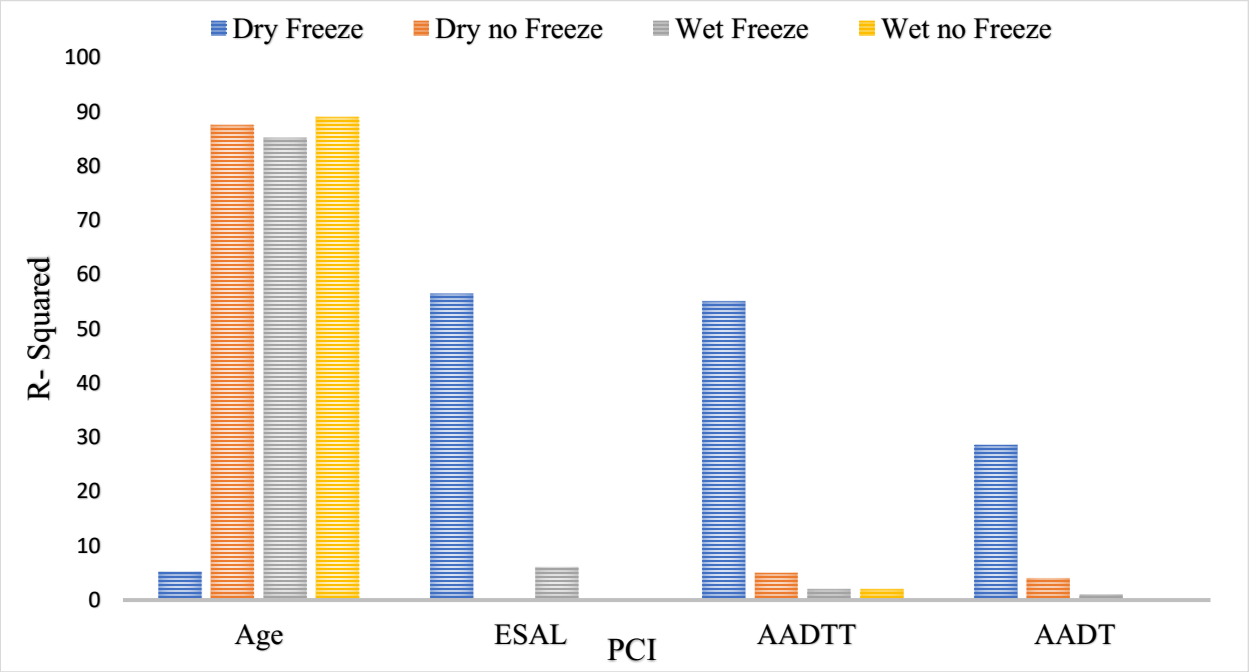

Figure 6-32: Sensitivity analysis of MLR for PCI based on traffic volume.

- **MLR Model Sensitivity Analysis for IRI**

A sensitivity analysis was conducted to determine the effects of input variables on the efficacy of the prediction models (IRI). The results of the sensitivity analysis for IRI are presented in Table (6-33) and Figure (6-33).

Table 6-33: Sensitivity analysis of prediction models for IRI based on traffic volume.

Independent Variable	R^2			
	Dry Freeze	Dry no Freeze	Wet Freeze	Wet no Freeze
Age	73.5	94.2	74.4	89.3
ESAL	6.0	4.0	7.0	0.194
AADTT	4.0	1.0	3.0	2.0
AADT	16.5	7.0	2.0	-

Based on Table (6-33) and Figure (6-33), the following conclusions can be drawn:

Dry Freeze: Compared with other variables, age is the most significant factor affecting the prediction model, and AADT has some impact on the prediction model. While ESAL and AADTT have minor effects on the model.

Dry no Freeze: Compared with other variables, age is the most significant factor affecting the prediction model, and others have some a statistical significance influence on the prediction model.

Wet Freeze: Compared with other variables, age is the most significant factor affecting the prediction model, and others have minor impacts on the prediction model.

Wet no Freeze: Compared with other variables, age is the most significant factor affecting the prediction model, and AADTT ESAL have minor effects on the prediction model. While AADT has no a statistical significance influence on the prediction model.

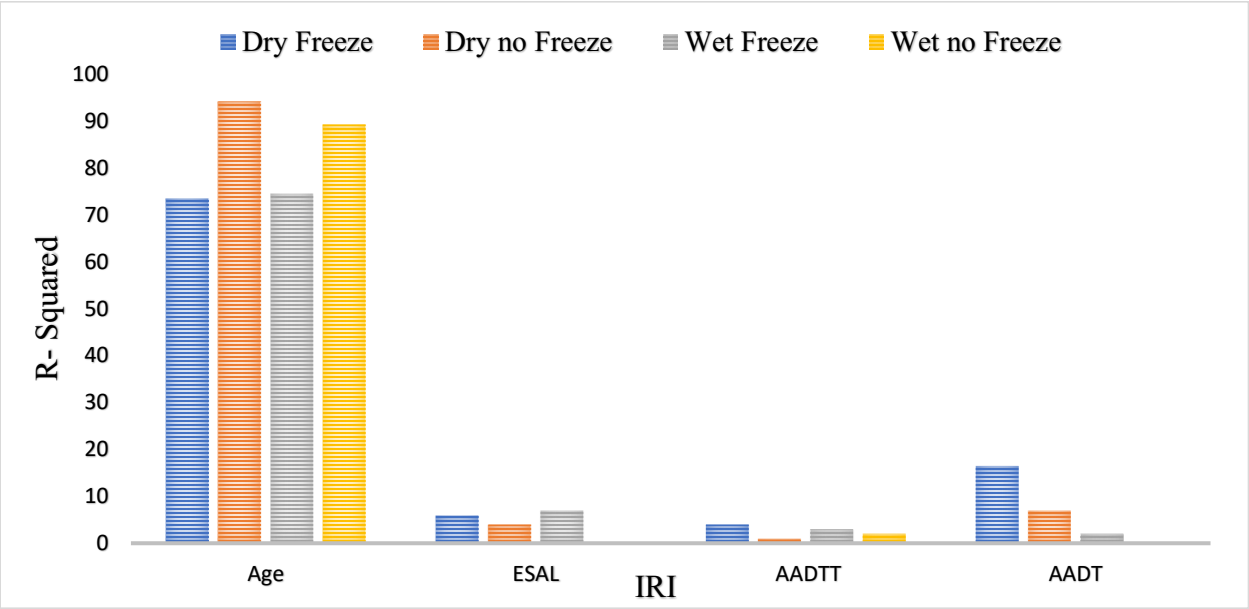

Figure 6-33: Sensitivity analysis of MLR for IRI based on traffic volume.

6.4.2 Modeling of Asphalt Pavement Performance Indices Using (ANNs) Technique

Artificial neural network has been used to train the data presented in Table (6-27). The ANNs technique aimed to model asphalt pavement performance indices (PCI and IRI) based on age and three traffic volume as input variables for four climate regions. The architecture of the designed network consists of one input layer with 4 parameters, three hidden layers, and an output layer (4-14-10-10-1). Figure (6-34) illustrates the architecture of the ANN.

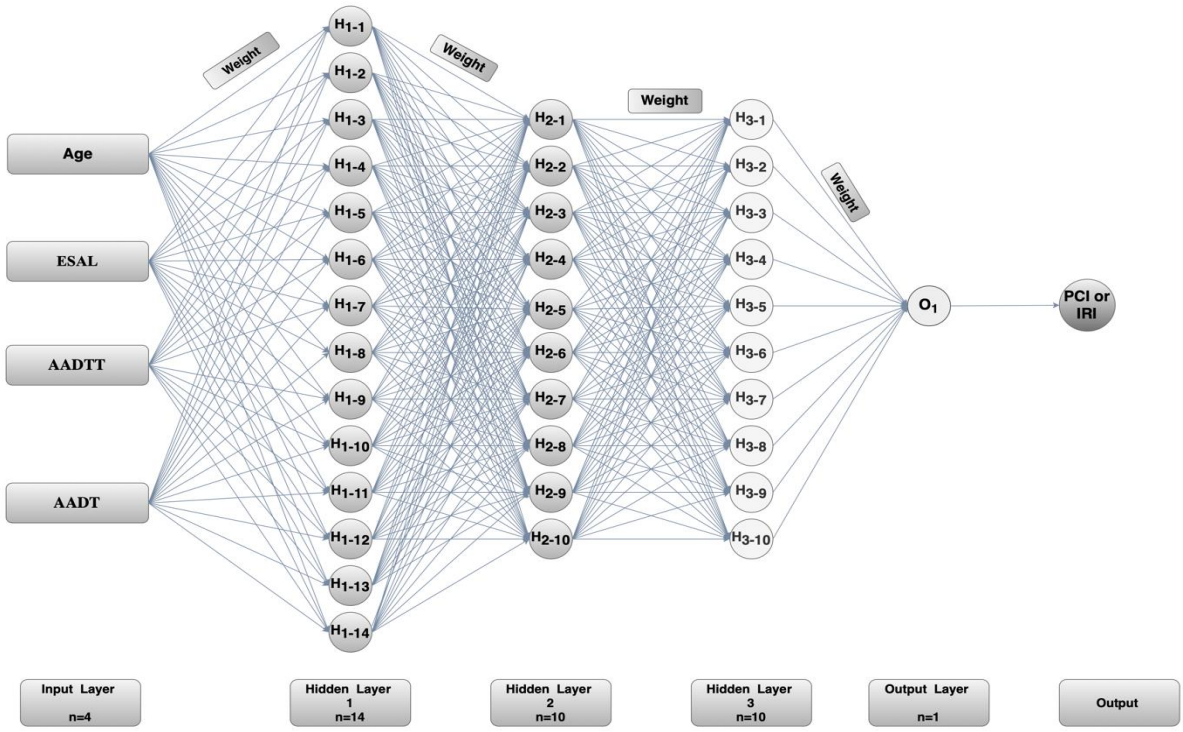

Figure 6-34: Architecture of ANN model for PCI and IRI based on traffic volume.

6.4.2.1 Modeling of Asphalt Pavement Performance Index (PCI)

Table (6-34) illustrates a summary of the PCI models by using an ANNs technique based on traffic volume for four climate regions.

Table 6-34: Performance of PCI models by using ANNs technique based on traffic volume.

Climate Regions	ANNs Models		
	Statistical Error Measures (PCI)		
	R^2	RMSE	MAE
Dry Freeze	99.2	0.89	0.89
Dry no Freeze	99.4	0.39	0.336
Wet Freeze	99.3	0.661	0.484
Wet no Freeze	98.5	1.868	1.34

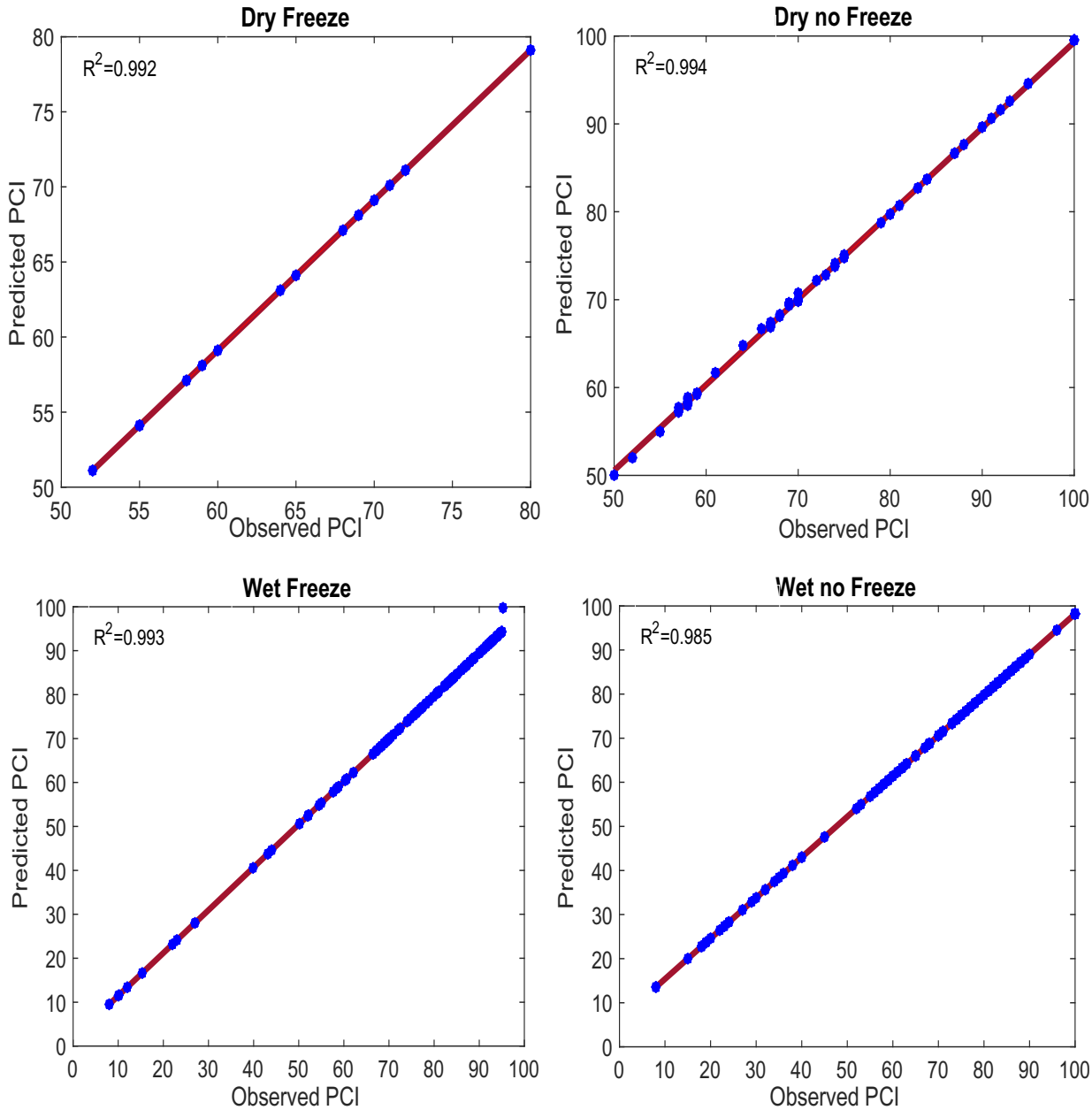

Figure 6-35: ANNs model goodness-of-fit results for IRI values based on traffic volume.

Based on Table (6-34) and Figure (6-35), the following conclusions can be drawn:

- **<u>Dry Freeze:</u>** The R^2value was 99.2%, while the RMSE and MAE values were 0.89% and 0.89%.

- **Dry no Freeze:** The R^2value was 99.4%, while the RMSE and MAE values were 0.39% and 0.336%.
- **Wet Freeze:** The R^2value was 99.3%, while the RMSE and MAE values were 0.661% and 0.484%.
- **Wet no Freeze:** The R^2value was 98.5%, while the RMSE and MAE values were 1.868% and 1.34%.

6.4.2.2 Modeling of Asphalt Pavement Performance Index (IRI)

Table (6-35) illustrates a summary of the IRI models by using an ANNs technique based on traffic volume for four climate regions.

Table 6-35: Performance of IRI models by using ANNs technique based on traffic volume.

Climate Regions	ANNs Models		
	Statistical Error Measures (IRI)		
	R^2	RMSE	MAE
Dry Freeze	99.3	0.008	0.006
Dry no Freeze	99	0.024	0.024
Wet Freeze	98.7	0.012	0.012
Wet no Freeze	98.5	0.052	0.039

Based on Table (6-35) and Figure (6-36), the following conclusions can be drawn:

- **Dry Freeze:** The R^2value was 99.3%, while the RMSE and MAE values were 0.008% and 0.006%.
- **Dry no Freeze:** The R^2value was 99 %, while the RMSE and MAE values were 0.024% and 0.024%.

- **<u>Wet Freeze:</u>** The R^2value was 98.7%, while the RMSE and MAE values were 0.012% and 0.012%.
- **<u>Wet no Freeze:</u>** The R^2value was 98.5%, while the RMSE and MAE values were 0.052% and 0.039%.

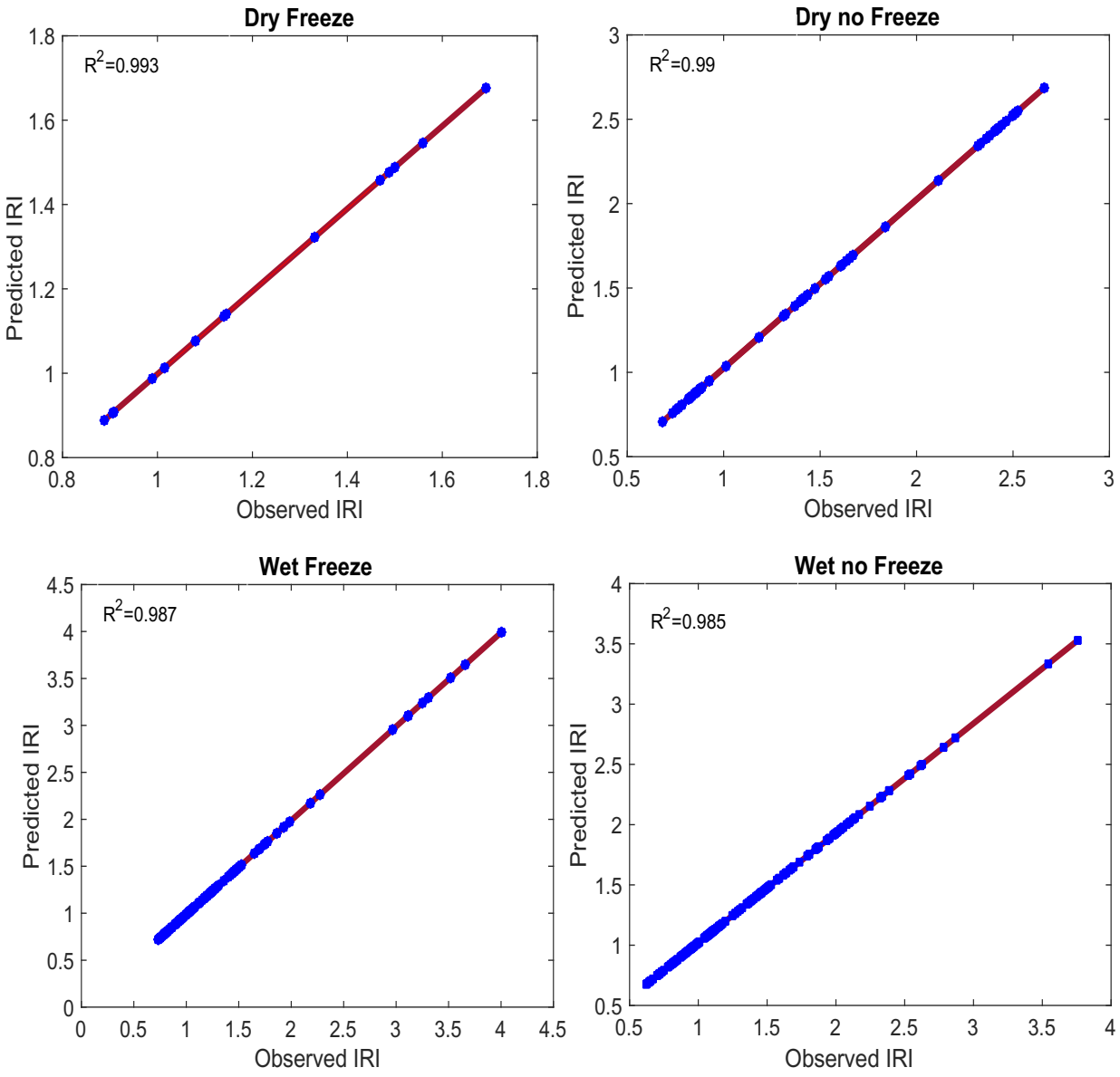

Figure 6-36: ANNs model goodness-of-fit results for IRI values based on traffic volume.

6.4.3 Validation of ANNs Models

A total of 408 observations obtained from the LTPP dataset for four climate regions investigations were used in ANNs modeling, where 70% of the data set was used for training, 15% for testing, and 15% for validation (checking) the network. Tables (6-36) and (6-37) show the results of the models for the validation dataset.

- **Validation of PCI Models**

The statistical error measures R^2 and RMSE were used to evaluate the performance of the ANNs models. Based on the R^2values, all models had a strong correlation, as their R^2values exceeded 98%, while with RMSE values, all models had a low error, as their error did not exceed 2.963%. Thus, the ANNs technique's ability to predict PCI models of traffic volume parameters was accurate. Table (6-36) illustrates Validation of PCI models for all sections in the four climate regions.

Table 6-36 : Validation of PCI models based on traffic volume parameters.

Climate Regions	**Statistical Error Measures (PCI)**					
	R^2			**RMSE**		
	Training	Testing	Validation	Traning	Testing	Validation
Dry Freeze	98.6	99.7	99.3	0.371	2.243	1.374
Dry no Freeze	99.1	99.4	100	0.355	2.431	1.245
Wet Freeze	99.9	100	99.8	0.469	1.124	0.451
Wet no Freeze	98.4	98.6	98.9	4.115	4.115	2.963

- **Validation of IRI Models**

The statistical error measures $R^2$and RMSE were used to evaluate the performance of the ANNs models. Based on the R^2 values, all models had a strong correlation, as their R^2 values exceeded 99%, while for RMSE values, all models had minor errors. Thus, the ANNs technique's ability to predict IRI models of traffic volume parameters was accurate. Table (6-37) illustrates Validation of IRI models for all sections in the four climate regions.

Table 6-37 : Validation of IRI models based on traffic volume parameters.

Climate Regions	**Statistical Error Measures (IRI)**					
	R^2			**RMSE**		
	Training	Testing	Validation	Traning	Testing	Validation
Dry Freeze	99.6	99.8	99.8	0.009	0.010	0.016
Dry no Freeze	99.7	100	100	0.023	0.097	0.028
Wet Freeze	99.9	99.9	99.6	0.016	0.071	0.025
Wet no Freeze	99.4	99.6	99.1	0.045	0.044	0.022

6.4.4 Comparison of the Models

To validate the developed models in this part, all models were evaluated by comparing MLR and ANNs techniques based on traffic volume for four climate regions, as shown in Tables (6-38) and (6-38).

6.4.4.1 Comparison of ANNs and MLR Models for PCI

The performance of the MLR models was compared with the performance of the ANNs models to evaluate the accuracy of the models in predicting pavement performance based on traffic volume

parameters. R^2, RMSE and MAE values were used to compare the performance of the models. Table (6-38) and Figures from (6-37) and (6-38) presented the comparison the MLR models to the ANNs models for PCI.

Table 6-38: Comparison of the MLR and ANNs models for PCI based on traffic volume.

Climate Regions	**Statistical Error Measures (PCI)**								
	MLR Generated			**ANNs Generated**			**Improvement (%)**		
	$\boldsymbol{R^2}$	**RMSE**	**MAE**	$\boldsymbol{R^2}$	**RMSE**	$\boldsymbol{MAE}$	$\boldsymbol{R^2}$	**RMSE**	$\boldsymbol{MAE}$
Dry Freeze	76.4	3.738	2.793	99.2	0.89	0.89	+22.98	+76.19	+68.13
Dry no Freeze	87.7	4.935	4.281	99.4	0.39	0.336	+11.77	+92.10	+92.15
Wet Freeze	85.7	7.486	5.631	99.3	0.661	0.484	+13.70	+91.17	+91.40
Wet no Freeze	88.1	7.458	5.939	98.5	1.868	1.34	+10.56	+74.95	+77.44

According to Table (6-38), several conclusions can be drawn:

- The statistics indicated that R^2values from the ANNs models were higher than the R^2values of the MLR models by 22.98%, 11.77%, 13.70%, and 9.54% for dry freeze, dry no freeze, wet freeze, and wet no freeze, respectively.
- The RMSE values of the ANNs models were less than the RMSE values of the MLR models by 76.19%, 92.10%, 91.17%, and 74.95% for dry freeze, dry no freeze, wet freeze, and wet no freeze, respectively.
- The MAE values of the ANNs models were less than the MAE values of the MLR models by 68.13%, 92.15%, 91.40%, and 77.44% for dry freeze, dry no freeze, wet freeze, and wet no freeze, respectively.

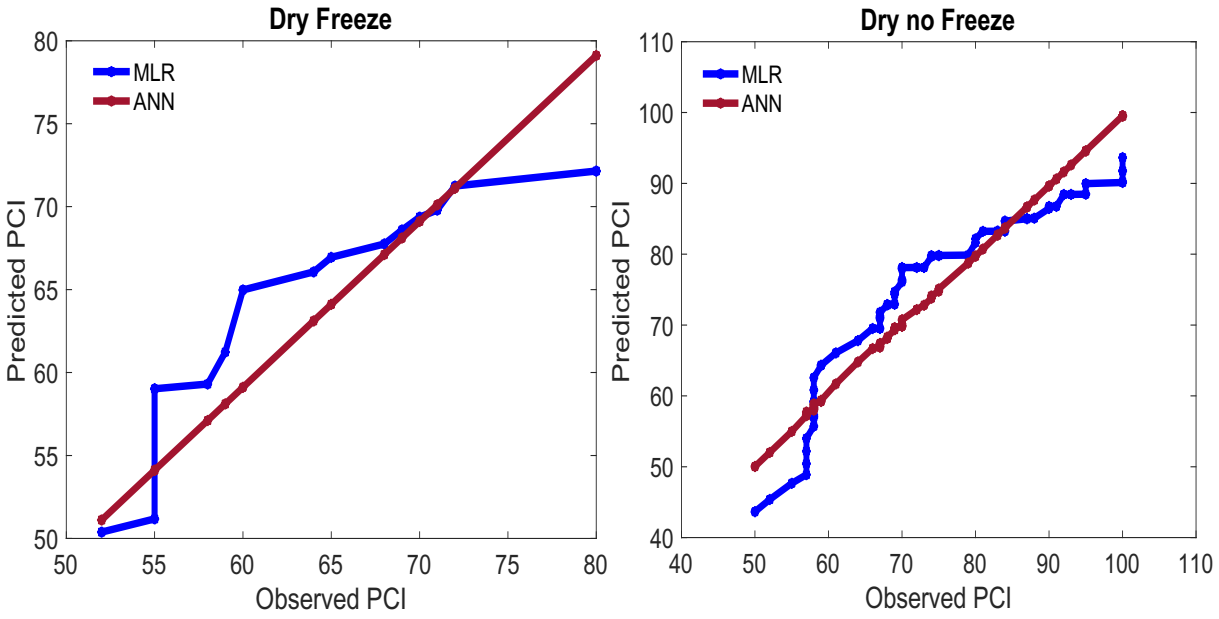

Figure 6-37: Fitness of MLR and ANNs models to PCI prediction based on traffic volume data from two climate regions: (left) dry freeze; (right)dry no freeze.

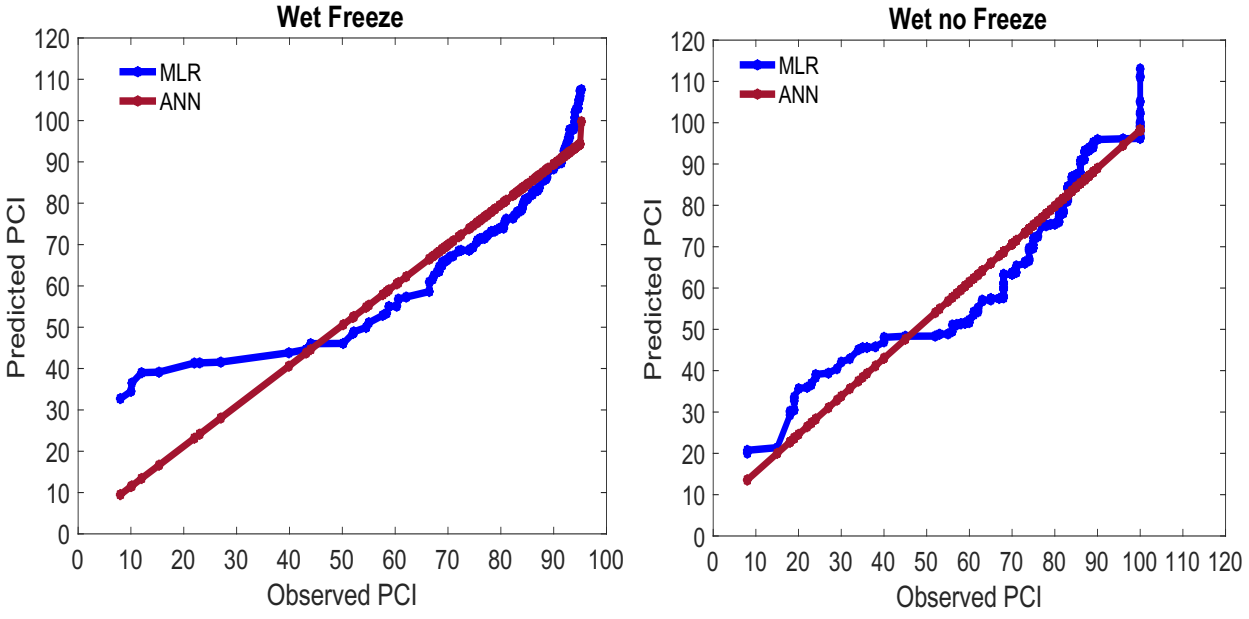

Figure 6-38: Fitness of MLR and ANNs models to PCI prediction based on traffic volume data from two climate regions: (left) wet freeze; (right)wet no freeze.

Based on Figures from (6-37) to (6-38), several conclusions can be drawn:

- The MLR approach has a slight corrugation while ANNs exhibits a straight line, which explains why ANN models tend to be more accurate.

Table (6-38), Figures (6-37), and (6-38) showed that the MLR and ANNs models have an ability to perform the prediction PCI models. In addition, the ANNs prediction models provided more accuracy than the MLR models under all climate conditions.

6.4.4.2 Comparison of ANNs and MLR Models for IRI

The performance of the MLR models was compared with the performance of the ANNs models to evaluate the accuracy of the models in predicting pavement performance based on traffic volume parameters. R^2, RMSE and MAE values were used to compare the performance of the models. Table (6-39) and Figures from (6-39) and (6-40) show the comparison the MLR models to the ANNs models for IRI.

Table 6-39: Comparison of the MLR and ANNs models for IRI based on traffic volume.

Climate Regions	**Statistical Error Measures (IRI)**								
	MLR Generated			**ANNs Generated**			**Improvement (%)**		
	R^2	**RMSE**	**MAE**	R^2	**RMSE**	**MAE**	R^2	**RMSE**	**MAE**
Dry Freeze	78.4	0.073	0.057	99.3	0.008	0.006	+20.75	+89.04	+89.47
Dry no Freeze	94.7	0.15	0.118	99	0.024	0.024	+4.34	+84.00	+79.66
Wet Freeze	75	0.304	0.216	98.7	0.012	0.012	+24.01	+96.05	+94.44
Wet no Freeze	89.4	0.18	0.093	98.5	0.052	0.039	+9.24	+71.11	+58.06

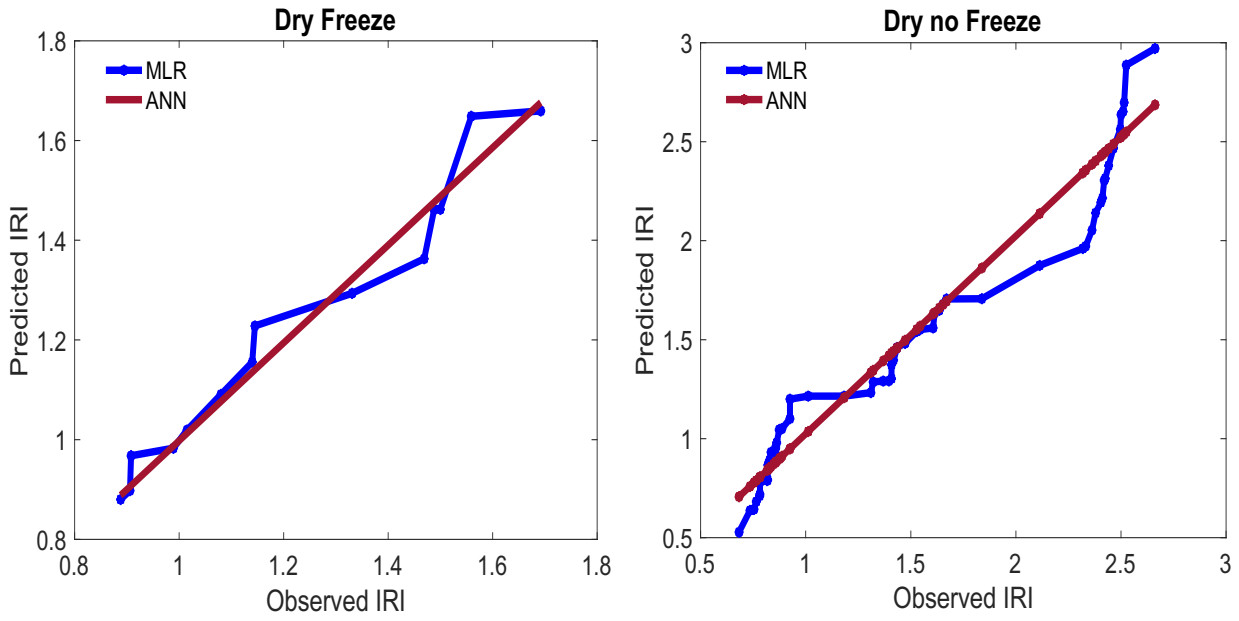

Figure 6-39: Fitness of MLR and ANNs models to IRI prediction based on traffic volume data from two climate regions: (left) dry freeze; (right)dry no freeze.

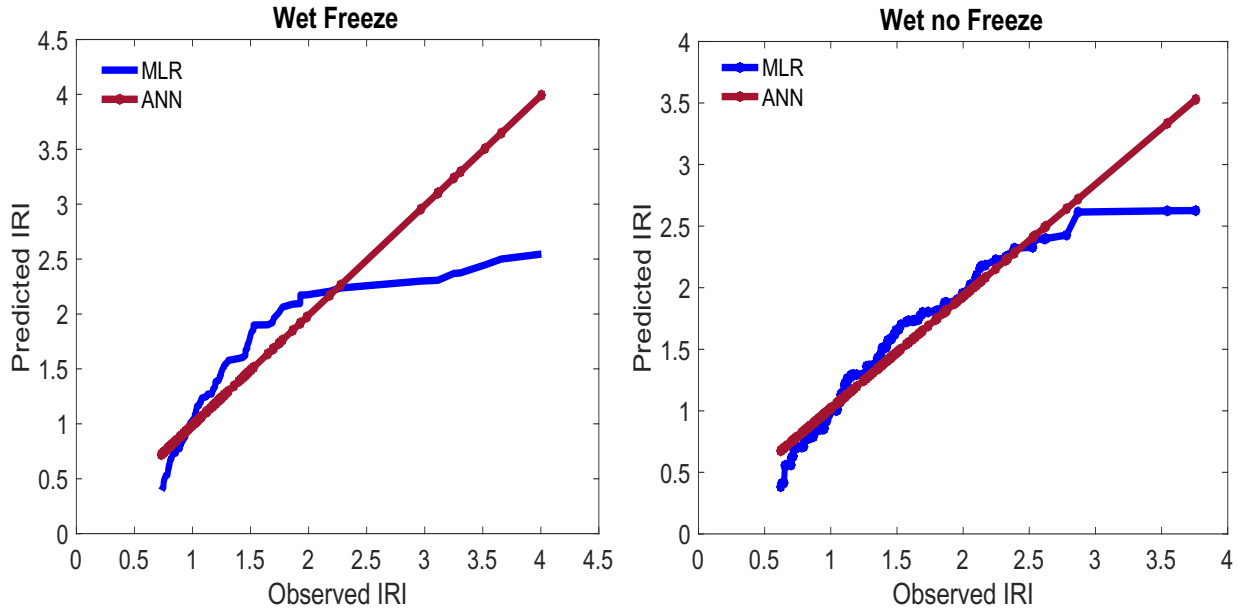

Figure 6-40: Fitness of MLR and ANNs models to IRI prediction based on traffic volume data from two climate regions: (left) wet freeze; (right)wet no freeze.

According to Table (6-39), Figures from (6-39) and (6-40), several conclusions can be drawn:

- The statistics indicated that R^2values from the ANNs models were higher than the R^2values of the MLR models by 20.75%, 4.34%, 24.01%, and 9.24% for dry freeze, dry no freeze, wet freeze, and wet no freeze, respectively.
- The RMSE values of the ANNs models were less than the RMSE values of the MLR models by 89.04%, 84%, 96.05%, and 71.11% for dry freeze, dry no freeze, wet freeze, and wet no freeze, respectively.
- The MAE values of the ANNs models were less than the MAE values of the MLR models by 89.47%, 79.66%, 94.44%, and 58.06% for dry freeze, dry no freeze, wet freeze, and wet no freeze, respectively.
- The MLR approach has a slight corrugation while ANN has a straight line, which explains why ANN models tend to be more accurate.
- Figures clearly show that the ANNs prediction models provided more accuracy than the MLR prediction models under different climate conditions.

Table (6-39), Figures (6-39), and (6-40) showed that the ANN prediction models provided more accuracy than the MLR models under all climate conditions.

The results of this study are consistent with some of the previous studies. For example, Ziari et al. (2015) developed various ANN networks to predict IRI using structural, traffic, and climate parameters. They used RMSE to evaluate the ANN model and achieved an RMSE of 0.012.

6.4.5 Summary

This part of the research focused on modeling asphalt pavement performance indices (PCI and IRI) based on traffic volume variables and studying the effect of these variables on asphalt pavement performance indices for four climate regions. Several important advantages were drawn from the MLR and the ANNs technique, as follows:

- The MLR and ANNs models have the ability to perform the prediction of PCI and IRI models. In addition, the ANNs prediction models provided more accuracy than the MLR models under four climate regions. The approaches have good accuracy since their R^2values exceed 75 and 98 % for MLR and ANN, respectively, as evidenced by the R^2 values.
- The ANNs method reduces the error value by a considerable amount compared to the MLR method for each climate region.

Chapter7: Field Survey (Case Study)

7.1 Field Survey (Case Study)

The case study site is located in St. John's, the capital of the province Newfoundland and Labrador, Canada. St. John's city has a wet freeze climate; all roads are negatively influenced by the challenging environment and ever-growing traffic volume. The case study focuses on studying the effect of pavement distress on determining pavement condition. These include the determination of PCI, IRI, and PSR of flexible pavement and developing reliable prediction models for St. John's roads, based on data obtained from the collected data over the past few years.

The PCI was computed using the ASTM International D6433-18 standard; the IRI values were measured using a smartphone application named TotalPave, and the PSR was obtained by distributing a questionnaire to drivers.

The present case study was divided into six phases as follows:

- Collect the pavement distress parameters for 19 road sections,
- Modeling of asphalt pavement performance indices using the (FIS) technique,
- Modeling the relationship between Indices PCI, IRI, and PSR using mathematical methods,
- Modeling of asphalt pavement performance indices using the (MLR) technique,
- Modeling of Asphalt Pavement performance indices using (ANNs), and
- Compare and validate the FIS, MLR, and ANNs models.

Eight pavement distress variables' effect were assessed and used to predict the PCI, IRI, and PSR models: fatigue cracking, block cracking, rutting, longitudinal cracking, transverse cracking, potholes, patching, and delimitation. The case study outline is presented in Figure (7-1).

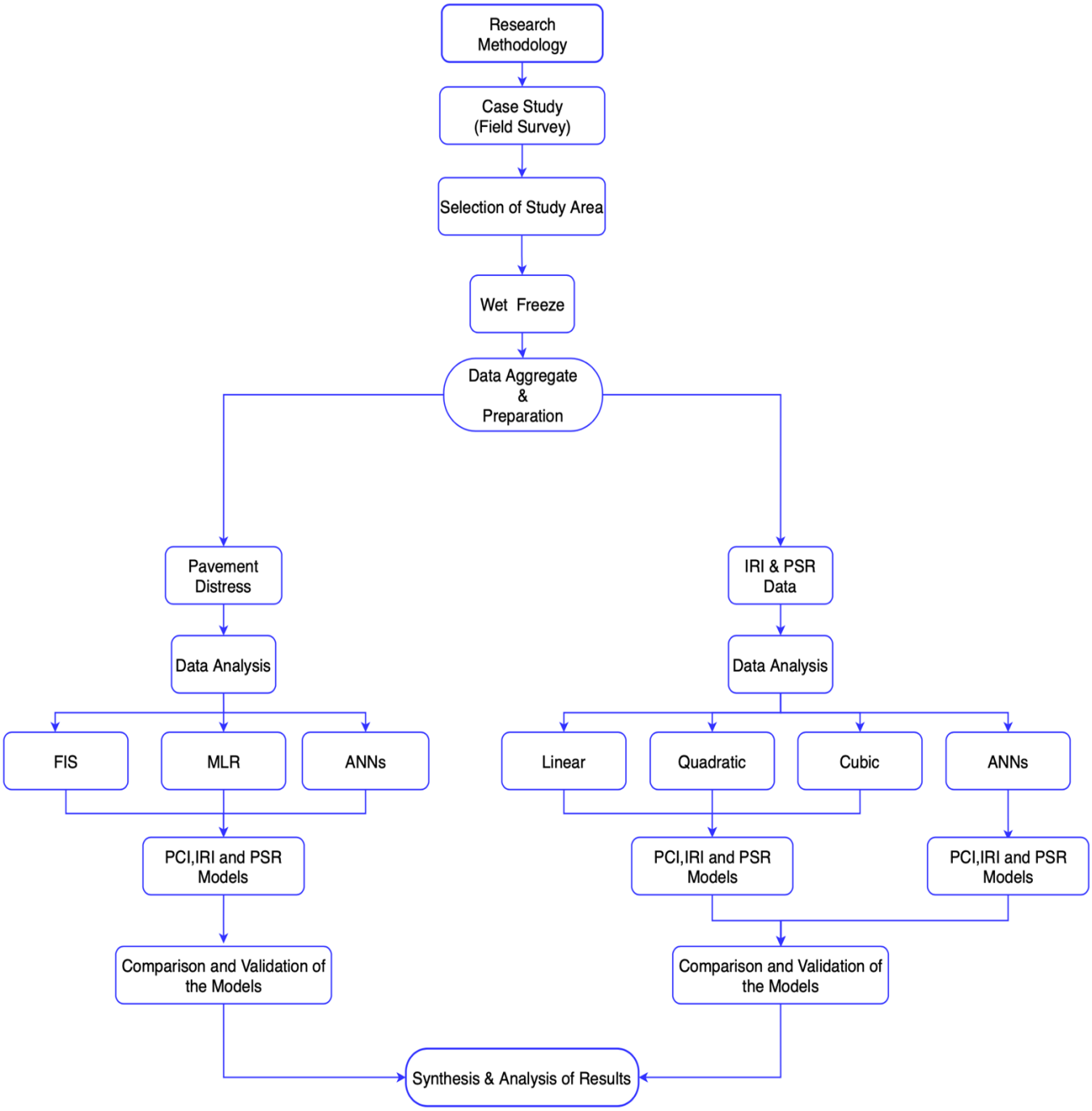

Figure7-1: Outline of the case study of research methodology.

7.2 Climate and Weather

Table (7-1) shows the available climate data for the last 90 years. The city is experiencing a harsh inclement climate, including an average snowfall of (330 mm /year) and temperature fluctuations (average low temp and average high temp) of -8.3 and 15.5 ° C, respectively. The average wind velocity is 21.5 km / h, with an annual precipitation average of 81%. Therefore, roads in this city suffer significant distresses, such as rutting, and potholes caused by moisture damage. This distress leads to substantial economic, health, and psychological problems for road users, due to increased travel time, increased accident rates, damage to vehicles and increased fuel usage.

Table 7-1: Weather conditions in the St. John's Newfoundland, Canada

Parameters	**unit**	**St. John's region (Wet Freeze)**
Age	**Year**	**90**
Average temp (low, high)	° C	(-8.3) to (+15.5)
Record daily (low, high)	° C	(-23.3) to (+29.5)
Total annual precipitation	(mm)	89-149
Total snowfall	Cm/year	27.58
Wind average	Km/h	21.5
Humidity	%	81

7.3 Smartphone Data Collection and Field Studies

The objective of collecting data on roads in St. John's was to evaluate pavement performance using three methods: (IRI), (PCI), and (PSR). The data collected contribute to creating models to predict the pavement condition via three methods (TotalPave smartphone application, visual inspection, and gathering drivers' opinions on driving comfort and road safety). To develop flexible pavement

performance and realize this research's objectives, researchers at Memorial University conducted a detailed field investigation of pavement conditions for 19 different roads.

The following sections overview the data collection methods and data processing techniques employed. The models developed in this section are particular for St. John's. A smartphone equipped with GPS and other sensors was used to collect data.

The smartphone and the holder were placed on the windshield, and then a TotalPave application was used to compile the data. This included roughness measurements of some major roads in St. John's, Newfoundland are mentioned in Table (7-2).

As specified by the TotalPave user guidelines, the vehicle was driven at a speed of (20-80 km / h) throughout data gatherings, as the IRI is sensitive to the same wavelengths of the profile, which causes vibrations in cars on roads at the designated speed (Sayers, 1995).

TotalPave can estimate IRI values based on the smartphone's vertical and horizontal motion. The motion along the vehicle's left-right, front-rear, and up-down directions is represented by the accelerometer's (x, y, z) axes. The data were obtained automatically and submitted to the application servers.

7.4 Study Area Location and Data Preparation

According to Canada's sixth annual climate change report (Government of Canada 2014), 28% of Canada's energy consumption is used in the transport sector. Road-driven vehicle transport constitutes the most considerable portion of this sector.

The number of vehicles in St. John's, Newfoundland, has increased by more than 100% in a short period due to a growing population. This ever-increasing trend influences the condition and efficiency of roads over time.

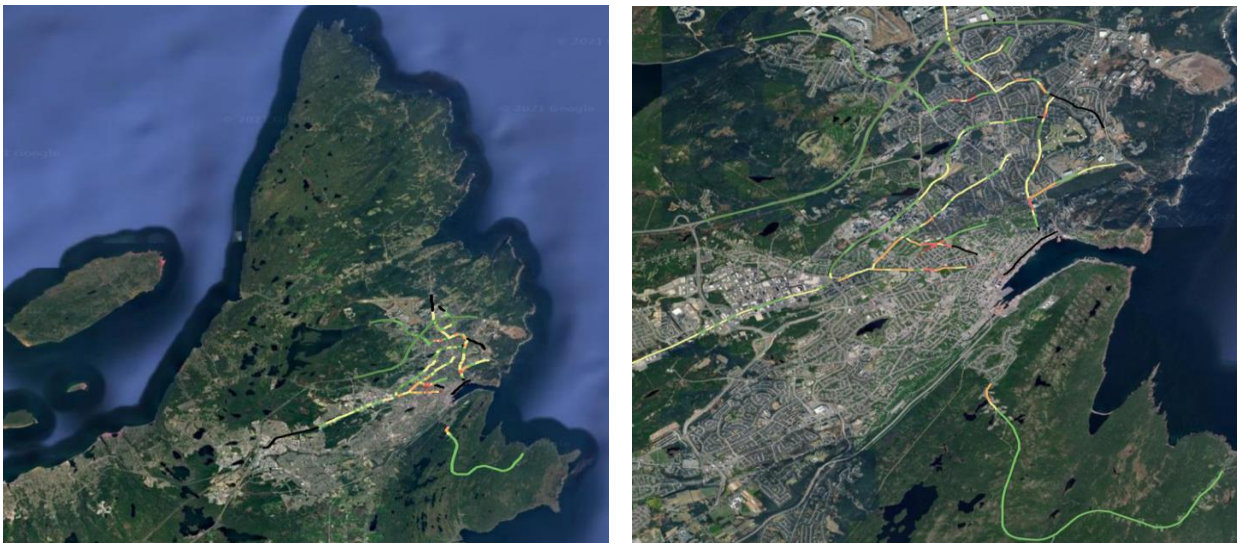

Figure 7-2: Map of the road network of the of St. John's.

The survey covered 19 different roads in St. John's (wet freeze climate) which were considered in this study. Pavement conditions in the selected sections ranged from very poor to excellent. The study examined a total of 58.3 km of road length, which included two Urban divided (7.7 km), sixteen Urban undivided (42 km), and one highway (8.6 km). The survey data collected in (2018 and 2021) have been used to develop asphalt performance models. Detailed information to classify IRI, PSR, and PCI were collected for all these roads. Table (7-2) shows a descriptive summary of the road network in St. John's selected for this study.

Ali et al. performed a distress survey on some road sections in St. John's, and they which was published at the 2021 (Journal of Transportation Engineering, Part B: Pavements). They also studied some roads other than the sections considered in the current analysis, and the survey was presented at the 2018 Conference of the Canadian Society for Civil Engineering (CSCE) (Ali et al., 2021., Ali et al., 2018).

Table 7-27: Details of study section.

Geometric Type	Road Name	Starting Coordinate	Ending Coordinate	Length (m)
Highway	Trans-Canada Highway	47.613080, -52.693132	47.572898, -52.778936	8600
Urban (Divided)	Prince Philip Dr	47.588916, -52.720251	47.561888, -52.749006	3900
	Portugal Cove Rd	47.595724, -52.726608	47.609546, -52.765798	3800
Urban (Undivided)	Elizabeth Ave Rd	47.563756, -52.739265	47.586281, -52.708537	3500
	Kenmount Rd	47.560475, -52.749060	47.533357, -52.831811	7000
	Torbay Rd	47.599852, -52.711999	47.638361, -52.724715	4500
	Logy Bay Rd	47.598178, -52.698031	47.581270, -52.704083	2000
	Kenna's Hill	47.580354, -52.704381	47.571455, -52.701725	1000
	Water St	47.570864, -52.697512	47.562220, -52.709403	1300
	King’s Bridge Rd	47.577570, -52.703921	47.571912, -52.701928	1000
	Blackhead Rd	47.539661, -52.712965	47.522431, -52.660019	8200
	Newfoundland Dr	47.595526, -52.725829	47.591908, -52.687005	3600
	Newtown Rd	47.569411, -52.731490	47.566484, -52.716049	1300
	Freshwater Rd	47.563767, -52.717459	47.561518, -52.745447	2200
	MacDonald Dr	47.590916, -52.718891	47.593944, -52.701323	1400
	Aberdeen Ave	47.619806, -52.718596	47.612738, -52.711725	1000
	Empire Ave	47.572286, -52.713828	47.565904, -52.729028	1400
	The Blvd	47.577727, -52.703588	47.584444, -52.684521	1600
	Highland Dr	47.604463, -52.717754	47.610121, -52.708517	1000

It was observed that damage caused by rutting and moisture (e.g., ravelling and potholes) are among the main types of distress observed on all roads in and around St. John's. Figure (7-3) displays representative photos of some of the road distress in the city. The severity levels were classified as the following, "Severe" for high severity, "Moderate" for moderate severity, and "Minimal" for low severity.

(a) Longitudinal Cracking (b)Transverse Cracking

(c) Structural Rutting (d) Abrasive Rutting

(d) Potholes (e) Fatigue Cracking

Figure 7-3: Representative photo showing different distress types in pavement sections.

7.5 Compilation and Analysis of Data

The following sections will concentrate on creating prediction models based on three indices: PCI, IRI, and PSR.

7.5.1 Pavement Condition Index (PCI)

Visual examination is essential to understanding all challenges facing the roads in St. John's, which suffer from severe structural and functional distress. Visual inspection information is used to determine the current pavement condition for PCI determination.

A two-step method was applied to the collected data using visual examination. First, the survey team drove across the chosen major and minor roads and collected pictures and videos of the road surfaces. These photos and clips were then manually processed and analyzed to understand the pavement performance. Secondly, the survey team walked along with the selected road areas for closer examination and gathering of road condition data. The distress was categorised and rated based on type and severity.

This research is expected to improve pavement service life by creating enhanced prediction models and improving traffic safety. PCI values were determined using the ASTM D6433-18 process. Around 60 km of road sections located within the St. John's municipality were visually examined, and the various distress characteristics were recorded. The PCI value calculation for Empire Avenue is presented in Table (7-3) as an example. Table (7-4) presents IRI, PSR, and PCI values measured for the 19 road sections.

Table 7-3: PCI determination from pavement distresses.

Empire Avenue Road (Section: I)							Area of Sample =720m^2	
Type of Distress	Rutting	Block	Fatigue	Long	Trans	Delamination	Pothole	Patching
Unit	(m^2)	(m^2)	(m^2)	(m^2)	(m^2)	(m^2)	(no)	(m^2)
Quantity	1.10	1.30	0	17	0	11	4	38
Level of Severity	Mb	Mb	-	Lc	-	Ha	Lc	Mb
Density (%)	0.15	0.18	0	2.35	0	1.52	0.55	5.24
Deduct Value	7	16	0	14	0	11	46	36
Total	130							
Corrected Deduct Value= 89								
PCI	100-89=11				Very poor			
Empire Avenue Road (Section: II)							Area of Sample =1440m^2	
Quantity	2.25	2.10	0	21	0	10.50	6	51
Level of Severity	Mb	Lc	-	Mb	-	Mb	Lc	Mb
Density (%)	0.16	0.15	0	1.47	0	0.74	0.42	3.57
Deduct Value	8	5	0	20	0	17	42	31
Total	123							
Corrected Deduct Value=87								
PCI	100-87=13				Very poor			
Ha = High severity, Mb = Medium severity, Lc = Low severity								

7.5.2 International Roughness Index (IRI)

IRI data were being captured by a smartphone application called "TotalPave". This application can capture the vertical movement resulting from the road's rough surface and calculate the IRI value in real-time. This application feature of no pre-or post-processing required for the pavement distress data obtained was the primary motivation behind this application's use in the study.

Furthermore, TotalPave is easy to use at a comparatively low cost. The TotalPave application was installed on a smartphone to gather the IRI data, then placed on the vehicle's windshield using a mobile phone holder. It was confirmed that minimal bumping and vibration of the phone occurred. To comply with TotalPave user guidelines, the vehicle was driven at a speed of between 20 and 80 kilometres per hour (km/h) throughout data gathering. The final IRI value for each road was stated as the arithmetic average of IRI values of all road sections. The average IRI data obtained for various road sections are illustrate in Table (7-4). As predicted, a high variation in IRI values was noted, based on the distress conditions. Specifically, Portugal Cove Road can be regarded as the best performing road among the city's roads. The freeway sections showed the lowest levels of roughness when all various types of roads were considered. Users felt less comfort because of the highest IRI value on Empire Avenue, followed by King's Bridge Road. Generally, most of these road sections showed high IRI values, suggesting bad road conditions.

7.5.3 Present Serviceability Rating (PSR)

This survey was carried out to gather drivers' opinions on driving comfort and road safety on a scale of five levels, namely very bad, poor, fair, good, and excellent. The survey was emailed to potential respondents (drivers that were mainly graduate students and employees of Memorial University). The percentage of opinions was determined to evaluate (PSR) values for the chosen road sections. A low value of serviceability means that the road surface was compromised by numerous difficulties and was in poor condition. The PSR value for most of these road sections was between 2 and 3, suggesting that the roads were fair to good. The results collected from the pavement serviceability survey carried out during this research are summarised in Table (7-4).

Table 7-4: IRI, PSR, and PCI values of the road sections.

Type	Road Name	IRI (2018)	IRI (2021)	PSR (2018)		PCI (2018)		PCI (2021)	
				I	II	I	II	I	II
Highway (Divided)	Trans-Canada Highway	1.09	1.10	3.22	3.47	75	74	71	73
Urban (Divided)	Prince Philip Dr	2.22	2.44	3.25	3.30	68	67	55	55
	Portugal Cove Rd	1.77	1.88	2.84	2.89	60	64	61	64
Urban (Undivided)	Elizabeth Ave Rd	5.3	6.02	2.593	2.591	23	14	21	13
	Kenmount Rd	2.59	3.10	2.84	3.0	49	45	43	39
	Torbay Rd	3.04	3.29	2.90	2.91	44	33	48	37
	Blackhead Rd	2.13	2.53	2.91	2.99	49	61	41	57
	Logy Bay Rd	3.98	5.83	2.87	2.96	23	41	19	22
	Kenna's Hill	4.28	3.94	2.73	2.77	33	-	40	-
	Water St	3.63	2.25	2.75	2.89	48	20	60	44
	King's Bridge Rd	5.68	4.37	2.75	2.60	17	20	35	35
	Newfoundland Dr	3.89	3.42	2.68	2.80	21	19	27	25
	Newtown Rd	4.39	4.78	2.82	2.82	32	37	28	31
	Freshwater Rd	3.50	4.26	2.70	2.75	41	44	37	37
	MacDonald Dr	2.16	2.77	3.31	3.47	57	67	54	54
	Aberdeen Ave	2.11	2.80	3.20	2.43	50	58	53	43
	Empire Ave	4.05	4.10	2.43	2.61	11	13	11	13
	The Blvd	3.19	3.87	2.93	2.96	44	37	41	32
	Highland Dr	2.94	2.59	3.27	3.20	45	62	56	71

7.6 Modeling of Asphalt Pavement Performance Indices using (FIS)

This part of the research attempts to implement one of the soft computing methods in pavement serviceability evaluation. The FIS has been applied to 19 St. John's roads as a case study in areas where roads of St. John's suffer from the eight distress types: rutting, fatigue cracking, block

cracking, longitudinal and transverse cracking, patching, potholes, and delamination. The fuzzy model uses iterations of the severity of the deterioration as inputs to create prediction models (PCI and IRI).

7.6.1 Methodology Fuzzy Inference System

As mentioned in chapter 4, a methodology based on a case study to evaluate road pavements using soft computing techniques has been proposed. The case study presented two models estimating the FPCI and FIRI, based on the data collected. Three trade-off steps were followed during the analysis, the Fuzzification, Normalization, and Defuzzification modules, as demonstrated in Figure (7-4).

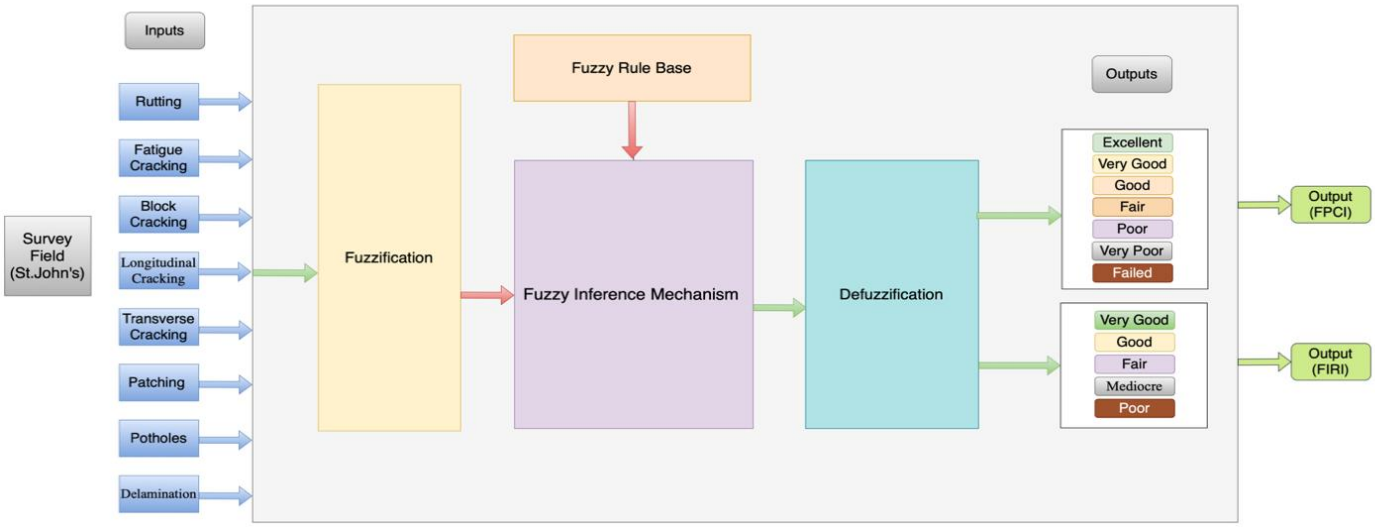

Figure 7-4: Diagram of a pavement classification on FIS.

7.6.1.1 Data Pre-processing and Feature Selection

After the data were collected and revised for 19 roads in St. John's, the fuzzy model was prepared with eight independent parameters of the distress types.

Table 7-5: Distress types and number of membership functions to evaluate PCI and IRI.

Distress of type	Category	Number of MF	Description
Rutting	Input	Minimal, Moderate, Severe	Extremely important
Fatigue Cracking	Input	Minimal, Moderate, Severe	Relatively important
Block Cracking	Input	Minimal, Moderate, Severe	Important
Longitudinal Cracking	Input	Minimal, Moderate, Severe	Important
Transverse Cracking	Input	Minimal, Moderate, Severe	Moderately important
Patching	Input	Minimal, Moderate, Severe	Moderately important
Potholes	Input	Minimal, Moderate, Severe	Relatively important
Delamination	Input	Minimal, Moderate, Severe	Relatively important
IRI	Output	Poor, Mediocre, Fair, Good, Very Good	Extremely important
PCI	Output	Failed, Very Poor, Poor, Fair, Good, Very Good, Excellent	Extremely important

7.6.1.2 Membership Functions

The membership functions for the input and output variables functions have been determined. The membership functions for all input variables are categorised as Minimal, Moderate, and Severe. The output variables have seven PCI membership functions classified as: Very Poor, Poor, Fair, Good, Very Good, and Excellent. Similarly, the output variables have five IRI membership functions classified as: Poor, Mediocre, Fair, Good. and Very Good (ASTM International D6433-18). As mentioned in chapter 4, for each input and output (PCI and IRI), the x-axis reflects the distress density, while the y-axis is a membership function varying between [0 to 1]. '0' indicates no statistical relationship, and '1' indicates a strong relationship.

7.6.1.3 Fuzzy Rule Generation:

Generating the rules is the major challenge in FIS through the second phase. It was complicated to generate all rules concerning all previous combinations. The classification model's generation

rules described in this work are difficult and complex because they consist of eight inputs and one output. The Tables (7-6) (7-7) Rule base was formed for FIS, for PCI, and IRI, respectively.

Table 7-6: Fuzzy rules for PCI by 19 road sections.

Rule No	Distress type (Input)								PCI (Output)
	Rutting	Fatigue Cracking	Block Cracking	Longitudinal Cracking	Transverse Cracking	Patching	Potholes	Delamination	
1	Minimal	Minimal	Minimal	Minimal	Minimal	Minimal	Minimal	Minimal	Excellent
2	Minimal	Minimal	Minimal	Moderate	Minimal	Minimal	Minimal	Minimal	Excellent
3	Minimal	Minimal	Minimal	Severe	Minimal	Minimal	Minimal	Minimal	Very Good
4	Minimal	Minimal	Minimal	Minimal	Severe	Minimal	Minimal	Minimal	Good
5	Minimal	Severe	Minimal	Moderate	Minimal	Minimal	Minimal	Minimal	Good
6	Minimal	Moderate	Minimal	Minimal	Severe	Minimal	Minimal	Minimal	Good
7	Minimal	Moderate	Minimal	Minimal	Minimal	Minimal	Minimal	Minimal	Good
8	Moderate	Minimal	Minimal	Minimal	Minimal	Minimal	Minimal	Minimal	Good
9	Minimal	Moderate	Minimal	Moderate	Severe	Minimal	Minimal	Moderate	Good
10	Minimal	Moderate	Minimal	Moderate	Minimal	Minimal	Minimal	Minimal	Fair
11	Minimal	Minimal	Minimal	Moderate	Moderate	Minimal	Minimal	Minimal	Fair
12	Minimal	Severe	Minimal	Minimal	Minimal	Minimal	Minimal	Moderate	Fair
13	Severe	Moderate	Minimal	Minimal	Minimal	Minimal	Minimal	Minimal	Poor
14	Minimal	Severe	Minimal	Minimal	Moderate	Minimal	Minimal	Minimal	Poor
15	Minimal	Moderate	Minimal	Minimal	Minimal	Moderate	Minimal	Minimal	Poor
16	Minimal	Minimal	Minimal	Moderate	Severe	Minimal	Minimal	Minimal	Poor
17	Minimal	Minimal	Minimal	Moderate	Moderate	Minimal	Minimal	Minimal	Very Poor
18	Moderate	Moderate	Minimal	Minimal	Moderate	Minimal	Minimal	Moderate	Very Poor
19	Minimal	Moderate	Minimal	Moderate	Severe	Minimal	Minimal	Moderate	Very Poor
20	Moderate	Minimal	Minimal	Minimal	Moderate	Minimal	Minimal	Minimal	Very Poor
21	Moderate	Severe	Minimal	Severe	Severe	Minimal	Minimal	Moderate	Very Poor
22	Minimal	Moderate	Minimal	Moderate	Moderate	Minimal	Minimal	Minimal	Very Poor
23	Moderate	Minimal	Minimal	Severe	Severe	Minimal	Minimal	Minimal	Very Poor
24	Minimal	Moderate	Minimal	Minimal	Moderate	Minimal	Minimal	Minimal	Failed
25	Minimal	Severe	Minimal	Moderate	Severe	Minimal	Minimal	Minimal	Failed
26	Moderate	Moderate	Minimal	Moderate	Severe	Minimal	Minimal	Minimal	Failed
27	Severe	Severe	Minimal	Moderate	Moderate	Minimal	Minimal	Moderate	Failed

Table 7-7: Fuzzy rules for IRI by 19 road sections.

Rule No	Distress type (Input)								IRI (Output)
	Rutting	**Fatigue Cracking**	**Block Cracking**	**Longitudinal Cracking**	**Transverse Cracking**	**Patching**	**Potholes**	**Delamination**	
1	Minimal	Minimal	Minimal	Minimal	Minimal	Minimal	Minimal	Minimal	Very Good
2	Minimal	Minimal	Minimal	Minimal	Severe	Minimal	Minimal	Minimal	Very Good
3	Minimal	Minimal	Minimal	Minimal	Moderate	Minimal	Minimal	Minimal	Very Good
4	Moderate	Moderate	Minimal	Minimal	Minimal	Minimal	Minimal	Minimal	Good
5	Minimal	Minimal	Minimal	Minimal	Moderate	Minimal	Minimal	Moderate	Good
6	Moderate	Minimal	Minimal	Moderate	Minimal	Minimal	Minimal	Minimal	Fair
7	Minimal	Moderate	Minimal	Severe	Moderate	Minimal	Minimal	Minimal	Fair
8	Moderate	Minimal	Minimal	Moderate	Moderate	Minimal	Minimal	Minimal	Mediocre
9	Minimal	Minimal	Minimal	Severe	Minimal	Minimal	Minimal	Minimal	Mediocre
10	Minimal	Minimal	Minimal	Severe	Minimal	Minimal	Minimal	Minimal	Mediocre
11	Severe	Moderate	Minimal	Minimal	Moderate	Minimal	Minimal	Minimal	Poor
12	Moderate	Minimal	Minimal	Severe	Moderate	Minimal	Minimal	Moderate	Poor
13	Severe	Severe	Minimal	Severe	Severe	Minimal	Minimal	Moderate	Poor

7.6.1.4 The Results of Pavement Section Classification

The system was evaluated using data collected for 19 road sections during 2018 and 2021. This technique created membership functions and rules by measuring fuzzy pavement classification efficiency. Four defuzzified methods (Centroid, Bisector, Som, and Lom) were used to find the R^2, the RMSE, and MAE, to display the level of agreement of the PCI and IRI values.

- **Fuzzy Pavement Condition Index (PCI)**

Table (7-8) presents the agreement level of the PCI values using four defuzzified methods. Figure (7-5) shows the relation between the observed PCI and fuzzified PCI for 19 road sections.

Table 7-8: Assessment various fuzzy inference systems' configurations for PCI.

Inference	Year	Defuzzification	Statistical Error Measures			Improvement (%)		
			R^2	RMSE	MAE	R^2	RMSE	MAE
Mamdani (Triangular)	**2018**	Centroid	96.6*	3.456*	2.919*	-	-	-
		Bisector	96.6	3.652	3.149	-	-	-
		Lom	96.1	4.136	3.541	-	-	-
		Som	95.9	4.751	3.595	-	-	-
	2021	Centroid	96.3	3.468	2.917	-0.31	-0.35	-0.07
		Bisector	96.0	3.68	3.167	-0.62	-0.76	-0.57
		Lom	96.1	4.11	3.50	0	+0.63	+1.58
		Som	95.5	4.805	3.639	-0.42	+1.19	-1.21

*Indicates the best results for each fuzzy system in the column.

The goodness of fit statistics of the 19 road sections in Table (7-8) provides the following observation:

- **Centroid method:** The results indicated that the R^2, RMSE, and MAE values were 96.6%, 3.456%, and 2.919%, respectively.
- **Bisector method:** The results indicated that the R^2, RMSE, and MAE values were 96.6%, 3.652%, and 3.149%, respectively.
- **Lom method:** The results indicated that the R^2, RMSE, and MAE values were 96.1 %,4.136%, and 3.541%, respectively.
- **Som method:** The results indicated that the R^2, RMSE, and MAE values were 95.9%,4.751%, and 3.595%, respectively.

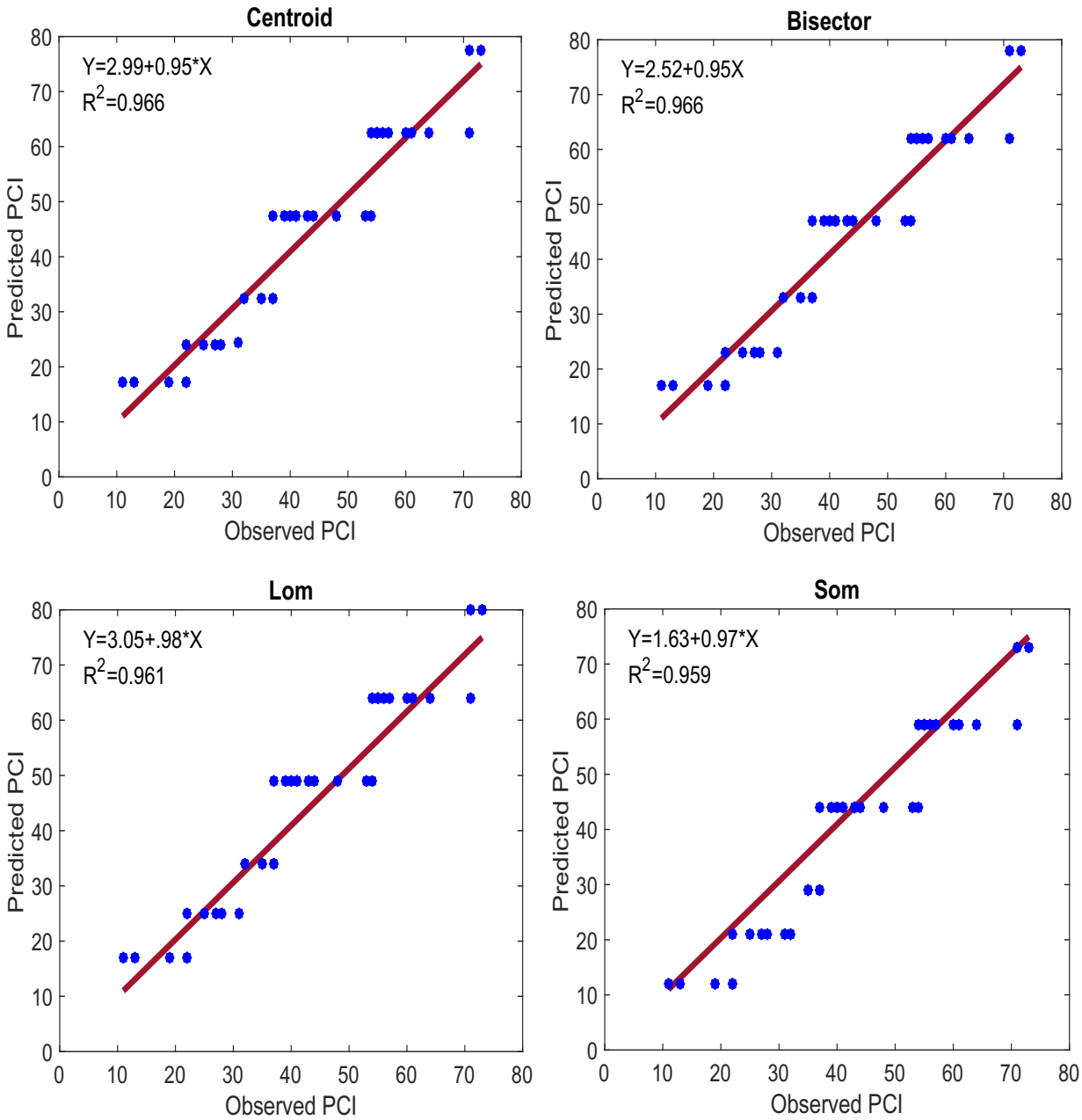

Figure 7-5: Fuzzy inference system for PCI(2018).

The results illustrated that the centroid method yields a more accurate result (R^2= 96.6%, RMSE =3.456%, and MAE=2.919%) than other methods. However, the Som method shows the lowest values out of the four methods, (R^2= 95.9%, RMSE =4.751% and MAE=3.595%).

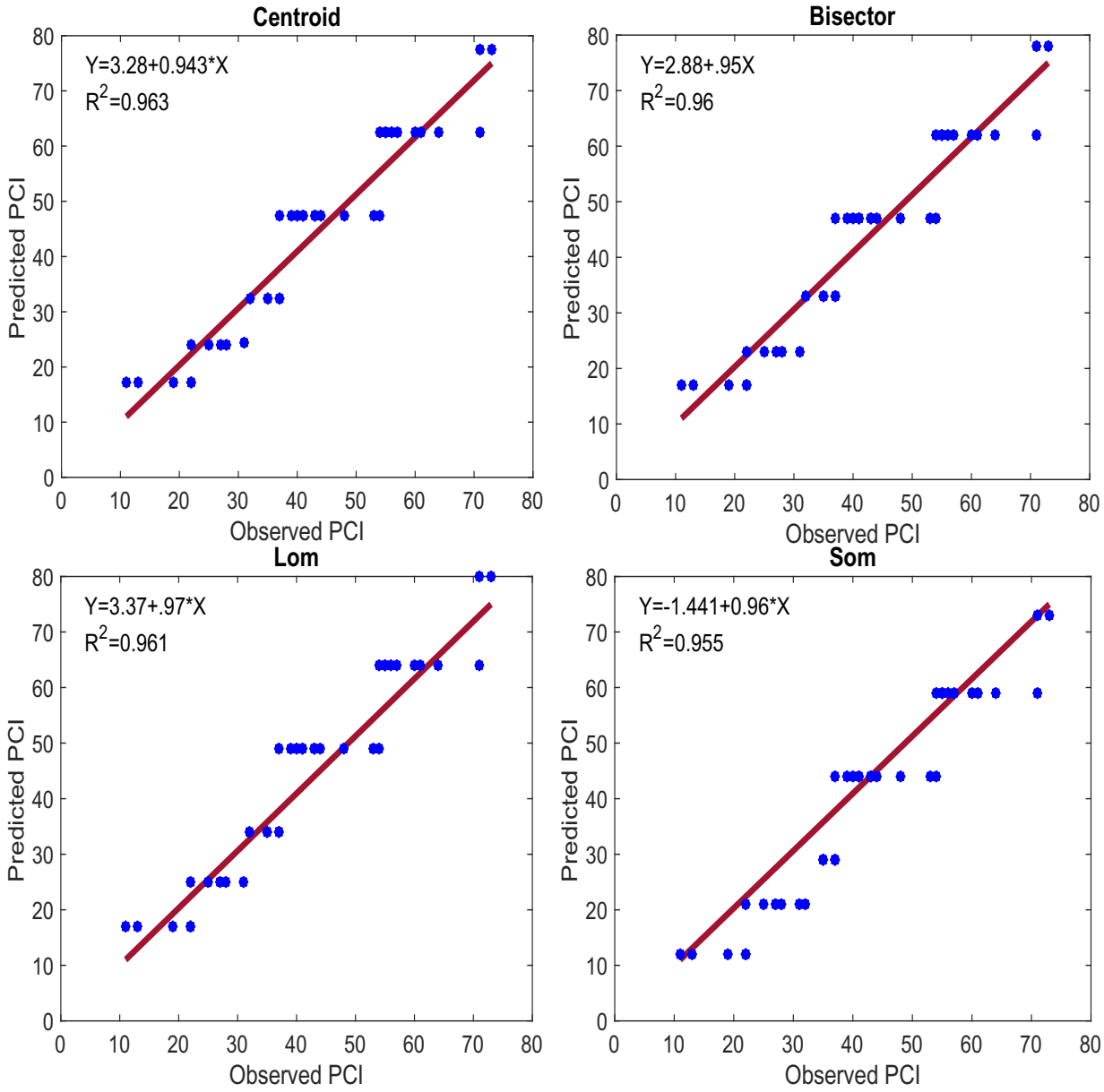

Figure 7-6: Fuzzy inference system for PCI (2021).

- **Fuzzy International Roughness Index (IRI)**

Table (7-9) presents the agreement level of the PCI values using four defuzzified methods Figure (7-6) showed the relation between the observed IRI and fuzzified IRI for 19 road sections.

Table 7-9: Assessment various fuzzy inference systems' configurations for IRI.

Inference	Year	Defuzzification	Statistical Error Measures			Improvement (%)		
			R^2	RMSE	MAE	R^2	RMSE	MAE
Mamdani (Triangular)	**2018**	Centroid	88.3*	0.567*	0.446*	-	-	-
		Bisector	88.1	0.675	0.523	-	-	-
		Lom	88.2	0.671	0.521	-	-	-
		Som	86.3	0.988	0.797	-	-	-
	2021	Centroid	88.5*	0.537*	0.409*	+0.226	+5.30	+8.30
		Bisector	87.2	0.54	0.411	-1.02	+20.0	+21.41
		Lom	86.5	0.662	0.506	-1.93	+1.34	+2.88
		Som	87.2	0.637	0.431	+1.03	+35.52	+45.92

*Indicates the best results for each fuzzy system in the column.

The goodness of fit statistics of the 19 road sections in Table (7-9) provides the following observation:

- **Centroid method:** The results indicated that the R^2, RMSE, and MAE values were 88.3%, 0.567%, and 0.446%, respectively.
- **Bisector method:** The results indicated that the R^2, RMSE, and MAE values were 88.1%, 0.675%, and 0.523%, respectively.
- **Lom method:** The results indicated that the R^2, RMSE, and MAE values were 88.2 %,0.671%, and 0.521%, respectively.
- **Som method:** The results indicated that the R^2, RMSE, and MAE values were 86.3%, 0.988%, and 0.797%, respectively.

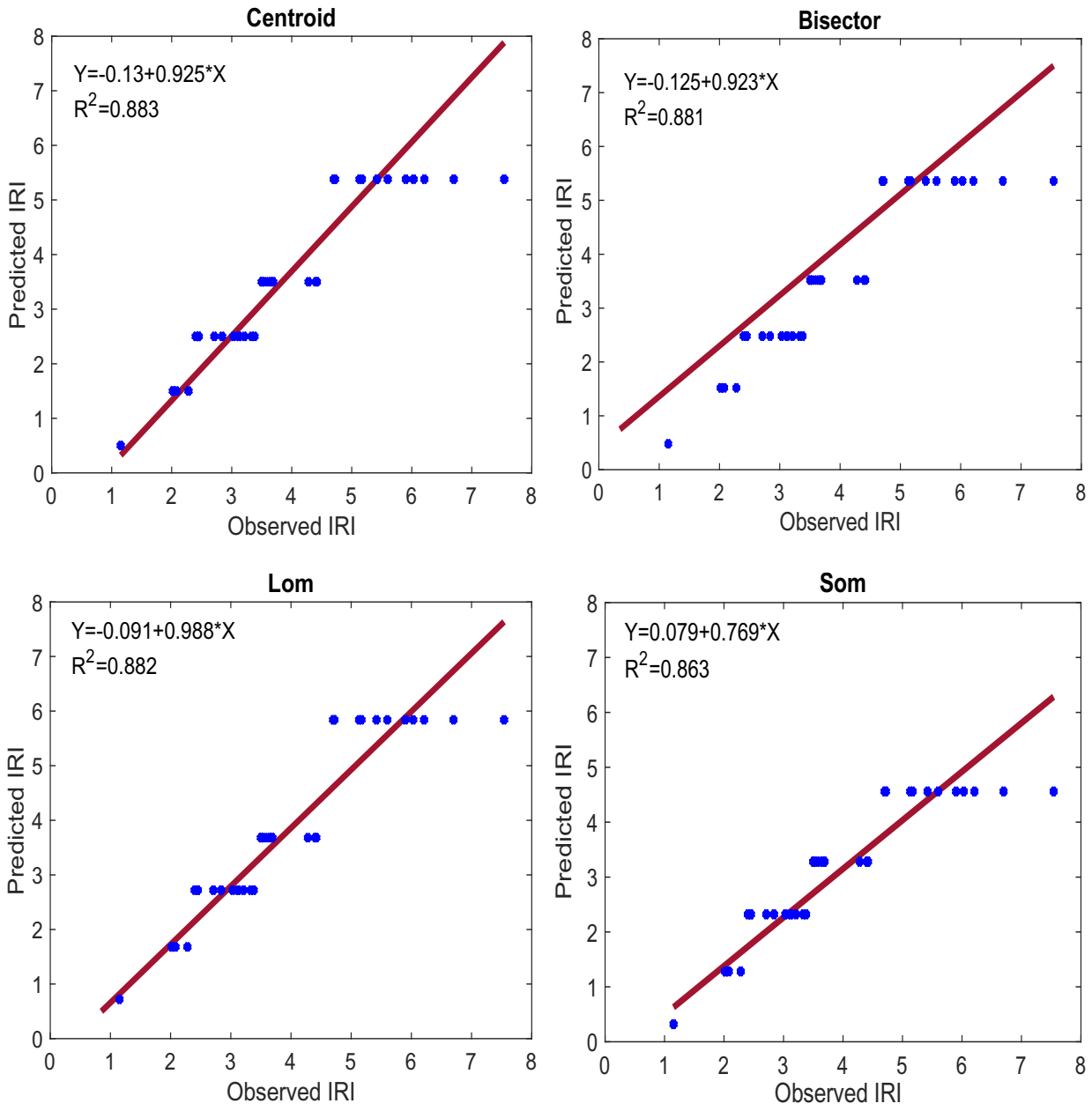

Figure 7-7: Fuzzy inference system for IRI(2018).

The results illustrated that the centroid method yields a more accurate result (R^2= 88.3%, RMSE =0.567%, and MAE=0.446%) than other methods.

The Bisector method showed the lowest values of the four methods (R^2= 88.1 %, RMSE =0.675% and MAE=0.523%).

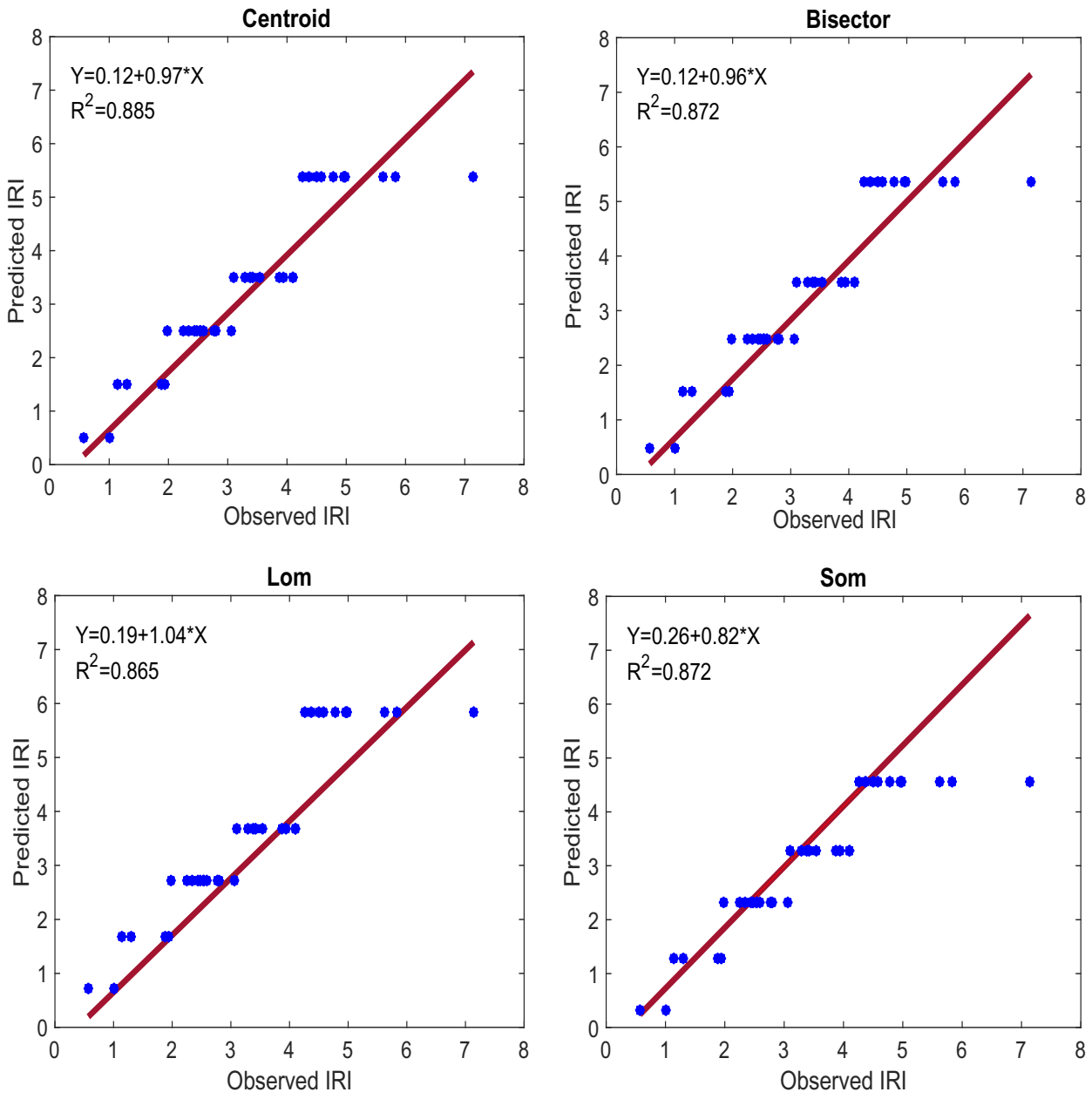

Figure 7-8: Fuzzy inference system for IRI (2021).

7.7 Modeling the Relationship Between Indices PCI, IRI, and PSR Using Mathematical and (ANNs)Techniques

7.7.1 Modeling the Relationship Between Indices PCI, IRI, and PSR Using Mathematical Methods

This section seeks to shed light on the relationship between IRI, PSR, and PCI based on field surveys for (2018 and 2021). Three mathematical methods (linear, quadratic, and cubic) have been used to develop a correlation between (PCI and IRI,) (PCI and PSR), and (IRI and PSR). Analysis was carried out by the SPSS programme to determine the correlation between these indicators. The correlation was assessed using R^2 values, RMSE, and MAE. Figures (7-9) to (7-11) present relationships among (PCI and IRI), (PCI and PSR), and (IRI and PSR), respectively. Equations from (7-1) to (7-9) summarised the regression models and presented the relation between (PCI and IRI,) (PCI and PSR), and (IRI and PSR) as follows:

1- Equations from (7-1) to (7-13) present the regression models and the relation between PCI and IRI using linear, quadratic, and cubic, respectively:

$$\boldsymbol{PCI = 85.657 - 11.380(IRI)} \qquad \textbf{7-1}$$

The correlation coefficient (R^2) of this relationship is **89.5%.**

$$\boldsymbol{PCI = 100.092 - 0.195(IRI) + 0.978(IRI)^2} \qquad \textbf{7-2}$$

The correlation coefficient (R^2) of this relationship is **91.6%.**

$$\boldsymbol{PCI = 80.645 - 1.44(IRI) - 3.87(IRI)^2 - 0.387(IRI)^3} \qquad \textbf{7-3}$$

The correlation coefficient (R^2) of this relationship is **92.9%.**

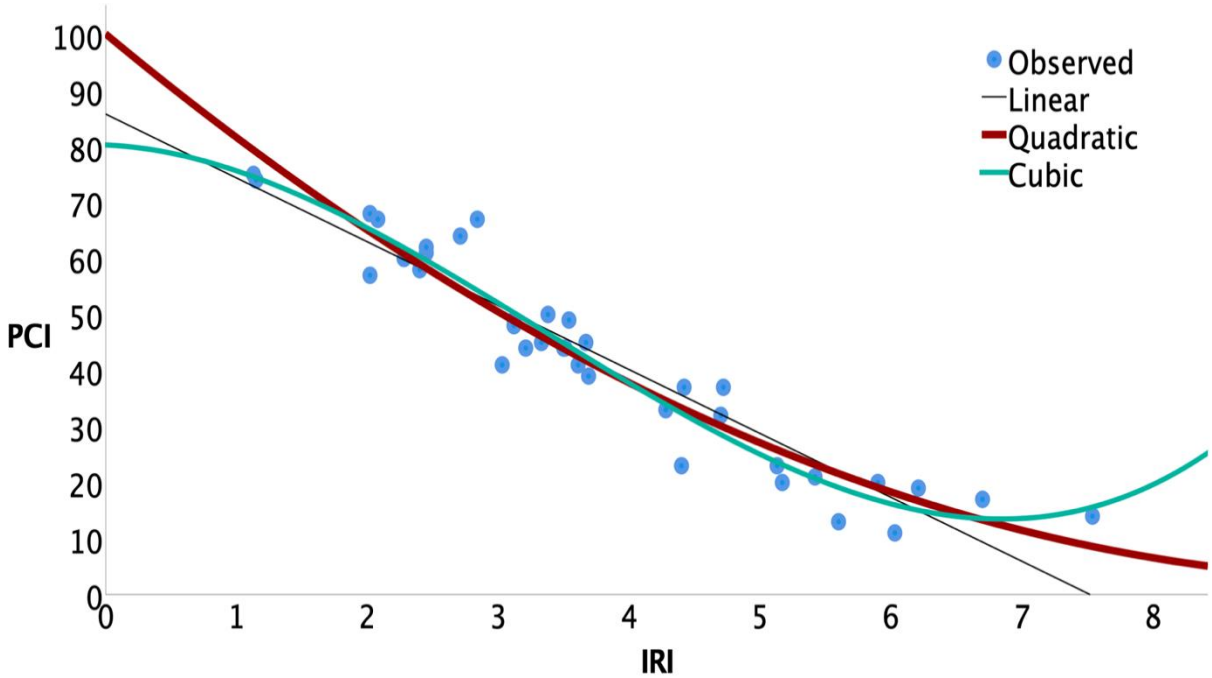

Figure7-9: PCI versus IRI plot.

2- Equations from (7-4) to (7-6) present the regression models and the relation between PCI and PSR using linear, quadratic, and cubic, respectively:

$$\mathbf{PCI} = -\ \mathbf{111.055} + \mathbf{53.54}\ (\mathbf{PSR}) \qquad \textbf{7-4}$$

The correlation coefficient (R^2) of this relationship is **55.7%.**

$$\boldsymbol{PCI} = -\mathbf{286} + \mathbf{1.72} \times \mathbf{10^2}(\boldsymbol{PSR}) - \mathbf{20.14}(\boldsymbol{PSR})^{\mathbf{2}} \qquad \textbf{7-5}$$

The correlation coefficient (R^2) of this relationship is **56.5%.**

$$\boldsymbol{PCI} = \mathbf{1.46} \times \mathbf{10^3} - \mathbf{1.63} \times \mathbf{10^3}(\boldsymbol{PSR}) + \mathbf{5.98} \times \mathbf{10^2}(\boldsymbol{PSR})^{\mathbf{2}} - \mathbf{70.21}(\boldsymbol{PSR})^{\mathbf{3}} \qquad \textbf{7-6}$$

The correlation coefficient (R^2) of this relationship is **57.3%.**

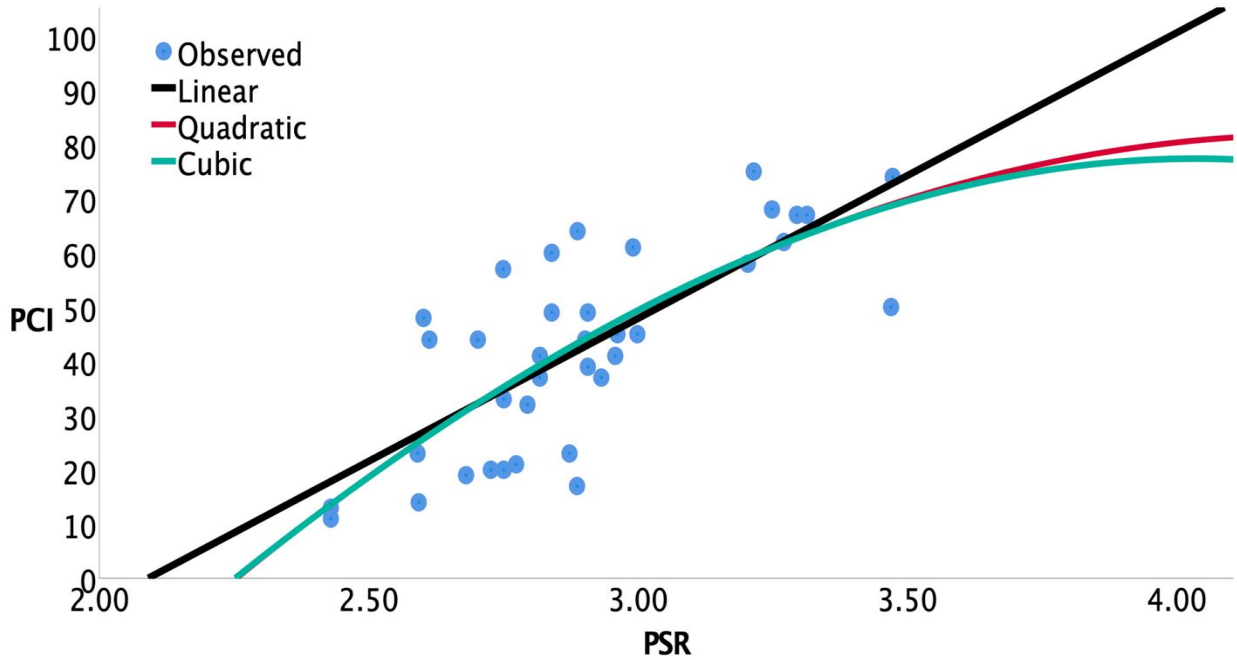

Figure 7-10: PCI versus PSR plot.

3- Equations from (7-7) to (7-9) present the regression models and the relation between IRI and PSR using linear, quadratic, and cubic, respectively:

$$\boldsymbol{IRI = 14.8 - 3.80\,(PSR)} \qquad \textbf{7-7}$$

The correlation coefficient (R^2) of this relationship is **42%.**

$$\boldsymbol{IRI = 27.39 - 12.36(PSR) + 1.45(PSR)^2} \qquad \textbf{7-8}$$

The correlation coefficient (R^2) of this relationship is **42.5%.**

$$\mathrm{IRI} = \boldsymbol{-1.22\times 10^2 + 1.42\times 10^2(\mathrm{PSR}) - 51.48(PSR)^2 + 6.01(PSR)^3} \qquad \textbf{7-9}$$

The correlation coefficient (R^2) of this relationship is **43.4%.**

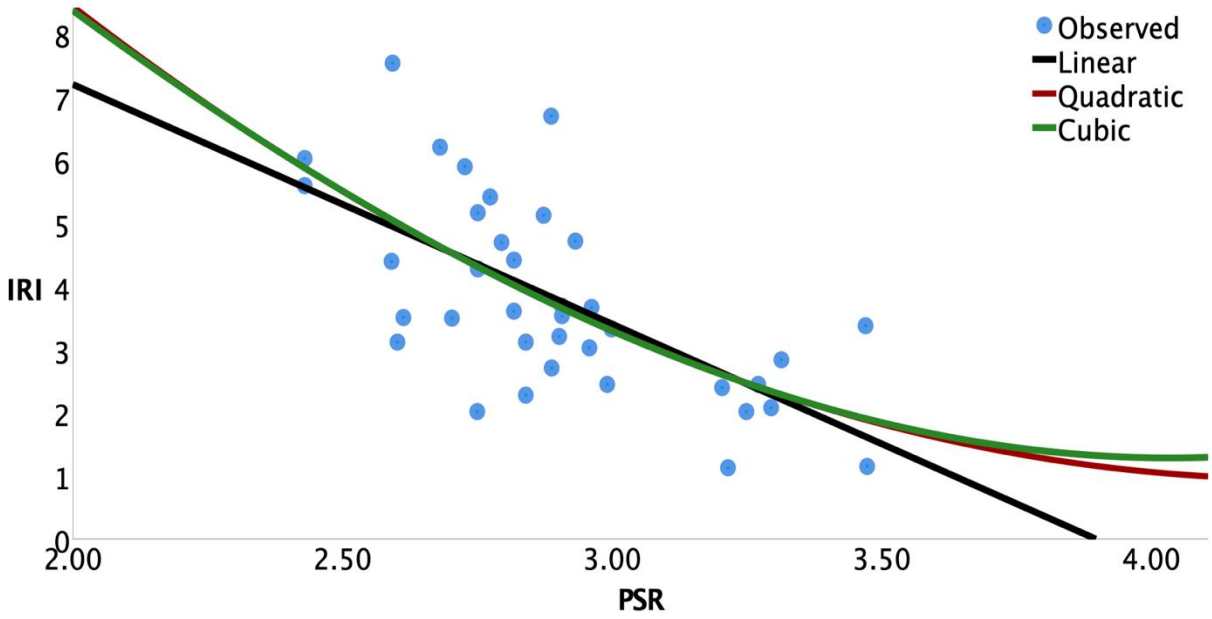

Figure7-11: IRI versus PSR plot.

7.7.2 Comparison and Validation of the Models

The performance of the linear method was compared with the performance of the quadratic and cubic methods to evaluate the accuracy of the models in predicting pavement performance based on pavement distress parameters. R^2, RMSE and MAE values were used to compare the performance of the models. Table (7-10) presents the comparison among (PCI&IRI), (PCI&PSR), and (IRI&PSR).

Table 7-10: Correlation between IRI, PCI & PSR.

Correlation	Statistical Error Measures								
	Linear			Quadratic			Cubic		
	R^2	RMSE	MAE	R^2	RMSE	MAE	R^2	RMSE	MAE
PCI &IRI	89.5	5.956	4.68	91.6	5.216	4.145	92.9	4.899	3.744
PCI&PSR	55.7	12.3	9.82	56.5	13.27	11.3	57.3	12.10	9.48
IRI&PSR	42.0	1.925	1.496	42.5	1.72	0.91	43.4	1.16	0.90

According to Table (7-10), several observations can be drawn:

- **PCI &IRI:** The results indicated that the R^2, RMSE, and MAE values of the cubic models improved by 3.66%, 17.75%, 20%,1.4%, 6.08%, and 9.67% compared to the linear models and quadratic model, respectively.
- **PCI&PSR: The** results indicated that the R^2, RMSE, and MAE values of the cubic models improved by 2.79%, 1.63%, 3.46%,1.4%, 8.82%, and 16.11% compared to the linear models and quadratic model, respectively.
- **IRI&PSR:** The results indicated that the R^2, RMSE, and MAE values of the cubic models improved by 2.07%, 39.74%, 39.84%, 2.07%, 32.56%, and 1.10% compared to the linear models and quadratic model, respectively.

Results showed that the cubic had the best fit in all cases with less error between the observed and predicted values, compared to linear and quadratic methods.

7.7.3 Modeling the Relationship between Indices Using (ANNs) Technique

Artificial neural networks have been used to develop effective and accurate models. These models were used to predict the relationship between the (PCI&IRI), (PCI&PSR), and (IRI &PSR) obtained from the field survey. The architecture of the designed network consisted of one input layer with one variable, three hidden layers, and an output layer. The model's performance was assessed using the three common methods of R^2value, RMSE, and MAE. Figures (7-12) to (7-14) present the ANNs prediction results for PCI, IRI, and PSR models. Table (7-11) show the performance of PCI models.

Table 7-11: Performance of PCI models.

Indicators	Statistical Error Measures (PCI)		
	R^2	RMSE	MAE
PCI &IRI	94.6	4.275	2.924
PCI&PSR	75.4	9.272	5.994
IRI&PSR	70.0	0.841	0.539

Table (7-11) shows the R^2, RMSE and MAE values were as follows:

- **PCI &IRI:** The R^2value was 94.6%, while the RMSE and MAE values were 4.275% and 2.924%.
- **PCI&PSR:** The R^2value was 75.4%, while the RMSE and MAE values were 9.272% and 5.994%.
- **IRI&PSR:** The R^2value was 70.0%, while the RMSE and MAE values were 0.841% and 0.539%.

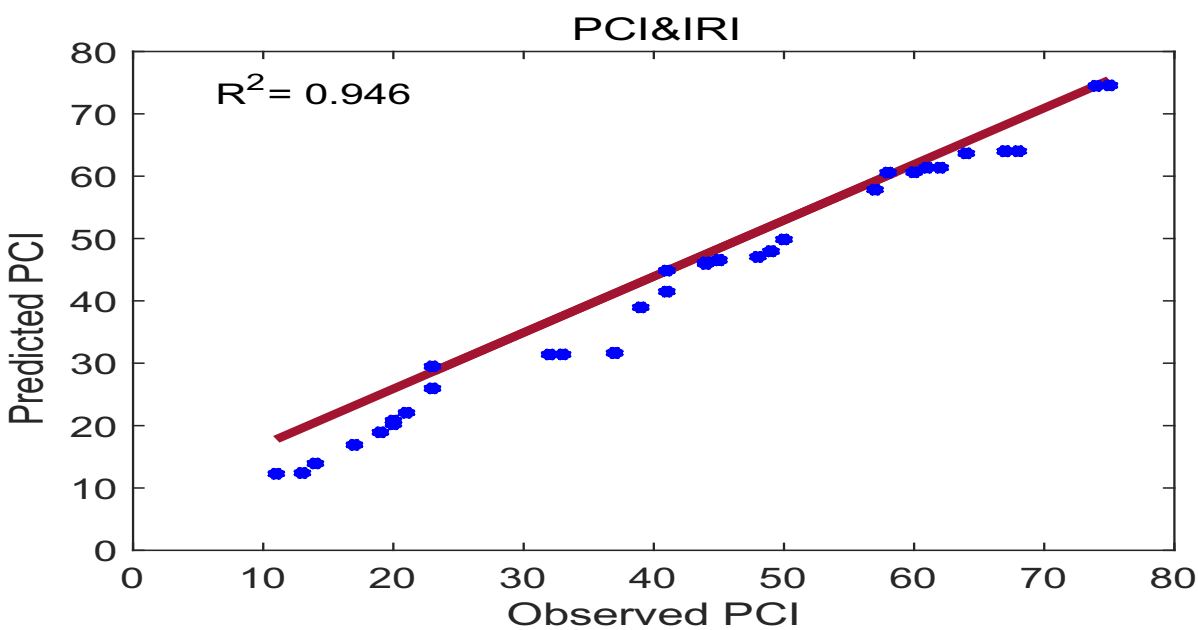

Figure 7-12: Performance of the ANNs for predicting PCI model from IRI.

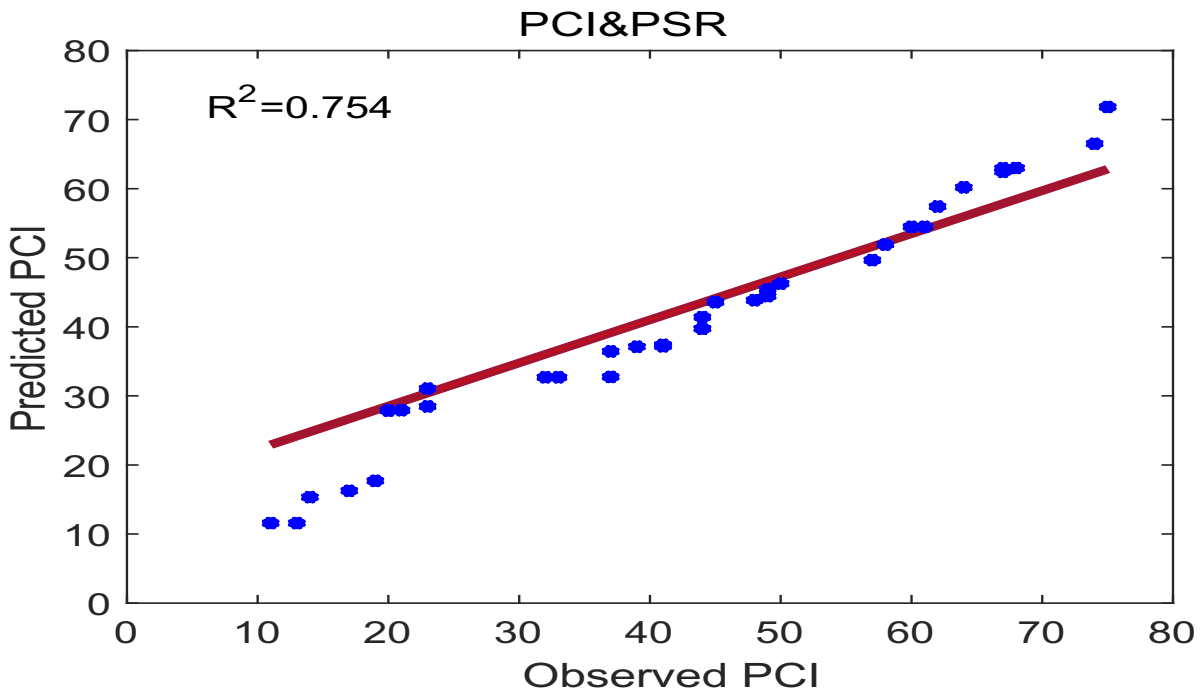

Figure 7-13: Performance of the ANNs for predicting PCI model from PSR.

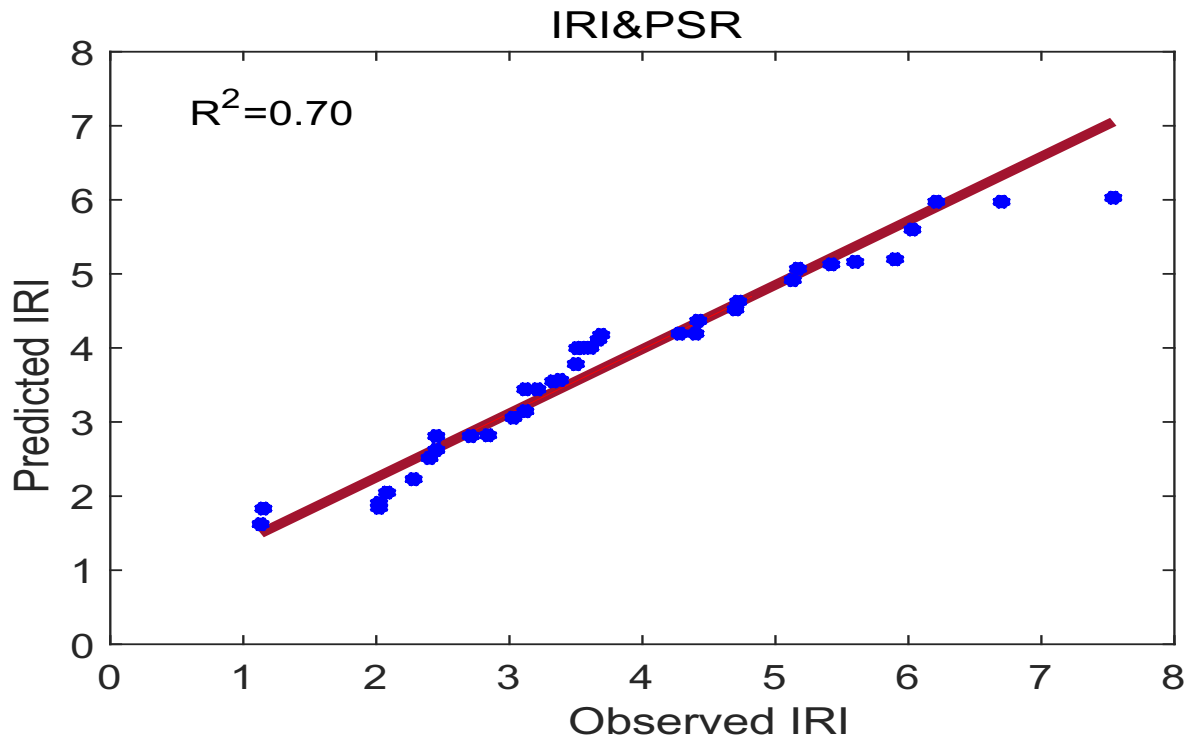

Figure 7-14: Performance of the ANNs for predicting IRI model from PSR.

7.7.4 Comparison and Validation of the Models

To validate the prediction models developed, the R^2, RMSE, and MAE methods were used to validate the cubic and ANNs techniques. In all cases, the calculated R^2 were strong, RMSE, and MAE values were found to be low, as shown in Table (7-12).

Table 7-12: Comparison of the Cubic models to ANNs models.

Climate Region	Statistical Error Measures (PCI)								
	Cubic Generated			ANNs Generated			Improvement (%)		
	R^2	RMSE	MAE	R^2	RMSE	MAE	R^2	RMSE	MAE
PCI &IRI	92.9	4.899	3.744	94.6	4.275	2.924	+1.80	+12.74	+21.90
PCI&PSR	57.3	12.10	9.48	75.4	9.272	5.994	+24.01	+23.37	+36.77
IRI&PSR	43.4	1.16	0.90	70.0	0.841	0.539	+38.00	+27.50	+40.11

Table (7-12) shows the comparison of the cubic models with ANNs models; a summary of the findings as follows:

- **PCI &IRI:** The results indicated that the R^2, RMSE, and MAE values of the ANNs models improved by 1.80%, 12.74%, and 21.90%, compared to the cubic models.
- **PCI&PSR:** The results indicated that the R^2, RMSE, and MAE values of the ANNs models improved by 24.01%, 23.37%, and 36.77%, compared to the cubic models.
- **IRI&PSR:** The results indicated that the R^2, RMSE, and MAE values of the ANNs models improved by 38%, 27.5%, and 40.11%, compared to the cubic models.

According to the results, the cubic models could estimate the PCI values from the IRI, PCI from PSR, and IRI from PSR with reasonable accuracy. The results showed the ANNs technique has

the best fit and high accuracy in all cases, with less error between observed and predicted values than the cubic method.

7.8 Modeling of Asphalt Pavement Performance Indices Using (MLR) Technique

Research in this part focuses on using pavement distress variables to model asphalt pavement performance indices (PCI, IRI, and PSR). Pavement distress parameters were input variables, and pavement performance indices (PCI, IRI, and PSR) were output parameters. Five prediction models were developed using (MLR) technique from the collected data. The PCI, IRI, and PSR regression models are shown in Table (7-13). These consider surface pavement distress: rutting, fatigue cracking, block cracking, longitudinal cracking, transverse cracking, potholes, patching, and delamination.

Table 7-13: PCI, IRI, and PSR models based on field survey.

Model	**PCI**		**IRI**		**PSR**
	2018	**2021**	**2018**	**2021**	**2018**
$\mathbf{R^2}$	48.0	63.0	39	53.2	54
Constant	39.73	36.294	3.58	4.006	3.00
Rutting	0.84	0.972	-0.06	-0.078	0.01
Fatigue Cracking	1.24	1.367	-0.12	0.194	0.02
Block Cracking	0.04	-0.161	-0.03	-0.222	-0.05
Longitudinal Cracking	-0.10	0.628	0.03	-0.067	-0.01
Transverse Cracking	0.10	-0.975	-0.02	0.081	0.01
Patching	-0.08	0.036	0.01	-0.004	-0.01
Potholes	0.22	-0.008	-0.01	-0.014	0.01
Delamination	-1.29	-2.552	0.08	0.15	-0.01

The PCI, IRI, and PSR regression models shown in equations (7-10) to (7-14) were as follows:

1-Factors Influencing PCI

Table (7-13) shows two regression models developed using PCI values and surface pavement distress data. The PCI (2018) model was negatively correlated with longitudinal cracking, patching, and delamination. The PCI (2018) model was positively correlated with rutting, fatigue cracking, block cracking, transverse cracking, and potholes. Equation (7-10) described the relationship between The PCI (2018) and surface pavement distress as follow:

$$\boldsymbol{PCI_{2018} = 39.73 + 0.84\ X_1 + 1.24\ X_2 + 0.04\ X_3 - 0.10\ X_4 + 0.10\ X_5 - 0.08\ X_6 + 0.22\ X_7 - 1.29\ X_{10}} \qquad \textbf{7-10}$$

The correlation coefficient (R^2) of this relationship is **48%.**

The PCI (2018) model was negatively correlated with block cracking, transverse cracking, potholes, and delamination. The PCI (2018) model was positively correlated with rutting, fatigue cracking, longitudinal cracking, and patching. Equation (7-11) described the relationship between The PCI (2018) and surface pavement distress as follows:

$$\boldsymbol{PCI_{2021} = 36.294 + 0.972\ X_1 + 1.367\ X_2 - 0.161\ X_3 + 0.628\ X_4 - 0.975\ X_5 + 0.036\ X_6 - 0.008 X_7 - 2.552\ X_{10}} \qquad \textbf{7-11}$$

The correlation coefficient (R^2) of this relationship is **63%.**

2-Factors Influencing IRI

Table (7-14) shows two regression models developed using IRI values and surface pavement distress data. The IRI (2018) model was negatively correlated with rutting, fatigue cracking, block cracking, transverse cracking, and potholes. The IRI (2018) model had positively correlated with

longitudinal cracking, patching, and delamination. Equation (7-12) described the relationship between IRI and surface pavement distress as follows:

$$\boldsymbol{IRI_{2018} = 3.58 - 0.06\, X_1 - 0.12\, X_2 - 0.03\, X_3 + 0.03\, X_4 - 0.02\, X_5 + 0.01\, X_6 - 0.01\, X_7 + 0.08\, X_{10}} \qquad \textbf{7-12}$$

The correlation coefficient (R^2) of this relationship is **39%.**

The IRI (2021) model was negatively correlated with rutting, block cracking, longitudinal cracking, patching, and potholes. The IRI (2021) model had positively correlated with fatigue cracking, transverse cracking, and delamination. Equation (7-13) described the relationship between IRI and surface pavement distress as follows:

$$\boldsymbol{IRI_{2021} = 4.006 - 0.078\, X_1 + 0.194\, X_2 - 0.222\, X_3 - 0.067\, X_4 + 0.081\, X_5 - 0.004\, X_6 - 0.014\, X_7 + 0.15\, X_{10}} \qquad \textbf{7-13}$$

The correlation coefficient (R^2) of this relationship is **53.2%.**

<u>3-Factors Influencing PSR</u>

Table (7-14) shows one regression model developed using PSR values and surface pavement distress data. The PSR model was negatively correlated with block cracking, longitudinal cracking, patching, and delamination. The PSR model was positively correlated with rutting, fatigue cracking, transverse cracking, and potholes. Equation (7-14) described the relationship between the PSR and surface pavement distress as follows:

$$\boldsymbol{PSR = 3.0 + 0.01\, X_1 + 0.02\, X_2 - 0.05\, X_3 - 0.01\, X_4 + 0.01\, X_5 - 0.01\, X_6 + 0.01\, X_7 - 0.001 X_{10}} \qquad \textbf{7-14}$$

The correlation coefficient (R^2) of this relationship is **54%.**

7.8.1 Validation for PCI and IRI Models

After the validation test, Table (7-14) illustrates the reduction in R^2, RMSE, and MAE values for all sections. Figures (7-15) and (7-16) present the errors and linear relation for the two periods (2018 and 2021).

Table 7-14: Validation of PCI models based on pavement distress.

Indicator	MLR			Validation			Reduction % (±)		
	R^2	RMSE	MAE	R^2	RMSE	MAE	R^2	RMSE	MAE
PCI (2018)	48	14.051	11.368	45	14.227	11.98	-6.25	-1.24	-5.11
IRI (2018)	39	1.046	0.827	35.8	1.253	1.036	-8.21	-16.52	-20.17
PCI (2021)	63	9.932	7.844	61.4	9.135	7.22	-2.54	+8.02	+7.96
IRI (2021)	53.2	0.751	0.605	46.5	0.802	0.613	-12.6	-6.36	-1.31

Based on Table (7-14), Figures (7-15), and (7-16), the following conclusions can be drawn:

- **PCI (2018):** The results indicated that the reduction of R^2 and RMSE, and MAE values was insignificant. The accuracy reductions were 6.25%,1.24%, and 5.11%, respectively. Thus, the MLR method's ability to accurately predict PCI models of the pavement distress models was good.
- **PCI (2021):** The results indicated that the reduction of R^2 and RMSE, and MAE values was insignificant. The accuracy reductions were 2.54%, 8.02%, and 7.96%, respectively. Thus, the MLR method's ability to accurately predict PCI models of the pavement distress models was good.
- **IRI (2018):** The results indicated that the reduction of R^2 and RMSE, and MAE values was insignificant. The accuracy reductions were 8.21%,16.52%, and 20.17%, respectively.

Thus, the MLR method's ability to accurately predict IRI models of the pavement distress models was good.

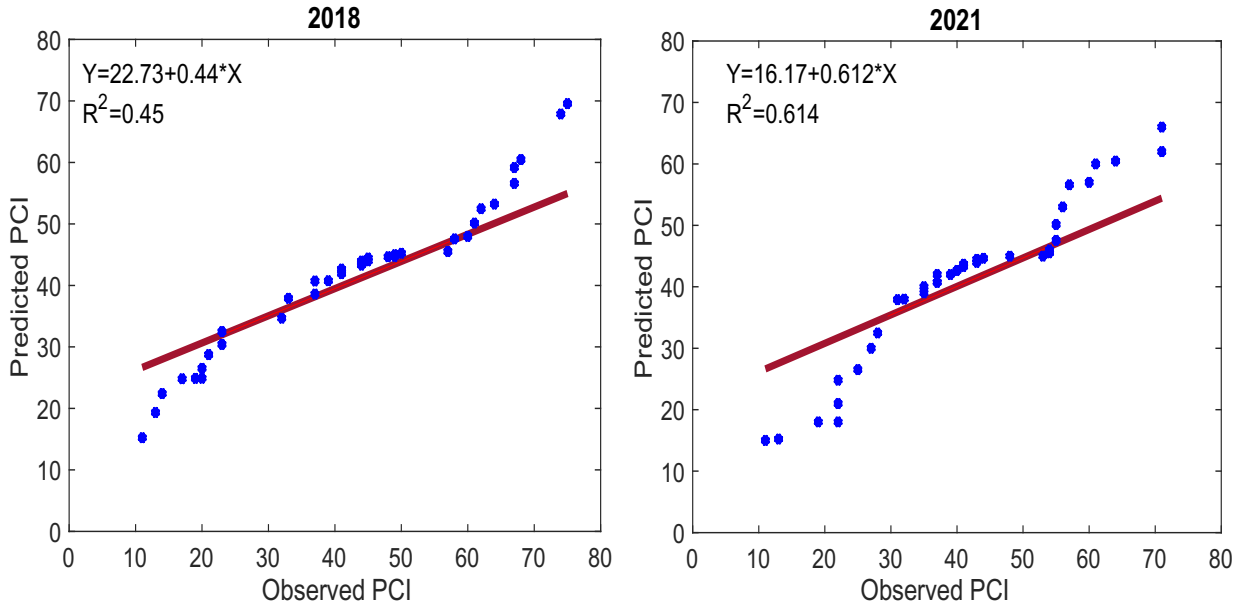

Figure 7-15:Accuracy of the prediction PCI values based on surface pavement distress: left (2018), and right (2021).

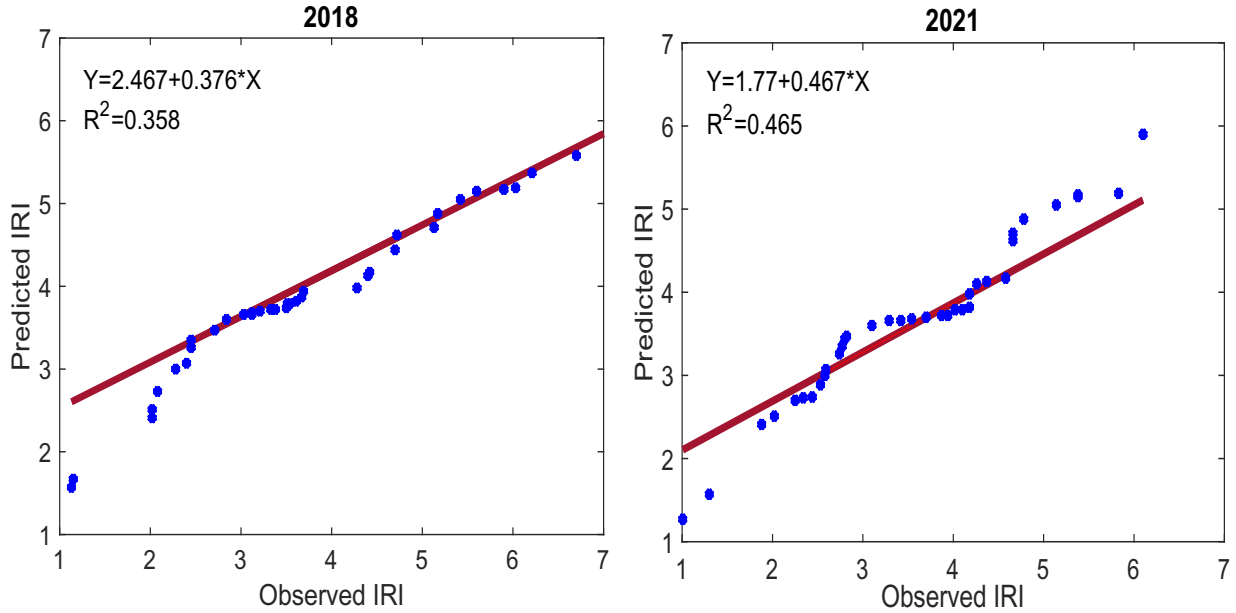

Figure 7-16: Accuracy of the prediction IRI values based on surface pavement distress: left (2018), and right (2021).

- **IRI (2021):** The results indicated that the reduction of R^2 and RMSE, and MAE values was insignificant. The accuracy reductions were 12.6%,6.36%, and 1.31%, respectively. Thus, the MLR method's ability to accurately predict IRI models of the pavement distress models was good.

7.8.2 Cronbach's alpha

Cronbach's alpha calculates inner consistency, i.e., how closely associated a group of parameters is. This test is used to calculate reliability, and it is worth noting that an alpha high value does not mean the calculation is one-dimensional. Cronbach's alpha can be written according to the number of test objects and the average correlation between the parameters. Equation (7-20) presented the formula for the Cronbach alpha for conceptual purposes:

$$\boldsymbol{\alpha} = \frac{\boldsymbol{N_c}}{\boldsymbol{v}+(\boldsymbol{N}-\mathbf{1})\boldsymbol{c}} \qquad \textbf{7-15}$$

where:

N is equal to the number of items, c is the average inter-item covariance among the items, and v equals the average variance.

Table 7-15: Reliability statistics.

Case Processing Summary			Reliability Statistics		
	N	%	Cronbach's Alpha	Cronbach's Alpha Based on Standardized Items	Number of Items
Valid	38	82.6	0.973	0.973	37
Excluded	8	17.4			
Total	46	100			

The alpha coefficient for the 37 items is (97.3%), suggesting that the items have relatively high internal consistency.

Note that a 70% or higher reliability coefficient is considered "acceptable" in most research situations.

Table 7-16: Summary item statistics.

Summary Item Statistics							
	Mean	Minimum	Maximum	Range	Maximum Minimum	Variance	N of Items
Item Means	2.988	2.316	3.526	1.211	1.523	0.080	37
Item Variances	0.704	0.453	1.121	0.668	2.474	0.031	37

7.9 Modeling of Asphalt Pavement Performance Indices Using (ANNs) Technique

The Artificial neural network has been used to train the data presented in Table (7-3). The ANNs technique aimed to model asphalt pavement performance indices (PCI, IRI, and PSR) based on eight surface pavement distresses. The input variables were rutting, fatigue cracking, block cracking, longitudinal and transverse cracking, patching, potholes, and delamination, while (PCI, IRI, and PSR) were the output variables. The network architecture consisted of one layer of 7 nodes and three hidden layers of nodes. Table (7-17) presents the performance of the ANNs model for PCI, IRI, and PSR. The model's performance was assessed using the three standard methods of R^2value, RMSE, and MAE. Within wet climatic zones, 19 road sections of flexible pavement have been chosen. The models were trained on 70% of the data, tested on15%, and validated on 15%; the results showed a good ability of the pavement distress models to predict the PCI, IRI, and PSR values. Table (7-17) shows the R^2, RMSE and MAE values of the PCI, IRI, and PSR models. The highest R^2 value was 99.6 % in the case of PSR for (2018). The lowest R^2value was 98.6 % and was observed for IRI model for (2018). The lowest RMSE and MAE values were

(0.007), (0.005) and were observed for PSR (2018). Figures (7-17) to (7-19) present the ANNs prediction results for PCI, IRI, and PSR, respectively.

Table 7-17: Summary of PCI, IRI, and PSR models of ANNs developed.

Indicators	**ANNs Models**					
	Model (2018)			**Model (2021)**		
	R^2	**RMSE**	**MAE**	R^2	**RMSE**	**MAE**
PCI	98.6	0.888	0.734	99.3	0.72	0.592
IRI	99.2	0.276	0.234	99.5	0.16	0.16
PSR	99.6	0.007	0.005	-	-	-

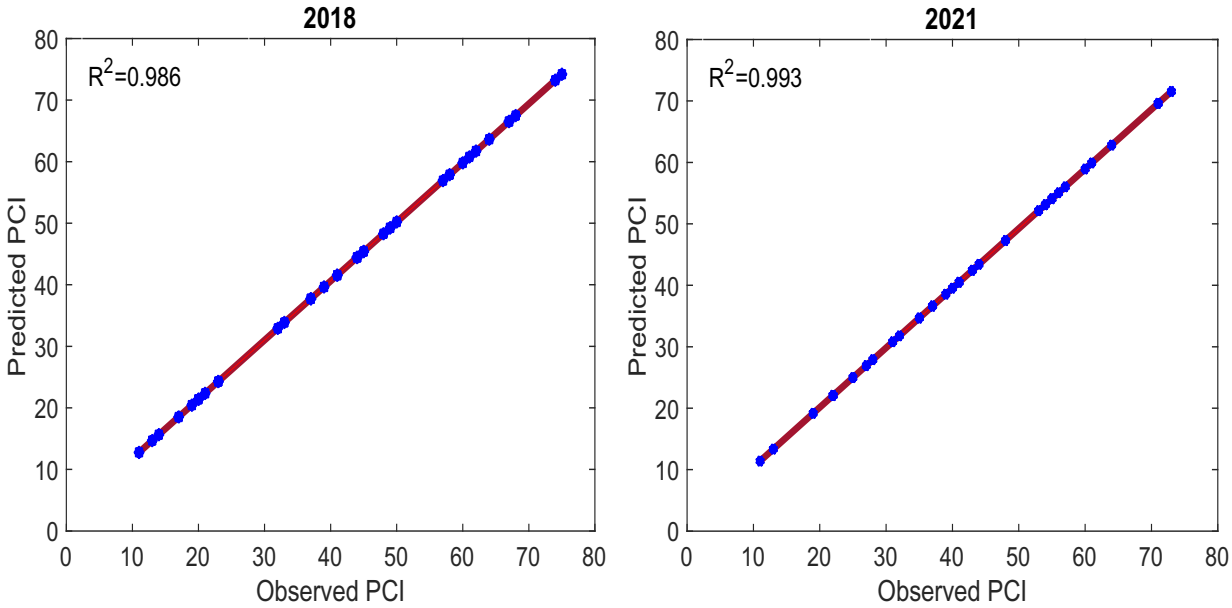

Figure 7-17: ANNs model goodness-of-fit results for PCI values based on pavement distress: left (2018), and right (2021).

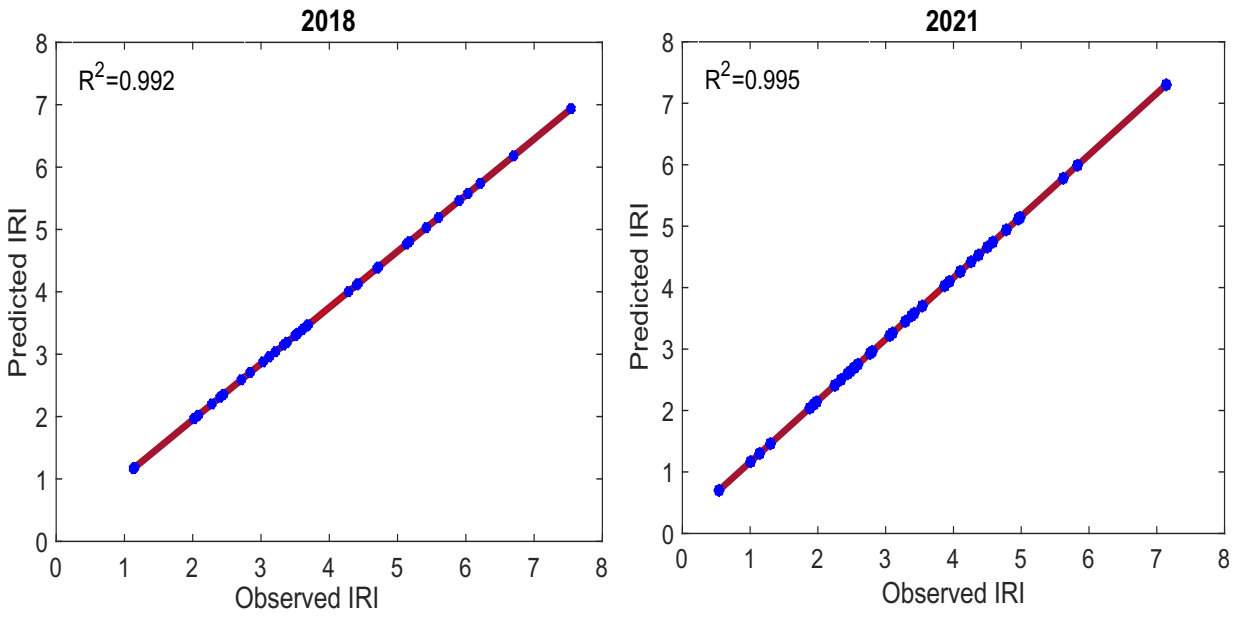

Figure 7-18: ANNs model goodness-of-fit results for IR values based on pavement distress: left (2018), and right (2021).

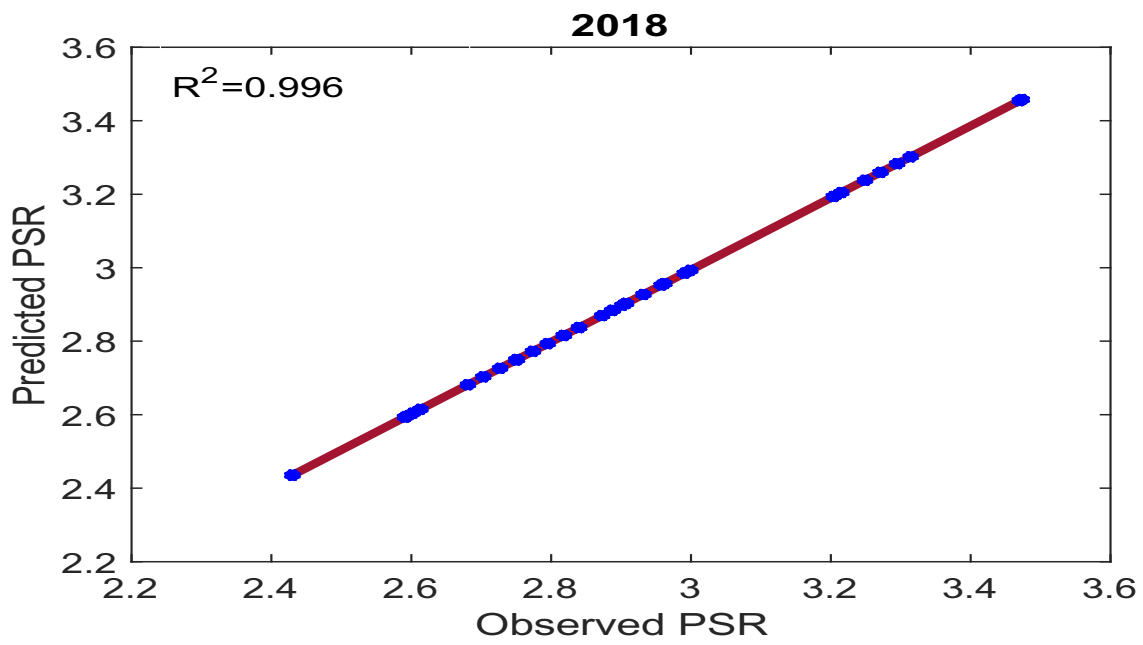

Figure 7-19: ANNs model goodness-of-fit results for PSR values based on pavement distress (2018).

7.9.1 Comparison and Validation of the Models

To validate the developed models in this part, all models were evaluated by comparing MLR, FIS, and ANNs techniques based on pavement distress, as shown in Tables (7-18), (7-19) and (7-20).

7.9.2 Comparison and Validation of MLR, FIS, and ANNs Models for PCI

The performance was compared among MLR, FIS, and ANNs models to evaluate the accuracy of the models in predicting pavement performance, based on pavement distress parameters. R^2, RMSE and MAE values were used to measure and compare the performance of the models. Table (7-18), Figures (7-20), and (7-21) present the comparison the MLR models to the ANNs models for PCI.

Table 7-18: Comparison among MLR, FIS, and ANNs models for PCI.

Technique	Year					
	2018			2021		
	R^2	RMSE	MAE	R^2	RMSE	MAE
MLR Generated	48.0	14.051	11.368	63.0	9.932	7.844
FIS Generated	96.6	3.456	2.919	96.3	3.468	2.917
ANNs Generated	98.6	0.888	0.734	99.3	0.72	0.592

According to Table (7-18), Figures (7-20), and (7-21), several conclusions can be drawn:

- **<u>PCI (2018):</u>**
  - The statistics indicated R^2values from the ANNs and FIS models were higher than the R^2values of the MLR models more than 50%.

- The RMSE value of the ANNs model was less than the RMSE values of the FIS and the MLR models by 74.31% and 99.4%, respectively.
- The RMSE value of the FIS model was less than the RMSE value of the MLR model by 75.4%.
- The MAE value of the ANNs model was less than the MAE values of the FIS and the MLR models by 74.85% and 93.54%, respectively.

- **PCI (2021):**
  - The statistics indicated that the R^2value from the ANNs model was higher than the R^2values of the MLR model by 36.56 %.
  - The RMSE value of the ANNs model was less than the RMSE value of the MLR model by 92.75%.
  - The MAE value of the ANNs model was less than the MAE value of the MLR model by 92.45 %.
  - Figures (7-20) and (7-21) clearly show that the ANNs prediction models provided more accuracy than the FIS and MLR prediction models.
  - The ANNs technique has the best fit and good accuracy in all cases, with less error between observed and predicted values than the FIS and MLR methods.

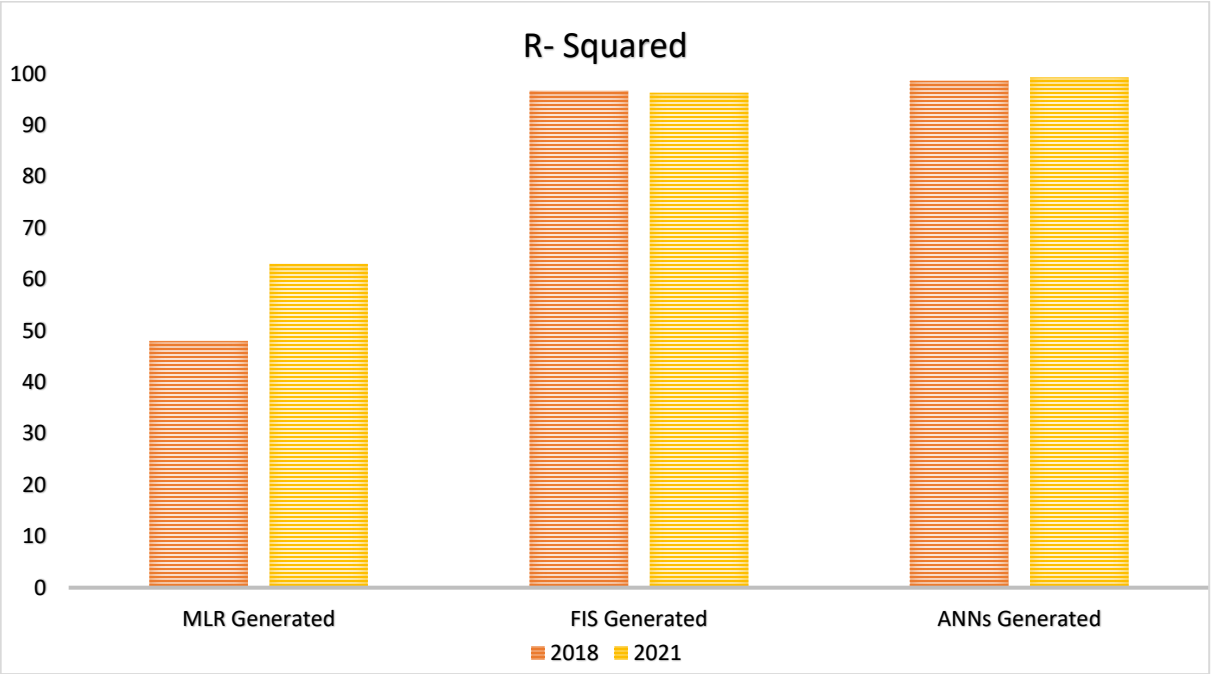

Figure 7-20: Fitness of MLR, FIS, and ANNs models to PCI prediction based on pavement distress data (2018 and 2021).

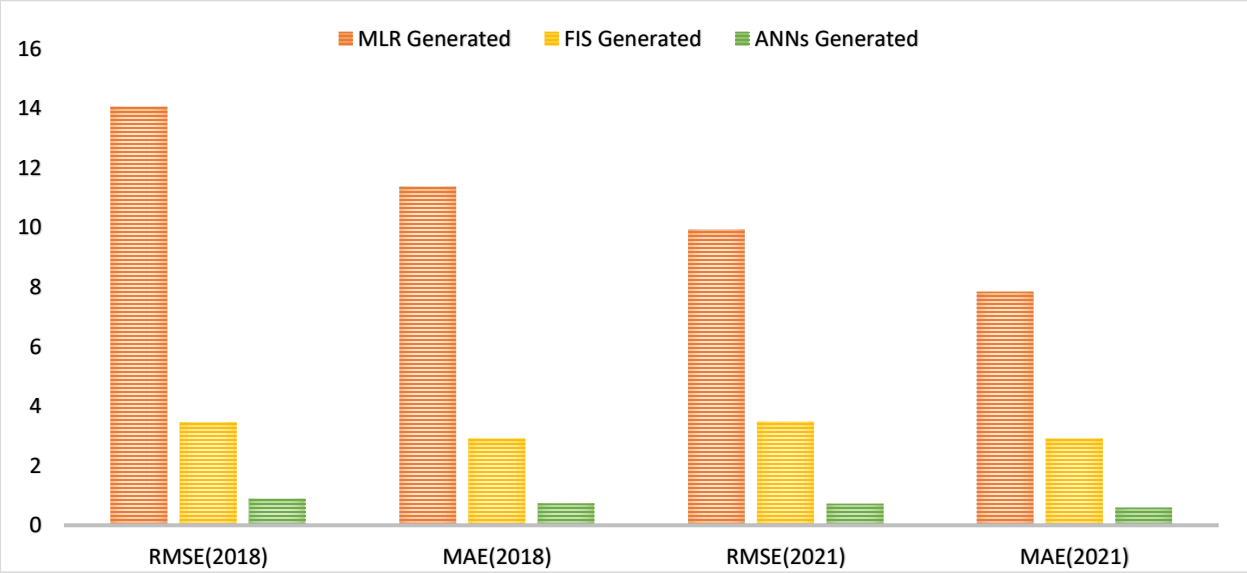

Figure 7-21: Fitness of MLR and ANNs models to PCI prediction based on pavement distress data (2018 and 2021).

7.9.3 Comparison and Validation of MLR, FIS, and ANNs Models for IRI

The performance was compared among MLR, FIS, and ANNs models to evaluate the accuracy of the models in predicting pavement performance based on pavement distress parameters. R^2, RMSE and MAE values were used to measure and compare the performance of the models. Table (7-19), Figures (7-22), and (7-23) present the comparison of the MLR models to the ANNs models for IRI.

Table 7-19: Comparison among MLR, FIS, and ANNs models for IRI.

Indicator	Technique	2018			2021		
		R^2	RMSE	MAE	R^2	RMSE	MAE
IRI	**MLR Generated**	39	1.046	0.827	53.2	0.751	0.605
	FIS Generated	88.3	0.567	0.446	88.5	0.54	0.411
	ANNs Generated	99.2	0.276	0.234	99.5	0.16	0.16

According to Table (7-19), Figures (7-22), and (7-23), several conclusions can be drawn:

- **<u>IRI (2018):</u>**
  - The statistics indicated the R^2 value from the ANNs model was higher than the R^2values of the FIS and the MLR models by 60.69% and 10.99%, respectively.
  - The statistics indicated the R^2value from the FIS model was higher than the R^2value of the MLR model by 55.83%.
  - The RMSE value of the ANNs model was less than the RMSE values of the FIS and the MLR models by 51.32% and 73.6%, respectively.

- The RMSE value of the FIS model was less than the RMSE value of the MLR model by 45.79%.
- The MAE value of the ANNs model was less than the MAE values of the FIS and MLR models by 47.53% and 71.70%, respectively.

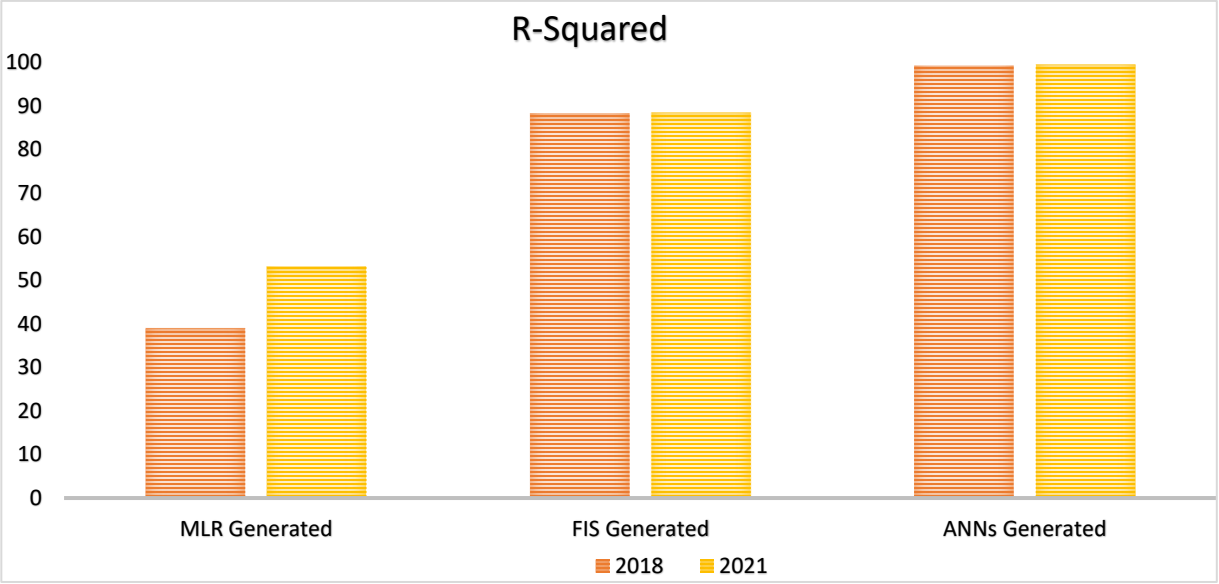

Figure 7-22: Fitness of MLR, FIS, and ANNs models to IRI prediction based on pavement distress data (2018 and 2021).

- **<u>IRI (2021):</u>**

- The statistics indicated that the R^2 value from the ANNs model was higher than the R^2 values of the MLR model by 46.5 %.
- The RMSE value of the ANNs model was less than the RMSE value of the MLR model by 78.70%.
- The MAE value of the ANNs model was less than the MAE value of the MLR model by 73.55 %.

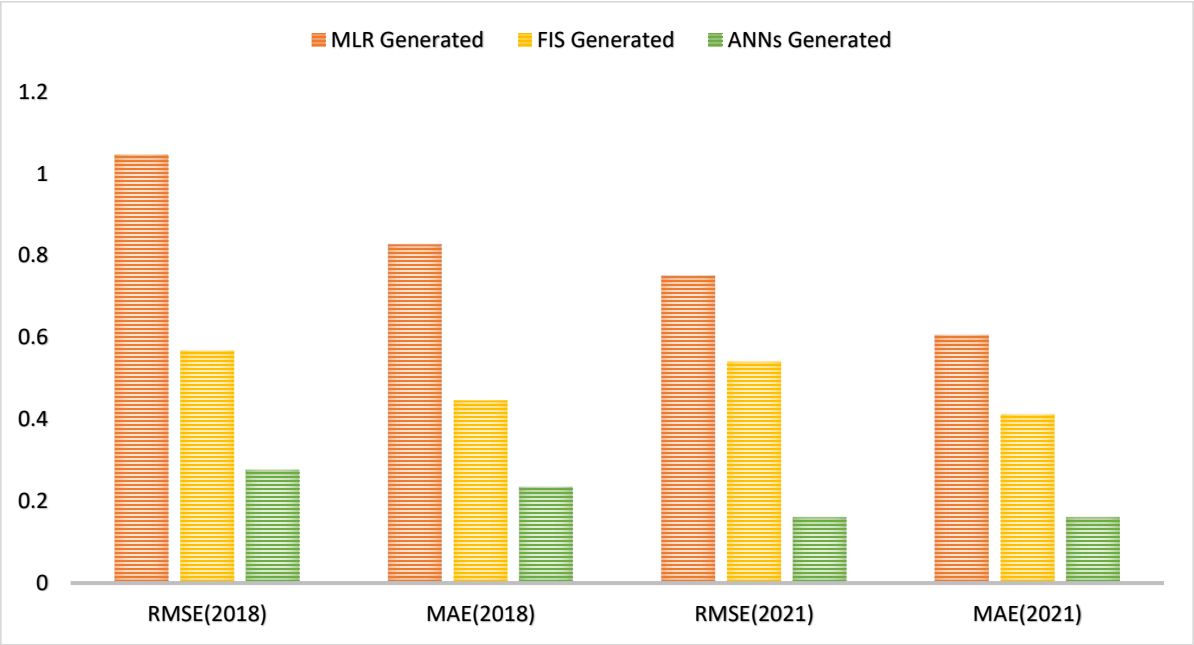

Figure 7-23: Fitness of MLR and ANNs models to IRI prediction based on pavement distress data (20182021).

7.9.4 Comparison and Validation of MLR and ANNs Models for PSR

The models predict pavement performance based on pavement distress parameters. R^2, RMSE and MAE values were used to measure and compare the performance of the models. Table (7-20) and Figure (7-24) present the comparison of the MLR models to the ANNs models for PSR.

Table 7-20: Comparison of the MLR models to the ANNs models.

Indicator	Technique	2018		
		R^2	RMSE	MAE
PSR	MLR Generated	54.0	0.45	0.368
	ANNs Generated	99.6	0.007	0.005

- The statistics indicate that the R^2value from the ANNs model was higher than the R^2value of the MLR model by 45.78%.

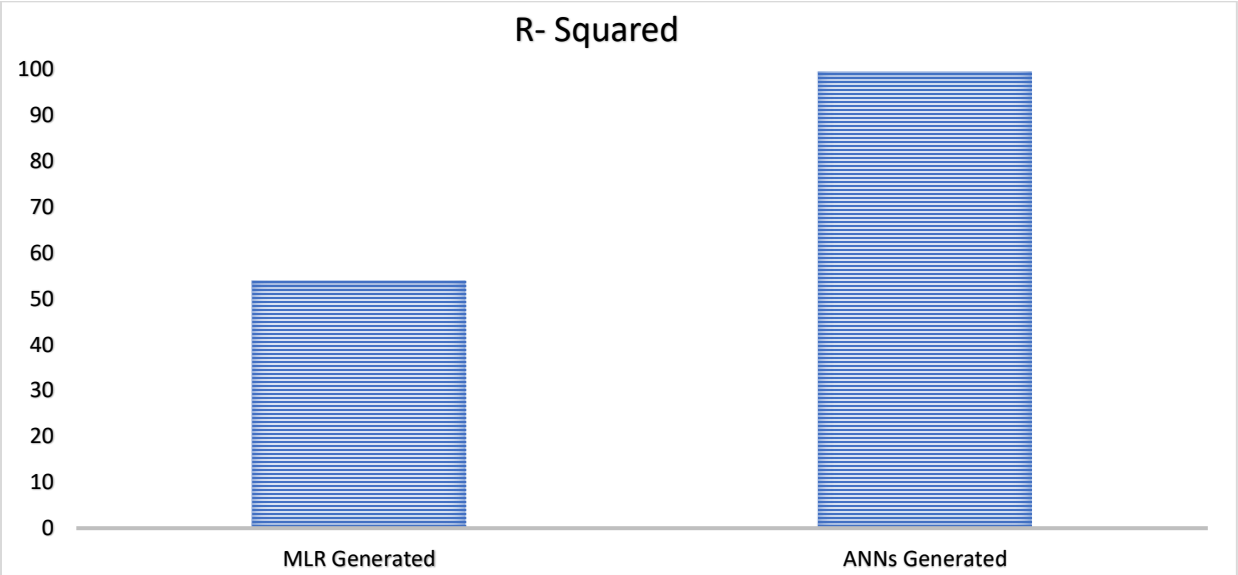

Figure 7-24: Fitness of MLR and ANNs models to PSR prediction based on pavement distress data (2018).

- The RMSE value of the ANNs model was less than the RMSE value of the MLR model by 98.44%.
- The MAE value of the ANNs model was less than the MAE value of the MLR model by 98.64%.

7.9.5 MLR Model sensitivity analysis for PCI, IRI, and PSR

A sensitivity analysis was conducted to determine the effects of input variables on the efficacy of prediction models PCI, IRI, and PSR. The results of the sensitivity analysis were presented in Table (7-21), and Figures (7-25) and (7-26) were as follows:

Table 7-21: Sensitivity analysis of prediction models for PCI, IRI, and PSR.

Parameters	R^2				
	2018			**2021**	
	PCI	**IRI**	**PSR**	**PCI**	**IRI**
Rutting	18.3	17.4	25.8	17.1	5.4
Fatigue Cracking	13.3	13.3	15.1	14.4	10
Block Cracking	2.5	3.3	-	1.2	1.7
Longitudinal Cracking	11.4	13.7	10.9	8.1	11.7
Transverse Cracking	0.4	-	0.1	4.1	0.1
Patching	19.0	11.0	11.7	16.6	3.2
Potholes	-	0.1	0.3	0.9	0.8
Delamination	19.1	12.9	14.4	19.0	5.4

Table (7-21) and Figures (7-25) and (7-26) present the following conclusions:

PCI (2018): Compared with other variables, rutting, patching, and delamination are the most significant variables on the prediction model. Fatigue cracking and longitudinal cracking have some effects on the PCI model. Block cracking and transverse cracking have minor effects on the PCI model, while potholes have no effect on the prediction model.

PCI (2021): Compared with other variables, rutting, patching, and delamination are the most significant variables on the prediction model. Fatigue cracking, and longitudinal cracking have some effects on the PCI model, while block cracking, transverse cracking, and potholes have minor effects on the PCI model.

IRI (2018): Compared with other variables, rutting is the most significant effect on the prediction model. Fatigue cracking, longitudinal cracking, patching, and delamination have some impacts on the prediction model, while block cracking and potholes have minor effects on the prediction model.

IRI (2021): Compared with other variables, longitudinal and fatigue cracking are the most significant effect on the prediction model. Rutting, block cracking, patching, and delamination have some effects on the prediction model, while transverse cracking and potholes have minor effects on the prediction model.

PSR (2018): Compared with other variables, rutting is the most significant effect on the prediction model. Fatigue cracking, longitudinal cracking, patching, and delamination have some impacts on the prediction model, while transverse cracking and potholes have minor effects on the prediction mode.

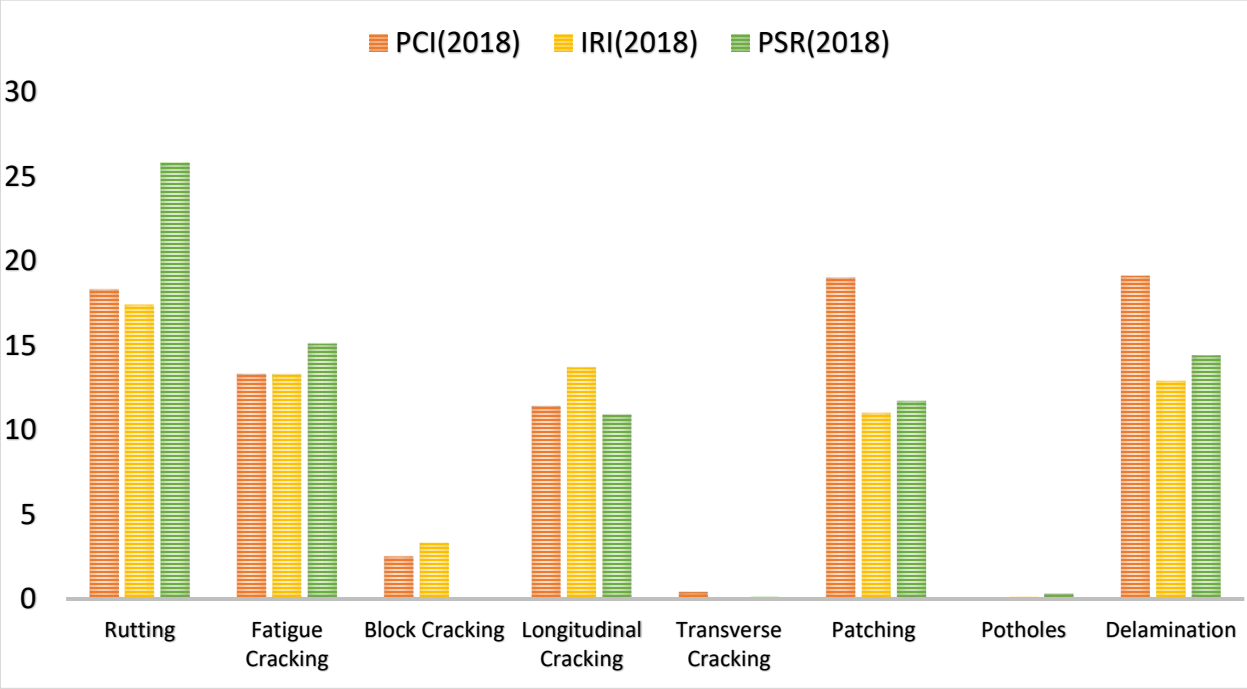

Figure 7-25: Sensitivity analysis of MLR for PCI, IRI, and PSR (2018).

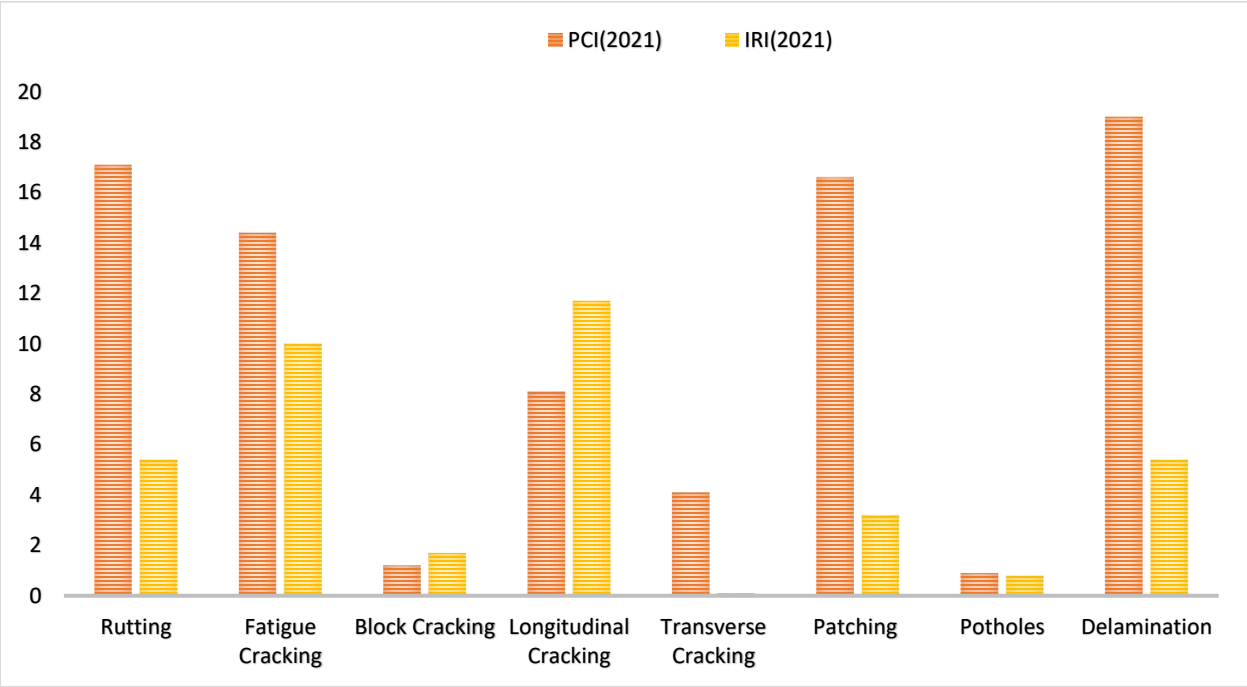

Figure 7-26: Sensitivity analysis of MLR for PCI and IRI (2021).

7.10 Summary

This case study investigated 19 road sections for 2018 and 2021 in St. John's, Newfoundland, Canada. Pavement distress of varying types was analyzed, and performance indicators were collected. St. John's has a very harsh climate due to a plethora of snowfall and freeze thaws in the winter season, plenty of rain throughout the year, and copious temperature fluctuations. Here are some conclusions are drawn from this research:

- The extensive maintenance work carried out by St. John's municipality between 2018 and 2021 affect road performance. It was improvement in the performance of the roads that received maintenance, while the roads not assigned for maintenance work had a worse performance than previously.
- Based on Table (7-4), the maintenance work carried out by St. John's municipality between 2018 and 2021could affect road performance. It was clear the improvement in the

performance of some roads sections that maybe have been received maintenance, while the others were worse, due to its have not been received any maintenance.

- According to FHWA, pavement conditions are poor if the IRI value exceeds 2.7 m/km. Table (7-4) showed that 81% of road sections were classified as poor in 2018, and around 84% of road sections were classified as poor in 2021.
- The ANNs technique has the best fit and high accuracy in all cases with less error between observed and predicted values than the FIS and MLR methods.

Chapter8: Conclusions and Recommendations

8.1 Conclusions

This thesis has included the investigation of typical and advanced characterization methods to model asphalt pavement performance indices and better understand the effect of various variables on pavement performance. In general, the results presented can be applied to evaluate pavement performance and predict future pavement conditions.

The study's general goal was to apply comprehensive research to model Asphalt Pavement Performance Indices (PCI& IRI) and compute various parameters' effects on pavement performance. The ultimate goal was to identify the most significant parameters that optimize pavement performance to provide longer road life. This chapter summarizes the extensive numerical work, the conclusions drawn from the work results, and an advanced understanding of soft computing mechanisms using the Fuzzy Inference System, Multiple Linear Regression, and Artificial Neural Network. Recommendations for potential future research arising from this study are also discussed. The proposed methods to estimate PCI and IRI of pavement performance are promising but still need validation with a more significant amount of different data. Analytical models and numerical simulations (such as Fuzzy Inference System models, Multiple Linear Regression models, and Artificial neural network models) can be used to predict models for pavement performance (PCI and IRI) and compare results with observed data. The results of the work and analysis revealed the following:

Modeling of Asphalt Pavement Performance Indices Using (FIS)

To modeling asphalt pavement performance indices, a fuzzy inference system (FIS) has been used to compute the fuzzy- pavement condition index (FPCI) and fuzzy international roughness index

(FIRI). The long-term pavement performance (LTPP) database and field Survey of St. John's, Newfoundland, Canada have been used to develop membership functions. Based on the results obtained from this analysis technique, fuzzy classification systems presented a strong correlation level and low percentage error for the prediction models.

According to FIS-based PCI and IRI models, the technique proved to optimize a few of the advantages drawn from this study as follows:

- As a direct result of using the fuzzy inference system approach, human involvement is limited for the decision process and distress classification.
- Pavement engineers can effectively identify pavement conditions and enhance decision-making by employing this methodology.
- Incorporating additional sections with different types of distress and severity helped the system learn and develop additional rules, which improved the models' results.
- The results indicated that the centroid method yields a more accurate prediction PCI model (R^2= 98.3%, RMSE =4.957%, and MAE=4.243%) than other methods (Bisector, Lom, Som). The Lom method has the most significant Improvement among methods (R^2= 2.85%, RMSE =37.72% and MAE=27.45%). This means that the accuracy of models was enhanced by adding just 30 sections increased accuracy.
- The results indicated that the centroid method yields a more accurate prediction IRI model (R^2= 92.9%, RMSE =0.285%, and MAE=0.227%) than other methods (Bisector, Lom, Som). The Lom method has the most significant Improvement among methods (R^2= 2.83%, RMSE =19.90% and MAE=20.70%). This means that the accuracy of models was enhanced when added just 30 sections increased the accuracy.

- The sensitivity analysis revealed that rutting and transverse cracking had the most significant impact on FPCI fuzzified classification compared to other distress types.
- The sensitivity analysis showed that rutting and patching had the most significant impact on FIRI fuzzified classification compared to other distress types for pavement performance prediction.

Modeling the Relationship Between Asphalt Pavement Performance Indices (PCI &IRI)

This part of the research sought to clarify the relationship between two performance indicators (PCI and IRI) using the LTPP data for four climate regions in the U.S. and Canada. Several important conclusions can be drawn from this part, as follow:

- The results indicate that three methods (linear, quadratic, and cubic) are able to predict PCI by using IRI data.
- The results indicated that the most accurate models were the Cubic models, compared to Linear and Quadratic models, in all cases of climate regions.
- The results indicated that the ANNs models were more accurate than cubic models for four climate regions.

Modeling of Asphalt Pavement Performance Indices Using (MLR)and (ANNs)

Pavement distress, traffic volume, and environmental parameters were studied as input variables for modeling asphalt pavement performance indices in this part of the study. The conclusions are as follows:

- Based on the models related to pavement distress parameters of PCI and IRI, the R^2values range between 77% and 91.6% for PCI, and 70.7% and 90.6% for IRI using the MLR technique. However, the R^2value ranges between 98.3% and 99.8%, and between 97.5%

and 99.8%, respectively, to PCI and IRI using the ANNs technique. That's mean the ANNs prediction models provided more accuracy than the MLR models under all climate regions.

- Based on the models related to environmental parameters of PCI and IRI, the R^2 values range between 71.4% and 91.8% for PCI and between 74% and 90.2% for IRI using the MLR technique. Furthermore, the R^2values range between 98.7% and 99.8%, and between 98.9% and 99.9% for PCI and IRI using the ANNs technique. That's mean the ANNs prediction models provided more accuracy than the MLR models under all climate regions.
- Based on the models related to traffic volume parameters of PCI and IRI, the R^2values range between 76.4% and 88.1% for PCI and between 78.4% and 94.7 % for IRI using the MLR technique. The R^2value was between 98.5% and 99.4%, and 98.5% and 99.3% for PCI and IRI using the ANNs technique. That's mean the ANNs prediction models provided more accuracy than the MLR models under all climate regions.
- Based on the case study, here are some conclusions are drawn:
  - The extensive maintenance work carried out by St. John's municipality between 2018 and 2021 affect road performance. It was improvement in the performance of the roads that received maintenance, while the roads not assigned for maintenance work had a worse performance than previously.
  - According to results, the maintenance work carried out by St. John's municipality between 2018 and 2021 could affect road performance. It was clear the improvement in the performance of some roads sections that maybe have been received maintenance, while the others were worse, due to its have not been received any maintenance.

- According to FHWA, pavement conditions are poor if the IRI value exceeds 2.7 m/km. The results showed that 81% of road sections were classified as poor in 2018, and more than 84% of road sections were classified as poor in 2021.
- The results showed the fuzzy pavement classification of FPCI and FIRI was more accurate than the observed (PCI and IRI).
- The ANNs technique has the best fit and high accuracy in all cases with less error between observed and predicted values than the FIS and MLR methods.

8.2 Contribution to Knowledge

The following contributions are made based on current developments**:**

Asphalt Pavement Performance Indices based on Fuzzy Inference System

The current study presented a significant contribution of developing an effective system that can overcome the failure of traditional classification. In addition, this technique has a crucial advantage because it generates rules from large-scale distress data in a short time. With the FIS technique, the distress classification becomes more consistent. Using FIS has reduced human involvement in decision-making processes.

Development of Enhanced Models:

The current research employs soft computing techniques (FIS) and ANNs) to optimize prediction models. Using these optimization techniques, the most reasonable prediction model can minimize the discrepancies between predicted and measured data.

Pavement Performance Prediction

This research uses two data sources stored in the LTPP dataset and the field survey of St. John's city for different climate regions to Mode asphalt pavement performance indices in different climate regions. Models developed to predict pavement performance address several variables that influence pavement performance. MLR and ANNs techniques have been utilized to predict models for pavement performance. According to the results, the ANN technique was able to predict the PCI and IRI models with high accuracy, and the ANNs technique was able to predict models under various conditions and several variables, such as:

- Pavement distress,
- traffic volume, and
- environmental parameters.

Better Understanding of Different Pavement Performance in Different Climate Regions:

The current research provides prediction models for three fundamental parameters (pavement distress, traffic volume, and environmental) in four climate regions in the U.S. and Canada. Comparison among different models for each performance index (PCI) and (IRI) reveals variation in pavement performances. Comparison among methods permits understanding pavement performance behaviour and identifying terminal service life for the four regions. Adding more historical data on the four climate regions will aid in improving the model developed in this study.

Prediction Models Development based on soft computing concepts:

The current research develops new performance prediction models based on soft computing techniques. These models represent pavement performance more than traditional models based on empirical concepts.

Automation of the Soft Computing Calibration Process:

The current research provides an innovative approach to calibrating soft computing models and moving away from traditional techniques based mainly on "trial and error" approaches. This research provides a methodology to automate the calibration process fully and thus provide an opportunity for pavement engineers and experts to explore the application of different optimization techniques to the soft computing (FIS) and (ANNs) calibration problem, which is not possible using a traditional approach.

8.3 Recommendations

In the present study, only data for flexible pavement were used, but the same concepts and methods applied in work could conceivably be applied to studies on rigid pavements. Further, the sensitivity analysis could be extended to determine optimal values of minimum acceptable PCI and IRI levels. Additionally, correlations between a distresses-based PCI index as presented in FIS and a more general distresses-based PCI and IRI could lead to PCI and IRI models that are based on concepts involving machine learning. Other promising future research directions are as follows:

- The present research applied linear programming techniques, ANNs, and fuzzy logic to determine prediction models using calibration coefficients. The calibration process used here could lead to other optimization techniques being used in the calibration process.
- LTPP data needs quality control procedures, and the database should be completely redone according to stricter standards. This could lead to higher accuracy for future models.
- Correlations between empirical models and the ANNs and FIS models could be further developed as a way for transport agencies to change their current PMS models into machine learning-based models.

- The fuzzy system could be improved by changing membership function shapes or incorporating additional pavement section data.
- More and more pavement data on Canada and the U.S. become available, more realistic models can be developed. According to the municipality, the collected data can then be further categorized as different regional sets to make the models more site-specific.
- By optimizing the database design, it will be easier to create high-quality predictive models in the future. Updating the plan for data collection will reduce the cost of roads.

Publications

Journal Papers

- Ali, A., Usama Heneash., & Hussein, A. (2022). Development of Pavement Condition Index Using Artificial Neural Network Approach: Case Study. Submitted.
- Ali, A., Usama Heneash., & Hussein, A. (2022). Performance of Soft Computing Technique in Predicting the Pavement International Roughness Index: Case Study. Under review.
- Ali, A., Usama Heneash., Hussein, A., & Shahbaz Khan. (2022). Application of Artificial Neural Network Technique for Prediction of Pavement Roughness as a Performance Indicator. Under review.
- Ali, A., Heneash, U., Hussein, A., Ali, S., & Khan, S. (2023). Models Development for Asphalt Pavement Performance Index in Different Climate Regions Using Soft Computing Techniques. Journal of Soft Computing in Civil Engineering, 7(1), 20-42. doi: 10.22115/scce.2022.357135.1512
- Ali A, Heneash U, Hussein A, Eskebi, M. (2022). Predicting Pavement Condition Index Using Fuzzy Logic Technique. 7(7):91. https://doi.org/10.3390/infrastructures7070091.
- Ali, A., Dhasmana, H., Hossain, K., & Hussein, A. (2021). Modeling Pavement Performance Indices in Harsh Climate Regions. Journal of Transportation Engineering, Part B: Pavements, 147(4), 04021049.

Conference Papers

- Ali, A., Hossain, K., Dhasmana, H., Safiuddin, M., Bazan, C., and Hussein, A. (2018). Field Inspection and Classification of Pavement Distress of St. John's City in Newfoundland Canada. 7th International Materials Specialty Conference, Canadian Society for Civil Engineering. Presented.

- Ali, A., A., Hossain, K., Hussein, A., Swarna, S., Dhasmana, H., & Hossain, M. (2019). Towards development of PCI and IRI models for road networks in the City of St. John's. In Airfield and American Society of Civil Engineers (ASCE) International Conference on Highway Pavements and Airfield Technology. Chicago, Illinois, USA. Presented.

References

AASHTO, A. A. of S. H. and T. O. (1972). AASHTO Method.

AASHTO Guidefor Design of Pavement Structures.American Association of State Highway and Transportation Officials, Washington, D.C., 1985.

AASHTO. 2008a. Mechanistic-Empirical Pavement Design Guide: A Manual of Practice. Interim Edition, American Association of Highways and Transportation Officials.

ACRP. (2016). Pavement Maintenance Guidelines for General Aviation Airport Management. Pavement Maintenance Guidelines for General Aviation Airport Management.

Adlinge, S. S., & Gupta, P. a K. (2013). Pavement Deterioration and its Causes. Mechanical & Civil Engineering, 9–15. www.iosrjournals.org

Al-Suleiman, T. I., & Shiyab, A. M. S. (2003). Prediction of Pavement Remaining Service Life Using Roughness Data - Case Study in Dubai. International Journal of Pavement Engineering, 4(2), 121–129.

Ali, A., Hossain, K., Dhasmana, H., Safiuddin, M., Bazan, C., and Hussein, A. (2018). Field Inspection and Classification of Pavement Distress of St. John's City in Newfoundland Canada. 7th International Materials Specialty Conference, Canadian Society for Civil Engineering.

Ali, A., Dhasmana, H., Hossain, K., & Hussein, A. (2021). Modeling pavementm performance indices in harsh climate regions. Journal of Transportation Engineering, Part B: Pavements, 147(4), 04021049

Abaza, K. A., Ashur, S. A., Abu-Eisheh, S. A., & Rabay'a, A. (2001). Macroscopic optimum system for management of pavement rehabilitation. Journal of Transportation Engineering, 127(6), 493-500.

Alharbi, F. (2018). Predicting pavement performance utilizing artificial neural network (ANN) models. Graduate Theses and Dissertations, 16703

Arellano, G. L. (2006). Improving Pavements With Long-Term Pavement Performance : Products for Today and Tomorrow. September.

Arhin, S. A., Williams, L. N., Ribbiso, A., & Anderson, M. F. (2015). Predicting Pavement Condition Index Using International Roughness Index in a Dense Urban Area. Journal of Civil Engineering Research, 5(1), 10–17.

ASTM International. (2018). "ASTM D6433-18 Standard Practice for Roads and Parking Lots Pavement Condition Index Surveys." 10.1520/D6433-18, West Conshohocken, PA.

ASTM International. (2015). "ASTM E2840-11 Standard Practice for Pavement Condition Index Surveys for Interlocking Concrete Roads and Parking Lots." 10.1520/E2840-11R15, West Conshohocken, PA.

ASTM International. (2012). "ASTM E867-06 Standard Terminology Relating to Vehicle-Pavement Systems." 10.1520/E0867-06R12, West Conshohocken, PA.

Chandra, S., Sekhar, C. R., Bharti, A. K., & Kangadurai, B. (2012). Relationship between pavement roughness and distress parameters for Indian highways. Journal of Transportation Engineering, 139(5), 467-475.

Cao, R., Leng, Z., Hsu, S. C., & Hung, W. T. (2020). Modelling of the pavement acoustic longevity in Hong Kong through machine learning techniques. Transportation Research Part D: Transport and Environment, 83, 102366.

Ceylan, H., Gopalakrishnan, K., & Kim, S. (2009). Looking to the future: The next-generation hot mix asphalt dynamic modulus prediction models. International Journal of Pavement Engineering, 10(5), 341–352. https://doi.org/10.1080/10298430802342690

Chattopadhyay, S. (2006). Soft Computing Techniques in combating the complexity of the atmosphere- a review. 16.

Choi, J. H., Adams, T. M., & Bahia, H. U. (2004). Pavement roughness modeling using back-propagation neural networks. Computer-Aided Civil and Infrastructure Engineering, 19(4), 295–303.

Dehzangi, O., Zolghadri, M.J., Taheri, S., Fakhrahmad, S.M., 2007. Efficient Fuzzy Rule Generation: A New Approach Using Data Mining Principles and Rule Weighting. In: Fourth International Conference on Fuzzy Systems and Knowledge Discovery. IEEE, Haikou, pp. 134–139.

Dewan, S. A. (2004). Pavement Management and Asset Management Side-by-Side. 6th International Conference on Managing Pavements, 34, 12.

DOT, F. (2010). Airfiel Pavement Inspection Reference Manual. March.

Elton, D. J., & Juang, C. H. (1988). Asphalt pavement evaluation using fuzzy sets.

Transportation Research Record, 1196, 1–6.

Fathi, A., Mazari, M., Saghafi, M., Hosseini, A., & Kumar, S. (2019). Parametric study of pavement deterioration using machine learning algorithms. Airfield and highway pavements, 2019, 31-41.

Field, A., (2009). Discovering Statistics Using SPSS. 3 rd ed. London: SAGE Publication Ltd.

Fujita, Y., Shimada, K., Ichihara, M., & Hamamoto, Y. (2017, May). A method based on machine learning using hand-crafted features for crack detection from asphalt pavement surface images. In Thirteenth International Conference on Quality Control by Artificial Vision 2017 (Vol. 10338, pp. 117-124). SPIE.

Federal Highway Administration, U. (2009). Pavement distressesidentification manual for the NPS Road Inventory. Cycle 4, 1–25.

Fwa, T.F., Chan, W.F., Hoque, K.Z., 2000. Multi-Objective Optimisation for Pavement Maintenance Programming. J. Transp. Eng. 126, 367–374.

Fwa, T.F., 2006. The Handbook of Highway Engineering. Taylor & Francis, Boca Raton, FL.

FHWA, Federal Highway Administration. (2009). "LTPP Beyond FY 2009: What Needs to Be Done?" Washington, DC.

Government of Canada. (2014). "Canada's Sixth National Report on Climate Change: Actions to Meet Commitments Under the United Nations Framework Convention on Climate Change."

Inkoom, S., Sobanjo, J., Barbu, A., & Niu, X. (2019). Pavement crack rating using machine learning frameworks: Partitioning, bootstrap forest, boosted trees, Naïve bayes, and K-Nearest neighbors. Journal of Transportation Engineering, Part B: Pavements, 145(3), 04019031.

IBM Corporation. (2020). "IBM SPSS Statistics for Windows." Version 27.0, Armonk, NY.

Gagnon, M., Gaudreault, V., & Overton, D. (2008). Analysis in Brief Age of Public Infrastructure : A Provincial Perspective Age of Public Infrastructure : A Provincial.11,1-27.

Gaspard, K. (2014). International Journal of Pavement Engineering International roughness

index models for HMA overlay treatment of flexible and composite pavements.

Garber NJ, Hoel LA, Sadek AW (2011) Transportation infrastructure engineering. A multimodal integration SI edition. Cengage Learning Publishing Company, Toronto

Gavin, J., Dunn, L., & Juhasz, M. (2003). Long term performance monitoring of the Lamont test road. TAC/ATC 2003 - 2003 Annual Conference and Exhibition of the Transportation Association of Canada: The Transportation Factor.

Gershenson, C. (2003). Artificial neural networksfor Beginners. September 2003.

Ghanizadeh, A. R., & Fakhri, M. (2014). Prediction of frequency for simulation of asphalt mix fatigue tests using MARS and ANN. The Scientific World Journal, 2014(2005).

Gharaibeh et al. (1999). D Evelopment of P Olarographic S Ensors for. 5(June), 61–68.

Golabi, K., & Pereira, P. (2003). Innovative Pavement Management and Planning System for Road Network of Portugal. Journal of Infrastructure Systems, 9(2), 75–80.

Golroo, A., & Tighe, S. (2009). Use of soft computing applications to model pervious concrete pavement condition in cold climates. Journal of Transportation Engineering, 135(11), 791–800.

Government of Alberta, T. (2011). Engineering Consulting Guidelines for Highway , Bridge , and Water Projects.

Guisan et al. (2000). Effect of boundary layer conductance on the response of stomata to humidity. Plant, Cell & Environment, 8(1), 55–57.

Gupta, A., Kumar, P., & Rastogi, R.(2011). Pavement deterioration and maintenance model for low volume roads. International Journal of Pavement Research and Technology, 4(4),202.

Hall, K T, Correa, C. E., Carpenter, S. H., & Elliott, R. P. (1993). NCHRP W35 Appendiz A - Pavement DistressesTypes and Causes. DistressesIdentification Manual for the Long-Term Pavement Performance Project, 1–31.

Hall, Kathleen T., Correa, C. E., & Simpson, A. L. (2003). Performance of Flexible Pavement Rehabilitation Treatments in the Long-Term Pavement Performance SPS-5 Experiment. Transportation Research Record, 1823, 93–101.

Hein, D., & Watt, D. (2005). Municipal pavement performance prediction based on pavement condition data. TAC/ATC 2005 - 2005 Annual Conference and Exhibition of the Transportation Association of Canada: Transportation - Investing in Our Future, January

2005.

Hoang, N. D., & Nguyen, Q. L. (2019). A novel method for asphalt pavement crack classification based on image processing and machine learning. Engineering with Computers, 35(2), 487-498.

Hossain, M. I., Gopisetti, L. S. P., & Miah, M. S. (2019). International roughness index prediction of flexible pavements using neural networks. Journal of Transportation Engineering, Part B: Pavements, 145(1), 04018058

Hudson, W. R., Haas, R., & Pedigo, R. D. (1979). Pavement Management System Development. In National Cooperative Highway Research Program Report (Issue 215).

Infrastructur, C. E. S. C. and M. B. M. of T. and. (2011). 2012 Standard Specifications for Highway Construction 2012 STANDARD SPECIFICATIONS FOR.

Islam, S., Buttlar, W., Aldunate, R., & Vavrik, W. (2014). Measurement of Pavement Roughness Using Android-Based Smartphone Application. Transportation Research Record: Journal of the Transportation Research Board, 2457(January), 30–38.

Juang, C. H., & Chen, C. J. (1999). CRT-based liquefaction evaluation using artificial neural networks. Computer-Aided Civil and Infrastructure Engineering, 14(3), 221–229.

Kamel, N. I., Phang, W., Morris, J., & Haas, R. C. G. (1973). Layer Analysis of the Brampton Test Road and Application To Pavement Design. Highw Res Rec, 466, 113–126.

Karballaeezadeh, N., Ghasemzadeh Tehrani, H., Mohammadzadeh Shadmehri, D., & Shamshirband, S. (2020). Estimation of flexible pavement structural capacity using machine learning techniques. Frontiers of Structural and Civil Engineering, 14(5), 1083-1096.

Khazanovich, L., Darter, M., Bartlett, R., & McPeak, T. (1998). Common Characteristics of Good and Poorly Performing PCC Pavements. 204.

Kilareski, W. P., & Churilla, C. J. (1983). Pavement management for large highway networks. Journal of Transportation Engineering, 109(1), 33–45.

Labi, S., & Sinha, K. C. (2005). Life-cycle evaluation of flexible pavement preventive maintenance. Journal of transportation engineering, 131(10), 744-751.

Leiva-Villacorta, F., Vargas-Nordcbeck, A., & Timm, D. H. (2017). Non-destructive evaluation of sustainable pavement technologies using artificial neural networks. International Journal of Pavement Research and Technology, 10(2), 139–147.

Li, Z., Chau, C. K., & Zhou, X. (2005). Accelerated assessment and fuzzy evaluation of concrete durability. Journal of materials in civil engineering, 17(3), 257-263.

Llopis-Castelló, D., García-Segura, T., Montalbán-Domingo, L., Sanz-Benlloch, A., & Pellicer, E. (2020). Influence of pavement structure, traffic, and weather on urban flexible pavement deterioration. Sustainability, 12(22), 9717

Lytton, R. (1987). Concepts of pavement performance prediction and modeling. In Second North American Conference on Managing Pavements (p. G-1-G-33).

Mcclelland, J. L., & Rumelhart, D. E. (1986). The Apppeal of Paralled Distributed Processing.pdf (pp. 1–43).

Mehran. (2008). Fuzzy Modeling for Process Control. School of Electrical, Electronic and Computer Engineering, 28.

Miller, J. S., & Bellinger, W. Y. (2003). DistressesIdentification Manual for the Long-Term Pavement Performance Program. Publication of US Department of Transport, Federal Highway Administration, June, 129.

Mirzahosseini, M., Najjar, Y. M., Alavi, A. H., & Gandomi, A. H. (2013). {ANN}-Based Prediction Model for Rutting Propensity of Asphalt Mixtures. The 92nd Transportation Research Board (TRB) Annual Meeting, 386(330), Paper No. 13--2180.

Mahmood, M., 2014. Cross Validation of Multi Input Deterioration Prediction Model (MID-PM) for Network Level Pavement Management. Proceedings of the Inaugural College of Art, Design & Built Environment Doctoral Conference, Nottingham Trent University, 9th -10 th June, Nottingham, UK.

Mahmood, M. S. (2015). Network-level maintenance decisions for flexible pavement using a soft computing-based framework. Nottingham Trent University (United Kingdom).

Morova, N., Sargin, Ş., Terzi, S., Saltan, M., & Serin, S. (2012). Modeling Marshall stability of light asphalt concretes fabricated using expanded clay aggregate with artificial neural networks. INISTA 2012 - International Symposium on INnovations in Intelligent SysTems and Applications, May.

Múčka, P. (2017). International Roughness Index specifications around the world. Road Materials and Pavement Design, 18(4), 929–965.

NCHRP. (2004). Guide for Mechanistic–Empirical Design of New and Rehabilitated Pavement

Structures. Transportation Research Board of the National .

Nabipour, N., Karballaeezadeh, N., Dineva, A., Mosavi, A., Mohammadzadeh S, D., & Shamshirband, S. (2019). Comparative analysis of machine learning models for prediction of remaining service life of flexible pavement. Mathematics, 7(12), 1198.

Nitsche, P., Stütz, R., Kammer, M., & Maurer, P. (2014). Comparison of machine learning methods for evaluating pavement roughness based on vehicle response. Journal of Computing in Civil Engineering, 28(4), 04014015.

Nejad, F. M., Mehrabi, A., & Zakeri, H. (2015). Prediction of asphalt mixture resistance using neural network via laboratorial X-ray images'. Journal of Industrial and Intelligent Information Vol, 3(1).

Nejad, F. M., Motekhases, F. Z., Zakeri, H., & Mehrabi, A. (2015). An image processing approach to asphalt concrete feature extraction. Journal of Industrial and Intelligent Information, 3(1).

Ngwangwa, H. M., Heyns, P. S., Breytenbach, H. G. A., & Els, P. S. (2014). Reconstruction of road defects and road roughness classification using Artificial neural networkssimulation and vehicle dynamic responses: Application to experimental data. Journal of Terramechanics, 53(1), 1–18.

Norouzi, M., Nassiri, S., Haghi, N. T., & Bayat, A. (2014). Performance evaluation of asphalt overlays in Alberta using long term pavement performance specific pavement study 5 sections. International Journal of Pavement Research and Technology, 7(1), 60–68.

Park, K., Thomas, N. E., & Lee, K. W. (2007). Applicability of the international roughness index as a predictor of asphalt pavement condition. Journal of Transportation Engineering, 133(12), 706–709.

Perera, R. W., & Kohn, S. D. (2006). Ride Quality Performance of Asphalt Concrete Pavements Subjected to Different Rehabilitation Strategies. Airfield and Highway Pavement, 789–800.

Piryonesi, S. M. (2019). The application of data analytics to asset management: Deterioration and climate change adaptation in Ontario roads (Doctoral dissertation, University of Toronto (Canada)).

Prozzi and Madanat. (2004). Development of pavement deterioration models by combining experimental and field data sets. Proceedings of the International Conference on Applications of Advanced Technologies in Transportation Engineering, 10(March), 529–

536.

Psalmen Hasibuan, R., & Sejahtera Surbakti, M. (2019). Study of Pavement Condition Index (PCI) relationship with International Roughness Index (IRI) on Flexible Pavement. MATEC Web of Conferences, 258, 03019.

Puppala, A. J., & Chittoori, B. C. S. (2012). Transportation infrastructure settlement and heave distress: challenges and solutions. Journal of Zhejiang University SCIENCE A, 13(11), 850–857.

Rajagopal, A. S., & George, K. P. (1991). Pavement maintenance effectiveness. Transportation Research Record, 1276, 62–68.

Rasdorf et al. (2000). I nformation M anagement M anual. 1(1), 237–256.

Roberts, C. A., & Attoh-Okine, N. O. (1998). A Comparative Analysis of Two Artificial neural networksUsing Pavement Performance Prediction. Computer-Aided Civil and Infrastructure Engineering, 13(5), 339–348.

Salama, H. K., Chatti, K., & Lyles, R. W. (2006). Effect of Heavy Multiple Axle Trucks on Flexible Pavement Damage Using In-Service Pavement Performance Data. Journal of Transportation Engineering, 132(10), 763–770.

Sarie, F., Bisri, M., Wicaksono, A., & Effendi, R. (2015). Types of Road Pavement Damage for Road on Peatland , A Study Case in Palangka Raya , Central Kalimantan , Indonesia. 9(12), 53–59.

Slatter, P. E. (1987). Building expert systems: Cognitive emulation. Open University (United Kingdom).

Scott, G., & Engineer, T. A. (2012). Pavement Cracking : A Failure Indicator of Your Roads Changes to Professional Development Hour Requirements. XXXI(March).

sebaaly et al. (1996). Nevada ' s Approach to. 109–117.

Selvi. (2009). Traffic Accident Predictions Based on Fuzzy Logic Approach for Safer Urban Environments , Case Study İzmir Metropolitan Area. Area.

Shafabakhsh, G. H., Ani, O. J., & Talebsafa, M. (2015). Artificial neural network modeling (ANN) for predicting rutting performance of nano-modified hot-mix asphalt mixtures containing steel slag aggregates. Construction and Building Materials, 85, 136–143. https://doi.org/10.1016/j.conbuildmat.2015.03.060.

Shahin, M. Y., & Walther, J. A. (1990). Pavement Maintenance Management PAVER System. Tehchnical Department of the Army.

Singh, D., Zaman, M., & Commuri, S. (2013). Artificial Neural Network Modeling for Dynamic Modulus of Hot Mix Asphalt Using Aggregate Shape Properties. Journal of Materials in Civil Engineering, 25(1), 54–62.

Smith, S. D. (1999). I Mage Snr E Stimation U Sing. Syria, 0(June), 1.

Solhmirzaei, A., Azadi, S., & Kazemi, R. (2012). Road profile estimation using wavelet neural network and 7-DOF vehicle dynamic systems. Journal of Mechanical Science and Technology, 26(10), 3029–3036.

Sousa, S. I. V., Martins, F. G., Alvim-Ferraz, M. C. M., & Pereira, M. C. (2007). Multiple linear regression and artificial neural networksbased on principal components to predict ozone concentrations. Environmental Modelling and Software, 22(1), 97–103.

Sugeno M (1985) An introductory survey of fuzzy control. Inf Sci 36(1):59–83

Sun, L., & Gu, W. (2011). Pavement condition assessment using fuzzy logic theory and analytic hierarchy process. Journal of Transportation Engineering, 137(9), 648–655.

Svozil, D., Kvasnicka, V., and Pospichal, J., (1997). Introduction to multilayer feed-forward neural networks. Chemometrics and Intelligent Laboratory Systems, Elsevier, 39 (1), 43–62.

Tsao, S., Kehtarnavaz, N., Chan, P., & Lytton, R. (1994). Image-based expert-system approach to distress detection on CRC pavement. Journal of Transportation Engineering, 120(1), 52-64.

Tapkin, S., Çevik, A., & Uşar, Ü. (2010). Prediction of Marshall test results for polypropylene modified dense bituminous mixtures using neural networks. Expert Systems with Applications, 37(6), 4660–4670.

Tarefder, R. A., Saha, N., Hall, J. W., & Ng, P. T. T. (2008). Evaluating weak subgrade for pavement design and performance prediction: A case study of US 550. Journal of GeoEngineering, 3(1), 13–24.

Tayfur, G., Ozdemir, S., & Singh, V. P. (2003). Fuzzy logic algorithm for runoff-induced sediment transport from bare soil surfaces. Advances in Water Resources, 26(12), 1249–1256.

Tigdemir, M., Karasahin, M., & Sen, Z. (2002). Investigation of fatigue behaviour of asphalt concrete pavements with fuzzy-logic approach. International Journal of Fatigue, 24(8), 910.

Tıdemir, M. (2014). Re-evaluation of the AASHTO-flexible pavement design equation with neural network modeling. PLoS ONE, 9(11), 1–9.

Unit, P. S. (2010). Pavement Distressessurvey Manual Pavement Services Unit. June, 1–58.

West, R., Michael, J., Turochy, R., & Maghsoodloo, S. (2011). Use of data from specific pavement studies experiment 5 in the long-term pavement performance program to compare virgin and recycled asphalt pavements. Transportation Research Record, 2208, 82–89.

Yousefzadeh, M., Azadi, S., & Soltani, A. (2010). Road profile estimation using neural network algorithm. Journal of Mechanical Science and Technology, 24(3), 743–754.

Zadeh. (1965). Fuzzy Sets. Information and Control. 38(4), 656–657.

Zaman, M., Solanki, P., Ebrahimi, A., & White, L. (2010). Neural Network Modeling of Resilient Modulus Using Routine Subgrade Soil Properties. International Journal of Geomechanics, 10(1), 1–12.

Zeiada, W., Dabous, S. A., Hamad, K., Al-Ruzouq, R., & Khalil, M. A. (2020). Machine learning for pavement performance modelling in warm climate regions. Arabian journal for science and engineering, 45(5), 4091-4109

Ziari, H., Sobhani, J., Ayoubinejad, J., & Hartmann, T. (2015). Prediction of IRI in short and long terms for flexible pavements: ANN and GMDH methods. International Journal of Pavement Engineering, 17(9), 776–788.

Zeiada, W., Dabous, S. A., Hamad, K., Al-Ruzouq, R., & Khalil, M. A. (2020). Machine learning for pavement performance modelling in warm climate regions. Arabian journal for science and engineering, 45(5), 4091-4109.

Zimmerman, H. J. (1991). Fuzzy Set Theory and its Applications, Chapter 1.

Zofka, A., & Yut, I. (2012). Prediction of asphalt creep compliance using artificial neural networks. Archives of Civil Engineering, 58(2), 153–173.

Appendices

Appendix A: Data Extraction (LTPP dataset)

Table A-1: Pavement distress of each section with PCI and IRI.

State /Province	Country	Climate regions	Age	Rutting	Fatigue	Block	Long	Transverse	Patching	Potholes	Bleeding	Raveling	IRI	PCI
Washington	US	DRY Freeze	6	10	98.9	0	129	50	0	0	0	0	1.488	72
Washington	US	DRY Freeze	7	9	170	0	155.2	35	0	0	0	0	1.08	69
Washington	US	DRY Freeze	8	9	61.7	0	232.6	45	0	0	0	0	1.331	71
Washington	US	DRY Freeze	15	9	0.3	0	204.7	37	0	0	0	0	1.015	70
Washington	US	DRY Freeze	13	8	0	0	155.3	30	0	0	0	0	1.559	80
Washington	US	DRY Freeze	13	8	84.7	0	378.5	65	0	0	0	0	0.989	68
Washington	US	DRY Freeze	11	8	0	0	250.8	22	0	0	0	0	1.14	65
Washington	US	DRY Freeze	10	6	0	0	199.7	34	0	0	0	0	0.888	64
Washington	US	DRY Freeze	9	6	0	0	142.1	31	0	0	0	0	1.692	60
Washington	US	DRY Freeze	9	4	0	0	140.7	24	0	0	0	0	1.469	59
Washington	US	DRY Freeze	8	4	0	0	128.9	27	0	0	0	0	1.145	58
Wyoming	US	DRY Freeze	17	3	0	0	289.2	22	0	0	0	0	0.908	55
Wyoming	US	DRY Freeze	17	0	7.6	0	213.7	29	0	0	0	0	0.906	55
Wyoming	US	DRY Freeze	18	0	0	0	173.3	29	0	0	0	0	1.5	52
California	US	DRY no Freeze	32	16	39.9	0	136.6	140	0	0	0	0	0.819	100
California	US	DRY no Freeze	30	6	17.1	0	27.5	62	0	0	0	0	0.781	100
California	US	DRY no Freeze	29	3	16.5	0	182.3	3	0	0	0	0	1.606	100
California	US	DRY no Freeze	27	12	5.8	0	0	0	0	0	0	0	1.408	100
California	US	DRY no Freeze	25	4	5.8	0	43.9	21	0	0	0	0	2.379	100
California	US	DRY no Freeze	24	4	3.8	0	305.6	4	0	0	0	0	0.765	80
California	US	DRY no Freeze	23	7	1.5	0	0	1	0	0	0	0	0.683	95
California	US	DRY no Freeze	23	6	2.6	0	98.3	59	0	0	0	0	0.735	63
California	US	DRY no Freeze	21	5	1.3	0	0	0	0	0	0	0	0.754	92
California	US	DRY no Freeze	21	6	1.3	0	305.2	0	0	0	0	0	0.782	61
California	US	DRY no Freeze	20	6	0.8	0	2.8	11	0	0	0	0	0.783	62
California	US	DRY no Freeze	20	2	1.1	0	176.6	2	0	0	0	0	0.817	90
California	US	DRY no Freeze	19	5	0	0	1.7	9	0	0	0	0	0.82	88
California	US	DRY no Freeze	19	12	0	0	242.2	71	0	0	0	0	0.823	87
California	US	DRY no Freeze	19	0	0	0	0	0	0	0	0	0	0.828	83
Hawaii	US	DRY no Freeze	18	6	0	0	36.1	7	0	0	0	0	0.835	80
Hawaii	US	DRY no Freeze	18	5	0	0	0	8	0	0	0	0	0.848	80
Hawaii	US	DRY no Freeze	18	4	0	0	0	8	0	0	0	0	0.855	75

Hawaii	US	DRY no Freeze	18	5	0	0	1.2	9	0	0	0	0	0.874	74
Hawaii	US	DRY no Freeze	17	5	0	0	0	0	0	0	0	0	1.321	74
Hawaii	US	DRY no Freeze	17	5	0	0	0	1	0	0	0	0	1.408	73
Hawaii	US	DRY no Freeze	17	5	0	0	0	4	0	0	0	0	1.418	72
Hawaii	US	DRY no Freeze	16	5	0	0	0	0	0	0	0	0	1.434	70
Hawaii	US	DRY no Freeze	16	0	0	0	0	0	0	0	0	0	1.434	66
Hawaii	US	DRY no Freeze	16	5	0	0	0	0	0	0	0	0	1.473	65
Hawaii	US	DRY no Freeze	15	4	0	0	0	1	0	0	0	0	1.528	63
Hawaii	US	DRY no Freeze	15	0	0	0	0	0	0	0	0	0	1.544	61
Hawaii	US	DRY no Freeze	15	0	0	0	0	0	0	0	0	0	1.613	57
Hawaii	US	DRY no Freeze	15	0	0	0	0	0	0	0	0	0	1.636	56
Hawaii	US	DRY no Freeze	13	6	0	0	270.2	0	0	0	0	0	1.653	55
Hawaii	US	DRY no Freeze	13	5	0	0	270.1	3	0	0	0	0	1.67	55
New Mexico	US	DRY no Freeze	13	5	0	0	0	0	0	0	0	0	1.838	52
New Mexico	US	DRY no Freeze	13	5	0	0	0	12	1.5	0	0	0	2.113	69
New Mexico	US	DRY no Freeze	13	0	0	0	0	0	0	0	0	0	2.318	68
New Mexico	US	DRY no Freeze	13	5	0	0	2.4	1	0	0	0	76.3	2.332	70
New Mexico	US	DRY no Freeze	12	7	0	0	263.1	7	0	0	0	0	2.362	55
New Mexico	US	DRY no Freeze	11	4	0	0	0	0	0	0	0	0	2.404	81
New Mexico	US	DRY no Freeze	11	4	0	0	0	0	0	0	0	0	2.412	70
New Mexico	US	DRY no Freeze	11	5	0	0	0	0	0	0	0	0	2.42	54
New Mexico	US	DRY no Freeze	11	5	0	0	0	0	0	0	0	0	2.425	66
New Mexico	US	DRY no Freeze	11	4	0	0	85.6	0	0	0	0	0	2.441	67
New Mexico	US	DRY no Freeze	11	5	0	0	213.1	2	0	0	0	0	2.464	67
New Mexico	US	DRY no Freeze	10	3	0	0	0	0	0	0	0	0	2.497	67
New Mexico	US	DRY no Freeze	10	3	0	0	0	0	0	0	0	0	2.5	74
New Mexico	US	DRY no Freeze	10	2	0	0	22.8	0	0	0	0	0	2.525	62
New Mexico	US	DRY no Freeze	9	2	0	0	179	83	0	0	0	0	2.662	59
New Mexico	US	DRY no Freeze	9	3	0	0	153	37	0	0	0	0	0.925	59
New Mexico	US	DRY no Freeze	9	3	0	0	0	0	0	0	0	0	0.856	58
New Mexico	US	DRY no Freeze	9	3	0	0	0	0	0	0	0	0	1.369	58
New Mexico	US	DRY no Freeze	9	4	0	0	0	0	0	0	0	0	1.396	82
New Mexico	US	DRY no Freeze	7	5	0	0	60.9	22	0	0	0	0	1.012	58
New Mexico	US	DRY no Freeze	7	3	0	0	36.9	19	0	0	0	0	0.857	58
New Mexico	US	DRY no Freeze	7	3	0	0	88.7	27	0	0	0	0	1.31	58
New Mexico	US	DRY no Freeze	7	4	0	0	102.7	41	0	0	0	0	1.183	57
New Mexico	US	DRY no Freeze	7	3	0	0	123.4	31	0	0	0	0	0.88	55

New Mexico	US	DRY no Freeze	6	3	0	0	23.4	17	0	0	0	0	0.877	56
New Mexico	US	DRY no Freeze	5	11	0	0	115.2	18	0	0	0	0	0.862	61
New Mexico	US	DRY no Freeze	5	4	0	0	112.4	13	0	0	0	0	0.887	91
New Mexico	US	DRY no Freeze	3	5	0	0	59.3	60	0	0	0	0	0.925	50
Idaho	US	Wet Freeze	3	0	5.4	0	29.5	0	0	0.00	0.00	0.00	4.005	8
Idaho	US	Wet Freeze	4	0	63.8	0	309	153	0	0.00	0.00	0.00	3.659	10
Idaho	US	Wet Freeze	4	0	3.7	0	20.4	0	0	0.00	0.00	0.00	3.519	10
Idaho	US	Wet Freeze	4	0	0	0	305	58	0	0.00	31.20	0.00	3.308	12
Idaho	US	Wet Freeze	4	0	63.8	0	309	152	0	0.00	0.00	0.00	3.251	15
Maine	US	Wet Freeze	5	0	0.9	0	329.1	113	0	0.00	5.50	0.00	3.116	22
Idaho	US	Wet Freeze	5	0	0	0	305	23	0	0.00	244.00	91.50	3.112	23
Idaho	US	Wet Freeze	5	0	0	0	305	17	0	0.00	0.00	547.20	2.967	27
Illinois	US	Wet Freeze	5	0	66.6	0	8.8	82	0	0.00	350.80	0.00	2.275	40
Maine	US	Wet Freeze	5	0	0	0	2.6	10	0	0.00	0.00	0.00	2.183	43
Michigan	US	Wet Freeze	5	0	0	0	0	11	0	0.00	0.00	556.60	1.985	44
Michigan	US	Wet Freeze	5	0	0	0	0	0	0	0.00	259.30	259.30	1.929	50
Michigan	US	Wet Freeze	5	0	0	0	0	2	0	0.00	0.00	0.00	1.929	52
Missouri	US	Wet Freeze	6	0	0	0	0	0	0	0.00	0.00	0.00	1.863	52
Michigan	US	Wet Freeze	6	0	0	0	26.3	0	0	0.00	0.00	0.00	1.775	52
Michigan	US	Wet Freeze	6	0	0	0	0	0	0	0.00	0.00	0.00	1.754	55
Michigan	US	Wet Freeze	6	0	0	0	0	0	0	0.00	0.00	0.00	1.742	55
Idaho	US	Wet Freeze	6	0	0	0	0	0	0	0.00	0.00	0.00	1.7	58
Idaho	US	Wet Freeze	6	3	0	0	0	0	0	0.00	0.00	0.00	1.691	58
Idaho	US	Wet Freeze	7	3	0	0	294.6	0	0	0.00	0.00	0.00	1.649	59
Michigan	US	Wet Freeze	7	3	0	0	64.4	0	0	0.00	0.00	0.00	1.526	60
Maine	US	Wet Freeze	7	4	3.1	0	19.1	18	0	0.00	0.00	0.00	1.526	61
Michigan	US	Wet Freeze	7	4	1	0	342.7	267	0	0.00	0.00	0.00	1.509	62
Michigan	US	Wet Freeze	7	4	0	0	0	0	0	0.00	0.00	0.00	1.501	66
Missouri	US	Wet Freeze	8	4	1.1	0	300	1	0	0.00	0.00	0.00	1.485	66
Idaho	US	Wet Freeze	8	4	0	0	298.1	6	0	0.00	0.00	0.00	1.473	67
Idaho	US	Wet Freeze	8	4	0	0	283.3	0	0	0.00	0.00	0.00	1.473	67
Idaho	US	Wet Freeze	8	5	7.5	0	14.5	0	0	0.00	0.00	0.00	1.458	68
Idaho	US	Wet Freeze	8	5	0	0	0	0	0	0.00	0.00	0.00	1.457	68
Missouri	US	Wet Freeze	9	5	0.9	0	306.3	173	0	0.00	274.00	0.00	1.457	68
Missouri	US	Wet Freeze	9	5	78.2	0	308.2	3	0	0.00	0.00	0.00	1.445	69
Maine	US	Wet Freeze	9	5	47.3	0	305.2	2	0	0.00	0.00	0.00	1.441	69
Missouri	US	Wet Freeze	9	5	0	0	0	0	0	0.00	0.00	0.00	1.433	69

Maine	US	Wet Freeze	9	5	0	0	120.6	0	0	0.00	10.80	0.00	1.416	69
Missouri	US	Wet Freeze	10	5	0	0	94.4	0	0	0.00	0.00	0.00	1.399	69
Maine	US	Wet Freeze	10	5	0	0	0	0	0	0.00	0.00	0.00	1.357	70
Maine	US	Wet Freeze	10	5	0	0	146	0	0	0.00	0.00	0.00	1.309	70
Illinois	US	Wet Freeze	10	5	0	0	0	0	0	0.00	0.00	0.00	1.293	70
Missouri	US	Wet Freeze	10	5	0	0	145.7	0	0	0.00	0.00	0.00	1.278	71
Missouri	US	Wet Freeze	10	6	218.7	0	305	35	0	0.00	0.00	305.00	1.274	72
Maine	US	Wet Freeze	10	6	2.1	0	313.2	293	0	0.00	0.00	0.00	1.274	72
Missouri	US	Wet Freeze	11	6	7.7	0	23.6	13	0	0.00	0.00	0.00	1.269	74
Michigan	US	Wet Freeze	11	6	0	0	295.3	22	0	0.00	305.00	0.00	1.257	74
Missouri	US	Wet Freeze	11	6	3.1	0	20.1	0	0	0.00	0.00	0.00	1.249	75
Michigan	US	Wet Freeze	11	6	91.5	0	0	0	0	0.00	0.00	0.00	1.247	75
Newfoundland	Canada	Wet Freeze	11	6	0	0	0	0	0	0.00	0.00	0.00	1.247	76
Newfoundland	Canada	Wet Freeze	11	6	0.4	0	171.7	33	0	0.00	0.00	0.00	1.242	76
Newfoundland	Canada	Wet Freeze	11	6	0	0	30.3	6	0	0.00	0.00	0.00	1.242	76
Missouri	US	Wet Freeze	11	6	0.6	0	325.5	190	0	0.00	0.00	0.00	1.235	76
Newfoundland	Canada	Wet Freeze	12	6	0	0	0	0	0	0.00	0.00	0.00	1.235	77
New Jersey	US	Wet Freeze	12	6	0	0	0	0	0	0.00	0.00	0.00	1.233	77
New Jersey	US	Wet Freeze	12	6	32.3	0	277	98	0	0.00	0.00	0.00	1.23	77
Missouri	US	Wet Freeze	12	6	0	0	0	0	0	0.00	0.00	0.00	1.229	77
Newfoundland	Canada	Wet Freeze	12	6	0	0	2300.4	20	0	0.00	0.00	0.00	1.222	78
Illinois	US	Wet Freeze	13	7	0	0	312.8	36	0	0.00	0.00	0.00	1.216	78
New Jersey	US	Wet Freeze	13	7	1.6	0	312.6	180	0	0.00	0.00	0.00	1.202	79
New Jersey	US	Wet Freeze	13	7	7.1	0	13.8	3	0	0.00	0.00	0.00	1.197	79
New Jersey	US	Wet Freeze	13	7	132.7	0	0	0	0	0.00	0.00	0.00	1.197	80
Newfoundland	Canada	Wet Freeze	13	7	1	0	10.4	4	0	0.00	0.00	0.00	1.196	81
Illinois	US	Wet Freeze	14	7	0	0	0	0	0	0.00	0.00	61.00	1.19	81
Newfoundland	Canada	Wet Freeze	14	7	0.8	0	162.7	171	0	0.00	0.00	0.00	1.177	81
New Jersey	US	Wet Freeze	14	7	0	0	167	1	0	0.00	0.00	0.00	1.176	81
Illinois	US	Wet Freeze	14	7	3.7	0	18.1	16	0	0.00	0.00	0.00	1.174	81
Illinois	US	Wet Freeze	14	7	0	0	36.7	17	0	0.00	0.00	0.00	1.167	82
New Jersey	US	Wet Freeze	14	7	0	0	150.5	13	0	0.00	0.00	0.00	1.151	82
Illinois	US	Wet Freeze	14	7	0	0	14.9	0	0	0.00	0.00	0.00	1.13	83
Montana	US	Wet Freeze	14	8	4.4	0	72.4	2	0	0.00	0.00	0.00	1.127	83
New Jersey	US	Wet Freeze	15	8	0	0	305.1	28	0	0.00	196.00	0.00	1.123	83
Montana	US	Wet Freeze	15	8	1	0	15.6	1	0	0.00	0.00	0.00	1.116	83
New Jersey	US	Wet Freeze	15	8	71.9	0	161.4	31	0	0.00	0.50	0.00	1.116	84

New Jersey	US	Wet Freeze	15	8	87.2	0	157	14	0	0.00	0.00	0.00	1.082	84
Montana	US	Wet Freeze	15	8	0	0	305	30	0	0.00	0.00	244.00	1.078	84
New Jersey	US	Wet Freeze	15	8	94.2	0	152.4	0	0	0.00	0.00	0.00	1.074	84
Montana	US	Wet Freeze	15	8	0	0	155.7	6	0	0.00	0.00	0.00	1.073	84
New Jersey	US	Wet Freeze	15	8	91.6	0	146.9	1	0	0.00	0.00	0.00	1.063	84
Michigan	US	Wet Freeze	15	8	6.7	0	95.1	27	0	0.00	0.00	0.00	1.058	84
Montana	US	Wet Freeze	15	8	58.5	0	245.5	23	0	0.00	0.00	0.00	1.051	84
New Jersey	US	Wet Freeze	15	8	5.9	0	63	17	0	0.00	0.00	0.00	1.043	85
Vermont	US	Wet Freeze	16	8	0	0	0	0	0	0.00	0.00	0.00	1.039	85
Montana	US	Wet Freeze	16	9	63.3	0	216	17	0	0.00	259.30	305.00	1.038	85
Montana	US	Wet Freeze	16	9	116.4	0	144.2	16	0	0.00	0.00	0.00	1.031	86
Montana	US	Wet Freeze	16	9	73.9	0	0	39	0	0.00	0.00	0.00	1.031	86
Vermont	US	Wet Freeze	17	9	0	0	7	0	0	0.00	4.70	82.40	1.031	87
Illinois	US	Wet Freeze	17	9	0	0	0	0	0	0.00	0.00	76.20	1.03	87
Montana	US	Wet Freeze	17	10	0.2	0	299.9	27	0	0.00	0.00	0.00	1.028	87
Montana	US	Wet Freeze	17	10	3.5	0	29.1	18	0	0.00	0.00	0.00	1.025	87
Vermont	US	Wet Freeze	17	10	31.8	0	20.7	85	0	0.00	0.00	0.00	1.02	87
Vermont	US	Wet Freeze	17	10	0	0	27	18	0	0.00	0.00	0.00	1.02	87
Michigan	US	Wet Freeze	17	10	28.4	0	0	39	0	0.00	0.00	0.00	1.018	88
Michigan	US	Wet Freeze	17	10	0	0	6.1	9	0	0.00	0.00	0.00	1.004	88
Vermont	US	Wet Freeze	17	10	0	0	2.3	5	0	0.00	0.00	0.00	0.999	88
Vermont	US	Wet Freeze	17	10	0	0	24.9	19	0	0.00	0.00	0.00	0.996	89
Vermont	US	Wet Freeze	17	10	0	0	0	5	0	0.00	0.00	0.00	0.98	89
Vermont	US	Wet Freeze	17	10	0	0	26.1	0	0	0.00	0.00	0.00	0.973	89
Vermont	US	Wet Freeze	18	10	0	0	0	0	0	0.00	0.00	0.00	0.965	89
Vermont	US	Wet Freeze	18	11	0	0	0	0	0	0.00	5.20	0.00	0.961	89
Montana	US	Wet Freeze	18	11		0			0	0.00	127.80	0.00	0.954	90
Illinois	US	Wet Freeze	18	11	0	0	0	0	0	0.00	21.00	500.50	0.946	90
Vermont	US	Wet Freeze	18	11	64.3	0	0	56	0	0.00	0.00	0.00	0.942	90
Michigan	US	Wet Freeze	18	11	0	0	10	0	0	0.00	0.00	0.00	0.942	91
Vermont	US	Wet Freeze	18	11	0	0	1.1	4	0	0.00	0.00	0.00	0.942	91
Vermont	US	Wet Freeze	19	11	0	0	6.8	6	0	0.00	0.00	0.00	0.939	91
Illinois	US	Wet Freeze	19	11	0	0	0.8	0	0	0.00	245.90	0.00	0.927	92
Michigan	US	Wet Freeze	19	12	0	0	289.5	18	0	0.00	0.00	0.00	0.924	92
Illinois	US	Wet Freeze	19	12	100.3	0	7.7	67	0	0.00	0.00	79.50	0.923	92
Vermont	US	Wet Freeze	19	12	73.2	0	2.7	93	0	0.00	0.00	564.30	0.906	92
Vermont	US	Wet Freeze	19	12	14.1	0	20.9	101	0	0.00	0.00	0.00	0.904	92

Illinois	US	Wet Freeze	19	12	0	0	36.3	39	0	0.00	0.00	0.00	0.899	92
Vermont	US	Wet Freeze	19	12	0	0	7.4	4	0	0.00	0.00	0.00	0.898	92
Michigan	US	Wet Freeze	20	12	0	0	0	0	0	0.00	0.00	0.00	0.892	92
Vermont	US	Wet Freeze	20	13	140.2	0	11.2	81	0	0.00	0.00	304.80	0.892	92
Michigan	US	Wet Freeze	20	13	181.8	0	26	67	0	0.00	0.00	0.00	0.864	93
Vermont	US	Wet Freeze	20	13	0	0	0	3	0	0.00	0.00	0.00	0.863	93
Vermont	US	Wet Freeze	20	14	0	0	0	0	0	0.00	0.00	0.00	0.859	93
Michigan	US	Wet Freeze	20	14	0	0	4.5	12	0	0.00	0.00	0.00	0.859	93
Vermont	US	Wet Freeze	20	14	0	0	24.2	3	0	0.00	0.00	0.00	0.845	93
Vermont	US	Wet Freeze	21	15	77.4	0	1.8	75	0	0.00	0.00	0.00	0.835	93
Vermont	US	Wet Freeze	21	15	2.3	0	96.2	150	0	0.00	0.00	0.00	0.822	93
Vermont	US	Wet Freeze	21	15	0	0	0	0	0	0.00	0.00	0.00	0.819	93
Indiana	US	Wet Freeze	21	15	0	0	0	0	0	0.00	12.00	500.50	0.819	93
Vermont	US	Wet Freeze	21	15	130.3	0	8.1	85	0	0.00	0.00	0.00	0.81	94
Michigan	US	Wet Freeze	22	15	0.4	0	163.5	136	0	0.00	0.00	0.00	0.808	94
Minnesota	US	Wet Freeze	22	15	0	0	56.2	28	0	0.00	7.60	0.00	0.805	94
Indiana	US	Wet Freeze	22	15	62.1	0	1.6	83	0	0.00	0.00	0.00	0.803	94
Indiana	US	Wet Freeze	22	15	114	0	3	84	0	0.00	0.00	0.00	0.796	94
Newfoundland	Canada	Wet Freeze	22	15	0	0	60.1	30	0	0.00	0.00	0.00	0.796	94
Minnesota	US	Wet Freeze	23	15	0	0	40.8	0	0	0.00	0.00	564.30	0.792	94
Newfoundland	Canada	Wet Freeze	24	16	162.1	0	1.5	85	0	0.00	0.00	0.00	0.787	94
Minnesota	US	Wet Freeze	25	16	163.9	0	1.5	103	0	0.00	0.00	76.20	0.786	94
Indiana	US	Wet Freeze	26	16	0	0	78	44	0	0.00	0.00	0.00	0.785	95
Minnesota	US	Wet Freeze	26	16	0	0	29.3	0	0	0.00	0.00	0.00	0.77	95
Illinois	US	Wet Freeze	26	17	0	0	0	0	0	0.00	0.00	0.00	0.757	95
Minnesota	US	Wet Freeze	26	18	0	0	3.7	0	0	0.00	0.00	0.00	0.756	95
Illinois	US	Wet Freeze	26	19	0	0	91.6	2	0	0.00	0.00	0.00	0.753	95
Michigan	US	Wet Freeze	26	21	5.6	0	82.8	5	0	0.00	0.00	0.00	0.751	95
Indiana	US	Wet Freeze	26	24	8.2	0	89.4	1	0	0.00	0.00	0.00	0.75	95
Newfoundland	Canada	Wet Freeze	27	26	22.3	0	92.6	2	0	0.00	259.30	305.00	0.744	95
Indiana	US	Wet Freeze	28	29	25.5	0	104.8	3	0	0.00	0.00	0.00	0.734	95
Newfoundland	Canada	Wet Freeze	28	0	0	0	15.8	1	0	0.00	0.00	0.00	0.732	95
Alabama	US	Wet no Freeze	1	14	0	0	152.8	0	0	0	0	0	0.621	100
Alabama	US	Wet no Freeze	1	0	0	0	0	0	0	0	0	0	0.627	100
Alabama	US	Wet no Freeze	1	0	0	0	0	0	0	0	0	0	0.641	100
Alabama	US	Wet no Freeze	1	0	0	0	0	0	0	0	0	0	0.646	100
Alabama	US	Wet no Freeze	3	0	0	0	0	1	0	0	0	0	0.653	100

Alabama	US	Wet no Freeze	3	0	0	0	0	0	0	0	0	0	0.67	100
Alabama	US	Wet no Freeze	3	0	0	0	18.2	0	0	0	0	0	0.7	100
Alabama	US	Wet no Freeze	4	0	0	0	164.6	0	0	0	0	0	0.702	100
Alabama	US	Wet no Freeze	4	0	0	0	0	0	0	0	0	0	0.713	100
Alabama	US	Wet no Freeze	4	0	0	0	0	0	0	0	0	0	0.716	100
Alabama	US	Wet no Freeze	5	0	31.6	0	0	16	0	0	0	0	0.717	100
Alabama	US	Wet no Freeze	5	0	0	0	0	0	0	0	0	0	0.72	100
Alabama	US	Wet no Freeze	5	0	0	0	15.5	0	0	0	0	0	0.735	100
Alabama	US	Wet no Freeze	5	0	0	0	0	11	0	0	0	0	0.735	100
Alabama	US	Wet no Freeze	5	0	0	0	0.4	7	0	0	0	0	0.749	100
Alabama	US	Wet no Freeze	5	0	75.6	0	27.4	26	0	0	0	0	0.778	100
Arkansas	US	Wet no Freeze	5	0	377.9	0	0	0	0	0	0	0	0.785	100
Arkansas	US	Wet no Freeze	5	0	6.2	0	14.9	5	0	0	0	0	0.796	100
Arkansas	US	Wet no Freeze	6	0	0	0	10.1	38	0	0	0	0	0.8	100
Arkansas	US	Wet no Freeze	6	1	2.3	0	97.8	2	0	0	0	0	0.811	100
Arkansas	US	Wet no Freeze	6	1	1.2	0	0	1	0	0	0	0	0.813	100
Arkansas	US	Wet no Freeze	6	1	0	0	0	0	0	0	0	0	0.815	100
Arkansas	US	Wet no Freeze	6	1	1	0	0	0	0	0	0	0	0.825	100
Arkansas	US	Wet no Freeze	6	1	0	0	0	0	0	0	0	0	0.834	100
California	US	Wet no Freeze	6	1	0	0	0	0	0	0	0	0	0.84	96
California	US	Wet no Freeze	6	1	0	0	0	0	0	0	0	0	0.847	90
California	US	Wet no Freeze	6	3	2.4	0	12.6	16	0	0	0	0	0.847	89
California	US	Wet no Freeze	6	3	0	0	0	0	0	0	0	0	0.869	89
California	US	Wet no Freeze	7	3	0	0	0	0	0	0	0	0	0.871	89
California	US	Wet no Freeze	7	3	0	0	0	0	0	0	0	0	1.364	89
California	US	Wet no Freeze	7	3	0	0	0	2	0	0	0	0	1.363	88
California	US	Wet no Freeze	7	3	0	0	39.2	1	0	0	0	0	1.352	88
California	US	Wet no Freeze	7	3	187.6	0	81.4	72	0	0	0	0	1.352	88
California	US	Wet no Freeze	7	4	0	0	126.5	4	0	0	0	0	1.352	88
California	US	Wet no Freeze	7	4	0	0	0	0	0	0	0	0	1.319	88
Florida	US	Wet no Freeze	7	4	0	0	0	0	0	0	0	0	1.302	88
Florida	US	Wet no Freeze	7	4	0	0	0.7	0	0	0	0	0	1.287	87
Florida	US	Wet no Freeze	7	4	0	0	0	4	0	0	0	0	1.269	87
Florida	US	Wet no Freeze	7	4	0	0	0	0	0	0	0	0	1.267	87
Florida	US	Wet no Freeze	7	4	0	0	0	1	0	0	0	0	1.249	87
Florida	US	Wet no Freeze	7	4	0	0	0	2	0	0	0	0	1.246	87
Florida	US	Wet no Freeze	7	4	7.3	0	7.6	2	0	0	0	0	1.196	87

Florida	US	Wet no Freeze	7	4	108.9	0	15.8	16	0	0	0	0	1.176	87
Florida	US	Wet no Freeze	8	4	2.6	0	5.2	1	0	0	0	0	1.164	87
Florida	US	Wet no Freeze	8	4	20.1	0	3.3	14	0	0	0	0	1.154	87
Florida	US	Wet no Freeze	8	4	0	0	0	0	0	0	0	0	1.15	86
Florida	US	Wet no Freeze	8	4	22.6	0	53..3	16	0	0	0	0	1.15	86
Florida	US	Wet no Freeze	8	4	15.2	0	9.8	5	0	0	0	0	1.136	86
Florida	US	Wet no Freeze	9	4	0	0	0	1	0	0	0	0	1.123	86
Florida	US	Wet no Freeze	9	4	11.4	0	8.9	4	0	0	0	0	1.12	86
Florida	US	Wet no Freeze	9	4	0	0	0	0	0	0	0	0	1.113	85
Florida	US	Wet no Freeze	9	4	8.4	0	7.6	1	0	0	0	0	1.11	85
Florida	US	Wet no Freeze	9	4	319.3	0	60.4	57	0	0	0	0	1.108	85
Florida	US	Wet no Freeze	9	4	7.3	0	8.2	2	0	0	0	0	1.108	85
Florida	US	Wet no Freeze	9	4		0			0	0	0	0	1.104	85
Florida	US	Wet no Freeze	9	4	318.3	0	27.6	5	0	0	0	0	1.104	84
Florida	US	Wet no Freeze	9	5	29.9	0	2.9	7	0	0	0	0	1.104	84
Florida	US	Wet no Freeze	9	5	0	0	0	3	0	0	0	0	1.104	84
Florida	US	Wet no Freeze	10	5	0	0	138.5	6	0	0	0	0	1.103	84
Florida	US	Wet no Freeze	10	5	365.7	0	32.9	113	0	0	0	0	1.098	83
Florida	US	Wet no Freeze	10	5	0	0	0	0	0	0	0	0	1.093	83
Florida	US	Wet no Freeze	10	5	56.6	0	96.5	90	0	0	0	0	1.093	83
Florida	US	Wet no Freeze	10	5	0	0	0	0	0	0	0	0	1.088	83
Florida	US	Wet no Freeze	10	5	18.8	0	63.2	116	0	0	0	0	1.085	83
Florida	US	Wet no Freeze	10	5	83.5	0	0	0	0	0	0	0	1.081	83
Florida	US	Wet no Freeze	11	5	7.5	0	181.8	1	0	0	0	0	1.078	83
Florida	US	Wet no Freeze	11	5	0	0	0	0	0	0	0	0	1.074	83
Florida	US	Wet no Freeze	11	5	0	0	1	0	0	0	0	0	1.074	83
Florida	US	Wet no Freeze	11	6	0	0	0	0	0	0	0	0	1.068	83
Florida	US	Wet no Freeze	11	6	0	0	0	3	0	0	0	0	1.064	83
Florida	US	Wet no Freeze	11	6	0	0	0	0	0	0	0	0	1.064	83
Florida	US	Wet no Freeze	11	6	1.3	0	89.2	6	0	0	0	0	1.062	83
Florida	US	Wet no Freeze	11	6	0	0	130.4	67	0	0	0	0	1.061	82
Florida	US	Wet no Freeze	11	6	7.7	0	78.4	6	0	0	0	0	1.052	82
Georgia	US	Wet no Freeze	12	6	1.4	0	99.2	45	0	0	0	0	1.05	82
Georgia	US	Wet no Freeze	12	6	0	0	26.9	13	0	0	0	0	1.045	82
Hawaii	US	Wet no Freeze	12	6	152.4	0	0	3	0	0	0	0	1.041	82
Hawaii	US	Wet no Freeze	12	6	0	0	152.3	0	0	0	0	0	1.008	82
Hawaii	US	Wet no Freeze	12	6	2.6	0	337.1	27	0	0	0	0	1.005	82

Hawaii	US	Wet no Freeze	12	6	0	0	0	0	0	0	0	0	1.002	82
Hawaii	US	Wet no Freeze	12	6	0	0	304.1	3	0	0	0	0	0.998	82
Hawaii	US	Wet no Freeze	12	6	0	0	0	7	0	0	0	0	0.994	82
Hawaii	US	Wet no Freeze	12	6	25.9	0	9.7	15	0	0	0	0	0.988	81
Hawaii	US	Wet no Freeze	13	6	0	0	0.2	19	0	0	0	0	0.985	81
Hawaii	US	Wet no Freeze	13	6	43.9	0	23.2	39	0	0	0	0	0.97	81
Hawaii	US	Wet no Freeze	13	6	13.4	0	94.6	61	0	0	0	0	0.969	81
Hawaii	US	Wet no Freeze	13	6	0	0	15.8	59	0	0	0	0	0.96	80
Hawaii	US	Wet no Freeze	13	7	0	0	0	0	0	0	0	0	0.959	80
Hawaii	US	Wet no Freeze	13	7	0	0	0.8	4	0	0	0	0	0.952	79
Hawaii	US	Wet no Freeze	13	7	0	0	0	1	0	0	0	0	0.951	78
Hawaii	US	Wet no Freeze	13	7	0	0	1.2	0	0	0	0	0	0.949	78
Hawaii	US	Wet no Freeze	13	7	0.7	0	1.4	7	0	0	0	0	0.948	78
Mississippi	US	Wet no Freeze	13	7	0	0	0	0	0	0	0	0	0.947	77
Mississippi	US	Wet no Freeze	13	7	0	0	0	5	0	0	0	0	0.944	77
Mississippi	US	Wet no Freeze	14	7	3.4	0	3.2	26	0	0	0	0	0.938	76
Mississippi	US	Wet no Freeze	14	7	0	0	17.2	22	0	0	0	0	0.926	76
Mississippi	US	Wet no Freeze	14	7	29.4	0	46.3	2	0	0	0	0	0.918	76
Mississippi	US	Wet no Freeze	14	7	0	0	122	0	0	0	0	0	0.912	75
Mississippi	US	Wet no Freeze	15	7	3	0	0	0	0	0	0	0	0.906	75
Mississippi	US	Wet no Freeze	15	7	0.5	0	286.8	93	0	0	0	0	0.906	75
Mississippi	US	Wet no Freeze	15	7	0	0	0	1	0	0	0	0	0.894	75
Mississippi	US	Wet no Freeze	15	7	0	0	3	0	0	0	0	0	0.884	74
Mississippi	US	Wet no Freeze	15	7	0	0	15.2	0	0	0	0	0	0.877	74
Mississippi	US	Wet no Freeze	15	7	1.7	0	31.9	25	0	0	0	0	1.366	74
Mississippi	US	Wet no Freeze	15	8	0	0	0	0	0	0	0	0	1.38	74
Mississippi	US	Wet no Freeze	16	8	0.9	0	0	6	0	0	0	0	1.383	74
Mississippi	US	Wet no Freeze	16	8	0	0	7.7	10	0	0	0	0	1.387	74
Mississippi	US	Wet no Freeze	16	8	0.6	0	30.8	5	0	0	0	0	1.393	73
Mississippi	US	Wet no Freeze	16	8	0	0	153.3	0	0	0	0	0	1.402	73
North Carolina	US	Wet no Freeze	16	8	0	0	0.1	2	0	0	0	0	1.418	73
North Carolina	US	Wet no Freeze	16	8	0	0	0	1	0	0	0	0	1.418	73
North Carolina	US	Wet no Freeze	16	8	0	0	0	0	0	0	0	0	1.422	71
North Carolina	US	Wet no Freeze	17	8	0.3	0	287.8	116	0	0	0	0	1.429	71
North Carolina	US	Wet no Freeze	17	8	4.7	0	307.2	107	0	0	0	0	1.433	70
North Carolina	US	Wet no Freeze	17	8	0	0	97.5	1	0	0	0	0	1.444	70
Oklahoma	US	Wet no Freeze	17	8	0	0	0	0	0	0	0	0	1.45	70

Oklahoma	US	Wet no Freeze	17	8	185.5	0	117.7	100	0	0	0	0	1.451	70
Oklahoma	US	Wet no Freeze	17	8	57.4	0	42.3	11	0	0	0	0	1.454	70
Oklahoma	US	Wet no Freeze	17	8	1.1	0	151.5	3	0	0	0	0	1.455	70
Oklahoma	US	Wet no Freeze	17	8	0	0	0	0	0	0	0	0	1.455	70
Oklahoma	US	Wet no Freeze	17	9	0.3	0	0	6	0	0	0	0	1.456	68
Oklahoma	US	Wet no Freeze	17	9	0	0	0	1	0	0	0	0	1.46	68
Oklahoma	US	Wet no Freeze	17	9	0	0	0	0	0	0	0	0	1.461	68
Oklahoma	US	Wet no Freeze	17	9	0	0	0	2	0	0	0	0	1.474	68
Oklahoma	US	Wet no Freeze	18	9	20.7	0	59.8	23	0	0	0	0	1.484	68
Oklahoma	US	Wet no Freeze	18	9	10.7	0	9.3	21	0	0	0	0	1.491	68
Oklahoma	US	Wet no Freeze	18	9	67.1	0	10.6	73	0	0	0	0	1.499	68
Oklahoma	US	Wet no Freeze	18	9	2	0	43.9	4	0	0	0	0	1.506	68
Oklahoma	US	Wet no Freeze	18	9	2.9	0	5.2	19	0	0	0	0	1.508	68
Oklahoma	US	Wet no Freeze	18	9	1.8	0	6.1	17	0	0	0	0	1.514	68
Oklahoma	US	Wet no Freeze	18	9	3.7	0	0	9	0	0	0	0	1.517	68
Oklahoma	US	Wet no Freeze	19	9	6.9	0	313.6	4	0	0	0	0	1.529	68
Oklahoma	US	Wet no Freeze	19	9	0	0	0	0	0	0	0	0	1.57	68
Oklahoma	US	Wet no Freeze	19	9	38.7	0	334.1	99	0	0	0	0	1.584	67
Oklahoma	US	Wet no Freeze	19	9	0	0	1.2	0	0	0	0	0	1.589	65
Oklahoma	US	Wet no Freeze	19	9	47	0	23	94	0	0	0	0	1.616	65
Oklahoma	US	Wet no Freeze	19	10	0	0	141.1	0	0	0	0	0	1.619	65
Oklahoma	US	Wet no Freeze	19	10	3	0	0	9	0	0	0	0	1.633	65
Oklahoma	US	Wet no Freeze	19	10	30.7	0	13.6	20	0	0	0	0	1.64	63
Oklahoma	US	Wet no Freeze	19	10	2.3	0	107.9	16	0	0	0	0	1.662	63
South Carolina	US	Wet no Freeze	20	10	0	0	13.3	11	0	0	0	0	1.674	63
South Carolina	US	Wet no Freeze	20	10	0	0	0	2	0	0	0	0	1.689	62
South Carolina	US	Wet no Freeze	20	10	0.3	0	35.6	0	0	0	0	0	1.693	62
South Carolina	US	Wet no Freeze	20	10	0	0	0	0	0	0	0	0	1.735	62
South Carolina	US	Wet no Freeze	20	10	0	0	2	2	0	0	0	0	1.791	62
South Carolina	US	Wet no Freeze	20	10	0	0	0	0	0	0	0	0	1.805	61
South Carolina	US	Wet no Freeze	20	10	8	0	3.8	13	0	0	0	0	1.807	61
South Carolina	US	Wet no Freeze	21	10	91.3	0	149.5	37	0	0	0	0	1.85	60
South Carolina	US	Wet no Freeze	21	10	0	0	137.8	39	0	0	0	0	1.858	60
South Carolina	US	Wet no Freeze	21	10	0	0	159	39	0	0	0	0	1.859	60
South Carolina	US	Wet no Freeze	21	10	6.3	0	0	10	0	0	0	0	1.867	59
South Carolina	US	Wet no Freeze	21	10	79.3	0	99.1	0	0	0	0	0	1.868	59
South Carolina	US	Wet no Freeze	21	10	97	0	46.3	119	0	0	0	0	1.87	59

South Carolina	US	Wet no Freeze	21	10	18	0	267.2	72	0	0	0	0	1.875	58
South Carolina	US	Wet no Freeze	21	10	21.9	0	12.6	20	0	0	0	0	1.875	58
South Carolina	US	Wet no Freeze	21	10	0.9	0	237.8	193	0	0	0	0	1.932	57
Tennessee	US	Wet no Freeze	21	11	11.3	0	302.7	17	0	0	0	0	1.946	57
Tennessee	US	Wet no Freeze	21	11	12.9	0	18.6	37	0	0	0	0	1.954	56
Tennessee	US	Wet no Freeze	22	11	62.5	0	4.6	121	0	0	0	0	1.981	56
Tennessee	US	Wet no Freeze	22	11	6.6	0	12.8	31	0	0	0	0	1.99	55
Tennessee	US	Wet no Freeze	22	11	0	0	153.1	1	0	0	0	0	1.993	53
Tennessee	US	Wet no Freeze	22	11	0	0	1.5	13	0	0	0	0	1.994	52
Tennessee	US	Wet no Freeze	22	11	252.4	0	152.5	18	0	0	0	0	2.006	45
Texas	US	Wet no Freeze	22	11	19.2	0	34.4	57	0	0	0	0	2.013	40
Texas	US	Wet no Freeze	22	11	1.7	0	51.7	59	0	0	0	0	2.031	40
Texas	US	Wet no Freeze	22	12	1.1	0	0	0	0	0	0	0	2.038	38
Texas	US	Wet no Freeze	23	12	252.7	0	153.1	33	0	0	0	0	2.053	36
Texas	US	Wet no Freeze	23	12	0	0	0	0	0	0	0	0	2.053	35
Texas	US	Wet no Freeze	23	12	0	0	0	1	0	0	0	0	2.078	34
Texas	US	Wet no Freeze	24	12	0	0	172.9	3	0	0	0	0	2.094	32
Texas	US	Wet no Freeze	24	12	0.2	0	0.5	0	0	0	0	0	2.103	30
Texas	US	Wet no Freeze	25	12	0	0	12.3	31	0	0	0	0	2.125	29
Texas	US	Wet no Freeze	25	12	0	0	237.6	99	0	0	0	0	2.135	27
Texas	US	Wet no Freeze	25	12	0	0	62.6	5	0	0	0	0	2.14	24
Texas	US	Wet no Freeze	25	12	0	0	169.3	134	0	0	0	0	2.169	24
Texas	US	Wet no Freeze	26	13	0	0	1.4	9	0	0	0	0	2.246	23
Texas	US	Wet no Freeze	26	13	0	0	66.5	0	0	0	0	0	2.322	23
Texas	US	Wet no Freeze	26	13	0	0	0	0	0	0	0	0	2.322	22
Texas	US	Wet no Freeze	26	13	0	0	4.9	0	0	0	0	0	2.337	20
Texas	US	Wet no Freeze	27	13	0	0	1.8	14	0	0	0	0	2.385	19
Texas	US	Wet no Freeze	27	14	0	0	0	1	0	0	0	0	2.388	19
Texas	US	Wet no Freeze	27	14	0	0	244.3	3	0	0	0	0	2.526	19
Texas	US	Wet no Freeze	28	15	0	0	4.4	19	0	0	0	0	2.54	19
Texas	US	Wet no Freeze	28	15	4.8	0	156	41	0	0	0	0	2.614	18
Texas	US	Wet no Freeze	28	15	0	0	54.2	0	0	0	0	0	2.626	18
Texas	US	Wet no Freeze	29	15	0	0	152.5	0	0	0	0	0	2.782	18
Texas	US	Wet no Freeze	31	17	0	0	116.4	6	0	0	0	0	2.868	15
Texas	US	Wet no Freeze	31	22	13.7	0	17.8	53	0	0	0	0	3.543	8
Texas	US	Wet no Freeze	31	22	0	0	8.2	23	0	0	0	0	3.758	8

Table A-2: Presents the Environmental data of each section with PCI AND IRI in the U.S. and Canada.

State /Province	Country	Climate regions	AGE	TEMP AVG	FREEZE INDEX YR	NUMBER FREEZE DAYS	TOTAL ANN PRECIP	TOTAL SNOWFALL YR	WIND AVG	HUM	IRI	PCI
Washington	US	DRY Freeze	6	8.9	247.5	82	515.3	1080	5.10	66.5	1.488	72
Washington	US	DRY Freeze	7	9.9	310	120	462.4	2371	5.20	61	1.08	69
Washington	US	DRY Freeze	8	9.7	203.6	83	397.6	826	4.80	65	1.331	71
Washington	US	DRY Freeze	15	9.6	285	128	446	1963	5.50	62	1.015	70
Washington	US	DRY Freeze	13	9.3	86.4	117	435.9	659	4.70	62.5	1.559	80
Washington	US	DRY Freeze	13	9.2	189.1	133	493.9	2105	5.50	66.5	0.989	68
Washington	US	DRY Freeze	11	9	247.4	115	581.5	638	4.70	65	1.14	65
Washington	US	DRY Freeze	10	8.9	306	127	438.1	2012	4.90	66	0.888	64
Washington	US	DRY Freeze	9	8.6	301	113	386	671	4.5	62	1.692	60
Washington	US	DRY Freeze	9	7.7	514	89	702.6	1061	4.00	62.5	1.469	59
Washington	US	DRY Freeze	8	7.7	558	133	411.9	1462	5.00	66	1.145	58
Wyoming	US	DRY Freeze	17	6.4	691	97	345.1	590	4	57.5	0.908	55
Wyoming	US	DRY Freeze	17	6.4	588.8	121	478.4	535	5.1	58	0.906	55
Wyoming	US	DRY Freeze	18	4.9	726	110	399.3	425	4.8	52	1.5	52
California	US	DRY no Freeze	32	10.5	94.1	67	369.5	43	3.90	53.5	0.819	100
California	US	DRY no Freeze	30	10.5	182	54	411	34	3.90	53.5	0.781	100
California	US	DRY no Freeze	29	10.7	132.7	68	373.9	28	3.90	54	1.606	100
California	US	DRY no Freeze	27	11.1	52.3	59	287	53	3.90	55	1.408	100
California	US	DRY no Freeze	25	11.2	36.3	77	245.5	44	3.91	55	2.379	100
California	US	DRY no Freeze	24	11.4	99	67	346.1	62	3.60	55	0.765	80
California	US	DRY no Freeze	23	11.6	109	57	228.6	35	3.89	56	0.683	95
California	US	DRY no Freeze	23	11.9	84	64	261.8	55	7.00	56	0.735	63
California	US	DRY no Freeze	21	12.1	91	54	297.4	29	5.90	56	0.754	92
California	US	DRY no Freeze	21	12.1	48	61	298.9	58	7.20	56	0.782	61
California	US	DRY no Freeze	20	12.1	62	60	344.4	79	5.20	56	0.783	62
California	US	DRY no Freeze	20	15.1	1	57	472	44	4.20	56.5	0.817	90
California	US	DRY no Freeze	19	15.5	1	78	524.5	0	4.10	57	0.82	88
California	US	DRY no Freeze	19	15.6	1	76	392.7	25	4.10	57	0.823	87
California	US	DRY no Freeze	19	15.8	1	73	272.4	105	4.10	57	0.828	83
Hawaii	US	DRY no Freeze	18	15.8	1	53	486.3	79	4.40	57	0.835	80
Hawaii	US	DRY no Freeze	18	15.9	1	69	168.4	28	4.10	57.5	0.848	80
Hawaii	US	DRY no Freeze	18	16	19.8	71	405.2	81	3.85	57.5	0.855	75
Hawaii	US	DRY no Freeze	18	16.1	1	78	433.2	0	4.10	57.5	0.874	74

Hawaii	US	DRY no Freeze	17	16.1	1	45	382.2	184	4.10	58	1.321	74
Hawaii	US	DRY no Freeze	17	16.2	3.3	72	411.8	62	5.9	58	1.408	73
Hawaii	US	DRY no Freeze	17	16.2	6.5	77	656.4	70	4.10	58	1.418	72
Hawaii	US	DRY no Freeze	16	16.2	1	63	612.3	4	3.60	58.5	1.434	70
Hawaii	US	DRY no Freeze	16	16.2	1	55	385.2	4	3.90	59	1.434	66
Hawaii	US	DRY no Freeze	16	16.3	6	78	520.3	66	7.0	59	1.473	65
Hawaii	US	DRY no Freeze	15	16.3	1	62	554.4	21	3.60	59.5	1.528	63
Hawaii	US	DRY no Freeze	15	16.4	8.5	54	244.9	85	3.84	59.5	1.544	61
Hawaii	US	DRY no Freeze	15	16.4	1	70	476.2	0	3.60	59.5	1.613	57
Hawaii	US	DRY no Freeze	15	16.6	24.6	55	353	70	3.6	60	1.636	56
Hawaii	US	DRY no Freeze	13	16.6	31.3	71	377.2	74	3.60	60	1.653	55
Hawaii	US	DRY no Freeze	13	16.6	1	46	393.2	0	3.80	60	1.67	55
New Mexico	US	DRY no Freeze	13	16.8	1	51	181.4	70	7.2	60	1.838	52
New Mexico	US	DRY no Freeze	13	16.8	9.6	62	484.2	77	3.86	60	2.113	69
New Mexico	US	DRY no Freeze	13	17	4	58	291.1	58	5.2	60.5	2.318	68
New Mexico	US	DRY no Freeze	13	17.4	33	71	189.1	28	3.84	60.5	2.332	70
New Mexico	US	DRY no Freeze	12	17.5	12	62	189	66	3.9	60.5	2.362	55
New Mexico	US	DRY no Freeze	11	17.5	3	77	217	62	3.8	60.5	2.404	81
New Mexico	US	DRY no Freeze	11	17.8	1	55	205.8	77	3.5	60.5	2.412	70
New Mexico	US	DRY no Freeze	11	17.9	3.6	65	211.7	58	3.8	60.5	2.42	54
New Mexico	US	DRY no Freeze	11	18	6.8	74	128.4	74	4.5	62	2.425	66
New Mexico	US	DRY no Freeze	11	18.1	5	71	185.1	81	5.2	62	2.441	67
New Mexico	US	DRY no Freeze	11	20.7	1	69	50.7	29	3.80	62.5	2.464	67
New Mexico	US	DRY no Freeze	10	21.4	1	58	122.3	92	3.90	62.5	2.497	67
New Mexico	US	DRY no Freeze	10	24	1	83	207.1	77	3.60	63	2.5	74
New Mexico	US	DRY no Freeze	10	24	1	65	207.1	70	3.84	68	2.525	62
New Mexico	US	DRY no Freeze	9	24.3	1	50	249.1	38	3.80	68	2.662	59
New Mexico	US	DRY no Freeze	9	24.3	1	57	256.8	74	3.83	68	0.925	59
New Mexico	US	DRY no Freeze	9	24.3	1	53	249.1	58	3.86	68	0.856	58
New Mexico	US	DRY no Freeze	9	24.4	1	51	336.2	74	3.81	68	1.369	58
New Mexico	US	DRY no Freeze	9	24.5	1	71	286.3	35	4.10	68	1.396	82
New Mexico	US	DRY no Freeze	7	24.7	1	66	361.5	55	3.80	69	1.012	58
New Mexico	US	DRY no Freeze	7	24.7	1	67	361.5	62	3.85	69	0.857	58
New Mexico	US	DRY no Freeze	7	24.8	1	66	506.6	36	4.10	69	1.31	58
New Mexico	US	DRY no Freeze	7	24.8	1	55	209.3	28	3.80	69	1.183	57
New Mexico	US	DRY no Freeze	7	24.8	1	71	506.6	66	3.84	69.5	0.88	55
New Mexico	US	DRY no Freeze	6	24.8	1	72	209.3	0	3.82	70.5	0.877	56

New Mexico	US	DRY no Freeze	5	25	1	55	737.3	37	3.90	70.5	0.862	61
New Mexico	US	DRY no Freeze	5	25.2	1	55	607.8	21	3.81	70.5	0.887	91
New Mexico	US	DRY no Freeze	3		60.4	73	68.4	66	4.10	71	0.925	50
Idaho	US	Wet Freeze	3	13.1	111	103	1157.5	1233	6.11	75	4.005	8
Idaho	US	Wet Freeze	4	13.4	203	121	993.1	2438	5.95	70	3.659	10
Idaho	US	Wet Freeze	4	12.7	65	140	1277.7	2050	5.96	75	3.519	10
Idaho	US	Wet Freeze	4	12.7	912	123	1010.7	1403	5.91	67	3.308	12
Idaho	US	Wet Freeze	4	10.5	1351.6	142	1480.2	2200	5.78	61	3.251	15
Maine	US	Wet Freeze	5	7.9	628	108	1056	2162	5.64	73	3.116	22
Idaho	US	Wet Freeze	5	9.2	461.9	139	778.1	812	3.9	69.5	3.112	23
Idaho	US	Wet Freeze	5	6.8	691	112	1208.8	1865	5.40	69.5	2.967	27
Illinois	US	Wet Freeze	5	6.7	696	115	1251.9	1850	6	60	2.275	40
Maine	US	Wet Freeze	5	11.5	275.4	118	992.5	2713	4.5	74.5	2.183	43
Michigan	US	Wet Freeze	5	10.5	435	121	1105.9	2910	4	74	1.985	44
Michigan	US	Wet Freeze	5	5.8	992	117	1282.8	1895	5.15	74	1.929	50
Michigan	US	Wet Freeze	5	12	217.4	129	1103.7	1432	3.5	68	1.929	52
Missouri	US	Wet Freeze	6	12.4	85	130	1067.7	2715	4.40	72	1.863	52
Michigan	US	Wet Freeze	6	11.5	223	142	1386	2010	4	80	1.775	52
Michigan	US	Wet Freeze	6	6.3	742	101	363.9	1876	5.00	58	1.754	55
Michigan	US	Wet Freeze	6	13.1	269.9	92	1150.4	2550	4.50	72	1.742	55
Idaho	US	Wet Freeze	6	7	673.8	89	444.6	997	4.40	57.5	1.7	58
Idaho	US	Wet Freeze	6	6.6	667	94	483.2	2721	4.50	60	1.691	58
Idaho	US	Wet Freeze	7	7.1	563	93	409.8	3367	6.60	57	1.649	59
Michigan	US	Wet Freeze	7	5.8	877	103	444.9	1083	3.60	60	1.526	60
Maine	US	Wet Freeze	7	4.4	1240	92	1499.7	2697	6.26	71	1.526	61
Michigan	US	Wet Freeze	7	7.5	664	105	747.3	1062	6.25	74.5	1.509	62
Michigan	US	Wet Freeze	7	12	137.9	112	1094.9	2516	5.1	71	1.501	66
Missouri	US	Wet Freeze	8	12.5	211	106	1193.4	1083	6	75	1.485	66
Idaho	US	Wet Freeze	8	12.3	229.4	96	1083.4	2820	3.7	80	1.473	67
Idaho	US	Wet Freeze	8	5.4	834.8	100	569.4	2952	6.60	61	1.473	67
Idaho	US	Wet Freeze	8	11.9	283	104	1113.5	2500	6.02	68	1.458	68
Idaho	US	Wet Freeze	8	8.9	482.5	104	971.7	2456	6.00	69.5	1.457	68
Missouri	US	Wet Freeze	9	7.4	557	106	1010.2	836	4	70	1.457	68
Missouri	US	Wet Freeze	9	7.7	574.7	89	892	1880	5.35	64	1.445	69
Maine	US	Wet Freeze	9	6.4	842	85	1208.3	2683	5.25	75	1.441	69
Missouri	US	Wet Freeze	9	11.3	357.3	79	1065.9	1137	5.6	69.5	1.433	69
Maine	US	Wet Freeze	9	9.7	321	73	1484	1531	5.1	74.5	1.416	69

Missouri	US	Wet Freeze	10	13.4	159.5	85	980.2	1514	4.25	64	1.399	69
Maine	US	Wet Freeze	10	6.3	481.7	103	624.9	1320	6.50	62.5	1.357	70
Maine	US	Wet Freeze	10	6.6	522.1	94	502.7	4941	6.60	63	1.309	70
Illinois	US	Wet Freeze	10	6.4	787	89	435.5	2107	3.50	57.5	1.293	70
Missouri	US	Wet Freeze	10	4.3	901	95	667.6	1137	4.10	59.5	1.278	71
Missouri	US	Wet Freeze	10	13	187	90	1329.1	1681	6.14	74.5	1.274	72
Maine	US	Wet Freeze	10	13.7	123	119	857.4	1905	6.15	76	1.274	72
Missouri	US	Wet Freeze	11	12.8	164	107	1031.1	1457	6.12	69.5	1.269	74
Michigan	US	Wet Freeze	11	12.6	208.5	91	1594	3475	5.99	65	1.257	74
Missouri	US	Wet Freeze	11	11.4	1009	109	1219.4	2363	5.86	71	1.249	75
Michigan	US	Wet Freeze	11	5.5	1242.4	95	839.6	1237	5.72	70	1.247	75
Newfoundland	Canada	Wet Freeze	11	7.4	394	111	1189.1	902	5.48	42.5	1.247	76
Newfoundland	Canada	Wet Freeze	11	7.6	699.3	87	1002.6	1112	3.8	73	1.242	76
Newfoundland	Canada	Wet Freeze	11	7.6	663.8	113	946.7	3661	5.25	76	1.242	76
Missouri	US	Wet Freeze	11	6.5	784	115	925.5	2668	4.50	75	1.235	76
Newfoundland	Canada	Wet Freeze	12	5.9	585	109	1059.1	1530	5.25	72	1.235	77
New Jersey	US	Wet Freeze	12	6.8	679	112	1293.2	1062	5	57	1.233	77
New Jersey	US	Wet Freeze	12	5.9	902	115	857.3	3047	5.8	65.5	1.23	77
Missouri	US	Wet Freeze	12	7.5	472	111	1265.3	2092	5	72	1.229	77
Newfoundland	Canada	Wet Freeze	12	10.4	399.3	118	974.9	1925	4.6	68	1.222	78
Illinois	US	Wet Freeze	13	4.8	1053	101	1525.9	3025	6.22	68	1.216	78
New Jersey	US	Wet Freeze	13	12.4	191.8	113	1297.1	2517	6.04	66	1.202	79
New Jersey	US	Wet Freeze	13	14	116.3	87	1341.9	2525	6.05	64	1.197	79
New Jersey	US	Wet Freeze	13	11.5	201	133	1770.8	1003	4.50	74	1.197	80
Newfoundland	Canada	Wet Freeze	13	5.6	946	89	933.7	3250	5.74	74.5	1.196	81
Illinois	US	Wet Freeze	14	4.5	1277	91	904	1262	5.75	59.2	1.19	81
Newfoundland	Canada	Wet Freeze	14	5.5	1304.4	93	1046.6	3275	5.76	64.5	1.177	81
New Jersey	US	Wet Freeze	14	7.3	609.5	89	1403.1	2289	4.8	72.5	1.176	81
Illinois	US	Wet Freeze	14	6.6	890.1	85	1218.2	1880	5.05	57.5	1.174	81
Illinois	US	Wet Freeze	14	10.1	425	81	1445.1	1530	4.1	82	1.167	82
New Jersey	US	Wet Freeze	14	13.4	140	93	1227.5	2952	4	69	1.151	82
Illinois	US	Wet Freeze	14	7.1	657	113	437.8	879	4.80	60.5	1.13	83
Montana	US	Wet Freeze	14	5.2	738.9	95	1513.8	2473	6.25	70	1.127	83
New Jersey	US	Wet Freeze	15	13.5	120	87	990.5	1009	5.30	67.5	1.123	83
Montana	US	Wet Freeze	15	10.7	1100	99	1312.1	2350	4.30	65	1.116	83
New Jersey	US	Wet Freeze	15	11	1079	91	1203.1	920	5.89	72	1.116	84
New Jersey	US	Wet Freeze	15	8.2	590	141	1032.4	4174	5.65	70	1.082	84

Montana	US	Wet Freeze	15	6	1472	87	886.9	2425	5.68	70.5	1.078	84
New Jersey	US	Wet Freeze	15	7.1	639	91	938.5	3374	5.5	75.5	1.074	84
Montana	US	Wet Freeze	15	6.2	881	98	997.3	2092	4.5	75	1.073	84
New Jersey	US	Wet Freeze	15	5.5	878	101	1121.7	2289	6.25	71	1.063	84
Michigan	US	Wet Freeze	15	7.7	552	102	1166.3	1274	5.38	69	1.058	84
Montana	US	Wet Freeze	15	7.6	466	105	1395.9	2456	6.4	58	1.051	84
New Jersey	US	Wet Freeze	15	7.2	518	108	1061.4	3244	6.25	72	1.043	85
Vermont	US	Wet Freeze	16	11.6	345	112	1023.3	1764	4.50	65.5	1.039	85
Montana	US	Wet Freeze	16	8.7	336	114	1299.1	2259	5.45	76	1.038	85
Montana	US	Wet Freeze	16	8.6	457.8	85	931.6	2683	5.55	66	1.031	86
Montana	US	Wet Freeze	16	9.5	467	92	1275.8	2122	4.25	69.5	1.031	86
Vermont	US	Wet Freeze	17	11.7	297	78	1480.9	930	4.5	71	1.031	87
Illinois	US	Wet Freeze	17	7.3	742	97	349.9	2907	4.90	60.5	1.03	87
Montana	US	Wet Freeze	17	4.9	1531	80	825.5	2212	5.69	67.5	1.028	87
Montana	US	Wet Freeze	17	8.5	439.5	76	1234.1	1865	5.4	63	1.025	87
Vermont	US	Wet Freeze	17	6.1	649	72	1110.2	1486	3.6	68.5	1.02	87
Vermont	US	Wet Freeze	17	10.7	409	68	1347.4	1698	4.75	65.5	1.02	87
Michigan	US	Wet Freeze	17	10.2	366.4	62	928.5	1728	5	68	1.018	88
Michigan	US	Wet Freeze	17	12.9	238	56	1307.7	2107	5.5	69.5	1.004	88
Vermont	US	Wet Freeze	17	9.3	475	50	1182.8	2021	7	74.5	0.999	88
Vermont	US	Wet Freeze	17	10.8	157	44	1559.2	940	7.25	76	0.996	89
Vermont	US	Wet Freeze	17	5.8	740	81	691.9	4280	6.70	57	0.98	89
Vermont	US	Wet Freeze	17	6.5	539.8	103	636.8	2141	6.40	62	0.973	89
Vermont	US	Wet Freeze	18	5.7	788.8	83	497.2	1004	4.30	60.5	0.965	89
Vermont	US	Wet Freeze	18	12.2	308	86	1262.5	888	5.92	67	0.961	89
Montana	US	Wet Freeze	18	13.4	117	94	1197.7	1425	5.94	73	0.954	90
Illinois	US	Wet Freeze	18	6.4	878	97	1375.1	1653	5.25	57	0.946	90
Vermont	US	Wet Freeze	18	11.1	180	104	1170.7	2330	4.25	74	0.942	90
Michigan	US	Wet Freeze	18	13.1	87	98	1222.3	2141	4.5	67.5	0.942	91
Vermont	US	Wet Freeze	18	12.2	270.5	80	1197.5	3440	4.1	75	0.942	91
Vermont	US	Wet Freeze	19	7.9	458	119	418.4	2632	4.90	57	0.939	91
Illinois	US	Wet Freeze	19	13.1	127	115	1461.4	1596	4.50	72	0.927	92
Michigan	US	Wet Freeze	19	10.8	682.1	121	1288.8	10325	3.30	67	0.924	92
Illinois	US	Wet Freeze	19	7.1	759	123	1123.8	2077	5.36	68	0.923	92
Vermont	US	Wet Freeze	19	6.5	667.1	119	1368.4	1471	3.75	61	0.906	92
Vermont	US	Wet Freeze	19	8	437	115	1352.9	2668	3.8	62	0.904	92
Illinois	US	Wet Freeze	19	11.4	226	122	1062.5	2107	4.45	71	0.899	92

Vermont	US	Wet Freeze	19	13.9	110.1	134	1254.3	890	4	66	0.898	92
Michigan	US	Wet Freeze	20	12.5	274	146	981.8	4280	5	68	0.892	92
Vermont	US	Wet Freeze	20	7.3	852.6	96	1288.5	2577	4.50	74.5	0.892	92
Michigan	US	Wet Freeze	20	4.1	637	108	1463	2801	6.21	68	0.864	93
Vermont	US	Wet Freeze	20	6.2	857.3	115	1005	1895	4.3	80	0.863	93
Vermont	US	Wet Freeze	20	10.3	755	115	1881.2	2375	3.75	61	0.859	93
Michigan	US	Wet Freeze	20	6.6	663	111	1701.5	1274	5.5	57	0.859	93
Vermont	US	Wet Freeze	20	9.8	197	105	1042.9	1334	5.6	76	0.845	93
Vermont	US	Wet Freeze	21	5.9	1185	120	1370.3	2129	6.16	69.5	0.835	93
Vermont	US	Wet Freeze	21	6.6	940	97	1375.6	2353	6.18	76	0.822	93
Vermont	US	Wet Freeze	21	14.1	123.3	124	1475.3	1561	6.06	68	0.819	93
Indiana	US	Wet Freeze	21	13.6	233	89	1569.5	2785	6.08	69	0.819	93
Vermont	US	Wet Freeze	21	8.9	580	93	833.6	2187	5.66	73	0.81	94
Michigan	US	Wet Freeze	22	6.6	807	98	655.9	1024	5.71	59.5	0.808	94
Minnesota	US	Wet Freeze	22	7.4	467.3	97	989.2	3087	5.55	75.5	0.805	94
Indiana	US	Wet Freeze	22	8.3	607	102	948.1	3824	4.7	71.5	0.803	94
Indiana	US	Wet Freeze	22	9.2	405	99	985.2	3513	5.2	70	0.796	94
Newfoundland	Canada	Wet Freeze	22	5.9	665.3	101	1050.8	1486	5	68	0.796	94
Minnesota	US	Wet Freeze	23	7.8	661	104	973.4	2259	5.5	60.5	0.792	94
Newfoundland	Canada	Wet Freeze	24	12.2	1759	87	1169.9	1310	5.79	60.5	0.787	94
Minnesota	US	Wet Freeze	25	12.3	1164.7	108	1168.3	3789	6.40	71	0.786	94
Indiana	US	Wet Freeze	26	10	287.3	89	849	2099	4.1	72	0.785	95
Minnesota	US	Wet Freeze	26	6.9	721.1	85	1424.4	2077	5.25	62.5	0.77	95
Illinois	US	Wet Freeze	26	4.7	888.4	117	1629.7	1249	5.50	69.5	0.757	95
Minnesota	US	Wet Freeze	26	6	726	120	1070.7	1698	5	80	0.756	95
Illinois	US	Wet Freeze	26	7.3	651.5	114	1059.2	1441	6.5	72	0.753	95
Michigan	US	Wet Freeze	26	7.3	477	122	781.5	1471	5.39	67.5	0.751	95
Indiana	US	Wet Freeze	26	8.8	337	124	1100.8	3949	6.1	73	0.75	95
Newfoundland	Canada	Wet Freeze	27	11.1	772.2	110	1283.7	2338	5.84	55	0.744	95
Indiana	US	Wet Freeze	28	12.5	260.6	87	1223.7	1488	6.01	58	0.734	95
Newfoundland	Canada	Wet Freeze	28	9.8	303.2	94	1143.4	2319	5	70	0.732	95
Alabama	US	Wet no Freeze	1	16.8	36	60	1329.8	0	2.8	75	0.621	100
Alabama	US	Wet no Freeze	1	14.7	3.7	0	1533.3	0	5.5	70	0.627	100
Alabama	US	Wet no Freeze	1	13.7	11	10	731.3	0	5.3	67	0.641	100
Alabama	US	Wet no Freeze	1	13.7	34	47	1381	495	3	73	0.646	100
Alabama	US	Wet no Freeze	3	13.8	25.3	0	1587.5	0	6	66	0.653	100
Alabama	US	Wet no Freeze	3	14.4	28	38	1007.9	0	4.8	69	0.67	100

Alabama	US	Wet no Freeze	3	14.5	37.2	56	1006.7	0	6.4	60.5	0.7	100
Alabama	US	Wet no Freeze	4	14.5	6.4	5	1646.4	0	5.3	70	0.702	100
Alabama	US	Wet no Freeze	4	14.6	73.2	15	1032.4	373	4.75	68	0.713	100
Alabama	US	Wet no Freeze	4	14.7	176	5	1819.8	0	5.4	73	0.716	100
Alabama	US	Wet no Freeze	5	13.3	53	15	1651.1	31	5.25	63	0.717	100
Alabama	US	Wet no Freeze	5	13.4	38	29	853	72	2.85	68	0.72	100
Alabama	US	Wet no Freeze	5	13.6	84	46	1698	0	4	61.5	0.735	100
Alabama	US	Wet no Freeze	5	12.6	32	39	2149.7	0	3.25	62.5	0.735	100
Alabama	US	Wet no Freeze	5	12.8	9.3	8	1364.5	0	5.3	66	0.749	100
Alabama	US	Wet no Freeze	5	13.2	136.9	30	1482.7	0	4.5	59	0.778	100
Arkansas	US	Wet no Freeze	5	12.1	29	43	1960.5	1	5.1	69.5	0.785	100
Arkansas	US	Wet no Freeze	5	12.3	89	20	2161.4	109	4.65	63	0.796	100
Arkansas	US	Wet no Freeze	6	12.6	3	4	1868.8	0	3.2	72	0.8	100
Arkansas	US	Wet no Freeze	6	14.8	85	55	1648	0	4.1	75	0.811	100
Arkansas	US	Wet no Freeze	6	14.8	24.8	45	1466.9	710	3.5	75	0.813	100
Arkansas	US	Wet no Freeze	6	15	23	23	455.4	0	3.75	66.5	0.815	100
Arkansas	US	Wet no Freeze	6	15	9	73	1725.9	0	4	68	0.825	100
Arkansas	US	Wet no Freeze	6	15	36.3	0	1030	742	4.5	70	0.834	100
California	US	Wet no Freeze	6	15.1	48.2	66	1805.7	515	3.9	65.5	0.84	96
California	US	Wet no Freeze	6	15.2	115	68	1491.9	0	5.3	68	0.847	90
California	US	Wet no Freeze	6	15.3	4.1	35	806.5	410	7.3	59	0.847	89
California	US	Wet no Freeze	6	15.3	7	25	1499.4	0	5.1	67.5	0.869	89
California	US	Wet no Freeze	7	15.3	8.9	0	1325.5	44	7.3	64.5	0.871	89
California	US	Wet no Freeze	7	15.4	5.8	41	1236.7	33	3.5	69	1.364	89
California	US	Wet no Freeze	7	15.4	69	36	1473.3	223	5.5	66.5	1.363	88
California	US	Wet no Freeze	7	15.2	6	69	646.9	0	3	55	1.352	88
California	US	Wet no Freeze	7	15.2	6	64	1007.3	7	5.5	67	1.352	88
California	US	Wet no Freeze	7	16.1	82	36	1291.7	0	5.25	70	1.352	88
California	US	Wet no Freeze	7	16.1	102	4	1510	0	6.25	66	1.319	88
Florida	US	Wet no Freeze	7	16.1	10.8	5	1457.1	6	5	61.5	1.302	88
Florida	US	Wet no Freeze	7	16.3	31.1	53	965.7	0	3.2	55	1.287	87
Florida	US	Wet no Freeze	7	16.3	89	53	1418.8	0	4.3	67.5	1.269	87
Florida	US	Wet no Freeze	7	16.3	14.6	44	1209.3	44	4.15	63	1.267	87
Florida	US	Wet no Freeze	7	16.4	45	0	1663.3	0	6.4	66	1.249	87
Florida	US	Wet no Freeze	7	16.4	33.3	64	1501	367	6.2	65	1.246	87
Florida	US	Wet no Freeze	7	15.9	20.7	21	1099.8	7	3	68	1.196	87
Florida	US	Wet no Freeze	7	15.9	14	45	1574.1	19	4.6	73	1.176	87

Florida	US	Wet no Freeze	8	15.9	73.2	0	1050	0	6	38	1.164	87
Florida	US	Wet no Freeze	8	16	172	0	1042.9	0	4.7	74	1.154	87
Florida	US	Wet no Freeze	8	16	32	36	1554.9	0	5.1	70	1.15	86
Florida	US	Wet no Freeze	8	15.4	10	0	648.8	0	4.8	64	1.15	86
Florida	US	Wet no Freeze	8	15.4	88.5	0	861.8	0	5.8	67.5	1.136	86
Florida	US	Wet no Freeze	9	15.5	8	0	884.5	0	6	60.5	1.123	86
Florida	US	Wet no Freeze	9	15.5	83	24	548.3	0	2.7	54	1.12	86
Florida	US	Wet no Freeze	9	15.6	20.7	51	1525.4	315	3.7	68	1.113	85
Florida	US	Wet no Freeze	9	15.7	18	0	1096.4	8	4	67	1.11	85
Florida	US	Wet no Freeze	9	15.7	44.6	53	1823.5	91	4.75	70	1.108	85
Florida	US	Wet no Freeze	9	15.7	43	76	1658.6	52	4.5	65	1.108	85
Florida	US	Wet no Freeze	9	15.7	10	44	1357.1	229	6	66	1.104	85
Florida	US	Wet no Freeze	9	15.8	64	45	1243.6	661	3	67	1.104	84
Florida	US	Wet no Freeze	9	16.7	6.4	20	1375.9	0	4.8	69	1.104	84
Florida	US	Wet no Freeze	9	16.7	13.3	54	1511.4	655	5.3	66.5	1.104	84
Florida	US	Wet no Freeze	10	16.8	8	0	1552.8	0	6	63	1.103	84
Florida	US	Wet no Freeze	10	16.5	46	80	1340.8	8	4	62.5	1.098	83
Florida	US	Wet no Freeze	10	16.5	8.2	29	1003.7	0	5	66	1.093	83
Florida	US	Wet no Freeze	10	16.6	34	39	1220.9	0	3.3	70	1.093	83
Florida	US	Wet no Freeze	10	16.6	10.3	63	1514.4	417	3.1	70	1.088	83
Florida	US	Wet no Freeze	10	16.6	19	54	1691.3	25	2.75	59.5	1.085	83
Florida	US	Wet no Freeze	10	16.7	17.9	52	357.5	6	3.25	70	1.081	83
Florida	US	Wet no Freeze	11	16.7	8.9	45	1622.8	0	2.9	65.5	1.078	83
Florida	US	Wet no Freeze	11	16.4	43.8	0	1049.8	0	5.95	73	1.074	83
Florida	US	Wet no Freeze	11	16.4	35	55	679	456	7.1	64	1.074	83
Florida	US	Wet no Freeze	11	17.4	143	74	1809.9	7	3	68.5	1.068	83
Florida	US	Wet no Freeze	11	17.6	79.5	0	676.4	0	5.4	68	1.064	83
Florida	US	Wet no Freeze	11	17.7	27.8	0	1283.3	0	5.3	58	1.064	83
Florida	US	Wet no Freeze	11	17.7	3.3	0	1283.3	0	5.8	58	1.062	83
Florida	US	Wet no Freeze	11	17.1	14	35	1222.1	47	5	70	1.061	82
Florida	US	Wet no Freeze	11	17.1	4	20	1180.4	0	3.1	61.5	1.052	82
Georgia	US	Wet no Freeze	12	17.2	8	32	575	0	2.45	59	1.05	82
Georgia	US	Wet no Freeze	12	17.3	82	41	1146.3	682	6	54	1.045	82
Hawaii	US	Wet no Freeze	12	17.3	28	0	1790.2	0	4.25	67	1.041	82
Hawaii	US	Wet no Freeze	12	17.3	8	47	1786	345	4	72	1.008	82
Hawaii	US	Wet no Freeze	12	17.3	26.2	44	1786	0	5.5	37	1.005	82
Hawaii	US	Wet no Freeze	12	17.3	49	25	1146.3	661	5.35	64.5	1.002	82

Hawaii	US	Wet no Freeze	12	17.4	52	29	1600.2	1	3.2	64	0.998	82
Hawaii	US	Wet no Freeze	12	16.8	36	52	1329.8	0	2.5	74	0.994	82
Hawaii	US	Wet no Freeze	12	16.8	4	29	573.4	0	5.5	58	0.988	81
Hawaii	US	Wet no Freeze	13	17	8.6	0	1590.1	229	2.8	67	0.985	81
Hawaii	US	Wet no Freeze	13	17	4	55	1581.4	0	5.8	71	0.97	81
Hawaii	US	Wet no Freeze	13	17	6	41	1581.4	25	5.3	71	0.969	81
Hawaii	US	Wet no Freeze	13	17	8.6	45	1526.8	274	2.5	75	0.96	80
Hawaii	US	Wet no Freeze	13	18.2	106	56	3708.8	229	3	72	0.959	80
Hawaii	US	Wet no Freeze	13	18.3	12	25	4661.1	0	4.5	72	0.952	79
Hawaii	US	Wet no Freeze	13	18.4	108	48	1172.2	0	5.5	68.5	0.951	78
Hawaii	US	Wet no Freeze	13	18.5	31.8	30	1555.8	15	2.6	65	0.949	78
Hawaii	US	Wet no Freeze	13	18.5	185	70	4916.9	0	2.75	68	0.948	78
Mississippi	US	Wet no Freeze	13	18.6	29.8	66	3397.7	0	3.1	73	0.947	77
Mississippi	US	Wet no Freeze	13	18.1	94	20	1441.9	0	4.25	69	0.944	77
Mississippi	US	Wet no Freeze	14	18.2	18.2	43	1103	31	6.35	62	0.938	76
Mississippi	US	Wet no Freeze	14	18.2	17.7	41	1675.7	373	5.25	70	0.926	76
Mississippi	US	Wet no Freeze	14	18.2	45.1	0	1254.8	0	7.8	62	0.918	76
Mississippi	US	Wet no Freeze	14	17.8	0.7	53	1268	0	4.5	70	0.912	75
Mississippi	US	Wet no Freeze	15	17.8	2.1	53	1268	33	4.2	72	0.906	75
Mississippi	US	Wet no Freeze	15	17.9	3	74	1259.6	12	3.1	67	0.906	75
Mississippi	US	Wet no Freeze	15	18	124.6	0	950.9	0	5.3	67	0.894	75
Mississippi	US	Wet no Freeze	15	18	123	52	464.7	51	4.1	66	0.884	74
Mississippi	US	Wet no Freeze	15	18	65.5	32	1439.1	245	2.45	70.5	0.877	74
Mississippi	US	Wet no Freeze	15	18.1	0	82	1175.9	256	5.2	61.5	1.366	74
Mississippi	US	Wet no Freeze	15	19	9	1	875.2	0	2.8	62.5	1.38	74
Mississippi	US	Wet no Freeze	16	19	15	0	875.2	0	3.3	62.5	1.383	74
Mississippi	US	Wet no Freeze	16	19.1	2	54	2876.2	18	5.25	69	1.387	74
Mississippi	US	Wet no Freeze	16	19.1	0.2	20	1547.9	33	5.1	68	1.393	73
Mississippi	US	Wet no Freeze	16	19.2	32	29	1378.8	816	7.5	61.5	1.402	73
North Carolina	US	Wet no Freeze	16	19.4	6.3	0	1192.1	0	5.2	69	1.418	73
North Carolina	US	Wet no Freeze	16	19.6	9	51	1420.1	345	2.85	62	1.418	73
North Carolina	US	Wet no Freeze	16	19.6	3.4	53	1420.1	109	3.15	63	1.422	71
North Carolina	US	Wet no Freeze	17	18.6	13	87	1318.9	0	4.1	62.5	1.429	71
North Carolina	US	Wet no Freeze	17	18.6	12.7	35	1267.7	109	4.7	69.5	1.433	70
North Carolina	US	Wet no Freeze	17	18.7	33	64	1523.6	0	3.7	69.5	1.444	70
Oklahoma	US	Wet no Freeze	17	18.7	93	34	1390.5	57	4.5	64	1.45	70
Oklahoma	US	Wet no Freeze	17	18.8	20	3	938	0	2.5	65	1.451	70

Oklahoma	US	Wet no Freeze	17	18.9	0.4	63	3644.6	564	4.6	67.5	1.454	70
Oklahoma	US	Wet no Freeze	17	18.9	15	41	4053.6	91	4	69	1.455	70
Oklahoma	US	Wet no Freeze	17	18.6	20	55	1235.6	77	7	61.5	1.455	70
Oklahoma	US	Wet no Freeze	17	20.4	71.4	51	1480.9	0	5.15	68	1.456	68
Oklahoma	US	Wet no Freeze	17	20.4	0.6	41	1480.9	91	3.8	63.5	1.46	68
Oklahoma	US	Wet no Freeze	17	20.7	12	0	2774.4	0	3.95	71	1.461	68
Oklahoma	US	Wet no Freeze	17	20.8	172	63	2210.6	0	2.5	43.5	1.474	68
Oklahoma	US	Wet no Freeze	18	20.9	22.3	63	1920.6	0	4.6	68	1.484	68
Oklahoma	US	Wet no Freeze	18	20	55	46	1501.3	0	5.75	61.5	1.491	68
Oklahoma	US	Wet no Freeze	18	20	5.8	73	1501.3	0	7.1	68	1.499	68
Oklahoma	US	Wet no Freeze	18	20.1	73	74	1156.5	209	6.25	65.5	1.506	68
Oklahoma	US	Wet no Freeze	18	20.1	158	64	1156.5	95	5.8	60.5	1.508	68
Oklahoma	US	Wet no Freeze	18	20.1	1	20	1497.7	816	2.5	68	1.514	68
Oklahoma	US	Wet no Freeze	18	20.1	80	36	1497.7	682	3.3	68	1.517	68
Oklahoma	US	Wet no Freeze	19	20.2	42.3	0	1162.1	0	6	68	1.529	68
Oklahoma	US	Wet no Freeze	19	19.6	42	33	1048.7	0	3.25	64.5	1.57	68
Oklahoma	US	Wet no Freeze	19	19.8	81	37	1451.8	254	6	70	1.584	67
Oklahoma	US	Wet no Freeze	19	19.8	7	66	1451.8	419	5.5	67	1.589	65
Oklahoma	US	Wet no Freeze	19	19.9	8	0	695.1	0	3.1	68	1.616	65
Oklahoma	US	Wet no Freeze	19	21.8	11	41	1420.2	28	7.8	62.5	1.619	65
Oklahoma	US	Wet no Freeze	19	21.9	113	66	986.1	0	5.25	54	1.633	65
Oklahoma	US	Wet no Freeze	19	22	10	65	1024.4	916	4	67	1.64	63
Oklahoma	US	Wet no Freeze	19	22.1	51	35	1151.8	6	4.5	72.5	1.662	63
South Carolina	US	Wet no Freeze	20	22.2	9.5	48	1474.9	548	4.4	70	1.674	63
South Carolina	US	Wet no Freeze	20	22.3	7.3	0	732.1	0	5.8	69	1.689	62
South Carolina	US	Wet no Freeze	20	22.4	39	41	1890.5	0	4.5	74	1.693	62
South Carolina	US	Wet no Freeze	20	22.5	11	46	1077.3	6	3.5	61.5	1.735	62
South Carolina	US	Wet no Freeze	20	22.5	7.2	51	1163.9	15	6	62	1.791	62
South Carolina	US	Wet no Freeze	20	21.5	1	55	1516.1	415	6	68	1.805	61
South Carolina	US	Wet no Freeze	20	21.5	107	74	1041.7	0	2.5	68	1.807	61
South Carolina	US	Wet no Freeze	21	21.5	6	3	725.3	0	3.1	70	1.85	60
South Carolina	US	Wet no Freeze	21	21.6	19	5	886.1	0	4.5	65.5	1.858	60
South Carolina	US	Wet no Freeze	21	21.6	0.7	0	886.1	0	4.9	65.5	1.859	60
South Carolina	US	Wet no Freeze	21	21.7	44	32	1195.8	8	6	70.5	1.867	59
South Carolina	US	Wet no Freeze	21	21.7	61.5	87	965.5	0	5.3	67	1.868	59
South Carolina	US	Wet no Freeze	21	21.1	85	29	1213.9	373	3	67	1.87	59
South Carolina	US	Wet no Freeze	21	21.1	17.9	54	2227.5	268	2.5	67.5	1.875	58

South Carolina	US	Wet no Freeze	21	21.2	16	20	1107.2	91	6.8	62.5	1.875	58
South Carolina	US	Wet no Freeze	21	21.4	10	66	2620.7	736	4.25	69	1.932	57
Tennessee	US	Wet no Freeze	21	22.8	61	41	1145.6	31	5.25	69	1.946	57
Tennessee	US	Wet no Freeze	21	22.9	29	65	1401.6	18	6	64	1.954	56
Tennessee	US	Wet no Freeze	22	23.1	71	29	1480	456	2.75	67	1.981	56
Tennessee	US	Wet no Freeze	22	23.2	19	73	1663.6	0	4.85	63.5	1.99	55
Tennessee	US	Wet no Freeze	22	23.5	57	43	908.7	0	4.5	64.5	1.993	53
Tennessee	US	Wet no Freeze	22	23.6	4.1	53	1461.7	109	4.25	77	1.994	52
Tennessee	US	Wet no Freeze	22	23.6	3	35	1268.7	0	5.25	69.5	2.006	45
Texas	US	Wet no Freeze	22	22.7	5.9	48	1182.4	0	3.1	68.5	2.013	40
Texas	US	Wet no Freeze	22	22.8	28	0	765	0	4.2	67.5	2.031	40
Texas	US	Wet no Freeze	22	24.1	56.7	35	979.3	0	3.35	69.5	2.038	38
Texas	US	Wet no Freeze	23	24.1	19	74	1287	0	6.7	68	2.053	36
Texas	US	Wet no Freeze	23	24.3	21.2	48	1589.1	32	6.1	62.5	2.053	35
Texas	US	Wet no Freeze	23	24.6	60	70	895.5	781	5.4	59.5	2.078	34
Texas	US	Wet no Freeze	24	24	43	51	1661	0	5.4	70	2.094	32
Texas	US	Wet no Freeze	24	24.1	6	15	897.9	0	3.2	69.5	2.103	30
Texas	US	Wet no Freeze	25	23.8	0.7	30	992.8	0	4.25	65.5	2.125	29
Texas	US	Wet no Freeze	25	23.8	94.2	41	954.6	373	3.75	69	2.135	27
Texas	US	Wet no Freeze	25	23.9	3	53	1167.1	0	6.2	63	2.14	24
Texas	US	Wet no Freeze	25	23.7	10	71	792.7	682	4	66	2.169	24
Texas	US	Wet no Freeze	26	24.7	21.7	64	977.7	77	3.6	67	2.246	23
Texas	US	Wet no Freeze	26	24.6	38.1	46	1377.4	6	6.25	68.5	2.322	23
Texas	US	Wet no Freeze	26	24.6	43	87	1123.1	91	3.7	63	2.322	22
Texas	US	Wet no Freeze	26	24.7	3.4	32	1420.2	615	5.5	67.5	2.337	20
Texas	US	Wet no Freeze	27	24.7	13	41	1166.3	109	3.8	69.5	2.385	19
Texas	US	Wet no Freeze	27	24.8	21	56	918	0	3	62	2.388	19
Texas	US	Wet no Freeze	27	24.9	5	35	1064.9	0	3.1	69.5	2.526	19
Texas	US	Wet no Freeze	28	25.2	1	50	743.9	102	3.75	61.5	2.54	19
Texas	US	Wet no Freeze	28	25	1	0	941.1	0	4	66	2.614	18
Texas	US	Wet no Freeze	28	25	69	23	1397.9	0	4	59	2.626	18
Texas	US	Wet no Freeze	29	25	4	20	959.6	0	4.1	60.5	2.782	18
Texas	US	Wet no Freeze	31	25.5	5	84	1153.1	373	4.5	65	2.868	15
Texas	US	Wet no Freeze	31	25.5	50.8	74	1377.5	425	2.65	62.5	3.543	8
Texas	US	Wet no Freeze	31	25.6	10	1	963.6	0	4	64.5	3.758	8

Table A-3: Presents the Traffic volume data of each section with PCI AND IRI in the U.S. and Canada.

State /Province	Country	Climate regions	AGE	ESAL	AADTT	AADT	IRI	PCI
Washington	US	DRY Freeze	6	6844	46	16790	1.488	72
Washington	US	DRY Freeze	7	6888	53	19398	1.08	69
Washington	US	DRY Freeze	8	6913	54	19710	1.331	71
Washington	US	DRY Freeze	15	5325	42	15330	1.015	70
Washington	US	DRY Freeze	13	7616	53	6466	1.559	80
Washington	US	DRY Freeze	13	9975	77	28105	0.989	68
Washington	US	DRY Freeze	11	7074	56	20440	1.14	65
Washington	US	DRY Freeze	10	5044	41	14965	0.888	64
Washington	US	DRY Freeze	9	47446	182	66430	1.692	60
Washington	US	DRY Freeze	9	7300	57	20805	1.469	59
Washington	US	DRY Freeze	8	6957	55	20075	1.145	58
Wyoming	US	DRY Freeze	17	47803	183	66978	0.908	55
Wyoming	US	DRY Freeze	17	43304	167	60955	0.906	55
Wyoming	US	DRY Freeze	18	41420	160	24320	1.5	52
California	US	DRY no Freeze	32	85797	426	155490	0.819	100
California	US	DRY no Freeze	30	6028	16	5856	0.781	100
California	US	DRY no Freeze	29	739530	1938	591090	1.606	100
California	US	DRY no Freeze	27	720372	2865	263580	1.408	100
California	US	DRY no Freeze	25	5000	15	5475	2.379	100
California	US	DRY no Freeze	24	57728	166	60590	0.765	80
California	US	DRY no Freeze	23	59670	165	60225	0.683	95
California	US	DRY no Freeze	23	26455	154	56210	0.735	63
California	US	DRY no Freeze	21	156578	381	139065	0.754	92
California	US	DRY no Freeze	21	18155	953	347845	0.782	61
California	US	DRY no Freeze	20	718404	2865	1045725	0.783	62
California	US	DRY no Freeze	20	36000	202	73730	0.817	90
California	US	DRY no Freeze	19	95010	330	120780	0.82	88
California	US	DRY no Freeze	19	23520	496	38192	0.823	87
California	US	DRY no Freeze	19	33921	200	73200	0.828	83
Hawaii	US	DRY no Freeze	18	42555	208	75920	0.835	80
Hawaii	US	DRY no Freeze	18	91489	309	113094	0.848	80
Hawaii	US	DRY no Freeze	18	46920	139	46704	0.855	75
Hawaii	US	DRY no Freeze	18	139437	689	251485	0.874	74
Hawaii	US	DRY no Freeze	17	1028796	2237	816505	1.321	74
Hawaii	US	DRY no Freeze	17	67105	194	70810	1.408	73

Hawaii	US	DRY no Freeze	17	40000	55	20130	1.418	72
Hawaii	US	DRY no Freeze	16	57856	167	60955	1.434	70
Hawaii	US	DRY no Freeze	16	13954	37	13505	1.434	66
Hawaii	US	DRY no Freeze	16	528717	2106	768690	1.473	65
Hawaii	US	DRY no Freeze	15	21243	49	17885	1.528	63
Hawaii	US	DRY no Freeze	15	32127	187	68255	1.544	61
Hawaii	US	DRY no Freeze	15	440321	1752	639480	1.613	57
Hawaii	US	DRY no Freeze	15	26000	84	30660	1.636	56
Hawaii	US	DRY no Freeze	13	95570	309	113094	1.653	55
Hawaii	US	DRY no Freeze	13	570867	2278	831470	1.67	55
New Mexico	US	DRY no Freeze	13	115252	354	129210	1.838	52
New Mexico	US	DRY no Freeze	13	70938	270	98820	2.113	69
New Mexico	US	DRY no Freeze	13	67518	172	62780	2.318	68
New Mexico	US	DRY no Freeze	13	12585	31	11315	2.332	70
New Mexico	US	DRY no Freeze	12	179040	452	164980	2.362	55
New Mexico	US	DRY no Freeze	11	183332	909	331785	2.404	81
New Mexico	US	DRY no Freeze	11	181861	459	167535	2.412	70
New Mexico	US	DRY no Freeze	11	158008	373	136145	2.42	54
New Mexico	US	DRY no Freeze	11	44000	229	83585	2.425	66
New Mexico	US	DRY no Freeze	11	123355	612	223380	2.441	67
New Mexico	US	DRY no Freeze	11	4851	11	4015	2.464	67
New Mexico	US	DRY no Freeze	10	754004	3000	1098000	2.497	67
New Mexico	US	DRY no Freeze	10	1028796	2237	816505	2.5	74
New Mexico	US	DRY no Freeze	10	33284	197	71905	2.525	62
New Mexico	US	DRY no Freeze	9	194089	490	178850	2.662	59
New Mexico	US	DRY no Freeze	9	86049	297	108405	0.925	59
New Mexico	US	DRY no Freeze	9	109000	481	175565	0.856	58
New Mexico	US	DRY no Freeze	9	889578	3538	1294908	1.369	58
New Mexico	US	DRY no Freeze	9	40000	252	92232	1.396	82
New Mexico	US	DRY no Freeze	7	807427	3216	1173840	1.012	58
New Mexico	US	DRY no Freeze	7	29000	157	57305	0.857	58
New Mexico	US	DRY no Freeze	7	751944	3000	1095000	1.31	58
New Mexico	US	DRY no Freeze	7	119267	594	216810	1.183	57
New Mexico	US	DRY no Freeze	7	1085824	2361	861765	0.88	55
New Mexico	US	DRY no Freeze	6	43646	214	78324	0.877	56
New Mexico	US	DRY no Freeze	5	48585	138	50370	0.862	61
New Mexico	US	DRY no Freeze	5	38000	210	76650	0.887	91

New Mexico	US	DRY no Freeze	3	78000	239	87474	0.925	50
Idaho	US	Wet Freeze	3	116880	468	170820	4.005	8
Idaho	US	Wet Freeze	4	128000	567	206955	3.659	10
Idaho	US	Wet Freeze	4	82000	375	137250	3.519	10
Idaho	US	Wet Freeze	4	411658	1320	481800	3.308	12
Idaho	US	Wet Freeze	4	32534	160	58560	3.251	15
Maine	US	Wet Freeze	5	76000	262	95630	3.116	22
Idaho	US	Wet Freeze	5	68948	195	71175	3.112	23
Idaho	US	Wet Freeze	5	247218	1178	429970	2.967	27
Illinois	US	Wet Freeze	5	285000	776	283240	2.275	40
Maine	US	Wet Freeze	5	75000	224	81760	2.183	43
Michigan	US	Wet Freeze	5	45000	187	68442	1.985	44
Michigan	US	Wet Freeze	5	69058	220	80300	1.929	50
Michigan	US	Wet Freeze	5	73361	480	175200	1.929	52
Missouri	US	Wet Freeze	6	52000	207	75762	1.863	52
Michigan	US	Wet Freeze	6	17527	126	45990	1.775	52
Michigan	US	Wet Freeze	6	244112	760	277400	1.754	55
Michigan	US	Wet Freeze	6	40000	217	79205	1.742	55
Idaho	US	Wet Freeze	6	79690	212	77380	1.7	58
Idaho	US	Wet Freeze	6	75515	199	72635	1.691	58
Idaho	US	Wet Freeze	7	61816	290	105850	1.649	59
Michigan	US	Wet Freeze	7	70314	224	81760	1.526	60
Maine	US	Wet Freeze	7	115000	525	191625	1.526	61
Michigan	US	Wet Freeze	7	119811	480	72960	1.509	62
Michigan	US	Wet Freeze	7	64576	172	62780	1.501	66
Missouri	US	Wet Freeze	8	358207	1150	419750	1.485	66
Idaho	US	Wet Freeze	8	99327	395	144175	1.473	67
Idaho	US	Wet Freeze	8	265640	1254	457710	1.473	67
Idaho	US	Wet Freeze	8	449377	1437	524505	1.458	68
Idaho	US	Wet Freeze	8	48454	188	68620	1.457	68
Missouri	US	Wet Freeze	9	53564	151	55115	1.457	68
Missouri	US	Wet Freeze	9	576006	1843	672695	1.445	69
Maine	US	Wet Freeze	9	111602	446	162790	1.441	69
Missouri	US	Wet Freeze	9	207420	644	235704	1.433	69
Maine	US	Wet Freeze	9	557444	1782	652212	1.416	69
Missouri	US	Wet Freeze	10	72646	189	46116	1.399	69
Maine	US	Wet Freeze	10	142000	450	164250	1.357	70

Maine	US	Wet Freeze	10	35000	158	57828	1.309	70
Illinois	US	Wet Freeze	10	79795	214	78324	1.293	70
Missouri	US	Wet Freeze	10	88762	282	103212	1.278	71
Missouri	US	Wet Freeze	10	355999	1914	698610	1.274	72
Maine	US	Wet Freeze	10	363255	1700	620500	1.274	72
Missouri	US	Wet Freeze	11	96000	290	105850	1.269	74
Michigan	US	Wet Freeze	11	69445	450	164250	1.257	74
Missouri	US	Wet Freeze	11	60718	220	80300	1.249	75
Michigan	US	Wet Freeze	11	38000	208	75920	1.247	75
Newfoundland	Canada	Wet Freeze	11	274319	1250	456250	1.247	76
Newfoundland	Canada	Wet Freeze	11	111602	446	162790	1.242	76
Newfoundland	Canada	Wet Freeze	11	87439	564	53580	1.242	76
Missouri	US	Wet Freeze	11	82000	375	136875	1.235	76
Newfoundland	Canada	Wet Freeze	12	58586	210	76860	1.235	77
New Jersey	US	Wet Freeze	12	39000	212	77380	1.233	77
New Jersey	US	Wet Freeze	12	89000	405	148230	1.23	77
Missouri	US	Wet Freeze	12	92000	348	127020	1.229	77
Newfoundland	Canada	Wet Freeze	12	67139	469	171654	1.222	78
Illinois	US	Wet Freeze	13	91659	292	106580	1.216	78
New Jersey	US	Wet Freeze	13	326409	1609	587285	1.202	79
New Jersey	US	Wet Freeze	13	31167	130	47450	1.197	79
New Jersey	US	Wet Freeze	13	399412	1280	467200	1.197	80
Newfoundland	Canada	Wet Freeze	13	379224	1210	442860	1.196	81
Illinois	US	Wet Freeze	14	53000	286	104390	1.19	81
Newfoundland	Canada	Wet Freeze	14	55046	155	56575	1.177	81
New Jersey	US	Wet Freeze	14	354698	1615	591090	1.176	81
Illinois	US	Wet Freeze	14	107000	330	120780	1.174	81
Illinois	US	Wet Freeze	14	239049	1167	425955	1.167	82
New Jersey	US	Wet Freeze	14	143255	446	162790	1.151	82
Illinois	US	Wet Freeze	14	527140	1690	616850	1.13	83
Montana	US	Wet Freeze	14	47000	247	90402	1.127	83
New Jersey	US	Wet Freeze	15	61737	168	61488	1.123	83
Montana	US	Wet Freeze	15	377683	1860	680760	1.116	83
New Jersey	US	Wet Freeze	15	76000	338	123370	1.116	84
New Jersey	US	Wet Freeze	15	102000	465	169725	1.082	84
Montana	US	Wet Freeze	15	313696	1430	521950	1.078	84
New Jersey	US	Wet Freeze	15	105518	420	153720	1.074	84

Montana	US	Wet Freeze	15	210707	656	239440	1.073	84
New Jersey	US	Wet Freeze	15	361781	1160	423400	1.063	84
Michigan	US	Wet Freeze	15	226712	1146	418290	1.058	84
Montana	US	Wet Freeze	15	260840	1190	434350	1.051	84
New Jersey	US	Wet Freeze	15	396627	1270	463550	1.043	85
Vermont	US	Wet Freeze	16	163000	473	172645	1.039	85
Montana	US	Wet Freeze	16	154000	705	257325	1.038	85
Montana	US	Wet Freeze	16	76000	305	111325	1.031	86
Montana	US	Wet Freeze	16	122881	657	239805	1.031	86
Vermont	US	Wet Freeze	17	91000	379	138335	1.031	87
Illinois	US	Wet Freeze	17	100474	602	219730	1.03	87
Montana	US	Wet Freeze	17	41132	200	73000	1.028	87
Montana	US	Wet Freeze	17	114847	457	167262	1.025	87
Vermont	US	Wet Freeze	17	108752	435	158775	1.02	87
Vermont	US	Wet Freeze	17	79000	248	90768	1.02	87
Michigan	US	Wet Freeze	17	117000	404	147460	1.018	88
Michigan	US	Wet Freeze	17	478022	1530	558450	1.004	88
Vermont	US	Wet Freeze	17	146456	586	213890	0.999	88
Vermont	US	Wet Freeze	17	190000	597	217905	0.996	89
Vermont	US	Wet Freeze	17	182000	565	206225	0.98	89
Vermont	US	Wet Freeze	17	83664	483	176778	0.973	89
Vermont	US	Wet Freeze	18	157388	490	178850	0.965	89
Vermont	US	Wet Freeze	18	70628	225	82125	0.961	89
Montana	US	Wet Freeze	18	102018	325	118625	0.954	90
Illinois	US	Wet Freeze	18	201071	626	228490	0.946	90
Vermont	US	Wet Freeze	18	118752	474	173484	0.942	90
Michigan	US	Wet Freeze	18	141000	402	147132	0.942	91
Vermont	US	Wet Freeze	18	106616	424	154760	0.942	91
Vermont	US	Wet Freeze	19	561114	1799	242865	0.939	91
Illinois	US	Wet Freeze	19	116880	468	170820	0.927	92
Michigan	US	Wet Freeze	19	303828	1380	505080	0.924	92
Illinois	US	Wet Freeze	19	58000	205	74825	0.923	92
Vermont	US	Wet Freeze	19	45964	170	62050	0.906	92
Vermont	US	Wet Freeze	19	158030	492	179580	0.904	92
Illinois	US	Wet Freeze	19	169000	528	193248	0.899	92
Vermont	US	Wet Freeze	19	72190	200	73000	0.898	92
Michigan	US	Wet Freeze	20	174000	530	193450	0.892	92

Vermont	US	Wet Freeze	20	75542	240	87840	0.892	92
Michigan	US	Wet Freeze	20	123386	392	143472	0.864	93
Vermont	US	Wet Freeze	20	84165	542	197830	0.863	93
Vermont	US	Wet Freeze	20	16151	80	29200	0.859	93
Michigan	US	Wet Freeze	20	19520	98	21756	0.859	93
Vermont	US	Wet Freeze	20	278400	1269	463185	0.845	93
Vermont	US	Wet Freeze	21	119282	380	138700	0.835	93
Vermont	US	Wet Freeze	21	69058	220	80300	0.822	93
Vermont	US	Wet Freeze	21	50000	202	73730	0.819	93
Indiana	US	Wet Freeze	21	60805	172	62780	0.819	93
Vermont	US	Wet Freeze	21	34485	184	67160	0.81	94
Michigan	US	Wet Freeze	22	232000	633	231045	0.808	94
Minnesota	US	Wet Freeze	22	65481	299	109135	0.805	94
Indiana	US	Wet Freeze	22	48000	217	79205	0.803	94
Indiana	US	Wet Freeze	22	234450	1149	419385	0.796	94
Newfoundland	Canada	Wet Freeze	22	343282	1592	581080	0.796	94
Minnesota	US	Wet Freeze	23	73391	481	175565	0.792	94
Newfoundland	Canada	Wet Freeze	24	15432	78	28470	0.787	94
Minnesota	US	Wet Freeze	25	125210	668	142284	0.786	94
Indiana	US	Wet Freeze	26	420395	1343	491538	0.785	95
Minnesota	US	Wet Freeze	26	94798	302	110230	0.77	95
Illinois	US	Wet Freeze	26	80672	257	93805	0.757	95
Minnesota	US	Wet Freeze	26	52677	195	32175	0.756	95
Illinois	US	Wet Freeze	26	579222	1854	676710	0.753	95
Michigan	US	Wet Freeze	26	48089	167	60955	0.751	95
Indiana	US	Wet Freeze	26	253309	1189	435174	0.75	95
Newfoundland	Canada	Wet Freeze	27	141000	645	236070	0.744	95
Indiana	US	Wet Freeze	28	17272	82	30012	0.734	95
Newfoundland	Canada	Wet Freeze	28	108500	433	158045	0.732	95
Alabama	US	Wet no Freeze	1	14582	85	31025	0.621	100
Alabama	US	Wet no Freeze	1	74419	235	86010	0.627	100
Alabama	US	Wet no Freeze	1	163000	472	172280	0.641	100
Alabama	US	Wet no Freeze	1	266000	991	361715	0.646	100
Alabama	US	Wet no Freeze	3	22707	173	61415	0.653	100
Alabama	US	Wet no Freeze	3	195000	413	150745	0.67	100
Alabama	US	Wet no Freeze	3	69941	224	81760	0.7	100

Alabama	US	Wet no Freeze	4	69941	224	81760	0.702	100
Alabama	US	Wet no Freeze	4	24375	146	53290	0.713	100
Alabama	US	Wet no Freeze	4	43610	253	92345	0.716	100
Alabama	US	Wet no Freeze	5	29000	148	54020	0.717	100
Alabama	US	Wet no Freeze	5	62000	208	75920	0.72	100
Alabama	US	Wet no Freeze	5	141752	493	180438	0.735	100
Alabama	US	Wet no Freeze	5	52257	256	93696	0.735	100
Alabama	US	Wet no Freeze	5	115552	410	149650	0.749	100
Alabama	US	Wet no Freeze	5	26192	92	33580	0.778	100
Arkansas	US	Wet no Freeze	5	50399	94	34310	0.785	100
Arkansas	US	Wet no Freeze	5	73000	193	70445	0.796	100
Arkansas	US	Wet no Freeze	6	376914	1529	558085	0.8	100
Arkansas	US	Wet no Freeze	6	136328	498	181770	0.811	100
Arkansas	US	Wet no Freeze	6	59000	121	44165	0.813	100
Arkansas	US	Wet no Freeze	6	76500	295	81420	0.815	100
Arkansas	US	Wet no Freeze	6	453000	1338	488370	0.825	100
Arkansas	US	Wet no Freeze	6	78537	291	106215	0.834	100
California	US	Wet no Freeze	6	10654	83	30378	0.84	96
California	US	Wet no Freeze	6	411000	1208	440920	0.847	90
California	US	Wet no Freeze	6	797000	3035	1107775	0.847	89
California	US	Wet no Freeze	6	65985	210	76650	0.869	89
California	US	Wet no Freeze	7	43187	210	76650	0.871	89
California	US	Wet no Freeze	7	24742	254	92964	1.364	89
California	US	Wet no Freeze	7	44180	491	179215	1.363	88
California	US	Wet no Freeze	7	30000	97	35405	1.352	88
California	US	Wet no Freeze	7	48876	206	75396	1.352	88
California	US	Wet no Freeze	7	48866	244	89060	1.352	88
California	US	Wet no Freeze	7	110599	214	78110	1.319	88
Florida	US	Wet no Freeze	7	28178	324	118260	1.302	88
Florida	US	Wet no Freeze	7	81070	346	126290	1.287	87
Florida	US	Wet no Freeze	7	117000	386	140890	1.269	87
Florida	US	Wet no Freeze	7	30000	92	33580	1.267	87

Florida	US	Wet no Freeze	7	70133	224	81984	1.249	87
Florida	US	Wet no Freeze	7	15374	54	19710	1.246	87
Florida	US	Wet no Freeze	7	566150	3219	788655	1.196	87
Florida	US	Wet no Freeze	7	94670	304	110960	1.176	87
Florida	US	Wet no Freeze	8	293053	1022	374052	1.164	87
Florida	US	Wet no Freeze	8	72365	307	112055	1.154	87
Florida	US	Wet no Freeze	8	80231	298	108770	1.15	86
Florida	US	Wet no Freeze	8	63000	219	79935	1.15	86
Florida	US	Wet no Freeze	8	36000	146	53436	1.136	86
Florida	US	Wet no Freeze	9	107000	354	129564	1.123	86
Florida	US	Wet no Freeze	9	58758	297	108405	1.12	86
Florida	US	Wet no Freeze	9	41966	147	53802	1.113	85
Florida	US	Wet no Freeze	9	711000	2360	861400	1.11	85
Florida	US	Wet no Freeze	9	22926	264	96360	1.108	85
Florida	US	Wet no Freeze	9	455359	1713	625245	1.108	85
Florida	US	Wet no Freeze	9	52000	169	61685	1.104	85
Florida	US	Wet no Freeze	9	89000	145	52925	1.104	84
Florida	US	Wet no Freeze	9	326211	1149	419385	1.104	84
Florida	US	Wet no Freeze	9	138587	251	91615	1.104	84
Florida	US	Wet no Freeze	10	58300	171	62586	1.103	84
Florida	US	Wet no Freeze	10	92496	296	108336	1.098	83
Florida	US	Wet no Freeze	10	308000	1146	419436	1.093	83
Florida	US	Wet no Freeze	10	47570	220	80300	1.093	83
Florida	US	Wet no Freeze	10	361814	1373	501145	1.088	83
Florida	US	Wet no Freeze	10	773000	2946	1075290	1.085	83
Florida	US	Wet no Freeze	10	91557	177	21948	1.081	83
Florida	US	Wet no Freeze	11	73000	267	97455	1.078	83
Florida	US	Wet no Freeze	11	40981	199	72834	1.074	83
Florida	US	Wet no Freeze	11	40402	198	72270	1.074	83
Florida	US	Wet no Freeze	11	71080	223	81395	1.068	83
Florida	US	Wet no Freeze	11	60000	209	76494	1.064	83
Florida	US	Wet no Freeze	11	39305	215	78690	1.064	83

Florida	US	Wet no Freeze	11	382594	1346	492636	1.062	83
Florida	US	Wet no Freeze	11	58800	465	70680	1.061	82
Florida	US	Wet no Freeze	11	648000	2467	900455	1.052	82
Georgia	US	Wet no Freeze	12	30999	351	128115	1.05	82
Georgia	US	Wet no Freeze	12	84552	297	108405	1.045	82
Hawaii	US	Wet no Freeze	12	21000	87	31755	1.041	82
Hawaii	US	Wet no Freeze	12	18892	81	29565	1.008	82
Hawaii	US	Wet no Freeze	12	92706	285	104025	1.005	82
Hawaii	US	Wet no Freeze	12	88461	224	81760	1.002	82
Hawaii	US	Wet no Freeze	12	58000	211	77015	0.998	82
Hawaii	US	Wet no Freeze	12	74000	316	115340	0.994	82
Hawaii	US	Wet no Freeze	12	203670	744	271560	0.988	81
Hawaii	US	Wet no Freeze	13	184000	608	222528	0.985	81
Hawaii	US	Wet no Freeze	13	448000	1334	486910	0.97	81
Hawaii	US	Wet no Freeze	13	22557	126	45990	0.969	81
Hawaii	US	Wet no Freeze	13	43466	490	179340	0.96	80
Hawaii	US	Wet no Freeze	13	27167	109	39785	0.959	80
Hawaii	US	Wet no Freeze	13	62934	222	40182	0.952	79
Hawaii	US	Wet no Freeze	13	37489	169	61854	0.951	78
Hawaii	US	Wet no Freeze	13	60320	173	63145	0.949	78
Hawaii	US	Wet no Freeze	13	125000	326	118990	0.948	78
Mississippi	US	Wet no Freeze	13	114840	461	168726	0.947	77
Mississippi	US	Wet no Freeze	13	18060	188	28576	0.944	77
Mississippi	US	Wet no Freeze	14	188000	526	192516	0.938	76
Mississippi	US	Wet no Freeze	14	69941	224	81760	0.926	76
Mississippi	US	Wet no Freeze	14	72000	134	49044	0.918	76
Mississippi	US	Wet no Freeze	14	56000	193	70445	0.912	75
Mississippi	US	Wet no Freeze	15	53684	264	96360	0.906	75
Mississippi	US	Wet no Freeze	15	43913	187	68255	0.906	75
Mississippi	US	Wet no Freeze	15	30396	344	125904	0.894	75
Mississippi	US	Wet no Freeze	15	213000	572	208780	0.884	74
Mississippi	US	Wet no Freeze	15	361168	1273	464645	0.877	74

Mississippi	US	Wet no Freeze	15	48476	186	67890	1.366	74
Mississippi	US	Wet no Freeze	15	25000	81	29565	1.38	74
Mississippi	US	Wet no Freeze	16	70346	298	108770	1.383	74
Mississippi	US	Wet no Freeze	16	43559	153	55845	1.387	74
Mississippi	US	Wet no Freeze	16	45870	209	76285	1.393	73
Mississippi	US	Wet no Freeze	16	68000	229	83585	1.402	73
North Carolina	US	Wet no Freeze	16	26000	82	30012	1.418	73
North Carolina	US	Wet no Freeze	16	208324	761	277765	1.418	73
North Carolina	US	Wet no Freeze	16	114000	375	136875	1.422	71
North Carolina	US	Wet no Freeze	17	729000	2777	1013605	1.429	71
North Carolina	US	Wet no Freeze	17	362649	837	305505	1.433	70
North Carolina	US	Wet no Freeze	17	34715	178	64970	1.444	70
Oklahoma	US	Wet no Freeze	17	13049	96	35040	1.45	70
Oklahoma	US	Wet no Freeze	17	77409	248	90520	1.451	70
Oklahoma	US	Wet no Freeze	17	453555	1701	622566	1.454	70
Oklahoma	US	Wet no Freeze	17	119205	511	186515	1.455	70
Oklahoma	US	Wet no Freeze	17	38000	144	52560	1.455	70
Oklahoma	US	Wet no Freeze	17	89341	287	104755	1.456	68
Oklahoma	US	Wet no Freeze	17	176900	1305	279270	1.46	68
Oklahoma	US	Wet no Freeze	17	294000	557	203862	1.461	68
Oklahoma	US	Wet no Freeze	17	22261	258	94170	1.474	68
Oklahoma	US	Wet no Freeze	18	84479	355	129575	1.484	68
Oklahoma	US	Wet no Freeze	18	82035	149	54534	1.491	68
Oklahoma	US	Wet no Freeze	18	88912	165	49335	1.499	68
Oklahoma	US	Wet no Freeze	18	329712	1240	452600	1.506	68
Oklahoma	US	Wet no Freeze	18	133199	259	94535	1.508	68
Oklahoma	US	Wet no Freeze	18	367522	1383	504795	1.514	68
Oklahoma	US	Wet no Freeze	18	70980	449	69146	1.517	68
Oklahoma	US	Wet no Freeze	19	73156	307	112362	1.529	68
Oklahoma	US	Wet no Freeze	19	31547	357	130305	1.57	68
Oklahoma	US	Wet no Freeze	19	41282	237	15642	1.584	67
Oklahoma	US	Wet no Freeze	19	55020	433	65816	1.589	65

Oklahoma	US	Wet no Freeze	19	73840	262	95630	1.616	65
Oklahoma	US	Wet no Freeze	19	19345	224	81760	1.619	65
Oklahoma	US	Wet no Freeze	19	465550	1753	639845	1.633	65
Oklahoma	US	Wet no Freeze	19	329015	1238	451870	1.64	63
Oklahoma	US	Wet no Freeze	19	402194	1322	482530	1.662	63
South Carolina	US	Wet no Freeze	20	43986	214	78110	1.674	63
South Carolina	US	Wet no Freeze	20	667000	2541	930006	1.689	62
South Carolina	US	Wet no Freeze	20	676000	2275	830375	1.693	62
South Carolina	US	Wet no Freeze	20	40979	179	65335	1.735	62
South Carolina	US	Wet no Freeze	20	22000	139	50874	1.791	62
South Carolina	US	Wet no Freeze	20	95196	327	119355	1.805	61
South Carolina	US	Wet no Freeze	20	42763	208	75920	1.807	61
South Carolina	US	Wet no Freeze	21	88520	671	244915	1.85	60
South Carolina	US	Wet no Freeze	21	176000	745	272670	1.858	60
South Carolina	US	Wet no Freeze	21	23966	130	47580	1.859	60
South Carolina	US	Wet no Freeze	21	438406	1773	648918	1.867	59
South Carolina	US	Wet no Freeze	21	111000	364	132860	1.868	59
South Carolina	US	Wet no Freeze	21	471540	1706	622690	1.87	59
South Carolina	US	Wet no Freeze	21	411230	803	139722	1.875	58
South Carolina	US	Wet no Freeze	21	78077	323	117895	1.875	58
South Carolina	US	Wet no Freeze	21	34956	162	59130	1.932	57
Tennessee	US	Wet no Freeze	21	386430	1448	529968	1.946	57
Tennessee	US	Wet no Freeze	21	55641	272	99280	1.954	56
Tennessee	US	Wet no Freeze	22	146135	246	89790	1.981	56
Tennessee	US	Wet no Freeze	22	148810	510	186150	1.99	55
Tennessee	US	Wet no Freeze	22	54290	207	75555	1.993	53
Tennessee	US	Wet no Freeze	22	79000	289	105485	1.994	52
Tennessee	US	Wet no Freeze	22	130000	449	163885	2.006	45
Texas	US	Wet no Freeze	22	69941	224	81760	2.013	40
Texas	US	Wet no Freeze	22	49968	155	56575	2.031	40
Texas	US	Wet no Freeze	22	65000	198	72270	2.038	38
Texas	US	Wet no Freeze	23	165330	1376	166496	2.053	36

Texas	US	Wet no Freeze	23	115000	380	138700	2.053	35
Texas	US	Wet no Freeze	23	44515	203	74095	2.078	34
Texas	US	Wet no Freeze	24	91133	321	117165	2.094	32
Texas	US	Wet no Freeze	24	5880	81	12555	2.103	30
Texas	US	Wet no Freeze	25	338382	1052	385032	2.125	29
Texas	US	Wet no Freeze	25	61000	168	61320	2.135	27
Texas	US	Wet no Freeze	25	363870	714	261324	2.14	24
Texas	US	Wet no Freeze	25	172134	699	255135	2.169	24
Texas	US	Wet no Freeze	26	708000	2696	984040	2.246	23
Texas	US	Wet no Freeze	26	50965	249	90885	2.322	23
Texas	US	Wet no Freeze	26	41866	203	74095	2.322	22
Texas	US	Wet no Freeze	26	76000	278	101470	2.337	20
Texas	US	Wet no Freeze	27	187245	684	249660	2.385	19
Texas	US	Wet no Freeze	27	76248	347	126655	2.388	19
Texas	US	Wet no Freeze	27	248422	905	331230	2.526	19
Texas	US	Wet no Freeze	28	159282	647	236155	2.54	19
Texas	US	Wet no Freeze	28	109803	350	127750	2.614	18
Texas	US	Wet no Freeze	28	39343	230	83950	2.626	18
Texas	US	Wet no Freeze	29	36344	154	56364	2.782	18
Texas	US	Wet no Freeze	31	35274	153	55845	2.868	15
Texas	US	Wet no Freeze	31	86684	366	133590	3.543	8
Texas	US	Wet no Freeze	31	363865	1282	467930	3.758	8

Appendix B: Data Extraction (St. John's city- Canada)

Table B-1: Presents the data from TotalPave (St. John's city- Canada).

Road Name	IRI 2018(m/km)	IRI 2021(m/km)	Length of section(m)
TRANS CANADA HWY	1.03	1.32	1000.00
TRANS CANADA HWY	0.91	1.19	1000.00
TRANS CANADA HWY	1.22	0.83	1000.00
TRANS CANADA HWY	1.17	1.34	1000.00
TRANS CANADA HWY	1.13	0.88	1000.00
TRANS CANADA HWY	1.15	0.82	1000.00
TRANS CANADA HWY	1.18	0.66	1000.00
TRANS CANADA HWY	1.01	1.01	613.36
TRANS CANADA HWY	1.01	0.75	1000.00
HIGHLAND DR	3.67	2.23	146.36
HIGHLAND DR	4.33	2.70	134.73
HIGHLAND DR	2.45	1.85	638.24
HIGHLAND DR	2.99	3.54	532.60
THE BOULEVARD	3.51	3.79	377.36
THE BOULEVARD	3.28	3.92	288.51
THE BOULEVARD	2.15	2.99	440.53
THE BOULEVARD	4.72	4.37	285.92
THE BOULEVARD	2.74	4.72	297.50
EMPIRE AVE	8.27	7.16	76.77
EMPIRE AVE	6.94	7.79	77.65
EMPIRE AVE	3.26	2.72	167.25
EMPIRE AVE	4.67	2.81	79.05
EMPIRE AVE	6.03	5.40	82.87
EMPIRE AVE	2.46	2.60	612.20

EMPIRE AVE	3.71	8.53	75.16
EMPIRE AVE	6.29	5.47	68.33
EMPIRE AVE	5.60	5.16	143.23
ABERDEEN AVE	2.11	2.80	436.43
MACDONALD DR	2.84	3.78	236.66
MACDONALD DR	0.81	2.32	89.50
MACDONALD DR	2.38	3.26	43.51
MACDONALD DR	1.68	4.59	40.45
MACDONALD DR	1.81	1.94	281.12
MACDONALD DR	2.02	2.55	185.05
MACDONALD DR	1.04	1.71	80.61
MACDONALD DR	2.60	3.63	204.80
MACDONALD DR	2.72	2.48	180.59
MACDONALD DR	1.60	2.27	156.37
FRESHWATER RD	2.18	3.44	27.80
FRESHWATER RD	3.51	4.34	194.11
FRESHWATER RD	2.51	3.83	100.03
FRESHWATER RD	3.40	4.80	159.81
FRESHWATER RD	2.52	4.23	96.78
FRESHWATER RD	3.61	4.60	216.01
FRESHWATER RD	2.97	3.85	91.64
FRESHWATER RD	3.16	3.80	102.62
FRESHWATER RD	3.69	4.59	97.39
FRESHWATER RD	3.16	5.54	187.58
FRESHWATER RD	3.56	4.30	137.95
FRESHWATER RD	2.43	1.84	89.13
FRESHWATER RD	3.68	3.14	255.46

FRESHWATER RD	4.25	4.54	105.23
FRESHWATER RD	5.28	4.70	156.26
FRESHWATER RD	5.78	8.32	61.08
FRESHWATER RD	3.50	3.91	218.48
FRESHWATER RD	2.01	2.87	42.58
FRESHWATER RD	2.52	4.23	96.78
FRESHWATER RD	3.61	4.60	216.01
FRESHWATER RD	3.51	4.34	194.11
FRESHWATER RD	2.51	3.83	100.03
FRESHWATER RD	3.40	4.80	159.81
FRESHWATER RD	2.18	3.44	27.80
FRESHWATER RD	2.97	3.85	91.64
FRESHWATER RD	3.16	3.80	102.62
FRESHWATER RD	3.69	4.59	97.39
FRESHWATER RD	3.16	5.54	187.58
FRESHWATER RD	3.56	4.30	137.95
FRESHWATER RD	2.43	1.84	89.13
FRESHWATER RD	3.68	3.14	255.46
FRESHWATER RD	4.25	4.54	105.23
FRESHWATER RD	4.82	4.70	156.26
FRESHWATER RD	5.78	8.32	61.08
FRESHWATER RD	3.50	3.91	218.48
FRESHWATER RD	2.01	2.87	42.58
NEWTOWN RD	3.37	3.39	92.53
NEWTOWN RD	4.70	5.28	280.14
NEWTOWN RD	4.42	4.92	205.74
NEWTOWN RD	3.49	3.30	107.19

NEWTOWN RD	4.33	5.54	63.66
NEWTOWN RD	5.73	5.64	76.27
NEWFOUNDLAND DR	2.60	2.89	141.99
NEWFOUNDLAND DR	3.05	2.59	91.08
NEWFOUNDLAND DR	4.77	4.05	214.58
NEWFOUNDLAND DR	6.21	1.83	117.00
NEWFOUNDLAND DR	3.41	3.10	84.54
NEWFOUNDLAND DR	1.22	3.12	75.65
NEWFOUNDLAND DR	3.64	2.94	122.78
NEWFOUNDLAND DR	3.39	3.44	107.45
NEWFOUNDLAND DR	2.92	2.02	219.52
NEWFOUNDLAND DR	2.94	5.36	180.13
NEWFOUNDLAND DR	6.42	5.86	135.30
NEWFOUNDLAND DR	4.51	3.56	104.89
NEWFOUNDLAND DR	3.76	2.86	55.08
NEWFOUNDLAND DR	4.34	3.49	229.79
NEWFOUNDLAND DR	2.81	4.06	80.92
NEWFOUNDLAND DR	4.00	1.97	190.44
NEWFOUNDLAND DR	4.18	4.04	276.32
WATER ST	4.05	3.20	87.36
WATER ST	3.20	2.97	303.55
WATER ST	4.53	2.75	92.30
WATER ST	2.97	2.52	144.51
WATER ST	3.61	2.29	140.97
WATER ST	3.25	2.06	27.30
WATER ST	4.29	1.83	186.51
WATER ST	5.17	1.60	61.58

WATER ST	3.65	1.37	146.47
WATER ST	3.39	1.14	116.09
WATER ST	1.48	1.92	34.91
KING'S BRIDGE RD	4.57	2.37	175.05
KING'S BRIDGE RD	5.41	11.57	28.36
KING'S BRIDGE RD	6.09	2.83	83.43
KING'S BRIDGE RD	6.70	3.40	127.25
KING'S BRIDGE RD	5.90	6.92	155.16
KENNA'S HILL	4.28	3.94	368.25
KING'S BRIDGE RD	3.98	5.83	106.80
LOGY BAY RD	3.97	4.09	142.89
LOGY BAY RD	1.05	1.45	104.36
LOGY BAY RD	5.13	3.91	128.35
LOGY BAY RD	1.44	2.87	70.48
LOGY BAY RD	3.65	3.08	99.04
LOGY BAY RD	3.03	3.56	278.94
LOGY BAY RD	3.76	5.97	101.20
LOGY BAY RD	1.63	1.76	65.90
LOGY BAY RD	3.10	3.90	65.76
LOGY BAY RD	3.43	3.28	176.68
LOGY BAY RD	2.78	3.45	292.96
LOGY BAY RD	2.20	4.03	104.74
LOGY BAY RD	1.91	3.64	173.20
LOGY BAY RD	1.08	1.19	78.45
LOGY BAY RD	1.06	0.77	24.60
LOGY BAY RD	1.11	1.44	116.59
BLACKHEAD RD	2.45	3.51	206.83

BLACKHEAD RD	3.54	4.66	439.53
BLACKHEAD RD	2.17	2.43	2571.66
BLACKHEAD RD	2.26	2.74	1199.58
BLACKHEAD RD	1.89	2.27	3829.73
TORBAY RD	2.75	3.82	72.84
TORBAY RD	3.69	3.83	248.62
TORBAY RD	2.83	2.48	234.53
TORBAY RD	2.89	2.00	160.48
TORBAY RD	3.85	3.83	206.76
TORBAY RD	2.40	4.27	241.23
TORBAY RD	2.79	3.59	318.77
TORBAY RD	3.36	1.63	30.15
TORBAY RD	2.02	1.82	17.82
TORBAY RD	3.64	3.93	193.08
TORBAY RD	2.47	1.54	162.16
TORBAY RD	2.24	4.41	90.99
TORBAY RD	3.21	3.04	319.38
PORTUGAL COVE RD	1.51	2.22	51.93
PORTUGAL COVE RD	1.10	2.14	110.61
PORTUGAL COVE RD	1.21	1.75	128.74
PORTUGAL COVE RD	3.45	2.99	360.07
PORTUGAL COVE RD	1.22	1.63	165.08
PORTUGAL COVE RD	2.46	1.62	154.31
PORTUGAL COVE RD	1.30	1.63	96.60
PORTUGAL COVE RD	0.88	2.27	76.41
PORTUGAL COVE RD	1.69	1.63	390.96
PORTUGAL COVE RD	1.09	1.34	501.59

PORTUGAL COVE RD	2.28	2.55	607.99
PORTUGAL COVE RD	1.42	1.57	1155.07
PORTUGAL COVE RD	2.71	2.85	110.84
KENMOUNT RD	2.04	3.01	151.48
KENMOUNT RD	1.49	2.60	103.12
KENMOUNT RD	2.26	3.24	1246.70
KENMOUNT RD	3.33	3.93	305.60
KENMOUNT RD	1.84	2.95	205.62
KENMOUNT RD	2.21	3.15	155.66
KENMOUNT RD	3.05	2.15	75.08
KENMOUNT RD	4.49	3.55	618.84
KENMOUNT RD	2.24	2.99	604.55
KENMOUNT RD	2.72	2.22	169.11
KENMOUNT RD	1.62	3.52	505.53
KENMOUNT RD	3.12	1.69	142.46
KENMOUNT RD	1.81	2.31	441.93
PRINCE PHILIP DR	1.69	1.82	179.20
PRINCE PHILIP DR	1.56	2.62	309.77
PRINCE PHILIP DR	1.39	2.42	158.72
PRINCE PHILIP DR	2.38	2.66	307.76
PRINCE PHILIP DR	2.78	3.34	992.07
PRINCE PHILIP DR	1.86	1.73	505.38
PRINCE PHILIP DR	2.02	2.26	213.68
PRINCE PHILIP DR	2.54	2.46	266.21
PRINCE PHILIP DR	4.01	3.46	89.09
PRINCE PHILIP DR	3.58	2.93	180.44
PRINCE PHILIP DR	2.08	1.39	228.11

PRINCE PHILIP DR	2.21	1.55	198.35
PRINCE PHILIP DR	1.16	1.59	361.24
ELIZABETH AVE	2.79	3.09	369.19
ELIZABETH AVE	2.92	2.53	36.68
ELIZABETH AVE	5.21	6.79	62.18
ELIZABETH AVE	3.57	2.98	169.72
ELIZABETH AVE	2.29	3.20	177.68
ELIZABETH AVE	3.46	3.32	34.22
ELIZABETH AVE	7.54	4.19	170.47
ELIZABETH AVE	2.66	3.53	187.79
ELIZABETH AVE	2.10	2.74	292.38
ELIZABETH AVE	1.87	3.58	98.92
ELIZABETH AVE	3.42	4.93	50.15
ELIZABETH AVE	3.38	3.95	45.61
ELIZABETH AVE	2.93	3.01	353.93
ELIZABETH AVE	2.94	3.36	35.49
ELIZABETH AVE	4.94	3.93	238.94
ELIZABETH AVE	4.43	4.59	181.44
ELIZABETH AVE	3.19	4.36	111.27
ELIZABETH AVE	3.48	3.88	83.96
ELIZABETH AVE	4.40	2.87	196.48
ELIZABETH AVE	4.79	4.07	217.75
ELIZABETH AVE	4.66	4.24	182.74
ELIZABETH AVE	4.00	3.63	57.79
ELIZABETH AVE	2.03	2.86	88.57
ELIZABETH AVE	3.30	2.92	106.33